

Fire Resistance of Concrete made with Portland and Slag Blended Cements

by

Alessandra Ferreira Bragança Mendes

Bachelor of Engineering



*A thesis submitted in fulfilment of the requirements for the degree
of Doctor of Philosophy*

Department of Civil Engineering

Monash University

October 2010

Notice 1

Under the Copyright Act 1968, this thesis must be used only under the normal conditions of scholarly fair dealing. In particular no results or conclusions should be extracted from it, nor should it be copied or closely paraphrased in whole or in part without the written consent of the author. Proper written acknowledgement should be made for any assistance obtained from this thesis.

Notice 2

I certify that I have made all reasonable efforts to secure copyright permissions for third-party content included in this thesis and have not knowingly added copyright content to my work without the owner's permission.

To Serafim Mendes and Maria Luisa Alves Ferreira

ABSTRACT

The fire resistance of concrete has become a major design concern due to various high profile fire incidents such as the collapse of the Twin Towers (September 11), USA and several tunnel fires around the world. Concrete although described as incombustible, undergoes physical and chemical transformations when exposed to elevated temperatures, as in a fire event.

Above 400°C, one of the main hydrates of ordinary Portland cement (OPC) paste, calcium hydroxide (CaOH_2) dehydrates into calcium oxide (CaO) causing the OPC paste to shrink and crack. After cooling and in the presence of air moisture, the CaO rehydrates into CaOH_2 causing the OPC paste to expand, crack and completely disintegrate. However, the long-term effects of the CaO rehydration on the mechanical properties of OPC pastes are unknown and therefore, are investigated by the present thesis.

In addition, the effects of elevated temperatures and CaOH_2 dehydration/ CaO rehydration on the microstructure and mechanical properties of concrete are still unclear. This issue has been of much debate and due to the conflicting nature of the available literature, is not fully understood. Therefore, this thesis investigates these effects on the microstructure and mechanical properties of OPC concrete.

Furthermore, despite the continuous growing popularity of ground granulated blast furnace slag (GGBFS or 'slag') as a partial replacement of OPC in concrete, limited research has focused on how this replacement influences the microstructure and mechanical properties of paste and concrete exposed to elevated temperatures. Therefore, this thesis also addresses this issue.

The study shows that partial replacement of OPC with slag resulted in a significant and beneficial reduction of the amount of CaOH_2 . An increase in the proportion of slag in the cement paste led to an improvement in the mechanical properties following exposure to temperatures beyond 400°C.

The long-term effects of CaO rehydration on the mechanical properties of OPC and OPC/slag pastes exposed to 800°C were investigated using differential

thermogravimetric analysis (DTG). Test results showed that CaO rehydration continued to take place throughout the period of one year, leading to a progressive deterioration of the OPC paste. After one year, the OPC paste completely disintegrated to a powder. In contrast, OPC/slag pastes were not affected by the progressive CaO rehydration as mechanical properties remained unchanged after one year.

The study of the role of paste hydrates, rather than CaOH_2 , in the deterioration of mechanical properties of OPC and OPC/slag pastes was performed by nuclear magnetic resonance (NMR), X-ray diffraction (XRD), infrared spectroscopy (IR) and Synchrotron NEXAFS. Test results showed differences in the resulting calcium silicate hydrate (C-S-H gel) and aluminate phases of OPC and OPC/slag pastes after exposure to elevated temperatures. This indicates that the silicate and aluminate phases play a role in the higher degree of deterioration observed for OPC pastes when compared to OPC/slag pastes.

The study of the effects of elevated temperatures on the mechanical properties of concrete revealed that OPC concrete heated to 800°C followed by exposure to air moisture presented strength loss of 65% while OPC pastes presented total strength loss and complete disintegration. This shows that the dehydration of CaOH_2 and rehydration of CaO is significantly less detrimental for OPC concrete than it is for OPC paste.

Techniques such as sorptivity tests and nitrogen adsorption were used to determine the differences in the CaO rehydration of paste and concrete. The rate of water absorption determines the growth rate of CaOH_2 crystals during CaO rehydration and ultimately the type of CaOH_2 crystals formed. Different rates of water absorption result in different CaOH_2 crystal formation. This leads to differences in levels of deterioration, which not always result in total disintegration of the constraining body. In this study, the rate of water absorption of OPC paste and concrete was found to significantly differ. The test results revealed that the extent of the deterioration is not only related to the CaO rehydration occurrence, but most importantly, it is related to the rate at which rehydration occurs, i.e., the rate of water absorption. The rate of water absorption is the determining factor controlling the extent of deterioration caused by CaO rehydration.

DECLARATION

In accordance with Monash University Doctorate Regulation 17/ Doctor of Philosophy and Master of Philosophy (MPhil) regulations the following declarations are made:

I hereby declare that this thesis contains no material which has been accepted for the award of any other degree or diploma at any university or equivalent institution and that, to the best of my knowledge and belief, this thesis contains no material previously published or written by another person, except where due reference is made in the text of the thesis.

This thesis includes three original papers published in peer reviewed journals and four unpublished publications. The core theme of the thesis is the study of the fire resistance of concrete blends. The ideas, development and writing up of all the papers in the thesis were the principal responsibility of myself, the candidate, working within the Department of Civil Engineering, Monash University under the supervision of Dr Frank Collins and Professor Jay Sanjayan.

In the case of Chapters 3-9 my contribution to the work involved the following:

| Thesis chapter | Publication title | Publication status* | Nature and extent of candidate's contribution |
|-----------------------|---|----------------------------|---|
| 3 | Phase transformations and mechanical strength of OPC/Slag pastes submitted to high temperatures | Published | Developing outline of research objective and hypothesis Laboratory/experimental investigation and analysis of results Writing, reviewing and editing of the paper |
| 4 | Long-term progressive deterioration following fire exposure of OPC versus slag blended cement pastes | Published | Developing outline of research objective and hypothesis Laboratory/experimental investigation and analysis of results Writing, reviewing and editing of the paper |
| 5 | Investigation of repair methods for preventing strength loss of ordinary Portland cement pastes after fire exposure | Submitted | Developing outline of research objective and hypothesis Laboratory/experimental investigation and analysis of results Writing, reviewing and editing of the paper |

| | | | |
|---|---|-----------|---|
| 6 | NMR, XRD, IR and Synchrotron NEXAFS spectroscopic studies of OPC and OPC/slag cement paste hydrates | Submitted | Developing outline of research objective and hypothesis Laboratory/experimental investigation and analysis of results Writing, reviewing and editing of the paper |
| 7 | NMR, XRD, IR and Synchrotron NEXAFS spectroscopic studies of OPC and OPC/slag cement paste hydrates after exposure to elevated temperatures | Submitted | Developing outline of research objective and hypothesis Laboratory/experimental investigation and analysis of results Writing, reviewing and editing of the paper |
| 8 | Effects of slag and cooling method on the progressive deterioration of concrete after exposure to elevated temperatures as in a fire event | Published | Developing outline of research objective and hypothesis Laboratory/experimental investigation and analysis of results Writing, reviewing and editing of the paper |
| 9 | Differences in the behaviour of cement paste and concrete after exposure to elevated temperatures, as in a fire event | Submitted | Developing outline of research objective and hypothesis Laboratory/experimental investigation and analysis of results Writing, reviewing and editing of the paper |

I have not renumbered sections of submitted or published papers in order to generate a consistent presentation within the thesis. Portable document format (PDF) of the published papers were resized and inserted in the relevant chapters while submitted papers were inserted in their submission manuscript format with figures redistributed for consistency.

Signed:



Date: 30 September 2010

ACKNOWLEDGEMENT

I would like to express my deep and sincere gratitude to my supervisor Professor Jay Sanjayan for the opportunity to work on this exciting project. His faith in me and untiring help during some of my most difficult moments have been invaluable to me. His support and encouragement, as well as his academic experience, have made this thesis possible.

I wish to express my warm and sincere thanks to my supervisor Dr Frank Collins. I am deeply grateful for his constant involvement, highly valuable guidance, timely advice and the friendship he and his family have offered me throughout the years. I hope our shared enthusiasm for materials science will see us work closely together in the future.

I extend my sincere gratitude to Dr Will Gates for his valuable contribution to my project. His contagious passion for science and research has broadened my skills and knowledge. I trust he will continue to spread his passion to many others.

My warm thanks to Jennifer Manson, Jenny, for the endless support and guidance during my candidature. I am sure she will be my friend for life.

I gratefully acknowledge all the friendly assistance provided by the late Graeme Rundle, Alan Taylor, Jeffrey Doddrell, Glenn Davis and Peter Dunbar. I also would like to thank Long Kim Goh for all his support and encouragement during my research work. My sincere thanks to Kevin Nievaart for his valuable technical input into this project but most importantly for the friendship shared during these years.

I wish to thank my precious friends Sara Moridpour and Cintia Dotto for their endless support during these years. I also would like to thank all my postgraduate colleagues, Nurses Kurucuk, Fern Yong, Rawaa Al-Safy, Mirela Magyar, Mobashwera Kabir, Siavash Hashemi, Ehsan Mazloumi, Zhu Pan and Ren Zhao. They all contributed to this journey in some way.

I wish to acknowledge the administrative staff from the Civil Engineering Department for their friendly assistance during my research, especially Chris Powell, Irene Sgouras, Helen Parker, Noi Souvandy and Rob Alexander.

My loving thanks to all my family and friends who have supported me from the distance separating Australia and Brazil, from day one and always. I also would like to thank my aussie family, The Tattersalls, for all the patience, prayers and love during these years.

My parents, Antonio and Giselda, have provided me with the opportunity to be where I am. They are my true inspiration. Inspired by them, I have the opportunity to be who I am. They have dedicated their lives to me, and to them I dedicate this thesis. I love them both, always.

To my fiancée Paul, my angel, my guiding light. He is my greatest gift, essential part of life. I thank him for being on this journey with me, for life.

To life!

LIST OF PUBLICATIONS

Refereed journal papers

1. Mendes A, Sanjayan J, Collins F (2008). Phase transformations and mechanical strength of OPC/Slag pastes submitted to high temperatures. *Materials and Structures* 41: 345-350.
2. Mendes A, Sanjayan J, Collins F (2009). Long-term progressive deterioration following fire exposure of OPC versus slag blended cement pastes. *Materials and Structures* 42: 95-101.
3. Mendes A, Sanjayan JG, Collins F (2010). Effects of slag and cooling method on the progressive deterioration of concrete after exposure to elevated temperatures as in a fire event. *Materials and Structures* DOI 10.1617/s11527-010-9660-2: Published online 31 August 2010.

Submitted journal papers

1. Mendes A, Gates WP, Sanjayan JG, Collins F. NMR, XRD, IR and Synchrotron NEXAFS spectroscopic studies of OPC and OPC/slag cement paste hydrates. *Materials and Structures*, submitted in January 2010.
2. Mendes A, Gates WP, Sanjayan JG, Collins F. NMR, XRD, IR and Synchrotron NEXAFS spectroscopic studies of OPC and OPC/slag cement paste hydrates after exposure to elevated temperatures. *Cement and Concrete Research*, submitted in July 2010.
3. Mendes A, Sanjayan JG, Gates WP, Collins F. Differences in the behaviour of cement paste and concrete after exposure to elevated temperatures, as in a fire event. *Cement and Concrete Composites*, submitted in June 2010.
4. Mendes A, Sanjayan JG, Collins F, Gates WP. Investigation of repair methods for preventing progressive strength loss of ordinary Portland cement pastes after fire exposure. *Materials and Structures*, submitted in August 2010.

TABLE OF CONTENTS

| | |
|---|-------------|
| Abstract | i |
| Declaration | iii |
| Acknowledgment | v |
| List of Publications | vii |
| Table of Contents..... | viii |
| | |
| 1 Introduction..... | 1 |
| 1.1 Overview | 1 |
| 1.2 Problem definition and objectives..... | 5 |
| 1.3 Thesis organization..... | 7 |
| 1.4 References | 8 |
| 2 Literature Review | 10 |
| 2.1 Fire resistance of concrete..... | 10 |
| 2.2 Paste..... | 12 |
| 2.2.1 Microstructure at room temperature..... | 12 |
| 2.2.2 Microstructure after exposure to elevated temperatures..... | 14 |
| 2.2.3 Summary..... | 20 |
| 2.3 Concrete..... | 21 |
| 2.3.1 The microstructure of concrete | 21 |
| 2.3.2 The pore structure of concrete..... | 26 |
| 2.3.3 Post-cooling regimes after elevated temperatures..... | 29 |
| 2.3.4 The role of aggregate at elevated temperatures..... | 31 |
| 2.3.5 Summary..... | 33 |
| 2.4 Partial replacement with slag | 36 |
| 2.4.1 Slag production | 36 |
| 2.4.2 Microstructure at room temperature | 36 |
| 2.4.3 Microstructure at elevated temperatures | 37 |
| 2.4.4 Summary..... | 39 |
| 2.5 Conclusions..... | 40 |
| 2.6 References | 41 |
| 3 Phase transformations and mechanical strength of OPC/Slag pastes submitted to high temperatures..... | 47 |
| 3.1 Overview | 47 |
| 3.2 Declaration for Thesis Chapter 3..... | 48 |
| 3.3 Publication..... | 50 |

| | |
|---|------------|
| 4 Long-term progressive deterioration following fire exposure of OPC versus slag blended cement pastes..... | 56 |
| 4.1 Overview | 56 |
| 4.2 Declaration for Thesis Chapter 4..... | 57 |
| 4.3 Publication..... | 59 |
| 5 Investigation of repair methods for preventing strength loss of ordinary Portland cement pastes after fire exposure..... | 66 |
| 5.1 Overview | 66 |
| 5.2 Declaration for Thesis Chapter 5..... | 67 |
| 5.3 Publication..... | 69 |
| 6 NMR, XRD, IR and Synchrotron NEXAFS spectroscopic studies of OPC and OPC/Slag cement paste hydrates..... | 84 |
| 6.1 Overview | 84 |
| 6.2 Declaration for Thesis Chapter 6..... | 85 |
| 6.3 Publication..... | 87 |
| 7 NMR, XRD, IR and Synchrotron NEXAFS spectroscopic studies of OPC and OPC/Slag cement paste hydrates after exposure to elevated temperatures..... | 124 |
| 7.1 Overview | 124 |
| 7.2 Declaration for Thesis Chapter 7..... | 125 |
| 7.3 Publication..... | 127 |
| 8 Effect of slag and cooling method on the progressive deterioration of concrete after exposure to elevated temperatures as in a fire event..... | 155 |
| 8.1 Overview | 155 |
| 8.2 Declaration for Thesis Chapter 8..... | 156 |
| 8.3 Publication..... | 158 |
| 9 Differences in the behaviour of cement paste and concrete after exposure to elevated temperatures, as in a fire event | 168 |
| 9.1 Overview | 168 |
| 9.2 Declaration for Thesis Chapter 9..... | 169 |
| 9.3 Publication..... | 171 |
| 10 Conclusions & future work..... | 198 |
| 10.1 Summary and conclusions..... | 198 |
| 10.2 Suggestions for future work | 202 |

Chapter 1

Introduction

1.1 Overview

Concrete is the most widely used engineering material in the world. It has excellent resistance to water, it can be formed into a variety of shapes and sizes and it is usually the cheapest and most readily available material in construction (Mehta and Monteiro 2006). Although concrete is generally considered to be a fire resistant material, the degradation processes experienced by concrete during and after fire exposure are still not clearly understood. Therefore, the structural safety of concrete structures exposed to a fire event is a major design consideration (Crozier and Sanjayan 1999; Eurocode 2 2005; Eurocode 4 2005; SP-255 2008).

A fire event in a structure can lead to major costs, both qualitative and quantitative losses. The qualitative losses relate to human lives. The quantitative losses include financial and environmental costs.

The loss of human lives is the most significant loss when a fire event occurs. The impact of a fire event upon humans can vary from injury to even the loss of life. In order to minimize and where possible eliminate human loss, many studies have focused on the fire resistance of structures.

The financial costs, as a result of a fire event in a structure, relate to the energy and resources expended repairing the structure or sometimes completely rebuilding it. These costs can be substantial in the short term. In addition, possible long-term costs may arise through legal action and assignment of liability where structures fail due to poor engineering construction and planning.

The environmental costs associated with a fire event include the impact on the surrounding eco-system through emission of fumes, production of waste and damage to existing environmental conditions.

1.1.1 Types of fires events

Standardised fires fall into three categories, depending upon the application: buildings; offshore/petrochemical; and tunnels (Khoury 2000). This is illustrated in Figure 1.1.

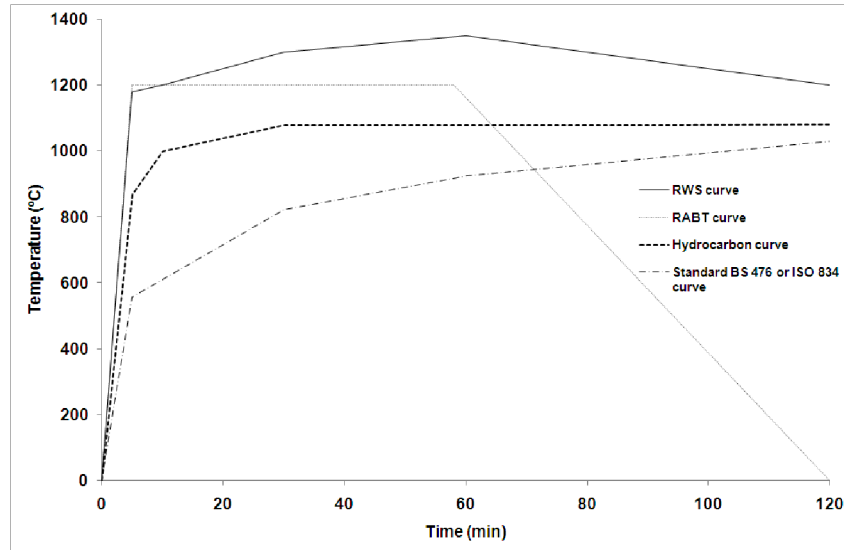


Figure 1.1 Fire categories and related fire curves. Adapted from (Khoury 2000)

The standard fire curve BS 476 (1987) or ISO 834 (1975) represents a typical building fire based upon a cellulosic fire in which the main fuel source is wood, paper and fabric. The standard fire curve corresponds to a severe fire, but not the severest fire possible (Khoury 2000).

In the 1970s, the oil company Mobil investigated hydrocarbon fuel fires and developed a temperature-time profile with a rapid temperature rise in the first 5 minutes of the fire up to 900°C and a peak of 1100°C. This research laid the foundation for test procedures to assess fire-protecting materials for the offshore and petrochemical industries (Khoury 2000).

The RWS Dutch fire curve models the severest hydrocarbon fire, rapidly exceeding 1200°C and peaking at 1350°C (melting temperature of concrete) after 60 minutes. A gradual decrease to 1200°C after 120 minutes is seen in the end of the fire curve. The RWS is intended to simulate tankers carrying petrol in tunnels with a fire load of 300 MW causing a fire for 2 hours. It represents the severest form of tunnel fire in terms of initial heating rates and maximum temperatures (Khoury 2000).

The RABT German fire curve represents a less severe fire scenario in tunnels than the RWS curve, reaching a maximum temperature of 1200°C (melting point of some aggregates) sustained up to 1 hour before decaying to ambient temperature (Khoury 2000).

1.1.2 Learning from actual fire events and costs

The fire resistance of concrete has become a major design consideration due to high profile fire incidents around the world.

In 1996, in the Channel Tunnel (a high speed railway tunnel running parallel beneath the English Channel (Kirkland 2002)) one of the heavy goods vehicles (HGV) on board of a shuttle train caught fire (Beard and Carvel 2005). The fire lasted for 10 hours and reached temperatures of up to 700°C (Ulm et al. 1999). Although no fatalities occurred, the tunnel was closed for 6 months at a loss of US\$ 1.5 million per day (Ulm et al. 1999).

In 1999, a HGV travelling through the Mont Blanc Tunnel from France to Italy caught fire halfway through the tunnel. The fire took 53 hours to be extinguished causing 39 deaths (Beard and Carvel 2005). Also in 1999, a fire incident occurred in the Tauern Tunnel, Austria causing severe casualties and damage. Four people died as a result of the fire, the tunnel was closed for 3 months and repairs costs and loss of toll fees exceeded US\$ 25 million (Leitner 2001). A view of the damaged tunnel is presented in Figure 1.2.



Figure 1.2 The Tauern Tunnel fire in 1999. Adapted from (Leitner 2001)

In Australia, the interest in fire safety design has escalated with the increased death rate and loss of property caused by fires in the last decade (Kong 2009). As shown in Figure 1.3, for the three year period between 2005 and 2007, the average fire death rate in Australia was 5.3 per million people (SCRGSP 2010).

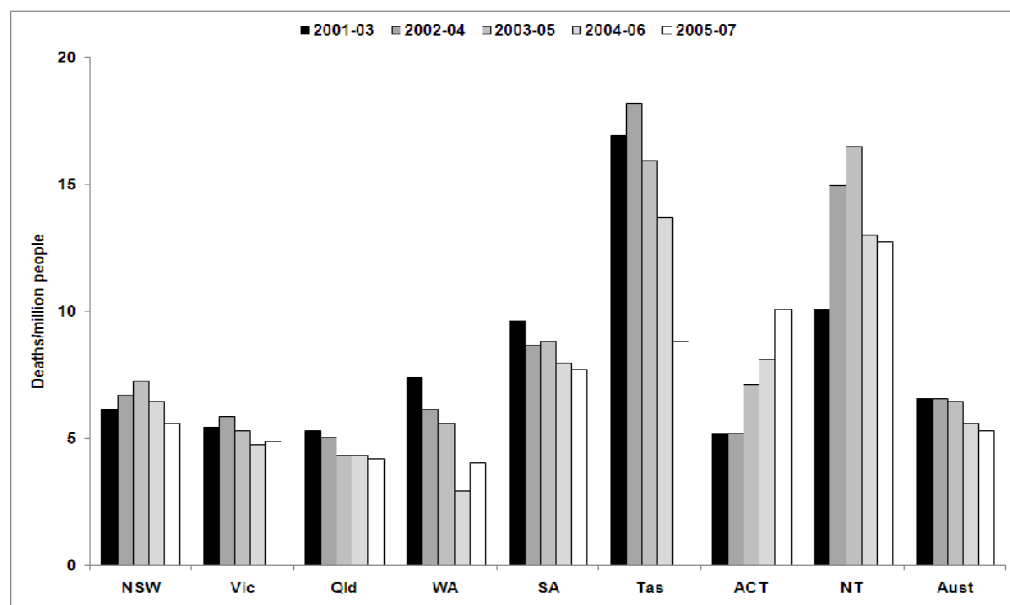


Figure 1.3 Annual fire death rate in Australia. Adapted from (SCRGSP 2010)

In terms of financial costs, the median dollar loss from structure fire (adjusted for inflation) is presented in Figure 1.4. Between 2006/2007, the median dollar loss has been as high as \$8,000 in South Australia (SA).

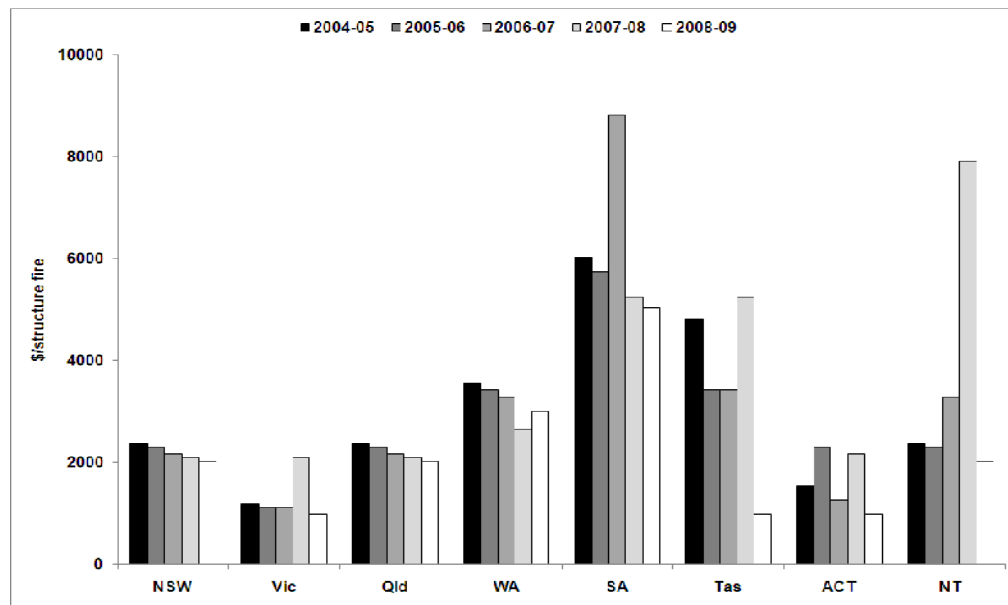


Figure 1.4 Median dollar loss per structure fire in Australia. Adapted from (SCRGSP 2010)

As described by Kong (2009), the types of structures ranged from houses to offices buildings, but the majority of the incidents reported were fires occurring in private residences. This has led to a growing realization of the importance of fire safety design of structures, including concrete structures.

1.2 Problem definition and objectives

Fire resistance is a concept applicable to elements of the building structure and not a material, but the properties of a material affect the performance of the element of which it forms a part (Khoury 2000).

Concrete, though not a refractory material, is incombustible and has good fire resistance properties (Lea 1970). Unlike wood and plastics, concrete does not emit fumes on exposure to elevated temperatures (Mehta and Monteiro 2006). However, one concern related to ordinary Portland cement (OPC) concrete when exposed to elevated temperatures, as in a fire event, is the deterioration of its mechanical

properties due to physical and chemical changes in the material during heating (Khoury 2000).

Above 400°C, one of the main hydrates of the OPC paste, calcium hydroxide (CaOH_2) dehydrates into calcium oxide (CaO) causing the OPC paste to shrink and crack (Lea and Stradling 1922; Dias et al. 1990). After cooling and in the presence of air moisture, CaO rehydrates into CaOH_2 , causing the OPC paste to expand and completely disintegrate (Petzold and Rohrs 1970).

However, the extent of deterioration caused by the CaOH_2 dehydration and CaO rehydration on the mechanical properties of OPC concrete exposed to temperatures above 400°C is still unclear.

Furthermore, it is unknown the effects of partial replacement of OPC with slag on the mechanical properties of paste and concrete exposed to elevated temperatures. Ground granulated blast furnace slag (GGBFS or 'slag') has been used as a partial replacement of OPC for decades (Daube and Bakker 1986). Slag is a by-product of iron and steel industries. It is obtained by rapidly quenching molten slag (granulation) with high pressure and high volume water sprays, resulting in a glassy material. Following grinding and blending with an alkali (such as OPC) the granulated, ground slag is cementitious.

Despite the continuous growing popularity of slag as partial replacement of OPC in concrete, limited research has been devoted into identifying the influence of this replacement on the microstructure and mechanical properties of paste and concrete exposed to elevated temperatures.

Therefore, this thesis aims to address the above issues, providing a better understanding of the effects of elevated temperatures on the:

- Microstructure of OPC paste and concrete;
- Mechanical properties of OPC paste and concrete;
- Microstructure of OPC/slag paste and concrete; and
- Mechanical properties of OPC/slag paste and concrete.

1.3 Thesis organization

This thesis is organized into ten chapters that are based on a series of seven scientific papers written during the course of the author's candidature. **Chapter 1** provides a review of the importance of the fire resistance of concrete and the objectives of the present thesis. **Chapter 2** presents a review of the published literature on the fire resistance of concrete. The review is divided in three parts: paste, concrete and paste/concrete partially replaced with slag. **Chapter 3** investigates the relationship between phase transformations (particularly CaOH_2 dehydration and CaO rehydration) and strength loss of OPC and OPC/slag pastes exposed to elevated temperatures. **Chapter 4** studies the long-term effects of exposure to elevated temperatures on the mechanical properties of OPC and OPC/slag pastes. **Chapter 5** investigates repair methods for preventing strength loss of OPC pastes after exposure to elevated temperatures. **Chapter 6** uses techniques such as nuclear magnetic resonance (NMR), X-ray diffraction (XRD), infrared spectroscopy (IR) and Synchrotron NEXAFS to characterize the paste hydrates (e.g. C-S-H, ettringite, monosulphate) of OPC and OPC/slag pastes. **Chapter 7** also uses NMR, XRD, IR, NEXAFS to study the effects of elevated temperatures on the paste hydrates of OPC and OPC/slag pastes. **Chapter 8** reports the effects of partial replacement with slag and cooling methods on the mechanical properties of concrete exposed to elevated temperatures. **Chapter 9** utilizes a number of different techniques such as sorptivity tests and nitrogen adsorption to investigate differences in the behaviour of cement paste and concrete after exposure to elevated temperatures. **Chapter 10** provides a summary of the key findings of the thesis as well as suggestions for future studies.

1.4 References

Beard A and Carvel R (2005) *The Handbook of Tunnel Fire Safety*. London, Thomas Telford Publishing.

BS 476 (1987) *Fire tests on building materials and structures*. The British Standards Institution.

Crozier D A and Sanjayan J G (1999) *Chemical and physical degradation of concrete at elevated temperatures*. Concrete in Australia March-May: 18-20.

Daube J and Bakker R (1986) *Portland Blast-Furnace Slag Cement: A Review*. Blended Cement, ASTM STP 897, Philadelphia. American Society for Testing Materials: 5-14

Dias W P S, Khoury G A and Sullivan P J E (1990) *Mechanical Properties of Hardened Cement Paste Exposed to Temperatures up to 700°C (1292°F)*. ACI Materials Journal 87(2): 160-166.

Eurocode 2 (2005) *Design of concrete structures - Part 1-2: General rules - Structural fire design (Including Irish National Annex)*. NSAI Standards.

Eurocode 4 (2005) *Design of composite steel and concrete structures - Part 1-2: General rules - Structural fire design (Including Irish National Annex)*. NSAI Standards.

ISO 834 (1975) *Fire resistance test - elements of building construction*. International Standard.

Khoury G A (2000) *Effect of fire on concrete and concrete structures*. Progress in Structural Engineering and Materials 2: 429-447.

Kirkland C J (2002) *The fire in the Channel Tunnel*. Tunnelling and Underground Space Technology 17: 129-132.

Kong D L (2009) *Fire Resistance of Geopolymer Concretes*. Civil Engineering Department, Monash University. PhD thesis.

Lea F C and Stradling R E (1922) *The resistance to fire of concrete and reinforced concrete*. Engineering 144: 341-344; 380-382.

Lea F M (1970) *The Chemistry of Cement and Concrete*. Edward Arnold (Publishers) Ltd.

Leitner A (2001) *The fire catastrophe in the Tauern Tunnel: experience and conclusions for the Austrian guidelines*. Tunnelling and Underground Space Technology 16(3): 217-223.

Mehta P K and Monteiro P J M (2006) *Concrete Microstructure, Properties, and Materials*. McGraw-Hill.

Petzold A and Rohrs M (1970) *Concrete for high temperatures*. London, Maclaren and Sons Ltd.

SCRGSP (2010) *Report on Government Services*. Review of Government Service Provision Part D - Chapter 9: 34-38.

SP-255 (2008) *Designing Concrete Structures for Fire Safety*. ACI-TMS Committee 216.

Ulm F J, Coussy O and Bazant Z P (1999) *The 'Chunnel' Fire. I: Chemoplastic Softening in Rapidly Heated Concrete*. Journal of Engineering Mechanics 125: 272-282.

Chapter 2

Literature Review

2.1 Fire resistance of concrete

Concrete is generally considered to be fire resistant when compared to building materials such as steel or timber. Concrete, though not a refractory material, is incombustible and has good fire resistance properties (Lea 1970). Unlike wood and plastics, concrete does not emit fumes or produce drip molten particles when burning and therefore, will not add to the fire load.

For these reasons concrete is said to have a high degree of fire resistance in the majority of applications, and can be described as virtually incombustible. When chemically combined, the main constituent materials of concrete (i.e. cement and aggregates) form a material that is essentially inert (Kong 2009).

However, when concrete is exposed to elevated temperatures, as in a fire event, two issues are of concern (Khoury 2000):

- Explosive spalling, which results in loss of material, reduction in section size and exposure of the reinforcing steel;
- Deterioration of mechanical properties caused by physical and chemical transformations.

Explosive spalling is the breaking off of layers or pieces of concrete from the surface of a structural element when it is exposed to both elevated and rapidly rising temperatures, as experienced in fires with heating rates typically 20-30°C/min (Khoury 2000). Sometimes the spalling can be explosive. The topic of spalling has been the subject of intensive research during the last two decades since the introduction of high strength concretes which was identified to have increased risk of spalling (Sanjayan and Stocks 1993). Hence, the spalling is not part of the scope of this thesis.

The present thesis focuses on the deterioration of mechanical properties of concrete caused by physical and chemical transformations experienced during

heating. Although this topic was first studied 90 years ago by Lea and Stradling (1922) who were pioneers on the investigation of those transformations occurring in concrete during heating, this topic has not been a major focus for concrete researchers during the subsequent years.

Analysing the behaviour of OPC mortars (cement paste and fine aggregate) exposed to elevated temperatures Lea and Stradling (1922) reported:

- A differential movement between the fine aggregate (sand) and cement due to the differential coefficients of thermal expansion;
- A breakdown of the cement paste, regardless of whether the aggregate was present or not.

Based on those findings and subsequent studies, the methodology of investigating the physical and chemical transformations experienced by concrete exposed to elevated temperatures is divided into two steps:

- i. The study of the cement paste; and
- ii. The study of the concrete as a whole, in which the cement paste, the aggregates and the interface between those are analysed.

This chapter is divided in three main sections. The first section provides a review of the literature concerning the cement paste microstructure at room temperature. In addition, it discusses the published literature on the effects of elevated temperatures on the microstructure and mechanical properties of the cement paste.

The second section focuses on the concrete as a whole, i.e., cement paste, aggregates and the interface between them. It reviews the published literature regarding the effects of elevated temperature on the microstructure and mechanical properties of concrete. Furthermore, this section presents a review concerning the aggregate behaviour when exposed to elevated temperatures.

The third section presents a review of the limited published data regarding the effects of partial replacement of OPC with slag on the microstructure and mechanical properties of paste and concrete exposed to elevated temperatures. Figure 2.1 illustrates how the literature review is structured to enable the

determination of the effects of elevated temperatures on the mechanical properties of concrete.

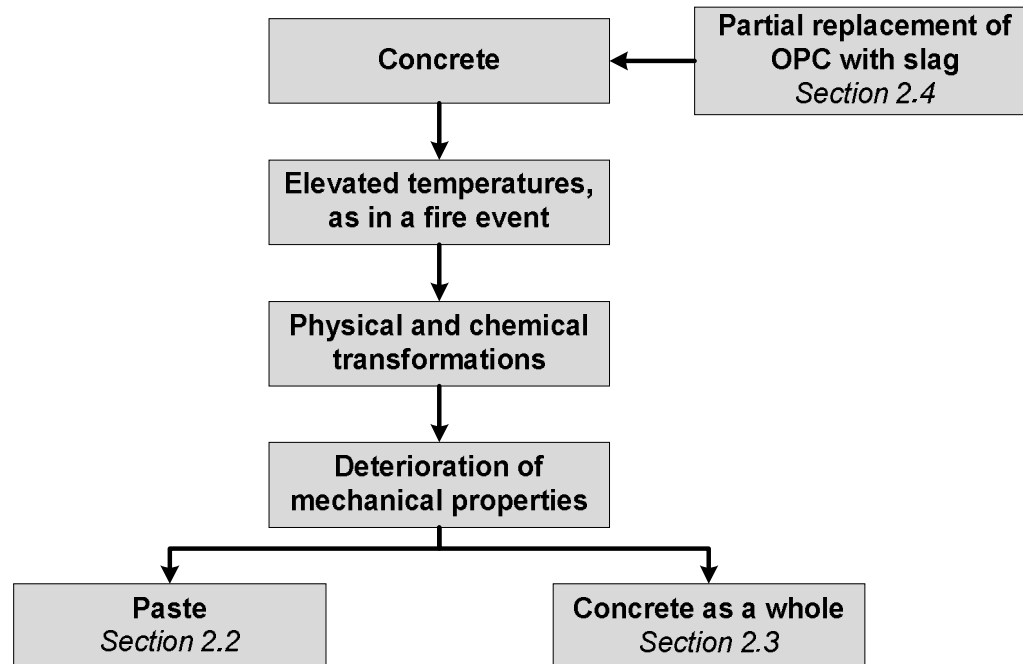


Figure 2.1 Analysis structure of concrete exposed to elevated temperatures

2.2 Paste

2.2.1 Microstructure at room temperature

The microstructure of the cement paste depends on the type, amount, size, shape, and distribution of the phases present in the paste.

Generally, as described by Mehta and Monteiro (2006), anhydrous ordinary Portland cement (OPC) has a chemical composition of C_3S , C_2S , C_3A and C_4AF . This is based on the common abbreviation system used by cement chemists (Taylor 1997; Mehta and Monteiro 2006):

- $C = CaO$; $S = SiO_2$; $A = Al_2O_3$; $F = Fe_2O_3$; $S = SO_3$; $H = H_2O$

The hydration process of the anhydrous OPC starts with dispersion in water. The OPC paste hydration is characterized by several stages, described by Odler (1998) as: pre-induction period (first minutes); induction period (first few hours); acceleration stage (3-12 hours after mixing) and the post- acceleration period (after days).

During the pre-induction period, as a result of the interaction between calcium, sulphate, aluminate, and hydroxyl ions, the needle-shaped crystals of ettringite (AFt) are formed. The paste hydrate ettringite has the general constitutional formula $[\text{Ca}_3(\text{Al,Fe})(\text{OH})_6.12\text{H}_2\text{O}]_2.X_3.x\text{H}_2\text{O}$, where 'x' is, normally at least, ≤ 2 . The 'X' represents one formula unit of a doubly charged, or with reservations, two formula units of a singly charged anion (Taylor 1997).

In the induction period (first few hours), large prismatic crystals of calcium hydroxide ($\text{Ca}(\text{OH})_2$) are formed. In addition, very small fibrous crystals of calcium silicate hydrates (C-S-H) begin to fill the empty space formerly occupied by water and the dissolving cement particles (Mehta and Monteiro 2006).

Following, the acceleration stage is controlled by the nucleation and growth of the resultant hydration products. The rate of tricalcium silicate (C_3S) hydration accelerates and the second stage of formation of C-S-H takes place. A noticeable hydration of dicalcium silicate (C_2S) also occurs (Odler 1998).

In the post-acceleration period, the hydration rate slows gradually, as the amount of still non-reacted material declines and the rate of the hydration process becomes diffusion-controlled. The C-S-H phase continues to be formed due to the continuous hydration of both C_3S and C_2S (Odler 1998). Depending on the alumina to sulphate ratio of the OPC, ettringite may become unstable and decompose to form monosulphate hydrate (AFm), which has a hexagonal-plate morphology (Mehta and Monteiro 2006). Monosulphate hydrate phase has the general formula $[\text{Ca}_2(\text{Al,Fe})(\text{OH})_6].X.x\text{H}_2\text{O}$, where 'X' denotes one formula unit of singly charged anion, or half a formula unit of a doubly charged anion (Taylor 1997).

Once the OPC paste hydration is complete, the main solid phases formed are: calcium silicate hydrate; calcium hydroxide; calcium sulfoaluminates hydrates; and unhydrated clinker grains.

2.2.1.1 Calcium silicate hydrate (C-S-H)

The calcium silicate hydrate phase, known as C-S-H gel, makes up to 50 to 60% of the volume of solids in a completely hydrated OPC paste. Therefore, the C-S-H gel is the most important phase determining the properties of the paste (Mehta and Monteiro 2006), being primarily responsible for the mechanical properties of the hydrated cement paste (Escalante-Garcia and Sharp 2004).

2.2.1.2 Calcium hydroxide (CaOH_2)

The calcium hydroxide, also known as portlandite, constitutes 20 to 25% of the volume of solids in the hydrated paste. Calcium hydroxide crystals consist of large crystals with distinctive hexagonal-prism morphology. Compared to C-S-H, the strength-contributing potential of CaOH_2 is limited as a result of considerably lower surface area (Mehta and Monteiro 2006).

2.2.1.3 Sulphoaluminates hydrates

The calcium sulfoaluminates hydrates relate to the ettringite and monosulphate hydrate phases presented in the hydrated paste. They occupy 15 to 20% of the solid volume in the hydrated paste. Therefore, they have a smaller role in the microstructure-mechanical properties relationship when compared to the C-S-H gel (Mehta and Monteiro 2006).

2.2.1.4 Unhydrated clinker grains

Finally, some unhydrated clinker grains may be found in the microstructure of hydrated pastes, depending on the particle size distribution of the anhydrous cement and the degree of hydration of the paste (Mehta and Monteiro 2006).

2.2.2 Microstructure after exposure to elevated temperatures

The relationship between the coefficient of expansion of OPC paste and the effect of dissociation of water from the hydrated paste has been reported by Lea and Stradling (1922). Their work found that OPC paste expands at temperatures up to 100°C then continually contracts up to 491°C. Above 491°C expansion commences again, taking place at a rate less than that occurring during the expansion previous to 100°C.

In addition, their work reported a range between 300°C and 500°C where water was expelled at a fairly constant rate. The total amount of expelled water was approximately 30% of the total combined water (i.e., chemically combined and physically adsorbed water driven off at temperatures above 98°C (capillary water)). They proposed that this greater loss of water was due to the breaking up of the calcium hydroxide (CaOH_2), one of the main hydrates of OPC paste. Lea and Stradling (1922) stated that CaOH_2 decomposes at about 400°C into calcium oxide (CaO) and water, as expressed in Equation 2.1:



Therefore, it was concluded that the hydrated portions of the OPC paste lose water and contract between 100°C and 491°C as a consequence of loss of water during dehydration of CaOH_2 .

Similarly, Dias et al. (1990) analysed the mechanical properties of OPC pastes exposed to temperatures of up to 700°C. Although no initial signs of distress were visible on the specimens when removed from the furnace, all specimens (heated to 400°C or above) exhibited severe cracking to the point of disintegration after a few days.

According to Petzold and Rohrs (1970), the reason for this cracking is the expansive and hence disruptive rehydration (due to reaction with airborne water vapour) of the CaO into CaOH_2 which is accompanied by a 44% volume increase. Based on that, Dias et al. (1990) concluded that 400°C is a critical temperature for OPC concrete, above which it cannot be sustained for any significant period without disintegration on subsequent post-cooled exposure to atmospheric moisture.

Furthermore, Dias et al. (1990) performed tests on mixes where OPC paste was partially replaced (i.e., 10, 25, and 40% by weight) with pulverized fly ash (PFA). According to them, the PFA would reduce the amount of CaOH_2 in the paste, due to pozzolanic reactions between the PFA and CaOH_2 . It was reported that even 10% PFA replacement completely eliminated all visible surface cracking due to post-cooled exposure to air following 600°C (Figure 2.2).

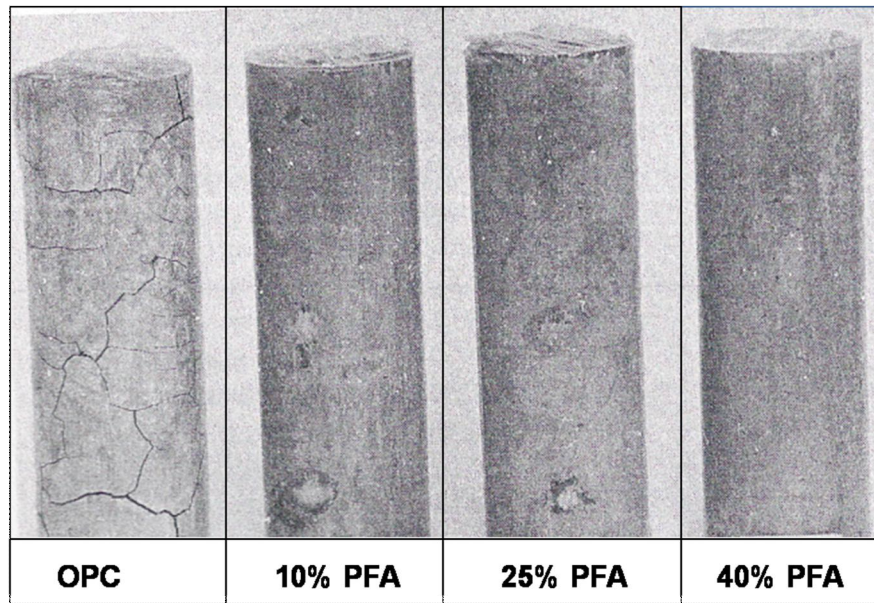


Figure 2.2 OPC paste and blends with PFA after exposure to 600°C. Adapted from (Dias et al. 1990)

The dehydration of CaOH_2 , responsible for the loss of strength in OPC paste exposed to temperatures above 400°C, was confirmed by different methods. The most used methods used in the investigation of paste exposed to elevated temperatures are:

2.2.2.1 Thermogravimetric analysis (TGA)

According to Harmathy (1968), dehydration of CaOH_2 is easily recognizable from a rapid weight loss indicated by thermogravimetric analysis. Thermogravimetric analysis (TGA) records changes in the weight of a material as a result of an increase in temperature. Alarcon-Ruiz et al. (2005) reported the use of thermal analysis in assessing the effect of temperature on a cement paste. They reported that the first weight loss observed between 100°C and 200°C was a result of dehydration reactions of several hydrates (carboaluminates, ettringite and in particular C-S-H). The second major weight loss, observed between 450°C and 500°C, was attributed to the dehydration of CaOH_2 . The third weight loss observed at 750°C was assigned to the decarbonation of calcium carbonate (CaCO_3). In addition, TGA analysis performed by Matesová et al. (2006) confirmed the temperature range around 500°C for the dehydration of CaOH_2 .

2.2.2.2 Neutron diffraction

Neutron diffraction was used by Castellote et al. (2004) in the studies of the composition and microstructural changes of cement pastes upon heating. In neutron diffraction, the neutrons can penetrate deep into materials in a non-destructive way providing information about the bulk of the samples. Neutrons are scattered by all elements, also the light ones like hydrogen isotopes; thus, information on moisture or hydrated elements can also be obtained (Castellote et al. 2004). Therefore, it is a useful tool to understand how the materials change and degrade. For the CaOH_2 , an abrupt decomposition was reported between 530°C and 560°C, leading to the transformation of CaOH_2 into CaO (lime).

2.2.2.3 Differential scanning calorimetry (DSC)

Differential scanning calorimetry (DSC) provides information regarding endothermic and exothermic reactions with changes in temperature. DSC was used to investigate the reactions occurring in OPC pastes with the increase in temperature (Sha et al. 1999). Sha et al. (1999) observed three major peaks in the DSC spectrum of OPC pastes, and their assignments are in accordance with the peaks obtained by other techniques as described above. The first peak, at approximately 100°C, was an endothermic reaction concluded to be a result of dehydration of C-S-H. The second major peak, between 400°C and 500°C, was related to the dehydration of CaOH_2 . The third peak, at approximately 750°C, was assigned to the decarbonation of CaCO_3 .

2.2.2.4 Scanning electron microscopy (SEM)

Scanning electron microscopy (SEM) has proved to be a valuable tool in the study of the microstructure of fire-damaged concrete (Lin et al. 1996). Their work reported changes in the cement paste after exposure to temperatures up to 900°C.

According to them, at room temperature, the C-S-H gel can be divided into 4 types: Type I covers fibrous particles, a few micrometer long, in the form of spine, prism, rod shape, or rolled sheet; Type II is a reticular or honeycomb-shaped structure formed in conjunction with Type I; Type III covers the nondescript or flattened particles under 0.1 μm ; Type IV is compact and has a dimpled appearance, which is generally formed in a later hydration period.

Furthermore, CaOH_2 is reported to appear as thin hexagonal plates. Ettringite forms into long rods or needles with parallel sides that have no branches. Monosulphate hydrate forms a thin hexagonal plate structure.

After exposure to 250°C , substantial changes from euhedral (well formed) platy crystals to subhedral were identified by Lin et al. (1996). In addition, anhedral grains (crystals showing no external crystal face) were also identified. According to Lin et al. (1996) these substantial changes are primarily due to the dehydration reactions occurring.

With the temperature increase to 400°C , loss of crystallinity from euhedral to anhedral resulted in cracks. Lin et al. (1996) reported that an endothermic reaction occurs exclusively between 440°C and 580°C due to the dehydration of CaOH_2 . After exposure to 500°C , platy calcium silicate hydrate was reported to be arranged in layers with interlayer acicular ettringite. In addition, Lin et al. (1996) affirmed that decarbonation of CaCO_3 occurs between 580°C and 900°C together with possible solid-solid phase transformation.

Lin et al. (1996) also reported the morphology of a sample after exposure to 900°C , followed by water-curing. According to them, CaOH_2 was formed as a result of rehydration of CaO , while long irregular fibrous hydrates of C-S-H gels were mingled with ettringite in voids of CaOH_2 crystals.

SEM studies on the physical and chemical changes of cement paste after exposure to elevated temperatures were also performed by Liu et al. (2006). SEM was used to observe the phase changes found with differential thermal analysis (DTA) and TGA. SEM images showed the presence of microcracks after 500°C , the temperature at which CaOH_2 dehydrates.

2.2.2.5 X-Ray diffraction (XRD)

Alonso and Fernandez (2004) used X-ray diffraction (XRD) to study the dehydration and rehydration processes of cement paste exposed to elevated temperatures. XRD is a valuable tool in the identification of polycrystalline phases of cement paste through the recognition of the X-ray patterns for each of the crystalline phases (Roncero et al. 2002). Therefore, it is useful to detect crystalline hydrates such as ettringite, monosulphate hydrate, CaOH_2 and others.

The XRD results obtained by Alonso and Fernandez (2004) showed that ettringite was not detected in temperatures above 100°C. Calcite (CaCO_3) peak increased in intensity up to 450°C and practically disappeared at 750°C. A progressive reduction of the peak related to CaOH_2 is observed when the temperature is increased above 450°C and complete disappearance occurred at 750°C. Further, CaO is also well identified after exposure to 750°C, which according to Alonso and Fernandez (2004), is a result of the CaOH_2 and CaCO_3 transformation. In addition, their work reported TGA tests results in accordance with the previous works described in Section 2.2.2.1.

2.2.2.6 ^{29}Si Magic Angle Spinning Nuclear Magnetic Resonance (^{29}Si MAS NMR)

Studies by Alonso and Fernandez (2004) recognized the importance of analysing one of the main hydration products, the C-S-H gel. According to them, the heating process induces a continuous dehydration of C-S-H gel with the increase in temperature.

Interpretation of ^{29}Si MAS NMR offers an efficient method to follow the hydration of C_3S in a qualitative and semi quantitative way because Si chemical shifts reflect the degree of condensation of SiO_2 tetrahedra (Hjorth et al. 1988). Therefore, it provides valuable information related to the formation of calcium silicate hydrate C-S-H gel. As demonstrated by Alonso and Fernandez (2004), ^{29}Si MAS NMR spectra results showed that the maximum transformation of the C-S-H gel is at 450°C. After exposure to 750°C, the C-S-H gel had completely disappeared and was mainly replaced by a new nesosilicate phase. According to them, this new nesosilicate formed is different in morphology than the initial anhydrous residue with less crystalline structure.

Furthermore, Alonso and Fernandez (2004) concluded that the heated cement paste is not stable within a wet atmosphere and rehydration takes place. According to their work, the new nesosilicate is transformed into C-S-H gel. In addition, CaOH_2 and ettringite are reformed. However, after 3 ½ months in a saturated chamber (100% RH) a progressive damage was reported with coarser cracking due to rehydration.

2.2.3 Summary

This section reported that CaOH_2 dehydration and CaO rehydration causes total strength loss and complete disintegration of OPC pastes exposed to temperatures above 400°C . A number of techniques were described in order to determine CaOH_2 dehydration and CaO rehydration. Figure 2.3 presents a summary of the main findings reported in this section.

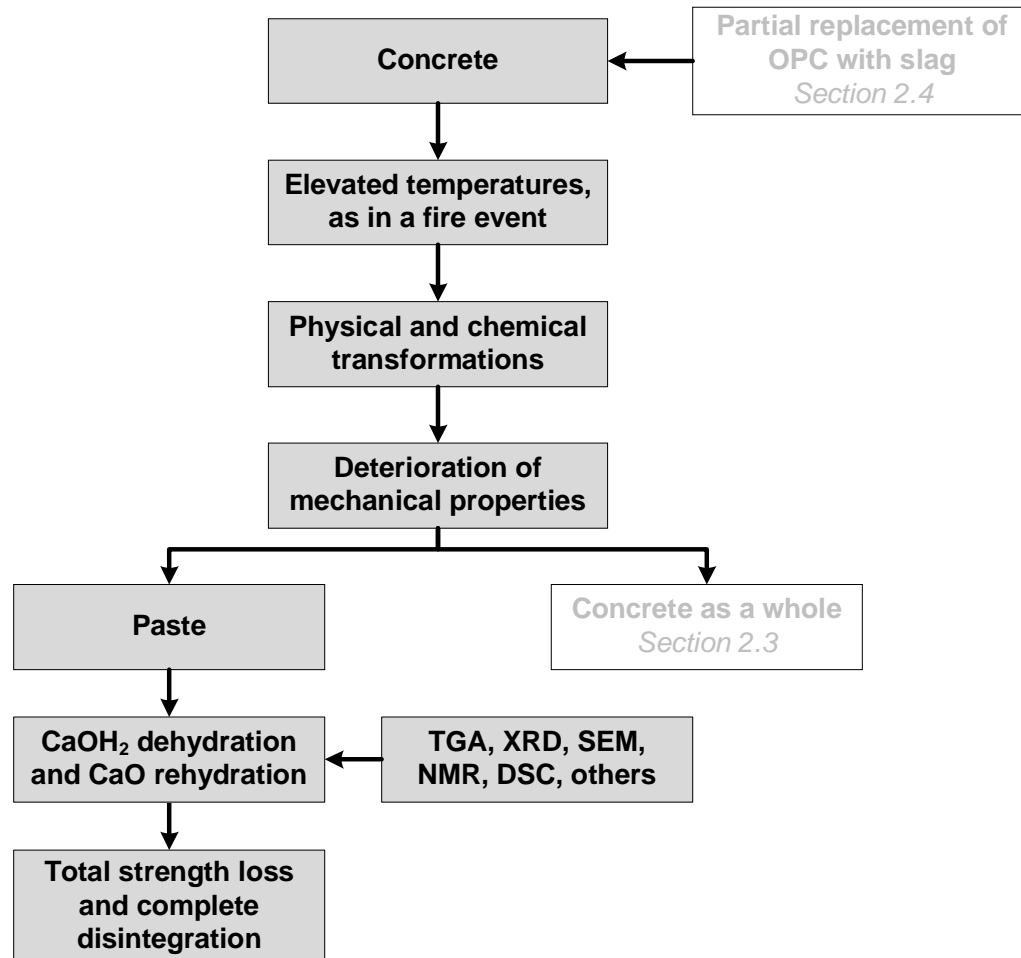


Figure 2.3 Summary of main findings reported for pastes exposed to elevated temperatures

2.3 Concrete

The deterioration of the mechanical properties of concrete exposed to elevated temperatures can be reduced by judicious design of the concrete mix (Khoury 2000). Therefore, consideration must be taken into the behaviour of the cement paste, aggregate, and the interface between them.

The present section reviews the effects of elevated temperatures on both the aggregates and the concrete as a whole, i.e., paste, aggregate and the interface between them.

Published data on the mechanical properties of concrete exposed to elevated temperatures taken from different sources differ substantially, and in several cases are contradictory (Khoury 1992). Therefore, interpreting the mechanical behaviour of concrete after exposure to elevated temperatures by an overall result can be misleading, unless materials and environmental factors are specified.

Four factors have been reported as the main factors determining the extent of deterioration experienced by concrete after exposure to elevated temperatures. These factors are:

- The microstructure of concrete;
- The pore structure of concrete;
- Post-cooling regimes after exposure to elevated temperatures; and
- Type of aggregate.

2.3.1 The microstructure of concrete

As discussed in Section 2.2 the microstructure of the OPC paste is the most important factor determining the extent of deterioration experience by the cement paste after exposure to elevated temperatures. In particular, one of the paste hydrates, CaOH_2 dehydrates into CaO above 400°C . When exposed to air moisture, the CaO rehydrates causing the OPC paste to expand and crack, leading to total strength loss and complete disintegration (Lea and Stradling 1922; Petzold and Rohrs 1970; Dias et al. 1990).

After analysing the effect of elevated temperatures on the mechanical properties of OPC paste, Lea and Stradling (1922) investigated the effects of elevated temperatures on concrete. Their work investigated OPC concrete (6 months old) exposed to 700°C. The specimens consisted of cube specimens (100 x 100 mm), composed of 1 part of cement, 2 parts of sand (Leighton Buzzard) and 4 parts of coarse aggregate (Rowley Rag – volcanic dolerite stone). The unheated strength was approximately 21 MPa. Following specimens dropped in water immediately after heating broke into pieces. For the specimens not dropped in water, the strength after cooling was approximately 6.2 MPa. Two days later the strength reduced to 5.3 MPa. Six days after heating, some specimens had crumbled to pieces whilst two had an average strength of 3.7 MPa.

According to Lea and Stradling (1922), none of these specimens had any cracks on the surface immediately after cooling down, however the cracks were clearly visible after a few days, as showed in Figure 2.4.

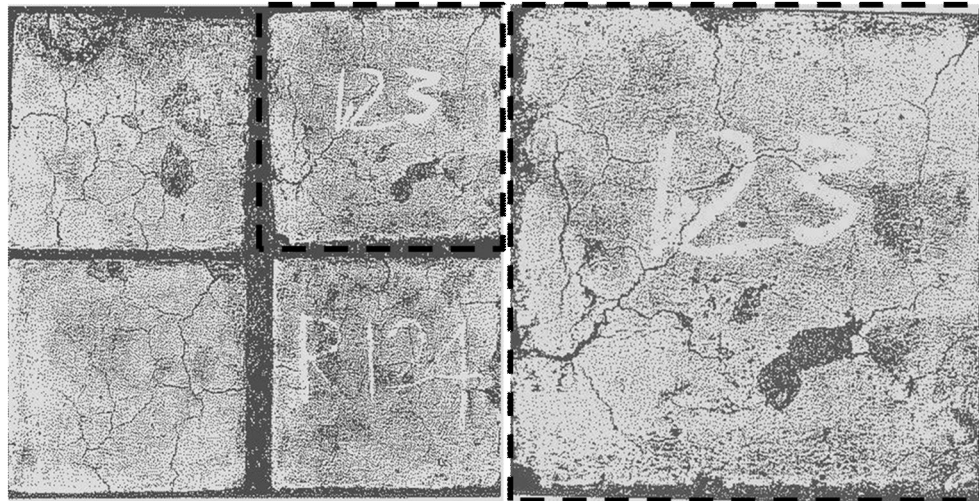


Figure 2.4 OPC concrete six days after exposure to 700°C. Dashed line refers to enlarged image. Adapted from Lea and Stradling (1922)

As per the OPC paste (Section 2.2), Lea and Stradling (1922) explained that the complete disintegration of some of the specimens, six days after heating, was due to dehydration of CaOH_2 into CaO . According to them, this is accompanied by a contraction of the concrete. Following cooling, the porosity of concrete allows airborne moisture to penetrate. The moisture hydrates the CaO into CaOH_2 , and as the latter occupies a considerably greater volume, causes the concrete to crack,

split and ultimately crumble (Lea and Stradling 1922). This is in accordance with the review of literature of OPC pastes exposed to elevated temperatures (Section 2.2.2).

A few decades later, Malhotra (1956) investigated the behaviour of concrete exposed to temperatures up to 600°C. His work concluded that the main factors affecting the crushing strength of concrete were: strength loss of the mortar; formation of cracks; and dehydration of CaOH_2 .

Khoury (1992) stated that, following Lea and Stradling (1922), it was recognized that the CaOH_2 dehydration could be the “Achilles’ heel” of concrete in elevated temperature applications. However, after reassessing literature of concrete strength at elevated temperatures, Khoury affirmed that there was scope for improvement within the temperature range of 300 to 600°C by considering material and environmental factors/mechanisms influencing the strength of concrete during the heat cycle and after cooling. Therefore, a significantly larger proportion of a structure exposed to elevated temperatures could remain serviceable and repairable, thus bringing about significant economic benefits (Khoury 1992).

In contrast to Lea and Stradling (1922), Sarshar and Khoury (1993) demonstrated that OPC concrete specimens exposed to 600°C presented no disintegration, while the residual strength was in the range of 40%. The aggregates (Lytag & firebrick) used in the concrete specimens were said to be thermally stable (Sarshar and Khoury 1993). Their work concluded that the absence of disintegration was due to the lower cement content in concrete (then cement paste and mortar), which according to them, would minimize the effects of CaOH_2 dehydration and CaO rehydration on the concrete. Sarshar and Khoury (1993) affirmed that when thermally stable aggregates are employed, the primary factor influencing the trend of strength against temperatures is the type of cement blend.

Chan et al. (1996) investigated the effects of elevated temperatures on the performance of high performance concrete (HPC) and normal strength concrete (NSC). The specimens were tested at an age of 90 days, and were heated up to 400°C, 600°C, 800°C, 1000°C and 1200°C, in which the maximum temperature was maintained for 1 hour. Following, specimens were allowed to cool down in air until room temperature was reached.

From the point of view of strength loss, there were three ranges of temperature behaviour: 20°C to 400°C, 400°C to 800°C and 800°C to 1200°C. Up to 400°C, only a small part of the original strength was lost, between 1 and 10% for HPC and about 15% for NSC. A severe compressive strength loss (85% for NSC) was observed within the 400°C to 800°C range. According to them, this was due to the fact that the cement paste, which is the main source of the strength in concrete, has experienced dehydration of C-S-H gel and loss of its cementing ability under those conditions. In addition, they reported that above 800°C, only a small part of the original compressive strength was left, about 9% to 20%. However, no disintegration of the concrete specimens was observed by Chan et al. (1996).

Crozier and Sanjayan (1999) discussed the physical and chemical transformations experience by concrete during exposure to elevated temperatures. Table 2.1 presents a summary of these transformations.

Table 2.1 Physical and chemical transformations of concrete at elevated temperatures (Crozier and Sanjayan 1999)

| Temperature (°C) | Physical and chemical transformations in concrete |
|------------------|--|
| 105 | Desorption of evaporable water from the pores |
| 120-140 | Dehydration of calcium aluminosulphate hydrates Consequently destruction of ettringite Impact on concrete structure |
| 200-300 | Dehydration and compaction of C-S-H phases |
| 400 | Substantial cracking and development of irregular shaped pores C-S-H crystallize on the cracks and pore surfaces Large CaOH ₂ crystalline compounds facilitate the development of internal stresses Weaking of the concrete structure The interface between paste and aggregates is weakened Strength reduction by 30% to 50% compared to 200°C to 300°C |
| 500 | Colour change to pink Strength loss of 70% Weak interface bond between paste and aggregates |
| 600 | Intensification of microcracks Dehydration of CaOH ₂ Starting point for disintegration of concrete structure Elimination of possibility of reuse after fire |

Handoo et al. (2002) investigated the physical and chemical transformations of OPC concrete exposed to temperatures up to 900°C. They investigated the mortar part of the concrete using XRD. The results showed a gradient between the amount of CaOH_2 at the outer surface and at the centre of the specimen. A gradual reduction in the CaOH_2 content was reported with an increase in temperature, which indicated gradual deterioration in concrete quality. They reported fast reduction in compressive strength of concrete exposed to beyond 500°C. Their work concluded that decomposition of CaOH_2 beyond 700°C at the surface and beyond 900°C at the centre resulted in total deterioration of concrete. In addition, Handoo et al. (2002) investigated the concrete morphology after exposure to elevated temperatures using SEM. The main transformations reported with the temperature rise are summarized in Table 2.2.

Table 2.2 Concrete morphology at different temperatures determined by SEM (Handoo et al. 2002).

| Temperature (°C) | Concrete morphology |
|------------------|--|
| 300 | Deformed CaOH_2 crystals |
| | Voids |
| | Transformation of CaOH_2 into CaCO_3 |
| 500 | Predominance of microcracks |
| | intermingled with voids |
| | Increased porosity |
| | Deformed CaOH_2 crystals and C-S-H gel |
| 600 - 800 | Significant changes in the morphology of concrete |
| | Predominance of microcracks |
| | intermingled with voids |
| | Voids increasing porosity |
| | Deformed CaOH_2 |
| | Disruptive C-S-H phase boundaries |

Arioz (2007) analysed the effect of elevated temperatures on the compressive strength of concrete containing either crushed limestone or river gravel. Prior to compressive strength testing, visual observations and weight loss measurements were made. During visual observations, no visible effects were found on the surface of the specimens heated up to 400°C. However, the concrete started to crack when the temperature increased to 600°C but the effect was not significant at that level. The cracks became very pronounced at 800°C and extensively increased at 1000°C, as presented in Figure 2.5. After exposure to 800°C, the residual strength

varied from 20% to 40% depending on the aggregate used. Above 1000°C, the residual strength was in the range of 15%.

As expected, the weight loss increased with the temperature rise. The reduction in weight gradually increased up to 800°C, however, there was a sharp jump in weight loss beyond that temperature. They stated that strength losses in concrete after exposure to elevated temperatures are related to the weight losses experienced with the temperature rise. Using DTA, they reported mass changes of -6.5%, -4.0%, -5.8% and -3.6% at the temperatures of 200°C, 390°C, 520°C and 700°C respectively. In addition, they reported that total strength loss and disintegration of concrete specimens only occurred in specimens exposed to temperatures above 1200°C (Arioz 2007).

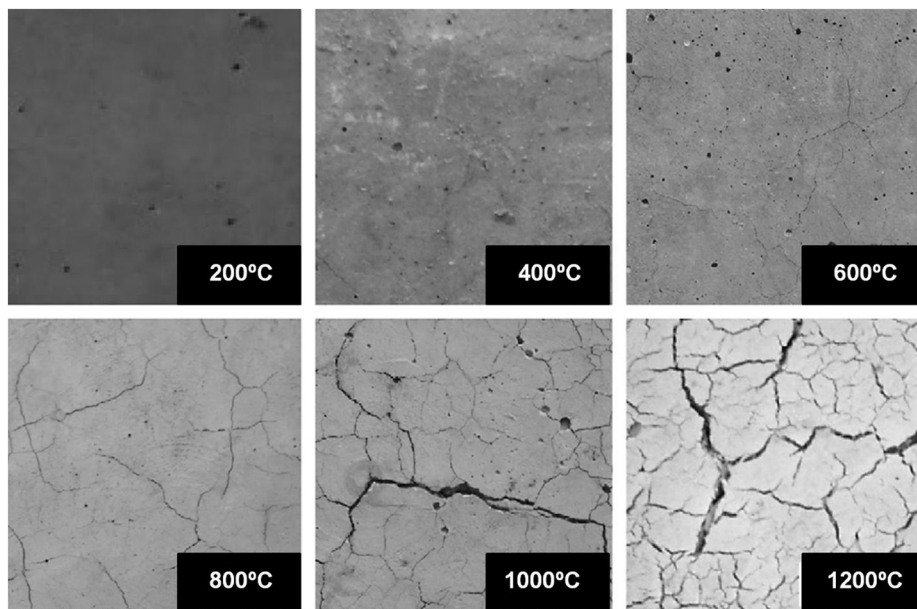


Figure 2.5 Visual observations of OPC concrete exposed to elevated temperatures. Adapted from (Arioz 2007)

2.3.2 Pore structure of concrete

The pore structure of the cement paste in concrete is, besides its chemical and mineralogical composition, of basic importance. This is due to the impact that pore structure has on a number of properties of mortar and concrete such as: physical and chemical resistance; temperature resistance, strength, thermal conductivity and others (Rostásy et al. 1980).

The cement paste in concrete has by volume a relatively large porosity, which can be defined in terms of void volume, capillary pores and gel pores. According to Bordallo and Aldridge (2010) the voids are formed on mixing, when air is entrapped into the mixture, and the resulting voids can vary in size from approximately 1 to 500 μm . Capillary pores have an average radius greater than 50 \AA and are originally water filled. When interconnected these pores dominate the water transport. Gel pores have a radius less than 50 \AA (Bordallo and Aldridge 2010). The water present in gel pores is more strongly bound water and can be removed only by drying (Korpa and Trettin 2006).

Exposure to elevated temperatures leads to a complete desiccation of the pore system. Rostásy et al. (1980) investigated the pore structure of OPC mortars exposed to elevated temperatures (up to 900°C).

According to them, the total pore volume increased with the increase of temperature, however not linearly. Heating to 600°C led to significant increase of the total pore volume. This increase is greater than one would expect from additional weight loss beyond 300°C. They suggested this was due to either an expansion of pores (by breakdown of partition walls) or microcracks have formed. Furthermore, the temperature increase to 900°C led to additional increase of pore volume (Rostásy et al. 1980).

As discussed in Section 2.3.1, Chan et al. (1996) investigated the effects of elevated temperatures on the performance of high performance concrete (HPC) and normal strength concrete (NSC). They reported that under elevated temperatures, both NSC and HPC experienced a change in pore size distribution, called the coarsening effect. According to them, this effect is one of the reasons for the strength loss at temperatures below 600°C. In addition, they stated that this effect also reduced the permeability and hence the durability of concrete exposed to elevated temperatures.

Chan et al. (2000) investigated the compressive strength and pore structure of concrete after exposure to temperatures up to 800°C. The partial replacement of OPC with silica fume and fly ash resulted in no disintegration for either normal strength concrete (NSC) or high performance concrete (HPC) exposed to 800°C, as seen in Figure 2.6, left. After exposure to 800°C, NC presented compressive

strength of 15.8 MPa while the different HPC blends presented 24.9, 38.7, 23.8 MPa. According to Chan et al. (2000), the loss of strength was related to the increase in porosity, Figure 2.6 right.

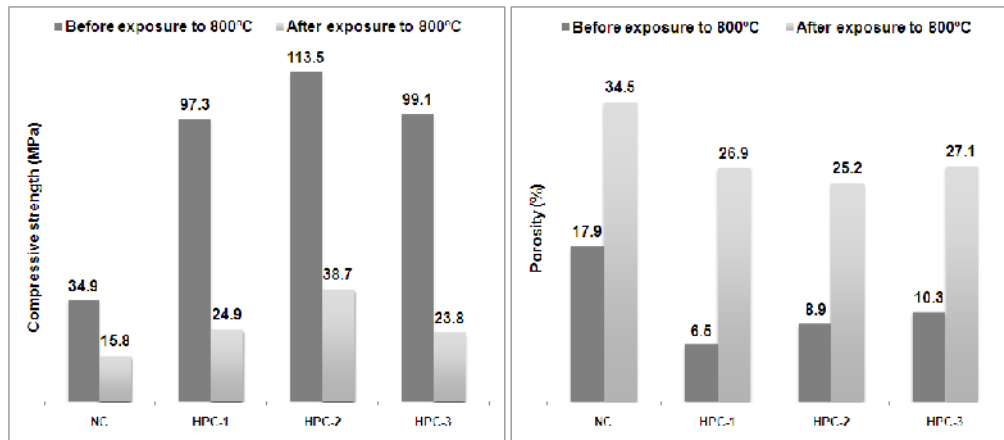


Figure 2.6 Compressive strength and porosity values for NSC and HPC after exposure to 800°C. Adapted from (Chan et al. 2000)

Based on experimental results, they provided a relationship between strength and corresponding porosity. This is illustrated in Figure 2.7. They concluded that porosity, pore size distribution, microcracks and others are important factors which determine the mechanical properties of concrete. Therefore, variation of pore structure, including porosity and pore size distribution, could be used to indicate degradation of mechanical properties of concrete exposed to elevated temperatures (Chan et al. 2000).

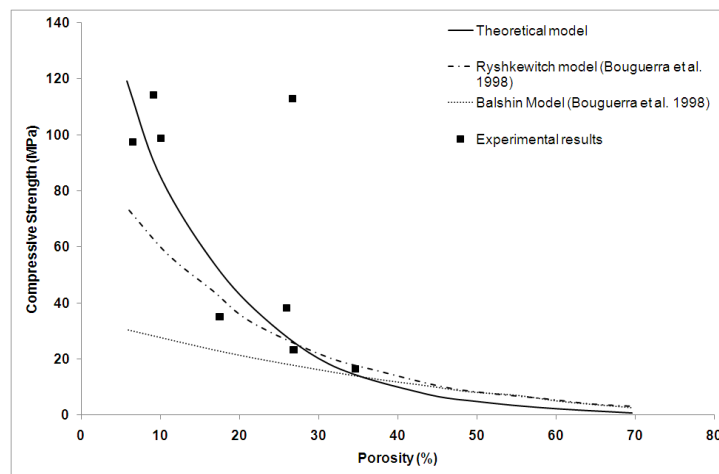


Figure 2.7 Relationship between compressive strength and porosity. Adapted from (Bouguerra et al. 1998; Chan et al. 2000)

Similar results were reported by Luo et al. (2000) while also analysing the effects of elevated temperatures on NSC and HPC concrete made with OPC, silica fume and fly ash. Their work reported that after exposure to 800°C and 1000°C, HPC had greater strength deterioration than NSC. HPC presented compressive strength of approximately 8 MPa (initial 97.3 MPa) while NSC presented 3 MPa (initial 35 MPa). In addition, HPC presented a greater increase in porosity after exposure to elevated temperatures when compared to NSC. Based on that, Luo et al. (2000) concluded that the greater porosity was the responsible factor for the greater strength deterioration of HPC concrete.

As discussed in Section 2.3.1, Handoo et al. (2002) investigated the effects of elevated temperatures on the concrete morphology. In addition, Handoo et al. (2002) concluded that the observed loss of strength at increasing temperatures may be related to the loss of bound water, increased porosity, and consequently increased permeability, which makes the concrete progressively more susceptible to further destruction.

2.3.3 Post-cooling regimes after elevated temperatures

Thermal stresses due to temperature gradient are more likely to cause cracking during cooling than during first heating, owing to the absence of transitional thermal creep during cooling (Khoury 1992). Since the transitional thermal creep does not take place during cooling, the internal stresses will not be subjected to appreciable relief (Khoury et al. 1986; Khoury 1992). Finally, the absorption of moisture can cause chemical changes and rehydration, which can be either beneficial or detrimental to concrete (Harada et al. 1972; Khoury et al. 1986; Sarshar and Khoury 1993).

Sarshar and Khoury (1993) investigated the effects of cooling methods on OPC concrete exposed to temperatures up to 600°C. Their work reported similar residual strength after slow cooling at 0.5°C/min and natural cooling (< 2°C/min). In addition, fast cooling (< 50°C/min) produced similar results to natural cooling and in certain cases it resulted in higher residual strengths. According to them, this may have been due to the longer time allowed at the slower rate for reabsorption of moisture from the environment. They added that, contrary to current belief, thermal stresses may not have been large enough to cause significant disruption even at rates of cooling as high as 50°C/min.

Furthermore, Sarshar and Khoury (1993) stated that quenching with water subjected the specimens to thermal shock, and saturated them with water, both being potentially detrimental to strength. Quenching of lightweight OPC concrete resulted in a greater reduction in residual strength when compared to firebrick OPC concrete. However, it resulted in lesser reduction when compared to the cement paste specimens. In addition, as discussed in Section 2.3.1, no disintegration was found for OPC concrete specimens.

Nassif et al. (1999) investigated the impact of water cooling after exposure to temperatures up to 470°C on limestone concrete using a stiffness damage test. They reported that sudden cooling unbalance internal equilibrium resulting in significant internal stresses and loss of stiffness, however no disintegration of the specimens was reported.

As discussed in Section 2.3.2 Luo et al. (2000) analysed the effects of elevated temperatures on NSC and HPC concrete made with OPC, silica fume and fly ash followed by either water cooling or furnace cooling. Furnace cooling consisted of turning the furnace off and removing the specimens once room temperature of the specimen was achieved. Their work reported that after 800°C, the residual compressive strength of concrete exposed to furnace cooling was 45% while specimens exposed to water cooling presented a residual strength of 32%, therefore 13% difference. After 1000°C, the difference was reduced to less than 1%. They concluded that the thermal gradient induced by the cooling methods was not the key cause of the specimen's damage. Whereas, according to them, the residual coarser pore volume and pore size distribution following curing had a more significant effect on residual strength (Luo et al. 2000).

Disintegration of concrete specimens were reported by Sakr and Hakim (2005). The OPC concrete made with gravel aggregate disintegrated after 3 hours of exposure to 750°C followed by air cooling. In contrast, specimens painted with fire protection material presented 2.95 MPa. In addition, non-painted specimens after 2 or 3 hours exposure to 750°C followed by water cooling completely disintegrated. Two main conclusions were reported by them. Firstly, they concluded that the fire protection material had no significant effect on compressive strength for temperatures higher than 500°C. Secondly, they concluded that water cooling led to

more reduction in compressive strength than air and foam cooling (Sakr and El-Hakim 2005).

Abramowicz and Kowalski (2005) investigated concrete made with siliceous aggregate heated to temperatures of 270°C, 370°C and 500°C. Cooling by 10 seconds of immersion in water was found not to produce any significant decrease of concrete strength. They concluded this was most likely due to insufficient thermal gradient arising within the short (10 seconds) immersion duration.

Husem (2006) reported disintegration of normal strength OPC concrete made with limestone aggregate after exposure to 800°C followed by water cooling. High strength OPC concrete presented 2.9 MPa after exposure to the same conditions. He concluded that OPC concrete may completely lose its strength if water spray cooling is used on a reinforced concrete building exposed to elevated temperatures as result of a fire.

Kowalski (2007) analysed the effects of cooling on the properties of concrete made with fly ash and siliceous aggregate. His work found that rapid cooling of the heated concrete had the highest influence on the strength loss when the maximum temperature was 330°C. Specimens cooled in laboratory air lost about 10% of their strength, while specimens cooled rapidly in water lost about 35% (5 minutes immersion in water) and 55% (20 minutes immersion in water). Kowalski (2007) attributed the reason for strength loss to microcracks that formed as a result of stresses induced by a temperature gradient. In the case of maximum temperature of 550°C, he suggested that the strength loss depended much less on the cooling process. According to his work, if the concrete has already been damaged during heating to 550°C, its internal stiffness would have been reduced. Hence, the induced stresses and resultant microcracking during cooling would be lower.

2.3.4 The role of aggregate at elevated temperatures

The interfacial bond between the aggregate and the paste is damaged at elevated temperatures (Harmathy 1993). In concrete, the aggregates undergo a progressive expansion on heating while the cement paste, beyond the point of maximum expansion, shrinks. The two opposing actions progressively weaken and crack the concrete. However, as described by Lea (1970), the various aggregates used in concrete differ considerably in their behaviour on heating.

The reason for the differences in aggregate behaviour during exposure to elevated temperatures is a result of the different thermal stabilities presented by the aggregates. Desirable features for high performance at elevated temperatures are: high thermal stability, low thermal expansion (which improves thermal compatibility with the cement paste) and rough angular surface, which improves the physical bond with the paste.

Khoury (2000) stated that the choice of aggregate is probably the most important when designing the concrete mix for elevated temperatures. The main differences between the most used concrete aggregates are:

Quartz: principal mineral constituent of sands and most gravels and a major constituent of the acid igneous rocks, expands steadily up to 573°C. At this temperature it undergoes a sudden expansion of 0.85%, caused by the transformation of 'low' quartz to 'high' quartz. This expansion has a disruptive action in any concrete in which quartz forms a major proportion of an aggregate (Eglinton 1998).

Siliceous gravel, flint and granite: spall when exposed to fire and are amongst the least resistant concrete materials (Eglinton 1998). According to Hertz (2005), siliceous aggregates have greater expansion than granite, basalt and limestone, and provide the greatest concrete damage of all. Flint is expected to break up at relatively low temperatures (below 350°C) (Khoury et al. 1985). In contrast, Khoury (1985) reported that granite exhibits thermal stability up to 600°C.

Sandstones: although containing quartz, do not cause a concrete to spall significantly. This is due to the fact that intergranular natural cementing material in sandstones shrinks on heating and thus, to some extent, counteracts the expansion of the quartz grains (Eglinton 1998). However, according to Eglinton (1998) the loss of strength in sandstone concrete on exposure to fire is often high and sandstones do not form good fire resistant aggregates.

Igneous rocks (basalt and dolerites): best fire resistant aggregates amongst the igneous rocks (Eglinton 1998). Basalt aggregate is thermally stable in temperatures up to 600°C and does not present phase change up to 800°C (Khoury et al. 1985).

Limestone: sedimentary dense limestone form good fire resistant aggregates (Eglinton 1998). Limestone is thermally stable up to 600°C (Khoury et al. 1985). In addition, the relative strength of concrete containing limestone aggregate was less affected by temperatures up to 1200°C when compared to concrete containing siliceous river gravel (Arioz 2007).

Broken brick: form a good aggregate in respect to fire resistance, provided it is free from quartz (Eglinton 1998).

Lightweight aggregates (pumice, foamed slag, expanded clay products): high resistance to fire, and concrete made from them has low heat conductivity. Their heat capacity, on the other hand, is less than that of heavier concretes (Eglinton 1998). Harada et al. (1972) reported that concrete containing pumicite had a strength loss of 60% after 400°C when compared to 40% presented by limestone and sandstone concretes. Xiao and König (2004) concluded that for temperatures up to 800°C, concrete containing lightweight aggregate had superior compressive strength when compared to concrete made with siliceous aggregate.

Air cooled blast furnace slag (ACS): makes the most fire resistant concretes (Eglinton 1998). High thermal stability was demonstrated by mortars made of ACS in temperatures up to 600°C (Shoaib et al. 2001).

2.3.5 Summary

As previously discussed, published data on the mechanical properties of concrete exposed to elevated temperatures taken from different sources differ substantially, and in several cases are contradictory (Khoury 1992). Therefore, Table 2.3 presents a summary of the published literature which has been discussed in details in Sections 2.3.1 to 2.3.4.

Table 2.3 Summary of the published literature on the deterioration of mechanical properties of concrete exposed to elevated temperatures

| Temperature (°C) | Deterioration of mechanical properties | Main factor resulting in deterioration | Reference |
|------------------|---|--|-----------------------------|
| 600 | Residual strength 40% | Microstructure/Post - cooling method | Sarshar and Khoury (1993) |
| | Residual strength 39% | Pore structure | Chan et al. (1996) |
| | Starting point for disintegration | Microstructure | Crozier and Sanjayan (1999) |
| 700 | Total strength loss and complete disintegration | Microstructure | Lea and Stradling (1922) |
| | Total strength loss and complete disintegration | Microstructure/Pore structure | Handoo et al. (2002) |
| 750 | Total strength loss and complete disintegration | Post-cooling method | Sakr and El-Hakim (2005) |
| 800 | Severe strength loss. Residual strength 15% | Microstructure | Chan et al. (1996) |
| | Residual strength of 10% | Type of aggregate/Post-cooling method | Xiao and Konig (2004) |
| | Residual strength 20% to 40% | Microstructure/Type of Aggregate | Arioz (2007) |
| | Residual strength of 45% | Pore structure | Chan et al. (2000)* |
| | Residual strength of 32% | Pore structure | Luo et al. (2000)* |
| | Total strength loss and complete disintegration | Post-cooling method | Husem (2006) |
| 1000 | Residual strength 15% | Microstructure/Type of Aggregate | Arioz (2007) |
| 1200 | Total strength loss and complete disintegration | Microstructure/Type of Aggregate | |

*Concrete made with OPC, silica fume and fly ash

As demonstrated by Table 2.3 the deterioration of the mechanical properties of concrete after exposure to elevated temperatures has been attributed to different factors. However, the role of each factor is still unclear, as represented by Figure 2.8.

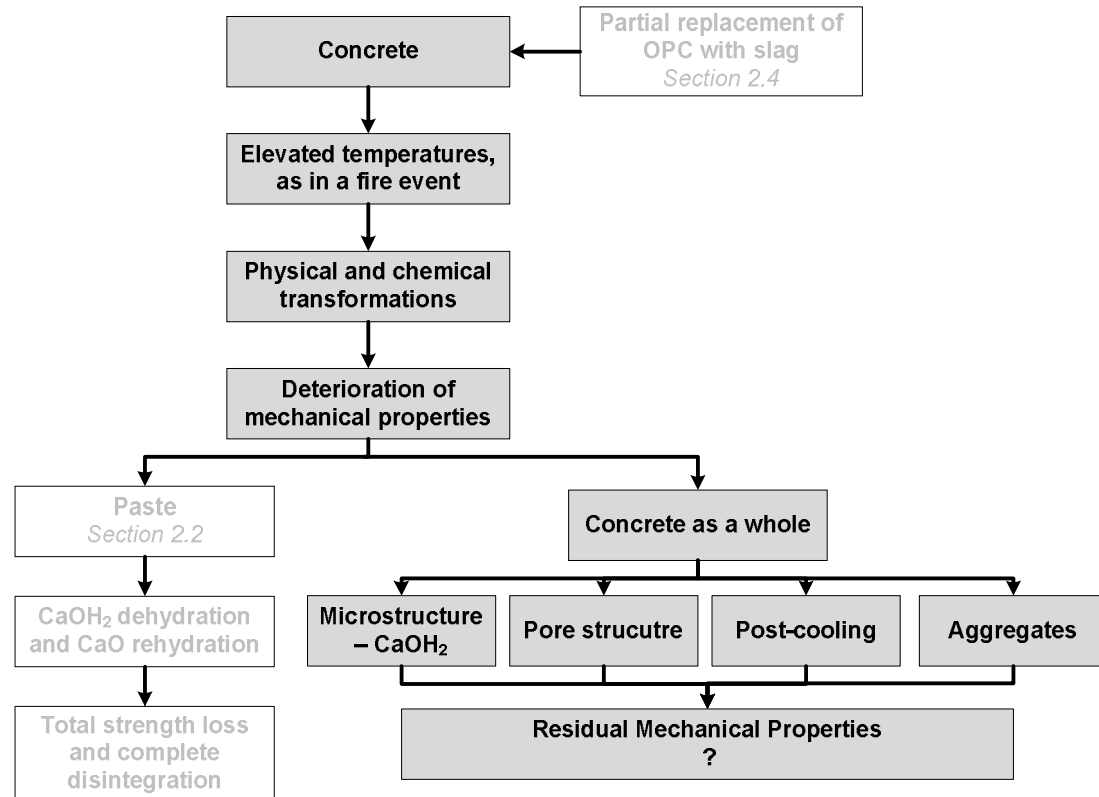


Figure 2.8 Main factors resulting in deterioration of mechanical properties of concrete exposed to elevated temperatures

2.4 Partial replacement with slag

2.4.1 Slag production

Slag is a by-product of the metallurgical process and its final composition dependent upon the raw materials and cooling processes used. The most common used slag is a by-product from the manufacture of iron and steel industry called blast furnace slag.

Blast furnace slag is formed as a liquid at 1350°C to 1550°C in the manufacture of iron. Following rapid cooling to below 800°C, it forms a glass which is a latent hydraulic cement. When dried and ground, it is called ground granulated blast furnace slag (GGBFS or 'slag') and often contains over 95% of glass (Taylor 1997).

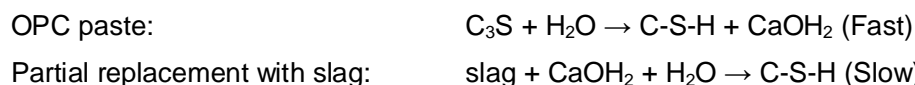
2.4.2 Microstructure at room temperature

The chemical composition of pure slag varies from 30% to 45% of CaO, 28% to 38% SiO₂, 5% to 20% Al₂O₃ and 1% to 18% MgO. The other minor constituents include oxides of sulphur, iron, titanium, manganese and alkaline metals (Bakharev 2001).

Partial replacement of OPC with slag is expected to result in hydration products essentially similar to those found in OPC paste (Taylor 1997). As per OPC pastes, the main hydrated phases in OPC/slag pastes are calcium silicate hydrate (C-S-H gel), calcium hydroxide (CaOH₂), sulphotoaluminate phases ettringite (AFt) and monosulphate hydrate (AFm) (Regourd et al. 1983; Richardson and Groves 1992). However, the quantities of CaOH₂ are expected to be significant lower in OPC/slag pastes when compared to OPC pastes.

Although in the short-term CaOH₂ production is accelerated by the presence of slag, in the long-term the CaOH₂ content of the hydrated binder is reduced by reaction with slag (Richardson and Groves 1992).

Slag, though not a pozzolan, reacts with CaOH₂ to form C-S-H gel in the paste (Mehta and Monteiro 2006). The equations below summarize this reaction:



2.4.3 Microstructure at elevated temperatures

Since the 1970s, numerous studies have been conducted in the hydration, microstructure and mechanical properties of slag blended cement and concretes (Kondo and Ohsawa 1968; Bensted 1976; Regourd 1980). However, little attention has been given to the effects of elevated temperatures on the microstructure and mechanical properties of those blends.

Lea (1970) referred to 'Portland blast furnace cement' as more resistant to fire than OPC. He suggested this may be attributed to the lower proportion of free CaOH_2 present in such cements.

Following Lea, one of the first investigations that focused on the behaviour of concrete made with slag blended cements exposed to elevated temperatures was conducted by Carette et al. (1982). Their work investigated the behaviour of concrete made with slag after long-term exposure to elevated temperatures. This means, not in a fire event, but in applications where concrete is constantly exposed to elevated temperatures, e.g. nuclear reactor pressure vessels, storage tanks for hot crude oil and hot water, coal gasification and liquefaction vessels, and pressure vessels used in the petrochemical industries. Their results indicated that the use of blast furnace slag as partial replacement for OPC in concrete, generally, did not improve the mechanical properties of concretes that have been exposed to sustained elevated temperatures.

Khoury et al. (1985) and Sullivan and Khoury (1986) studied the transient thermal strain behaviour of concrete during the first heating cycle under load to 600°C. Their work compared three different cement pastes OPC, OPC/fly ash, and sulphate resisting Portland cement (SRPC)/slag. It was reported that SRPC/slag paste presented the highest thermal shrinkage followed by OPC and OPC/fly ash pastes.

In addition, Khoury et al. (1985) conducted differential thermal analysis (DTA) to investigate the three abovementioned binder types. The three binder exhibited similar overall DTA trends with endothermic peaks at about 150°C and 500°C due to moisture loss and dissociation of CaOH_2 , respectively. However, the role of both fly ash and slag in reducing the amount of CaOH_2 formed during hydration was evident in the smaller endothermic peak areas of the cement blend.

In 1992, (Khoury) referred to a private communication with Grainger (1980) stating that when PFA or slag were employed as partial replacement of OPC, the losses normally found in the compressive strength above 300°C were reduced. In addition, an increase in strength for temperatures up to 550°C was observed. He concluded that this could be related to the reduced amount of CaOH_2 in the system, since PFA or slag react with CaOH_2 produced during the OPC hydration. Therefore, the partial replacement with PFA or slag would lead to an improvement in the mechanical properties after exposure to elevated temperatures (Khoury 1992).

Sharshar and Khoury (1993) reported that specimens containing PFA or slag (paste and concrete) performed significantly better than OPC specimens in temperatures up to 600°C. They concluded that the lesser CaOH_2 content of PFA and slag blends when compared to OPC paste and concrete, could explain at least in part their better performance.

Sha and Pereira (2001) used differential scanning calorimetry (DSC) to compare the thermal behaviour of slag with the thermal behaviour found in their previous work for OPC (Sha et al. 1999). The most significant reaction from the presence of slag in a (50% OPC/50% slag) paste was a large exothermic peak at around 573°C. This peak was identified as the crystallization of an amorphous phase. There was an overlap between the peak corresponding to the dehydration of CaOH_2 and the crystallization peak, which were in opposite directions as the former reaction absorbed heat while the latter released heat.

Xiao et al. (2006) investigated the mechanical properties of HPC-BFS (high-performance concrete/blast-furnace-slag) after exposure to elevated temperatures. When comparing the residual compressive strength of NSC (normal strength concrete) with HPC-BFS, it was reported that HPC-BFS had a better performance in temperatures up to 800°C.

Furthermore, Aydin (2008) studied the effects of elevated temperatures on OPC/slag mortars made with pumice aggregate. It was reported that these mortars showed no compressive strength loss after exposures up to 600°C followed by air cooling. They conclude that the OPC/slag pumice mortars are a promising multipurpose insulation material for structures exposed to elevated temperatures during service life.

2.4.4 Summary

This section reviewed the limited published literature on the effects of partial replacement of OPC with slag in pastes and concretes exposed to elevated temperatures. As discussed above, there are indications that the partial replacement with slag would lead to improvement of mechanical properties of paste after exposure to elevated temperatures. However, this is still unclear, especially for concrete exposed to elevated temperatures. A summary of this section is presented in Figure 2.9.

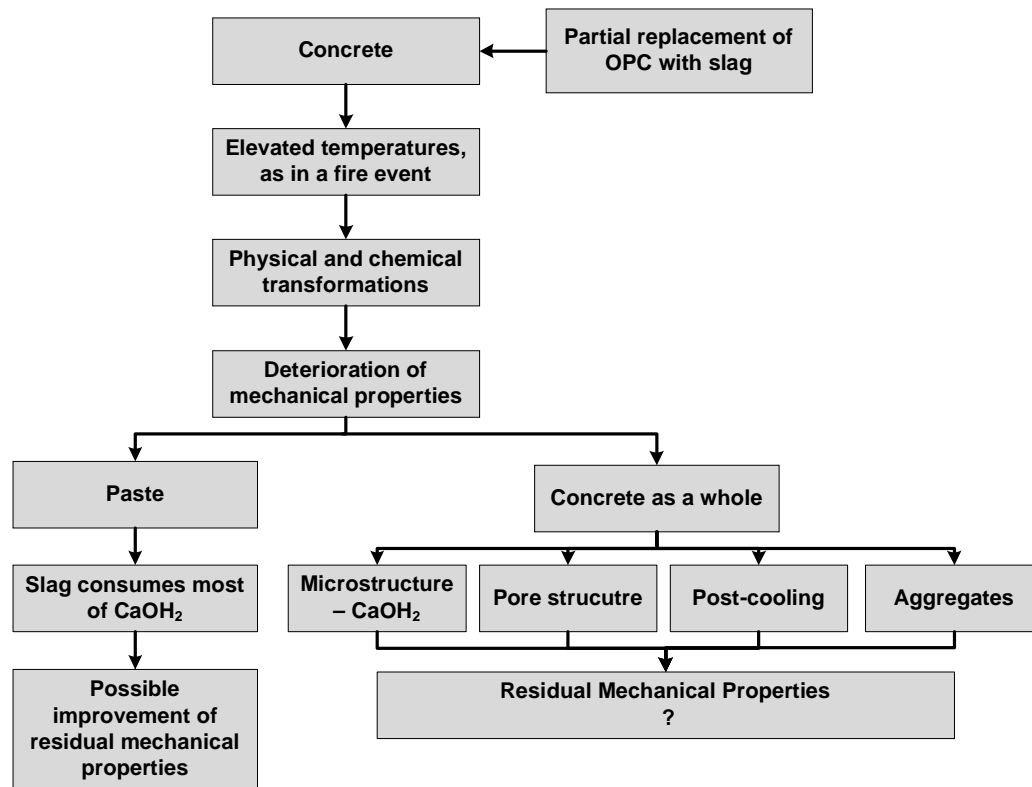


Figure 2.9 Limited published data on the effects of partial replacement of OPC with slag on the mechanical properties of paste and concrete exposed to elevated temperatures

2.5 Conclusions

Based on the literature review presented, it can be concluded that above 400°C, CaOH_2 dehydration and CaO rehydration cause severe deterioration in the mechanical properties of OPC pastes.

For the OPC concrete exposed to elevated temperatures, the role of CaOH_2 dehydration and CaO rehydration in the deterioration of mechanical properties has been of much debate and is yet not fully understood. Similarly, the roles of other factors such as pore structure of concrete and post-cooling methods are still unclear due to the conflicting nature of the available literature. Therefore, a number of studies are necessary to expand the understanding of the effects of elevated temperatures on the microstructure and mechanical properties of OPC concrete. The author aims to address this issue with this thesis.

In addition, knowledge of the effects of partial replacement of OPC with slag on the microstructure and mechanical properties of paste and concrete exposed to elevated temperatures is very limited. Therefore, this also forms part of the scope of this thesis.

Some of the broad research objectives addressed in this thesis include:

- The study of the phase transformations experienced by OPC and OPC/slag pastes during and after exposure to elevated temperatures and their effects on the mechanical properties of these pastes;
- The study of the role of paste hydrates in the deterioration of mechanical properties of OPC and OPC/slag pastes exposed to elevated temperatures;
- The study of the phase transformations experienced by OPC and OPC/slag concretes during and after exposure to elevated temperatures and their effects on the mechanical properties of these concretes;
- The investigation of the effects of different cooling methods on the mechanical properties of OPC and OPC/slag concrete exposed to elevated temperatures; and
- The study of the main differences between paste and concrete after exposure to elevated temperatures.

2.6 References

- Abramowicz M and Kowalski R (2005) *The influence of short time water cooling on the mechanical properties of concrete heated up to high temperature*. Journal of Civil Engineering and Management XI(2): 85-90.
- Alarcon-Ruiz L, Platret G, Massieu M and A Ehrlicher (2005) *The use of thermal analysis in assessing the effect of temperature on a cement paste*. Cement and Concrete Research 35: 609-613.
- Alonso C and Fernandez L (2004) *Dehydration and rehydration processes of cement paste exposed to high temperature environments*. Journal of Materials Science 39: 3015-3024.
- Arioz O (2007) *Effects of elevated temperature on properties of concrete*. Fire Safety Journal 42: 516-522.
- Aydin S (2008) *Development of a high-temperature-resistant mortar by using slag and pumice*. Fire Safety Journal 43: 610-617.
- Bakharev T (2001) *Alkali Activated slag concrete: chemistry, microstructure and durability*. Civil Engineering Department, Monash University. PhD thesis.
- Bensted J (1976) *Examination of the hydration of slag and pozzolanic cements by infrared spectroscopy*. II Cemento 73(4): 209-214.
- Bordallo H N and Aldridge L P (2010) *Concrete and Cement Paste Studied by Quasi-Elastic Neutron Scattering*. Z. Phys. Chem. 224: 183-200.
- Bouguerra A, Ledhem A, Barquin F, Dheilly R M and Queneudec M (1998) *Effect of microstructure on the mechanical and thermal properties of lightweight concrete prepared from clay, cement, and wood aggregates*. Cement and Concrete Research 28: 1179-1190.
- Carette G G, Painter K E and Malhotra V M (1982) *Sustained high temperature effect on concrete made with normal Portland cement, normal Portland cement and slag, or normal Portland cement and fly ash*. Concrete International July: 41-51.

Castellote M, Alonso C, Andrade C, Turrillas X and Campo J (2004) *Composition and microstructural changes of cement pastes upon heating, as studied by neutron diffraction*. Cement and Concrete Research 34: 1633-1644.

Chan S Y N, Peng G and Chan J K W (1996) *Comparison between high strength concrete and normal strength concrete subjected to high temperature*. Materials and Structures 29: 616-619.

Chan Y N, Luo X and Sun W (2000) *Compressive strength and pore structure of high-performance concrete after exposure to high temperature up to 800°C*. Cement and Concrete Research 30: 247-251.

Crozier D A and Sanjayan J G (1999) *Chemical and physical degradation of concrete at elevated temperatures*. Concrete in Australia March-May: 18-20.

Dias W P S, Khoury G A and Sullivan P J E (1990) *Mechanical Properties of Hardened Cement Paste Exposed to Temperatures up to 700°C (1292°F)*. ACI Materials Journal 87(2): 160-166.

Eglinton M (1998) *Resistance of Concrete to Destructive Agencies*. Hewlett P, Oxford, Elsevier: 299-340

Escalante-Garcia J I and Sharp J H (2004) *The chemical composition and microstructure of hydration products in blended cements*. Cement and Concrete Composites 26: 967-976.

Grainger B N (1980) Private communications - Central Electricity Research Laboratories Khoury G A UK.

Handoo S K, Agarwal S and Agarwal S K (2002) *Physicochemical, mineralogical, and morphological characteristics of concrete exposed to elevated temperatures*. Cement and Concrete Research 32: 1009-1018.

Harada T, Takeda J, Yamane S and Furumura F (1972) *Strength, elasticity and thermal properties of concrete subjected to elevated temperatures*. ACI SP SP34-21: 377-406.

Harmathy T Z (1968) *Determining the temperature history of concrete constructions following fire exposure*. ACI Journal 65(11): 959-964.

Harmathy T Z (1993) *Fire safety design and concrete*. Longman Scientific & Technical.

Hertz K D (2005) *Concrete Strength for fire safety design*. Magazine of Concrete Research 57(8): 445-453.

Hjorth J, Skibsted J and Jakobsen H J (1988) ^{29}Si MAS NMR studies of Portland cement components and effects of microsilica on the hydration reaction. Cement and Concrete Research 18(5): 789-798.

Husem M (2006) *The effects of high temperature on compressive and flexural strengths of ordinary and high-performance concrete*. Fire Safety Journal 41: 155-163.

Khoury G A (1992) *Compressive strength of concrete at high temperatures: a reassessment*. Magazine of Concrete Research 44(161): 291-309.

Khoury G A (2000) *Effect of fire on concrete and concrete structures*. Progress in Structural Engineering and Materials 2: 429-447.

Khoury G A, Grainger B N and Sullivan P J E (1985) *Transient thermal strain of concrete: literature review, conditions within the specimen and behaviour of individual constituents*. Magazine of Concrete Research 37(132): 131-144.

Khoury G A, Grainger B N and Sullivan P J E (1986) *Strain of concrete during first cooling from 600°C under load*. Magazine of Concrete Research 38: 3-12.

Kondo R and Ohsawa S (1968) *Studies on a method to determine the amount of granulated blast-furnace slag and the rate of hydration of slag in cements*. Proceedings of the Fifth International Symposium on the Chemistry of Cement, Tokyo. The Cement Association of Japan: 255-262

Kong D L (2009) *Fire Resistance of Geopolymer Concretes*. Civil Engineering Department, Monash University. PhD thesis.

Korpa A and Trettin R (2006) *The influence of different drying methods on cement paste microstructures as reflected by gas adsorption: Comparison between freeze-drying (F-drying), D-drying, P-drying and oven-drying methods*. Cement and Concrete Research 36(4): 634-649.

Kowalski R (2007) *The effects of the cooling rate on the residual properties of heated-up concrete*. Structural Concrete 8(1): 11-15.

Lea F C and Stradling R E (1922) *The resistance to fire of concrete and reinforced concrete*. Engineering 144: 341-344; 380-382.

Lea F M (1970) *The Chemistry of Cement and Concrete*. Edward Arnold (Publishers) Ltd.

Lin W M, Lin T D and Powers-Couche L J (1996) *Microstructure of Fire-Damaged Concrete*. ACI Materials Journal May-June: 199-205.

Liu X, Ye G, Schutter G D, Yuan Y and Taerwe L (2006) *Physicochemical change of cement pastes at elevated temperatures*. 2nd International Symposium on Advances in Concrete through Science and Engineering Quebec City, Canada

Luo X, Sun W and Chan S (2000) *Effect of heating and cooling regimes on residual strength and microstructure of normal strength and high performance concrete*. Cement and Concrete Research 30: 379-383.

Malhotra H L (1956) *The effect of temperature on the compressive strength of concrete*. Cement and Concrete Research 8(23): 85-94.

Matesova D, Bonen D and Surenda P S (2006) *Factors affecting the resistance of cementitious materials at high temperatures and medium heating rates*. Materials and Structures 39: 919-935.

Mehta P K and Monteiro P J M (2006) *Concrete Microstructure, Properties, and Materials*. McGraw-Hill.

Nassif A Y, Rigden S and Burley E (1999) *The effects of rapid cooling by water quenching on the stiffness properties of fire-damaged concrete*. Magazine of Concrete Research 51(4): 255-261.

Odler I (1998) *Hydration, Setting and Hardening of Portland Cement*. Hewlett P, Oxford, Elsevier: 241-289

Petzold A and Rohrs M (1970) *Concrete for high temperatures*. London, MacLaren and Sons Ltd.

- Regourd M (1980) *Structure and behaviour of slag Portland cement hydrates*. VIIth International Congress on the Chemistry of Cement: III -2/10-25
- Regourd M, Thomassin J H, Baillif P and Touray J C (1983) *Blast-furnace slag hydration. Surface analysis*. Cement and Concrete Research 13(4): 549-556.
- Richardson I G and Groves G W (1992) *Microstructure and microanalysis of hardened cement pastes involving ground granulates blast-furnace slag*. Journal of Materials Science 27: 6204-6212.
- Roncero J, Valls S and Gettu R (2002) *Study of the influence of superplasticizers on the hydration of cement paste using nuclear magnetic resonance and X-ray diffraction techniques*. Cement and Concrete Research 32(1): 103-108.
- Rostásy F S, Wei R and Wiedemann G (1980) *Changes of pore structure of cement mortars due to temperature*. Cement and Concrete Research 10(2): 157-164.
- Sakr K and El-Hakim E (2005) *Effect of high temperature or fire on heavy weight concrete properties*. Cement and Concrete Research 35(3): 590-596.
- Sanjayan G and Stocks L (1993) *Spalling of High-Strength Silica Fume Concrete in Fire*. ACI Materials Journal 90(2): 170-173.
- Sarshar R and Khoury G A (1993) *Material and environmental factors influencing the compressive strength of unsealed cement paste and concrete at high temperatures*. Magazine of Concrete Research 45(162): 51-61.
- Sha W, O'Neill E A and Guo Z (1999) *Differential scanning calorimetry study of ordinary Portland cement*. Cement and Concrete Research 29: 1487-1489.
- Sha W and Pereira G B (2001) *Differential scanning calorimetry study of hydrated ground granulated blast-furnace slag*. Cement and Concrete Research 31: 327-329.
- Shoaib M M, Ahmed S A and Balaha M M (2001) *Effect of fire and cooling mode on the properties of slag mortars*. Cement and Concrete Research 31: 1533-1538.
- Sullivan P J E and Khoury G A (1986) *Fire performance of various concrete deduced from strain measurements during first heating*. ACI SP 92: 175-196.
- Taylor H F W (1997) *Cement chemistry*. Wiltshire, Redwood Books.

Xiao J and Konig G (2004) *Study on concrete at high temperature in China: an overview*. Fire Safety Journal 39: 89-103.

Xiao J, Xie M and Zhang C (2006) *Residual Compressive behaviour of pre-heated high performance concrete with blast-furnace-slag*. Fire Safety Journal 41: 91-98.

Chapter 3

Phase Transformations and Mechanical Strength of OPC/Slag Pastes Submitted to High Temperatures

3.1 Overview

The literature review presented in Chapter 2 outlined the negative effects of the dehydration of calcium hydroxide (CaOH_2), one of the main hydrates of the cement paste, on the mechanical properties of ordinary Portland cement (OPC) pastes exposed to temperatures above 400°C . Chapter 3 is aimed to investigate the effects of CaOH_2 dehydration on OPC pastes partially replaced with slag and exposed to elevated temperatures.

This chapter is based on the publication of the same name as the chapter title in Materials and Structures Journal, 2008, Volume 41, pages 345-350. The paper presents an assessment of OPC and OPC/slag pastes exposed to elevated temperatures. It investigates the relationship between phase transformations and strength loss due to exposure to elevated temperatures up to 800°C . The mechanical properties are analysed by compressive strength tests while the phase transformations are investigated by thermogravimetric analysis (TGA).

3.2 Declaration for Thesis Chapter 3

Declaration by candidate

In the case of Chapter 3, the nature and extent of my contribution to the work was the following:

| Nature of contribution | Extent of contribution (%) |
|---|----------------------------|
| Developing outline of research objective and hypothesis Laboratory/experimental investigation and analysis of results Writing, reviewing and editing of paper | 90 |

The following co-authors contributed to the work. Co-authors who are students at Monash University must also indicate the extent of their contribution in percentage terms:

| Name | Nature of contribution | Extent of contribution (%) for student co-authors only |
|---------------|---|---|
| Jay Sanjayan | Developing outline of research objective and hypothesis Reviewing of paper | 5 |
| Frank Collins | Developing outline of research objective and hypothesis Reviewing of paper | 5 |

Candidate's
Signature



30 September 2010

Declaration by co-authors

The undersigned hereby certify that:

- (1) the above declaration correctly reflects the nature and extent of the candidate's contribution to this work, and the nature of the contribution of each of the co-authors.
- (2) they meet the criteria for authorship in that they have participated in the conception, execution, or interpretation, of at least that part of the publication in their field of expertise;
- (3) they take public responsibility for their part of the publication, except for the responsible author who accepts overall responsibility for the publication;
- (4) there are no other authors of the publication according to these criteria;
- (5) potential conflicts of interest have been disclosed to (a) granting bodies, (b) the editor or publisher of journals or other publications, and (c) the head of the responsible academic unit; and

(6) the original data are stored at the following location(s) and will be held for at least five years from the date indicated below:

Location(s)

| |
|--|
| Department of Civil Engineering, Monash University |
|--|

[Please note that the location(s) must be institutional in nature, and should be indicated here as a department, centre or institute, with specific campus identification where relevant.]

Signature 1



30 September 2010

Signature 2



30 September 2010

3.3 Publication

Materials and Structures (2008) 41:345–350
DOI 10.1617/s11527-007-9247-8

ORIGINAL ARTICLE

Phase transformations and mechanical strength of OPC/ Slag pastes submitted to high temperatures

Alessandra Mendes · Jay Sanjayan · Frank Collins

Received: 12 February 2007 / Accepted: 10 April 2007 / Published online: 25 May 2007
© RILEM 2007

Abstract Ground granulated blast furnace slag (GGBFS or “slag”) is a by product of the steel industry and is often used in combination with ordinary Portland cement (OPC) as a binder in concrete. When concrete is exposed to high temperatures, physical and chemical transformations lead to significant loss of mechanical strength. Past studies have reported changes in concrete where OPC is 100% of the binder, but there is a lack of published data on slag blended cements. This work provides better understanding of how slag blended cement pastes behave when exposed to high temperatures, when the critical transformations occur, and what the consequences in the structure of these pastes are. Thermogravimetric analysis made it possible to identify when the transformations occurred and the changes in mechanical strength in the cement paste. A unique outcome of this work is the lower damage presented by slag blended cements after exposure to high temperatures

Keywords Cement · Slag · Compressive strength · High temperatures · Thermogravimetric analysis

1 Introduction

The use of slag as a partial substitute for Portland cement (OPC) in blended cements and in ready mixed concrete not only lessens the amount of unused waste that is produced by the steel industry, but most importantly reduces the carbon dioxide emissions arising from cement making.

A key property of concrete is the durability when exposed to high temperatures (e.g. to provide resistance when exposed to accidental fire). Past studies have reported the concrete behavior when exposed to high temperatures where OPC is 100% of the binder, but there is a lack of published data on slag blended cements.

Two effects of high temperature on exposed mortars were reported [1]: (i) a differential movement between sand particles and cement paste due to different coefficients of thermal expansion; (ii) breakdown of cement paste, regardless of whether the sand is present or not. This investigation focuses on OPC and slag blended cement *pastes* and therefore examines Item (ii).

Lea and Stradling [1] reported the relation between the coefficient of expansion of OPC paste and the dissociation of water from the hydrated paste. Their work recognized that OPC paste expands at temperatures up to 93°C then continually contracts up to 491°C. Calcium hydroxide, $(\text{Ca}(\text{OH})_2)$, one of the products of the hydration of OPC, decomposes at approximately 400°C into calcium oxide (CaO) and water.

A. Mendes (✉) · J. Sanjayan · F. Collins
Department of Civil Engineering, Monash University,
Wellington Road, Clayton, VIC 3800, Australia
e-mail: Alessandra.mendes@eng.monash.edu.au



Following scanning electron microscope (SEM) analysis on samples exposed to temperatures between 600–800°C, significant changes in the morphology of heat-affected concrete were found, due to the predominance of microcracks and voids thereby increasing the porosity of concrete, deformed $\text{Ca}(\text{OH})_2$ crystals and disrupted C-S-H phase boundaries [2]. The observed loss of strength at increasing temperatures is likely be related to the microcracks. The loss of bound water and formation of microcracks also increases the porosity and consequently increases permeability.

When OPC paste is heated, the dehydration of $\text{Ca}(\text{OH})_2$ is easily recognizable from rapid loss of weight and consequently can be analysed by thermogravimetric analysis [3–5]. The disintegration of OPC pastes subjected to 400°C was attributed to the re-hydration of the dissociated $\text{Ca}(\text{OH})_2$ following cooling [6].

Neutron diffraction analysis showed that when $\text{Ca}(\text{OH})_2$ reaches an internal temperature (530–560°C), it decomposes abruptly, being transformed into CaO (lime). Ettringite thermally decomposes when it reaches 90°C. The C-S-H gel slightly decomposes as it gets dehydrated, disappearing at a temperature which depends on the dehydration of the gel (200–450°C). Part of the C-S-H that decomposes contributes to the increase in concentration of calcite and larnite (both remaining throughout the experiments) [7].

Khoury [8] suggested that calcium hydroxide dehydration and re-hydration could be the “Achilles heel” of concrete in high temperature applications. Petzold and Rohrs [9] reported similar occurrence, attributing the loss of strength to the re-hydration of CaO, which is accompanied by 44% increase of volume. The re-hydration of CaO during cooling was also used to explain the reduction in strength in the study of cement mortars [10]. Significant loss of strength after 400°C in OPC concrete specimens was attributed to the loss of crystal water, resulting in the reduction of the $\text{Ca}(\text{OH})_2$ [2]. Cracking and softening, followed by decrepitation of the concrete surface, were explained as a result of expansion followed by shrinkage of the OPC paste due to the transformation of $\text{Ca}(\text{OH})_2$ to CaO in the temperature range 450–500°C. [11].

Comparing sulphate-resisting Portland cement (SRPC) paste containing 50% of slag in the binder

composition with OPC paste, Khoury et al. [12] found that the role of slag in reducing the amount of $\text{Ca}(\text{OH})_2$ during hydration was evidenced by the observed lower DTA endothermic peaks for SRPC/slag blends around 550°C.

Analysing long term exposure of concrete to high temperatures, an investigation in the use of slag as partial replacement (i.e. 35% by weight) for OPC in the concrete binder was conducted [13]. It was found that, in general, the replacement did not improve the mechanical properties of concretes that have been exposed to sustained high temperatures. However data regarding binders with higher proportion of slag (than 35%) have not been published.

There is a lack of detailed investigations that report the performance of slag blended cement pastes under high temperature exposure conditions and the aim of this paper is to provide comparative data with OPC binders

2 Experimental procedure

Ordinary Portland cement (OPC) and ground granulated blast furnace slag (GGBFS or “slag”), conforming to the requirements of Australian Standard AS3972 were used as binder materials. The chemical composition and properties of the binders are summarised in Table 1.

Table 1 Chemical composition and properties of the binders

| Constituent/property % | OPC | Slag |
|----------------------------------|-------|------|
| SiO_2 | 19.90 | 32.5 |
| Al_2O_3 | 4.70 | 13 |
| Fe_2O_3 | 3.38 | 0.22 |
| MgO | 1.30 | 5.47 |
| CaO | 63.93 | 42.1 |
| Na_2O | 0.17 | 0.21 |
| TiO_2 | 0.245 | 1.08 |
| K_2O | 0.446 | 0.25 |
| MnO | 0.079 | 5.47 |
| P_2O_5 | 0.063 | Bd |
| SO_3 | 2.54 | 4.1 |
| LOI | 2.97 | 0.35 |
| Fineness, m^2/kg | 360 | 435 |
| Specific gravity | 3.15 | 2.92 |



In this investigation OPC was partially replaced (i.e., 35, 50 and 65% by weight) with slag. The term water/binder (w/b) ratio is used instead of the water/cement ratio to include both binder types mentioned above. The w/b ratio used was 0.5

Cylinder specimens of diameter 50 mm (1.97 in) and length 100 mm (3.94 in) were investigated. The specimens consisted of pastes, thus overcoming uncertainties arising from paste-aggregate differential properties. Twelve litres of each mixture (i.e. replacements 0, 35, 50 and 65% by weight with slag) were prepared. Water was first added, followed by the binders. The mixing was conducted in a mechanical mixer of 20 l of capacity, 80 rpm, for five minutes each mixture. The specimens were cast using a vibration table for better compaction. Specimens were de-molded after 24 h, followed by 14 days curing in lime-saturated water at 23°C.

Following curing, the specimens were oven-dried for 2 days at 60°C. Specimens were submitted to heat treatment in a *CEMLL Ceramic Engineering* furnace. Increasing temperature intervals of 100°C were applied, from 100 to 800°C, at a constant heating rate of 6.25°C/min until 50°C below the desired temperature, then 1 h until the desired temperature was reached, followed by 1 h at the desired temperature. For example, for 800°C heat treatment, constant heating rate of 6.25°C/min until 750°C, then 1 h between 750–800°C, and finally 1 h at 800°C. Specimens were cooled by furnace cooling, i.e., left to cool with furnace switched off, until the samples reached room temperature.

Specimens were tested for compressive strength in a *Baldwin—Universal Testing Machine* (120 WHVL – 120000 LB. CAP.) using a loading rate of 20 MPa/min. The TGA (thermogravimetric analysis) was conducted in a *TG92—Setaram*, with the temperature of the furnace programmed to rise at constant heating rate of 5°C/min up to 800°C, under air flow. The amount of test sample used ranged between 220 and 225 mg.

3 Results and discussion

3.1 Compressive strength

The weight loss after oven drying for 2 days at 60°C is presented in Table 2. Following drying, specimens were submitted to heat treatment in intervals of

Table 2 Weight loss (%) after drying for 2 days at 60°C

| Mixtures | Weight loss (%) |
|------------------|-----------------|
| 100% OPC | 5.85 |
| 65% OPC–35% Slag | 9.10 |
| 50% OPC–50% Slag | 10.79 |
| 35% OPC–65% Slag | 10.31 |

100°C, from 100 to 800°C. The weight loss after heat treatment is presented in Table 3. Compressive strength tests were conducted in this work rather than other mechanical test, e.g. tensile tests, as the structural aspect of the cement paste was the focus of this investigation. The compressive strength results for the different pastes are summarized in Fig. 1. Above 400°C, OPC samples presented a considerable decrease in compressive strength. All OPC specimens heated to 400°C or above exhibited severe cracking to the point of disintegration after a few days, presenting no strength. Similar results have been reported by others (summarised above).

The explanation of this phenomenon can be found in the fact that one of the main products of hydration of Portland cement is Ca(OH)_2 [1]. This dissociates into CaO at about 400°C, accompanied by contraction of the concrete. Concrete is porous and the water vapour from the air enables re-hydration of the CaO into Ca(OH)_2 . As Ca(OH)_2 occupies considerably greater volume than CaO it causes the concrete to crack and disintegrate [1].

3.2 Heat treatment effects

In this investigation an increase in the proportion of slag in the composition of the specimen provided not only significantly fewer visible surface cracks, but also an improvement in the strength. As shown in Fig. 2, 3 and 4, OPC specimens submitted to heat treatment after 400°C presented a large quantity of visual cracks when removed from the furnace, completely disintegrating after a few days, whereas 35, 50 and 65% slag specimens presented few to almost no visual cracks. It is likely that this reflects the decreasing amounts of Ca(OH)_2 present in the hydrated slag blended cement pastes compared with 100% OPC prior to heating, and hence the decreasing amount of disruption arising from re-formation of Ca(OH)_2 . This suggests that sufficient replacement of



Table 3 Weight loss (%) after heat treatment from 100 to 800°C

| Mixtures | 100°C | 200°C | 300°C | 400°C | 500°C | 600°C | 700°C | 800°C |
|------------------|-------|-------|-------|-------|-------|-------|-------|-------|
| 100% OPC | 1.39 | 17.81 | 23.35 | 22.96 | 24.80 | 28.83 | 30.69 | 29.95 |
| 65% OPC–35% Slag | 1.32 | 17.39 | 23.50 | 22.10 | 25.17 | 23.82 | 26.16 | 27.96 |
| 50% OPC–50% Slag | 1.14 | 16.99 | 21.99 | 21.70 | 24.71 | 23.17 | 25.77 | 26.89 |
| 35% OPC–65% Slag | 1.27 | 16.41 | 22.55 | 22.51 | 26.03 | 23.78 | 26.27 | 27.43 |

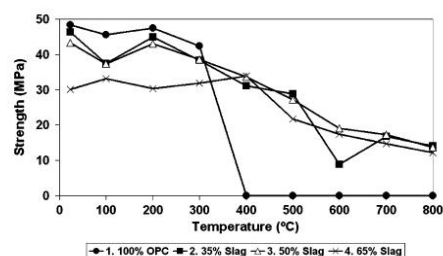


Fig. 1 Compressive strength of different pastes at various temperatures



Fig. 2 Different pastes after 500°C



Fig. 3 Different pastes after 800°C, first day out of the furnace

OPC with slag could reduce the harmful effects when pastes are heated above the critical temperature of 400°C for OPC pastes. Similar results were found when OPC was partially replaced with fly ash [6].



Fig. 4 Different pastes after 800°C, second day out of the furnace

3.3 Thermogravimetric analysis

To determine the quantity of $\text{Ca}(\text{OH})_2$ present in the OPC and OPC/slag blended cement pastes, thermogravimetric analysis was conducted in this work. As previously mentioned, as the dehydration of $\text{Ca}(\text{OH})_2$ is recognizable from a rapid weight loss, TGA and DTG studies could easily detect the dehydration in OPC paste [3]. Thermogravimetric analysis conducted on OPC paste, reported the dehydration of the $\text{Ca}(\text{OH})_2$ between 450 and 500°C, with the re-hydration occurring rapidly after heat treatment [14]. Our investigation (Fig. 5 and Fig. 6) shows a noticeably higher peak for the OPC paste at around 500°C whereas the intensity of the peak is significantly less for samples that have increasing propor-

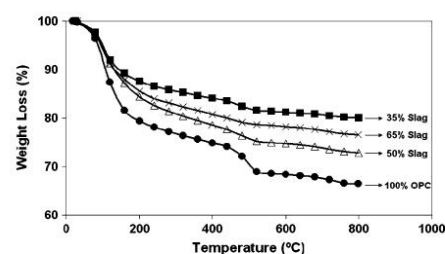


Fig. 5 TGA curves of the different pastes

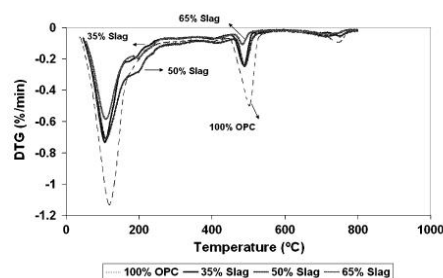


Fig. 6 DTG curves of the different pastes

tion of slag. For OPC, the DTG peak at 500°C is approximately -0.41 (%/min). However, for the sample containing 65% of replacement with slag the peak is approximately -0.1 (%/min). This shows that the OPC peak is four times greater than the 65% slag peak.

The presence of slag reduces the $\text{Ca}(\text{OH})_2$ concentration of the binder [15–17] and slag reacts with the $\text{Ca}(\text{OH})_2$ thereby forming calcium silicate hydrate and filling the weak transition zone [18, 19].

The reaction of slag with $\text{Ca}(\text{OH})_2$ and the resulting hydrated cement paste confirms the significantly improved performance to OPC.

4 Conclusions

The aim of this investigation was to provide published data on slag blended cement pastes exposed to high temperatures. Previous investigations have reported the critical temperature of 400°C for breakdown of OPC pastes. This phenomenon is due to the dissociation of $\text{Ca}(\text{OH})_2$ followed by re-hydration, leading the OPC to disintegration. In this investigation, the use of slag as a way of reducing the amount of $\text{Ca}(\text{OH})_2$ was studied with respect to behaviour when exposed to high temperatures. It was found that OPC cement pastes partially replaced with slag achieved a significant and beneficial reduction of the amount of $\text{Ca}(\text{OH})_2$ and an increase in the proportion of slag in the cement paste, in general, led to an improvement in the mechanical properties following exposure to temperatures beyond 400°C. Although the properties of concrete vary according to its constituents, this investigation considered as a first approach the analysis of the binding ingredients of

concrete, the cement paste. Future research on the other constituents of concrete, using different methods of investigations, e.g., microscope analysis, is therefore necessary (and currently underway) to gain a complete understanding of how concrete containing slag blended cements behave after exposure to high temperature.

Acknowledgments The authors gratefully acknowledge the Australian Research Council Discovery Grant No. DP0558463 for this research project.

References

1. Lea F, Stradling R (1922) The resistance of fire of concrete and reinforced concrete. *Engineering* 144: 341–344, 380–382
2. Handoo SK, Agarwal S, Agarwal SK (2002) Physico-chemical, mineralogical, and morphological characteristics of concrete exposed to elevated temperatures. *Cem Concr Res* 32:1009–1018
3. Harmathy TZ (1968) Determining the temperature history of concrete constructions following fire exposure. *ACI J* 65(11):959–964
4. Harmathy TZ (1993) Fire safety design & concrete. Longman Scientific & Technical
5. Matesova D, Bonen D, Surenda PS (2006) Factors affecting the resistance of cementitious materials at high temperatures and medium heating rates. *Mater Struct* 39:919–935
6. Khoury GA, Dias WPS, Sullivan PJE (1990) Mechanical properties of hardened cement paste exposed to temperatures up to 700°C. *ACI Mater J* 87:160–166
7. Castellote M, Alonso C, Andrade C, Turrillas X, Campo J (2004) Composition and microstructural changes of cement pastes upon heating, as studied by neutron diffraction. *Cem Concr Res* 34:1633–1644
8. Khoury GA (1992) Compressive strength of concrete at high temperatures: a reassessment. *Mag Concr Research* 44(161):291–309
9. Petzold A, Rohrs M (1970) Concrete for high temperatures, 2nd edn. MacLaren and Sons Ltd, London
10. Xiao J, Xie M, Zhang C (2006) Residual compressive behaviour of pre-heated high-performance concrete with blast-furnace-slag. *Fire Saf J* 41:91–98
11. Georgali B, Tsakiridis PE (2005) Microstructure of fire-damaged concrete. A case study. *Cem Concr Composites* 27(2):255–259
12. Khoury GA, Grainger BN, Sullivan PJE (1985) Transient thermal strain of concrete: literature review, conditions within specimen and behaviour of individual constituents. *Mag Concr Res* 37(132):131–144
13. Carette GG, Painter KE, Malhotra VM (1982) Sustained high temperatures effect on concretes made with normal Portland cement, normal Portland cement and slag, or normal Portland cement and fly ash. *Concr Int Design and Constr* 4(7):41–51



14. Alarcon-Ruiz L, Platret G, Massieu E, Ehrlacher A (2005) The use of thermal analysis in assessing the effect of temperature on a cement paste. *Cem Concr Res* 35:609–613
15. Saito M, Kawamura M (1989) Effect of fly ash and slag on the interfacial zone between cement and aggregate. In: Malhotra VM (ed) Paper presented at the 3rd international conference on Fly Ash, Silica Fume, Slag, and Natural Pozzolans in Concrete. Trondheim, Norway, ACI SP 114
16. Larbi JA, Bijen JM (1992) Effect of mineral admixtures on the cement paste-aggregate interface. In: Malhotra VM (ed) Paper presented at the 4th CANMET/ACI international conference on Fly Ash, Silica Fume, Slag, and Natural Pozzolans in concrete. Istanbul, Turkey, ACI SP-132
17. Nilsen U, Sandberg P, Folliard K (1992) Influence of mineral admixtures on the transition zone in concrete. In: Maso JC (ed) Paper presented at the RILEM international conference on interfaces in cementitious composites. E & FN Spon, London
18. Hooton RD (1997) Slag binders for enhanced performance of concrete. Paper presented at the international seminar on technical and environmental advantages of concrete containing Fly Ash and Slag, Ash Development Association of Australia, Australasian Slag Association, and Institution of Engineers, Sydney, Australia, 22 August 1997
19. Scrivener KL (1989) The microstructure of concrete. Paper presented at the materials science of concrete I, The American Ceramic Society, Westerville, Ohio



Chapter 4

Long-Term Progressive Deterioration following Fire Exposure of OPC versus Slag Blended Cement Pastes

4.1 Overview

Chapter 3 reported that above 400°C, calcium hydroxide (CaOH_2) dehydrates into calcium oxide (CaO) causing the ordinary Portland cement (OPC) paste to contract and crack. After cooling and during exposure to air moisture, CaO rehydrates into CaOH_2 , causing the OPC paste to expand and completely disintegrate, resulting in total strength loss. In contrast, partial replacement with slag resulted in consumption of most of the available CaOH_2 , consequently reducing the negative effects caused by the CaOH_2 dehydration and CaO rehydration.

The present Chapter 4 is based on the publication of the same name as the chapter title in Materials and Structures Journal, 2009, Volume 42, pages 95-101. It presents an assessment of the long-term effects of the CaO rehydration on the mechanical properties of OPC and OPC/slag pastes exposed to elevated temperatures. The investigation consists of visual observations, compressive strength tests and differential thermogravimetric analysis (DTG).

4.2 Declaration for Thesis Chapter 4

Declaration by candidate

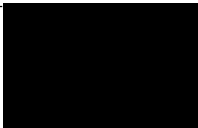
In the case of Chapter 4, the nature and extent of my contribution to the work was the following:

| Nature of contribution | Extent of contribution (%) |
|---|----------------------------|
| Developing outline of research objective and hypothesis Laboratory/experimental investigation and analysis of results Writing, reviewing and editing of paper | 90 |

The following co-authors contributed to the work. Co-authors who are students at Monash University must also indicate the extent of their contribution in percentage terms:

| Name | Nature of contribution | Extent of contribution (%) for student co-authors only |
|---------------|---|---|
| Jay Sanjayan | Developing outline of research objective and hypothesis Reviewing of paper | 5 |
| Frank Collins | Developing outline of research objective and hypothesis Reviewing of paper | 5 |

Candidate's
Signature



30 September 2010

Declaration by co-authors

The undersigned hereby certify that:

- (1) the above declaration correctly reflects the nature and extent of the candidate's contribution to this work, and the nature of the contribution of each of the co-authors.
- (2) they meet the criteria for authorship in that they have participated in the conception, execution, or interpretation, of at least that part of the publication in their field of expertise;
- (3) they take public responsibility for their part of the publication, except for the responsible author who accepts overall responsibility for the publication;
- (4) there are no other authors of the publication according to these criteria;
- (5) potential conflicts of interest have been disclosed to (a) granting bodies, (b) the editor or publisher of journals or other publications, and (c) the head of the responsible academic unit; and

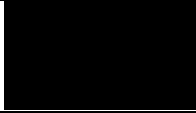
(6) the original data are stored at the following location(s) and will be held for at least five years from the date indicated below:

Location(s)


| |
|--|
| Department of Civil Engineering, Monash University |
|--|

[Please note that the location(s) must be institutional in nature, and should be indicated here as a department, centre or institute, with specific campus identification where relevant.]

Signature 1

| | |
|---|--------------------------|
|  | 30 September 2010 |
|---|--------------------------|

Signature 2

| | |
|---|--------------------------|
|  | 30 September 2010 |
|---|--------------------------|

4.3 Publication

Materials and Structures (2009) 42:95–101
DOI 10.1617/s11527-008-9369-7

ORIGINAL ARTICLE

Long-term progressive deterioration following fire exposure of OPC versus slag blended cement pastes

Alessandra Mendes · Jay G. Sanjayan ·
Frank Collins

Received: 3 December 2007 / Accepted: 27 February 2008 / Published online: 11 March 2008
© RILEM 2008

Abstract The normal practice of repairing fire-damaged concrete structures is to remove the visibly damaged portions and restore them with new concrete. However, little attention has been given to the long-term performance of fire exposed concrete which is not removed from the structure. This paper addresses this issue. Ordinary Portland cement (OPC) pastes, when exposed to a critical temperature of 400°C, undergo complete breakdown. This behaviour was attributed to the dehydration of Ca(OH)_2 , followed by the expansive rehydration of CaO. In contrast, partial replacement of the OPC binder with slag, had a beneficial effect in the mechanical properties of the paste after exposure to high temperatures, as slag significantly reduces the amount of available Ca(OH)_2 in the cement paste. The present work provides new data regarding the long-term (after the exposure event) effect of CaO rehydration in the OPC and OPC/slag pastes. After 1 year the ongoing effect of the CaO rehydration was severe in the OPC paste while OPC/slag blends were not affected by rehydration. Compressive strength and thermogravimetric results are presented to explain this behaviour.

Keywords Cement paste · Long-term effects · High temperatures · Mechanical properties · Differential thermogravimetric analysis

1 Introduction

When concrete is submitted to high temperatures as in a fire, physical and chemical transformations take place resulting in deterioration of its mechanical properties. This deterioration varies according to the concrete mix proportions and constituents and can be determined by complex physicochemical transformations occurring during heating [1].

The present work investigates both short- and long-term behaviour (up to 1 year) of pastes after an initial exposure to high temperatures. The long-term effect of high temperatures in Ordinary Portland cement (OPC) paste is compared to OPC/slag paste. Both physical and chemical transformations of the binders of the concrete are analysed.

The critical temperature of 400°C for the breakdown of OPC pastes due to the dehydration of calcium hydroxide Ca(OH)_2 , followed by the expansive rehydration of lime (CaO) after cooling, was confirmed by Mendes et al. [2].

Ca(OH)_2 plays an important role in the chemical and microstructural composition of the cement paste and therefore of the concrete [3]. Its effects in the mechanical properties of concrete have been studied since 1922 [4].

A. Mendes (✉) · J. G. Sanjayan · F. Collins
Department of Civil Engineering, Monash University,
Clayton Campus, Melbourne, VIC 3800, Australia
e-mail: alessandra.mendes@eng.monash.edu.au



Khoury [5] reported the phenomenon of dehydration of Ca(OH)_2 followed by rehydration of CaO , and classified those events as the “Achilles heel” of concrete. Petzold and Rohrs [6] also reported this phenomenon highlighting an expansion in volume of 44%.

Mendes et al. [2] reported similar expansion when OPC specimens submitted above 400°C completely disintegrated after a few days due to the expansion caused by the CaO rehydration.

In the past, previous works [7–10] have investigated this phenomenon in OPC paste using thermogravimetric analysis. More recently this analysis was conducted in OPC pastes and OPC/slag pastes [2]. It was found that OPC/slag pastes achieved a significant and beneficial reduction in the amount of Ca(OH)_2 that led to an improvement in the mechanical properties after exposure to temperatures beyond 400°C . While OPC paste specimens completely disintegrated after a few days following the heat treatment, OPC/slag specimens visibly presented very few, to almost no cracks.

Visual observation is usually the first step for the assessment of fire-damaged structures [11].

Aiming to provide data in the long-term effect of high temperatures in the cement paste, the work presented in this paper uses visual observations, compressive strength test and differential thermogravimetric analysis to report the behaviour of OPC pastes and OPC/slag pastes after 1 year following the initial heat exposure.

The outcome of this work shows the importance of not only an efficient repair of fire-damaged structures, but also a continuous monitoring of how those fire-damaged structures will behave in the long-term.

2 Experimental procedure

Aiming to investigate the long-term effect of rehydration in the cement paste, and therefore enabling a comparison between short- and long-term effect of the CaO rehydration, two different ages of paste specimens were analysed. One paste was exposed to 800°C heat treatment 1 year prior to compressive strength test and differential thermogravimetric analysis whereas the other paste was exposed to 800°C heat treatment 1 week before those analyses. Ordinary Portland cement (OPC) and ground granulated

blast furnace slag (GGBFS or “slag”), conforming the requirements of Australian Standard AS 3972, were used as binder materials. The chemical composition and properties of the binders are summarised in Table 1.

Short-term specimens are identified as ‘1 week’; i.e. specimens were exposed to 800°C heat treatment 1 week prior to the time when compressive strength and differential thermogravimetric analyses were conducted. Long-term specimens are identified as ‘1 year’ and were exposed to the same heat treatment 1 year prior to the compressive strength and differential thermogravimetric analyses.

In this investigation OPC was partially replaced (i.e. 35, 50 and 65% by weight) with slag, resulting in four different mixtures. The water/binder (w/b) ratio was maintained as 0.5 in all the mixes.

Cylinder specimens of 50 mm diameter and 100 mm length were prepared. Water was first added, followed by the binders. The mixing was conducted in a mechanical mixer of 20 l capacity, 80 rpm, for 5 min for each mixture. Three specimens of each mixture were cast and compacted on a vibration table. The specimens were de-molded after 24 h, followed by 14 days curing in lime-saturated water at 23°C . Before exposure to high temperatures, the specimens were oven-dried for 2 days at 60°C .

The heat treatment was conducted in a *CEMLL Ceramic Engineering* furnace. Specimens were submitted to 800°C using a constant heating rate of

Table 1 Chemical composition and properties of the binders

| Constituent/property (%) | OPC | Slag |
|-------------------------------------|-------|------|
| SiO_2 | 19.90 | 32.5 |
| Al_2O_3 | 4.70 | 13 |
| Fe_2O_3 | 3.38 | 0.22 |
| MgO | 1.30 | 5.47 |
| CaO | 63.93 | 42.1 |
| Na_2O | 0.17 | 0.21 |
| TiO_2 | 0.245 | 1.08 |
| K_2O | 0.446 | 0.25 |
| MnO | 0.079 | 5.47 |
| P_2O_5 | 0.063 | Bd |
| SO_3 | 2.54 | 4.1 |
| LOI | 2.97 | 0.35 |
| Fineness (m^2/kg) | 360 | 435 |
| Specific gravity | 3.15 | 2.92 |



6.25°C/min until 750°C, then 1 h between 750 and 800°C, and finally 1 h in 800°C.

Both short- and long-term specimens were kept in a sealed plastic bag after heat treatment until compressive strength and differential thermogravimetric analysis were conducted, 1 week and 1 year after the heat exposure, respectively.

Compressive strength testing was undertaken using a *Baldwin-Universal Testing Machine* (120WHVL-120000LB.CAP.), at a loading rate of 20 MPa/min.

Differential thermogravimetric analysis (DTG) was conducted in a *TG92—Setaram*, with the temperature of the furnace programmed to rise at constant heating rate of 5°C/min up to 800°C, under air flow. The amount of test sample used ranged between 220 and 225 mg.

3 Results and discussion

3.1 Visual observations

An assessment of a fire-damaged concrete structure generally starts with a visual observation of colour changes, crazing, cracking and spalling [12]. The present work also used visual assessment first before conducting other tests.

Mendes et al. [2] investigated the short-term effects of high temperature in OPC and OPC/slag pastes. It was found that OPC specimens heated to 400°C or above exhibited severe cracking to the point of disintegration after a few days following exposure. In contrast, 35, 50 and 65% slag replacement specimens presented few to almost no visual cracks when initially exposed above this temperature. The explanation of this phenomenon can be found in the fact that one of the main products of hydration of OPC is $\text{Ca}(\text{OH})_2$. This dissociates into CaO above 400°C. After cooling and in the presence of air moisture, the concrete paste suffers rehydration of the CaO into $\text{Ca}(\text{OH})_2$. As $\text{Ca}(\text{OH})_2$ occupies considerably a greater volume than CaO it causes the concrete to crack and disintegrate [4].

In the present work an analysis of the long-term effect of the CaO rehydration in OPC and OPC/slag pastes was carried out, followed by a comparison between short- and long-term effects of rehydration.



Fig. 1 Three OPC paste specimens (50 mm × 100 mm) immediately after 800°C heat treatment

3.1.1 Short-term effect of CaO rehydration

Figures 1 and 2 show the evolution of rehydration in OPC paste specimens after exposure to high temperature. Figure 1 presents three OPC paste specimens immediately after 800°C heat treatment. Figure 2 presents the same specimens as Fig. 1, 2 days after the heat treatment. The progressive deterioration due to the CaO rehydration in the OPC paste specimens is clearly noticeable.

3.1.2 Long-term effect of CaO rehydration

Figure 3 presents four different paste specimens: OPC and OPC/slag (35, 50 and 65%) 2 days after the 800°C heat treatment. The OPC specimen presented a large quantity of visual cracks when removed from the furnace, completely disintegrating after 2 days. On the other hand, the 35, 50 and 65% slag blended cement samples presented few to almost no cracks,



Fig. 2 Three OPC paste specimens (50 mm × 100 mm) 2 days after 800°C heat treatment



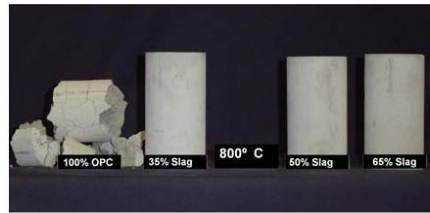


Fig. 3 Different specimens (50 mm × 100 mm), 2 days after 800°C heat treatment



Fig. 4 OPC and 50% Slag specimens 1 year after 800°C heat treatment

immediately and also 2 days after the heat treatment; therefore not being significantly affected by CaO rehydration. This reinforces that sufficient replacement of OPC with slag could reduce the harmful effects of CaO rehydration when pastes are heated above the critical temperature of 400°C for OPC pastes.

Samples shown in Fig. 3 were kept in a sealed plastic bag for 1 year. Figure 4 presents the appearance of the OPC and 50% Slag specimens at the end of this period (1 year).

For simplified presentation, only one OPC and one OPC/slag specimens are shown in Fig. 4. However, it is important to note that specimens with 35, 50 and 65% slag presented almost no cracks; and no visual distinction could be made between '1 week' and '1 year' specimens.

However, the same behaviour was not found for the OPC specimens. While there were no visual differences between '1 week' and '1 year' images for OPC/slag specimens, OPC specimens were progressively reduced to a powder 1 year after the 800°C heat treatment. In Fig. 4, it can be seen how severe the effects of CaO rehydration are for OPC

specimens. It needs also consideration that those severe results were found even though the specimens were stored in a sealed plastic bag in laboratory conditions, thus limiting the quantity of available air moisture, the main source of moisture for rehydration.

The results show the importance of monitoring fire-damaged structures long after the fire exposure for ongoing deterioration. Concrete is exposed to the air atmosphere in real in-service conditions where moisture is available, the main tool for CaO rehydration.

3.2 Compressive strength

Following visual observations, mechanical tests were used as a second step for the assessment of short- and long-term effects of CaO rehydration in OPC and OPC/slag pastes after high temperature exposure. Compressive strength tests were conducted and results are presented in Fig. 5.

The OPC paste specimens disintegrated after a few days of heat treatment presenting no compressive strength. Those specimens have suffered a progressive deterioration throughout 1 year, being reduced to a powder after this period.

In contrast, Fig. 5 shows that OPC/slag specimens had compressive strength results within the range of 11–14 MPa 1 week after the heat treatment. When analysing the strength after 1 year, it was found that OPC/slag blended cement pastes were not significantly affected during this time, maintaining the compressive strength in the range of 11–14 MPa.

Those results reinforce the notion that only OPC pastes have suffered both short- and long-term effects

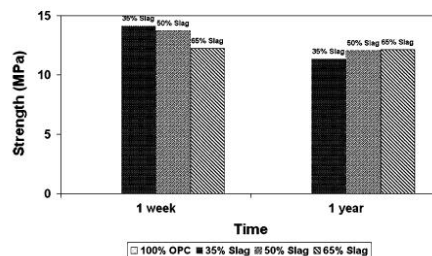


Fig. 5 Compressive strength results for the different mixtures, 1 week and 1 year after 800°C heat treatment



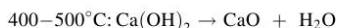
of CaO rehydration, while OPC/slag pastes are not significantly affected in short- and long-term after heat exposure.

3.3 Differential thermogravimetric analysis

To confirm the hypothesis that CaO rehydration is responsible for the long-term deterioration after heat treatment, differential thermogravimetric analysis (DTG) was conducted in OPC and 50% Slag specimens, both 1 week and 1 year after the 800°C heat treatment. The respective curves were then compared to the curve of a reference sample; i.e. paste specimen that has not been submitted to heat treatment.

3.3.1 OPC paste

Figure 6 shows that for the reference specimen (OPC reference), there are three rapid weight losses. The first weight loss, between 100 and 200°C, can be associated with the loss of capillary water. The second major weight loss, between 400 and 500°C, corresponds to the dehydration of $\text{Ca}(\text{OH})_2$. The third weight loss was found to occur at temperatures above 750°C and is a result of the decarbonation of calcium carbonate (CaCO_3) [10]. In summary, $\text{Ca}(\text{OH})_2$ and CaCO_3 undergo the following chemical transformations at the temperatures indicated:



When comparing DTG results of OPC specimens '1 week' and '1 year' after the 800°C heat treatment with specimens that were not heat treated, it can be seen that the peak related to the loss of capillary water (between 100 and 200°C) completely disappeared for heat treated samples. This is expected and confirms that there were no reabsorbed free water in the specimens. The weight loss found between 400 and 500°C indicates that $\text{Ca}(\text{OH})_2$ exists in the heat treated specimens, confirming that the CaO rehydration took place forming $\text{Ca}(\text{OH})_2$. Heat treated specimens contained higher amounts of $\text{Ca}(\text{OH})_2$ than the reference unheated specimen. This is a unique finding as it suggests that CaO rehydration not only has its source in the dissociation of $\text{Ca}(\text{OH})_2$, but also in the decarbonation of CaCO_3 .

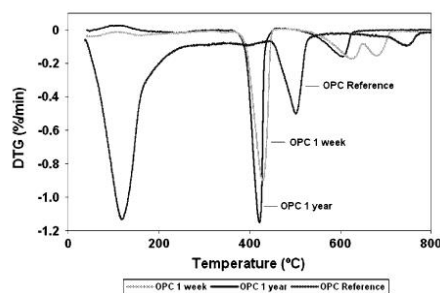


Fig. 6 Comparison between OPC specimens, reference, 1 week and 1 year after 800°C heat treatment

Above 750°C it can be seen that only the OPC reference has the third weight loss peak, confirming that no CaCO_3 was formed, indicating that its previous decarbonation was one of the sources for CaO rehydration and justifying therefore the higher quantity of $\text{Ca}(\text{OH})_2$ existed in heated specimens when compared to the unheated reference OPC specimen. Decarbonation was classified as an irreversible reaction by Short et al. [10].

Based on similar results, Short et al. [10] called the second weight loss peak, dehydration of $\text{Ca}(\text{OH})_2$, as a reversible reaction. Alonso and Fernandez [12] have also confirmed in their research in dehydration and rehydration processes of the cement paste exposed to high temperatures that the initial composition of $\text{Ca}(\text{OH})_2$ is recovered through rehydration.

When comparing the two OPC heat treated specimens, it was found that '1 year' specimens had a greater peak between 400 and 500°C than the '1 week' specimens. This shows that 1-year-old OPC specimens have a higher amount of $\text{Ca}(\text{OH})_2$ in their composition, indicating that rehydration continued with time. This explains the deterioration to powder found with the visual observations.

3.3.2 OPC/slag paste

Figure 7 presents the DTG curves for 50% Slag paste specimens. The curve for the 50% Slag reference specimen follows the same behaviour as the OPC reference specimen. However a different behaviour was found for 50% Slag heat treated specimens. While the quantity of $\text{Ca}(\text{OH})_2$ increased in OPC specimens throughout 1 year, an opposite behaviour for 50% slag



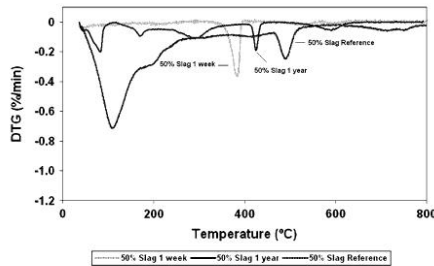


Fig. 7 Comparison between 50% Slag specimens, reference, 1 week and 1 year after 800°C heat treatment

was found. The greater peak between 400 and 500°C for 50% Slag 1 week shows that the quantity of $\text{Ca}(\text{OH})_2$ decreased throughout the period of 1 year. This implies that CaO rehydration in OPC/slag blends occurs within a short time after the heat treatment.

3.3.3 OPC paste versus OPC/slag paste

Figures 8 and 9 present a comparison between OPC and 50% Slag paste specimens for both short- and long-term effect, respectively. For short-term specimens, i.e. 1 week after the 800°C heat treatment, the peak which represents the dehydration of $\text{Ca}(\text{OH})_2$ is significantly greater for OPC paste specimens when compared to 50% Slag specimens. Thus the amount of $\text{Ca}(\text{OH})_2$ in the paste composition is higher for OPC specimens, showing that the rehydration of CaO is therefore greater in OPC.

In Fig. 9, for the long-term specimens, i.e. 1 year after the 800°C heat treatment, the difference between peak sizes at the temperature range of

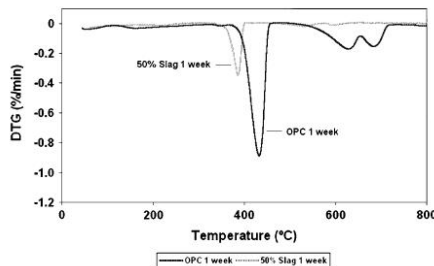


Fig. 8 Comparison between OPC and 50% Slag paste specimens 1 week after 800°C heat treatment

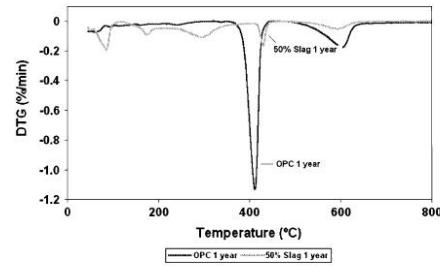


Fig. 9 Comparison between OPC and 50% Slag paste specimens 1 year after 800°C heat treatment

400–500°C was even greater than the difference for ‘1 week’ specimens, indicating that the rehydration of CaO throughout 1 year has much more significant effect in OPC pastes than in 50% Slag paste.

4 Conclusions

This work provides original data on the long-term progressive deterioration or otherwise of OPC and OPC/slag pastes following an initial exposure to high temperatures. Three steps were undertaken in this study: (i) visual observations, (ii) compressive strength tests and (iii) differential thermogravimetric analysis (DTG). To enable a comparison between short- and long-term behaviour of OPC and OPC/slag pastes after high temperature exposure two types of specimens were used: ‘1 week’ and ‘1 year’ after the 800°C heat treatment. Main results were:

1. Visual assessment of OPC paste 1 week after the 800°C heat treatment showed disintegration of the specimen while 1 year after those specimens were progressively reduced to powder. This long-term progressive deterioration of OPC paste has not been reported previously.
2. Visual assessment of OPC/slag paste 1 week after the 800°C heat treatment showed that specimens presented few to almost no cracks while 1 year after no significant change was found.
3. OPC paste presented no compressive strength after 800°C heat treatment. In the short-term, specimens suffered disintegration due to the CaO rehydration and in the long-term specimens were reduced to powder showing the

- long-term effects of CaO rehydration for OPC paste.
4. OPC/slag paste presented compressive strength in the range of 11–14 MPa 1 week after the 800°C heat treatment. No significant changes in compressive strength were found 1 year after the 800°C heat treatment.
 5. For OPC reference paste three main weight losses were found in differential thermogravimetric analysis. The first weight loss, between 100 and 200°C, is due to loss of capillary water, the second weight loss, between 400 and 500°C, is a result of the dehydration of Ca(OH)_2 , and the third weight loss, above 750°C is caused by the decarbonation of CaCO_3 .
 6. For OPC/slag reference paste similar behaviour to OPC paste was found. Differential thermogravimetric analysis has also showed the same three main weight losses.
 7. For OPC 800°C heat treated paste (1 week and 1 year after the 800°C heat treatment) the weight loss which corresponds to the dehydration of Ca(OH)_2 was detected. This confirms that rehydration of CaO into Ca(OH)_2 has occurred, resulting in an expansion of volume and therefore disintegration of the specimens.
 8. For OPC 800°C heat treated paste it was found that '1 year' specimens presented a higher amount of Ca(OH)_2 than '1 week' specimens, showing that for OPC paste the CaO rehydration phenomenon continues throughout the period of 1 year.
 9. For OPC/slag 800°C heat treated paste (1 week and 1 year) it was found that '1 week' specimens presented a higher amount of Ca(OH)_2 than '1 year' specimens. This shows that for those blends CaO rehydration occurs quickly after the heat treatment and reduces throughout the period of 1 year.
 10. Finally, when comparing OPC paste with OPC/slag paste it was found that both '1 week' and '1 year' OPC specimens presented a higher amount of Ca(OH)_2 than OPC/slag specimens, especially 1 year after the 800°C heat treatment. This confirms that OPC paste is more affected by the long-term effect of CaO rehydration than OPC/slag paste.

The results show that CaO rehydration progresses with time for OPC paste, resulting in severe deterioration in its structure, while this long-term effect is not found in OPC/slag blends. This implies that when a fire-damaged structure is repaired, a monitoring programme is needed to reassure the safety of the fire-damaged and in-service structure from long-term CaO rehydration damage.

Acknowledgment The authors gratefully acknowledge the Australian Research Council Discovery Grant No. DP0558463 for this research project.

References

1. Khoury GA (2000) Effect of fire on concrete and concrete structures. *Progr Struct Eng Mater* 2:429–447
2. Mendes A, Sanjayan J, Collins F (2008) Phase transformations and mechanical strength of OPC/Slag pastes submitted to high temperatures. *Mater Struct* 41:345–350
3. Diamond S (2001) Calcium hydroxide in cement paste and concrete—microstructural appraisal. *Materials science of concrete special volume: calcium hydroxide in concrete (USA)*. American Ceramic Society, Westerville, pp 37–58
4. Lea FC, Stradling RE (1922) The resistance to fire of concrete and reinforced concrete. *Engineering* 144:341–344, 380–382
5. Khoury GA (1992) Compressive strength of concrete at high temperatures: a reassessment. *Mag Concrete Res* 44:291–309
6. Petzold A, Rohrs M (1970) *Concrete for high temperatures*, 2nd edn. Maclaren and Sons Ltd, London
7. Harmathy TZ (1968) Determining the temperature history of concrete constructions following fire exposure. *ACI J* 65:959–964
8. Harmathy TZ (1993) *Fire safety design & concrete*. Longman Scientific & Technical, UK
9. Matesova D, Bonen D, Surenda PS (2006) Factors affecting the resistance of cementitious materials at high temperatures and medium heating rates. *Mater Struct* 39:919–935
10. Alarcon-Ruiz L, Platret G, Massieu M, Ehrlicher A (2005) The use of thermal analysis in assessing the effect of temperature on a cement paste. *Cement Concrete Res* 35:609–613
11. Short NR, Purkiss JA, Guise SE (2000) Assessment of fire damaged concrete using colour image analysis. *Constr Build Mater* 15:9–15
12. Alonso C, Fernandez L (2004) Dehydration and rehydration processes of cement paste exposed to high temperature environments. *J Mater Sci* 39:3015–3024



Chapter 5

Investigation of Repair Methods for Preventing Strength Loss of Ordinary Portland Cement Pastes after Fire Exposure

5.1 Overview

As discussed in Chapters 3 and 4, following exposure to elevated temperatures, ordinary Portland cement (OPC) paste presented total strength loss due to calcium oxide (CaO) rehydration. The present Chapter 5 investigates different repair methods to prevent strength loss of OPC pastes exposed to elevated temperatures.

This chapter is based on the publication of the same name as the chapter title submitted to Materials and Structures Journal in August 2010. This paper uses two different sealants, silicone and paraffin, with the aim to prevent moisture ingress into the OPC paste exposed to elevated temperatures, therefore preventing CaO rehydration. Visual observations and compressive strength tests were performed in OPC specimens uncoated or coated with either silicone or paraffin. The efficiency of the sealant was confirmed by infrared spectroscopy (IR) tests.

5.2 Declaration for Thesis Chapter 5

Declaration by candidate

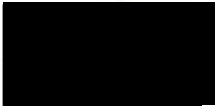
In the case of Chapter 5, the nature and extent of my contribution to the work was the following:

| Nature of contribution | Extent of contribution (%) |
|---|----------------------------|
| Developing outline of research objective and hypothesis Laboratory/experimental investigation and analysis of results Writing, reviewing and editing of paper | 85 |

The following co-authors contributed to the work. Co-authors who are students at Monash University must also indicate the extent of their contribution in percentage terms:

| Name | Nature of contribution | Extent of contribution (%) for student co-authors only |
|---------------|---|---|
| Jay Sanjayan | Developing outline of research objective and hypothesis Reviewing of paper | 5 |
| Frank Collins | Developing outline of research objective and hypothesis Reviewing of paper | 5 |
| Will P Gates | Developing outline of research objective and hypothesis Reviewing of paper | 5 |

Candidate's
Signature

| | |
|---|-------------------|
|  | 30 September 2010 |
|---|-------------------|

Declaration by co-authors

The undersigned hereby certify that:

- (1) the above declaration correctly reflects the nature and extent of the candidate's contribution to this work, and the nature of the contribution of each of the co-authors.
- (2) they meet the criteria for authorship in that they have participated in the conception, execution, or interpretation, of at least that part of the publication in their field of expertise;
- (3) they take public responsibility for their part of the publication, except for the responsible author who accepts overall responsibility for the publication;
- (4) there are no other authors of the publication according to these criteria;

- (5) potential conflicts of interest have been disclosed to (a) granting bodies, (b) the editor or publisher of journals or other publications, and (c) the head of the responsible academic unit; and
- (6) the original data are stored at the following location(s) and will be held for at least five years from the date indicated below:

Location(s)

| |
|--|
| Department of Civil Engineering, Monash University |
|--|

[Please note that the location(s) must be institutional in nature, and should be indicated here as a department, centre or institute, with specific campus identification where relevant.]

Signature 1



30 September 2010

Signature 2



30 September 2010

Signature 3



30 September 2010

5.3 Publication

Investigation of Repair Methods for Preventing Progressive Strength Loss of Ordinary Portland Cement Pastes after Fire Exposure

Alessandra Mendes¹, Jay G Sanjayan², Frank Collins¹, Will P Gates¹

¹*Civil Engineering Department, Monash University, Clayton VIC, Australia*

²*Faculty of Engineering and Industrial Sciences, Swinburne University of Technology, Hawthorn VIC, Australia*

Abstract

The present work investigates the use of two sealants (silicone and paraffin) to reduce the progressive strength loss of ordinary Portland cement (OPC) pastes following exposure to elevated temperatures due to the rehydration of CaO into CaOH₂. After oven exposure to 800°C and cooling to 100 °C, the sealants were applied to the samples to reduce moisture ingress from air. Coated and uncoated specimens were exposed to air moisture for 1 week. Compressive strength results revealed that OPC pastes coated with paraffin presented 15% of residual strength. On the other hand, the OPC pastes coated with silicone presented less than 2.5% while the uncoated specimens presented total strength loss and complete disintegration. Infrared spectroscopy confirmed these results, revealing that uncoated OPC pastes presented the highest peak intensity for CaOH₂. OPC pastes coated with silicone presented CaOH₂ peak 16 times more intense than the OPC pastes coated with paraffin. The latter presented a very minor CaOH₂ peak intensity, showing the efficiency of the paraffin in acting as a barrier to reduce the moisture ingress and therefore, CaO rehydration. When a concrete structure is exposed to a fire event, the effects of rehydration of CaO due to moisture ingress from air can be reduced by applying a coating to the exposed surfaces. This has shown to be an effective method in maintaining residual strength.

Keywords: OPC pastes, strength loss, fire exposure, repair

1 Introduction

One of the key properties of concrete is the durability when exposed to elevated temperatures, as in a fire event. Therefore, the fire resistance of concrete has been the focus of researchers since 1922 [1]. When concrete is exposed to elevated temperatures, physical and chemical transformations take place resulting in deterioration of its mechanical properties.

The critical temperature of 400°C for the breakdown of ordinary Portland cement (OPC) pastes has been reported [1-3]. Above 400°C, one of the main hydrates of the OPC paste, calcium hydroxide (CaOH_2) dehydrates into calcium oxide (CaO) causing the OPC paste to shrink and crack [1-3]. After cooling and in the presence of air moisture, CaO rehydrates into CaOH_2 causing expansion, total strength loss and complete disintegration of the OPC paste [3-5].

In contrast, the dehydration of CaOH_2 and rehydration of CaO caused no significant deterioration in pastes where OPC was partially replaced with slag [3, 4, 6]. Ground granulated blast furnace slag ('slag') is a by-product of the iron and steel industries. During hydration, slag consumes most of the available CaOH_2 [7], therefore reducing or even eliminating the negative effects of CaOH_2 dehydration and CaO rehydration. This is illustrated in Fig. 1, which presents the compressive strength of OPC and OPC/slag pastes exposed to temperatures up to 800°C. OPC/slag pastes consist of pastes in which the OPC has been partially replaced (i.e., 35, 50 and 65% by weight) with slag. This further confirms the negative effects caused by the CaO rehydration when the OPC paste is exposed to elevated temperatures.

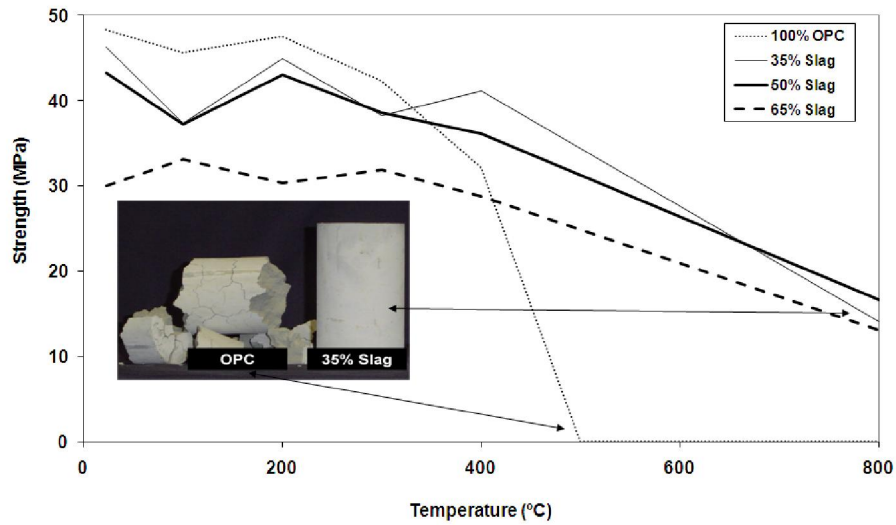


Fig. 1 OPC and OPC/slag pastes after exposure to temperatures up to 800°C

The progressive strength loss observed for OPC pastes exposed to elevated temperatures followed by exposure to moisture is of extreme concern as the majority of the concrete structures are built with OPC paste as the main binder of the aggregates. Therefore, this progressive strength loss should be considered a major repair issue for fire damaged structures. Unfortunately, this progressive strength loss of OPC pastes after a fire event is not widely recognised by engineers who are involved in the rehabilitation of these structures.

When a fire event occurs, emergency response by water extinguishing is usually undertaken, providing a ready supply of moisture for the rehydration of CaO. However, in some cases, not all of the structure is wetted by extinguishing and regions remain dry. Over time, ongoing exposure to air moisture would provide the necessary means for CaO rehydration and consequently, damage to the structure.

Based on that, the present work investigates two sealants that could potentially be used as a barrier to moisture ingress and therefore limit the CaO rehydration. The two sealants investigated are: soft paraffin and general purpose silicone. Following sealant application, the mechanical properties of the OPC paste were investigated by compressive strength tests. Infrared spectroscopy (IR) was conducted in order to determine the efficiency of the sealants in eliminating the negative effects of the CaO rehydration in OPC pastes after exposure to elevated temperatures.

2 Experimental procedure

Ordinary Portland cement (OPC) conforming to the requirements of Australian Standard AS 3972 was used as the binder material. Its chemical composition and properties are presented in Table 1. The OPC used in this study has a low C_3A content of < 5%.

Table 1 Chemical composition and properties of OPC

| Constituent/property | % weight |
|--------------------------------|----------|
| SiO ₂ | 19.90 |
| Al ₂ O ₃ | 4.70 |
| Fe ₂ O ₃ | 3.38 |
| MgO | 1.30 |
| CaO | 63.93 |
| Na ₂ O | 0.17 |
| TiO ₂ | 0.245 |
| K ₂ O | 0.446 |
| MnO | 0.079 |
| P ₂ O ₅ | 0.063 |
| SO ₃ | 2.54 |
| LOI | 2.97 |
| Fineness, m ² /kg | 360 |
| Specific gravity | 3.15 |

OPC paste cylinder specimens of diameter 50 mm and length 100 mm were investigated. The specimens consisted of pastes. The water/cement (w/c) ratio used was 0.5.

The mixture was prepared by adding water and the binder to a mechanical mixer of 20 litres of capacity, 80 rpm, followed by mixing for five minutes. The cylinder specimens were cast and compacted using a vibration table, and sealed with a plastic sheet and demolded after 24 hours. Demolding was followed by 28 days curing in lime-saturated water bath at 23°C.

Before exposure to elevated temperatures, the specimens were oven-dried for 2 days at 60°C. Following drying, heat exposure to 800°C was conducted. The heat treatment was as follows: constant heating rate of 6.25°C/min until 750°C, then 1 hour between 750-800°C, and finally 1 hour at 800°C. To limit moisture ingress in

the specimens, they were kept in the oven and cooled until the furnace temperature reduced to 100°C, following which the specimens were removed. Immediately after removal from the furnace the specimens were coated with a soft paraffin or a general purpose silicon. For easy reference those will be referred as 'paraffin' and 'silicone' throughout the manuscript. For comparison some specimens remained uncoated and will be referred as 'air moisture' to reflect their free exposure to air moisture.

Silicone is thermal stable in temperatures up to 250°C [8] and have high permeability to water vapour [9]. Paraffin has been reported to have a melting point of approximately 50°C [10] and a very low permeability to water vapour [11]. The paraffin application required constant repetition as the paraffin melted at the temperature of 100°C. The paraffin was reapplied when the temperature was ambient to a thickness layer ≥ 2 mm. The melting was not observed with the silicone, and an instant layer ≥ 2 mm was formed on the surface of the OPC paste specimens.

Following treatment with the coatings, all specimens (coated and uncoated) were exposed to air moisture in a controlled temperature room at 23°C and 80% relative humidity for one (1) week. After 1 week, compressive strength tests were conducted, using a loading rate of 20 MPa/min. The results reported are an average of 3 specimens for each of the 3 specimens variables investigated: paraffin, silicone and air moisture. Immediately after the compressive strength tests, Infrared spectroscopy (IR) was conducted using a FTS 3000 MX Excalibur Series Digilab fitted with a glow bar radiation source, a DTGS detector, dry CO₂-free air purge and an extended KBr beamsplitter. The sample space was continuously purged with dry nitrogen. As many as 512 acquisitions were co-added at a resolution of 2 cm⁻¹ on powdered specimens mixed (~ 5%) with sodium chloride (ACS). Each spectrum was referenced to NaCl and converted to Kubelka-Munk absorbance units for comparison.

3 Results and discussion

3.1 Visual observations

Visual observations are usually the first step undertaken during the assessment of a fire-damaged concrete structure as they enable the determination of colour changes, crazing, cracking and spalling [12]. In the present work the visual assessment was performed at: (a) immediately after removal from the furnace and application of paraffin, silicone or none; (b) one-week after air moisture exposure (after removal from furnace).

As described in Section 2, the OPC paste specimens were removed from the furnace at 100°C and the sealants were applied immediately after. The specimens presented minor visual cracks when removed from the furnace and prior to the sealant application. Once the paraffin was applied on the specimens, it immediately started to melt and became liquid. Continuous application was made until approximately 2-3 mm thickness was achieved. The paraffin was reapplied when the specimens reached room temperature.

For the silicone, the melting was not observed and a silicone layer ≥ 2 mm was formed instantly. For visual comparison, Fig. 2 presents 3 specimens immediately after removal from furnace/sealant application. The specimen on the left has been coated with paraffin. The specimen on the centre has been coated with silicone while the specimen on the right has not been coated and it is directly exposed to air moisture.

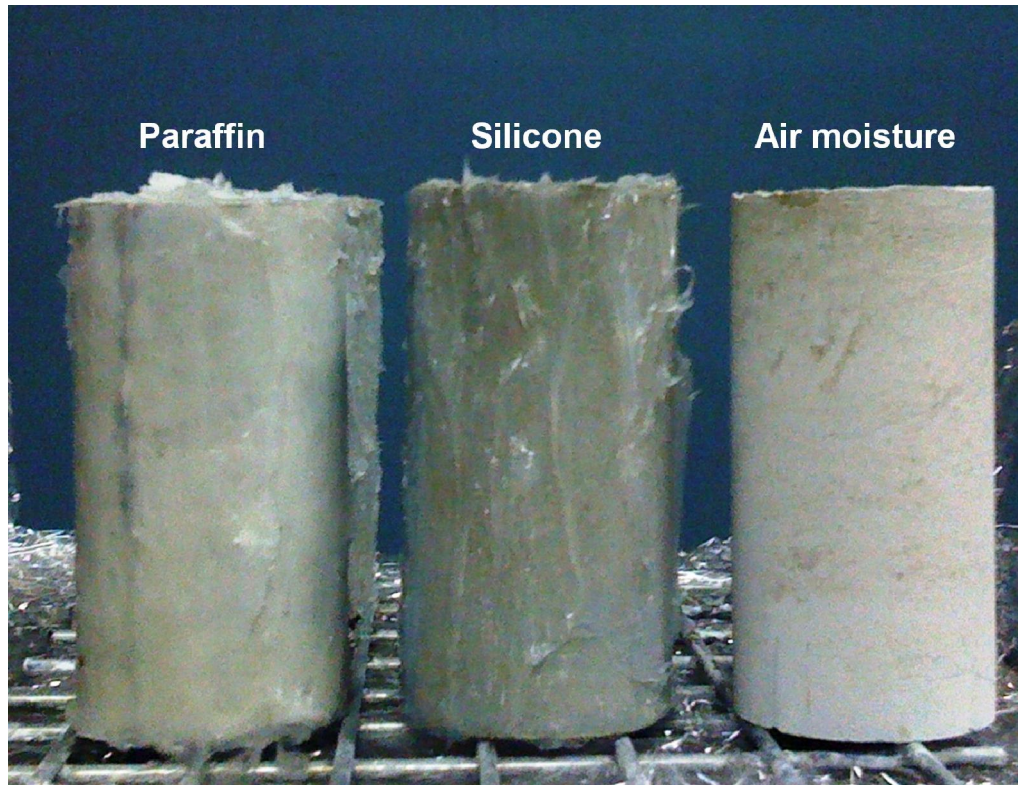


Fig. 2 OPC pastes specimens immediately after removal from furnace at 100°C followed by sealant application (left and centre specimens)

While only minor cracks were observed after removal from the furnace, Fig. 2 shows that there are no major visual differences between the specimens after the sealant application or the uncoated specimen labelled as 'air moisture'.

However, Fig. 3 shows that major differences are present after 1 week of air moisture exposure. For the specimens coated with paraffin no visual differences can be found between Fig. 2 and Fig. 3. For the specimens coated with silicone, Fig. 3 shows that 1 week exposure to air moisture has led to microcracks (bottom of the specimen). This is likely to be due to the high permeability to water vapour presented by the silicone [9]. This is better visualised in Fig. 4 (arrow). For the specimen with no sealant (labelled 'air moisture') large cracks appeared which led to complete disintegration of the specimen.

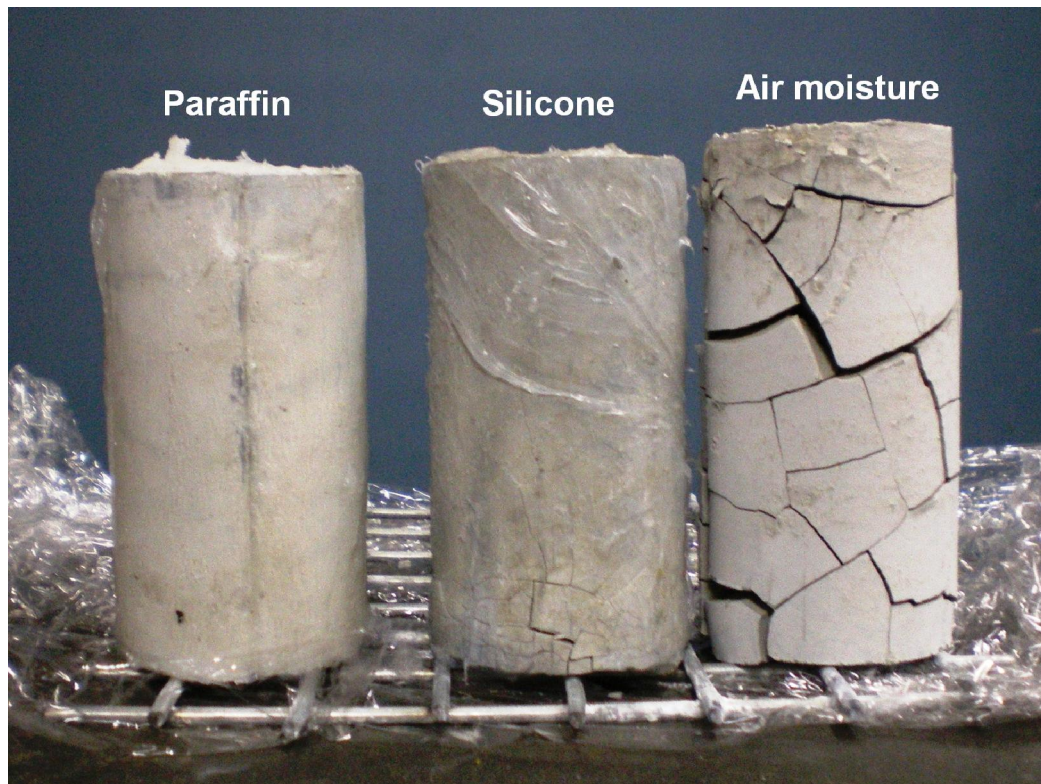


Fig. 3 OPC pastes specimens 1 week after exposure to air moisture



Fig. 4 Enlargement of OPC paste coated with silicone 1 week after exposure to air moisture

3.2 Compressive strength tests

Following visual observations, compressive strength tests were performed on all specimens. Fig. 5 presents the average residual compressive strength results for the OPC pastes coated with paraffin, silicone and uncoated samples after completion of heat exposure followed by 1 week of air moisture. The hot strength values are also presented, indicating that the exposure to 800°C caused the OPC pastes to lose 80% of the initial strength. After cooling and in the presence of air moisture for 1 week, the uncoated specimens ('air moisture') present total strength loss.

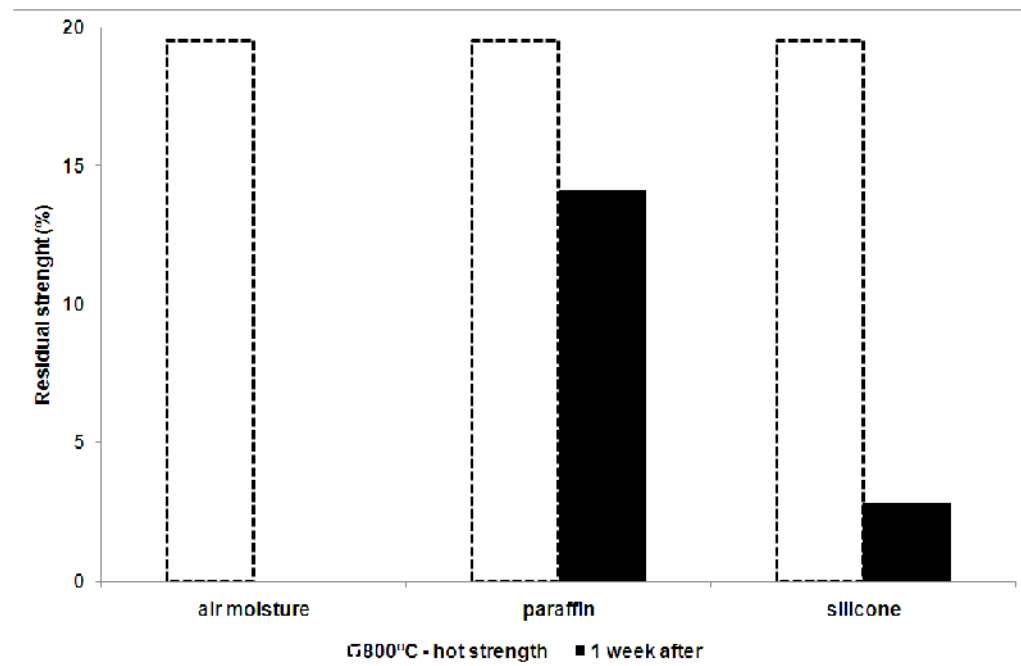


Fig. 5 Residual compressive strength of OPC pastes exposed to 800°C. Dashed line refers to the hot strength at 800°C. Black columns refer to the residual strength after 1 week of exposure to air moisture

As reported previously [3, 4], the total strength loss presented by OPC specimens after 800°C followed by exposure to air moisture is due to the dehydration of CaOH_2 followed by the rehydration of CaO .

For the coated specimens, a different scenario was found. The specimens coated with paraffin presented residual strength of almost 15%. On the other hand, specimens coated with silicone presented residual strength of less than 2.5%.

The difference in residual strength for the specimens coated with paraffin and silicone is related to the efficiency of the sealant in preventing the CaO rehydration, i.e., the ingress of moisture in the OPC pastes.

As described in Section 3.1, when the paraffin was applied to the OPC paste after removal from the furnace at 100°C, it melted (melting point ~ 50°C [10]) and became liquid possibly penetrating through the porous paste. This was not observed for the silicone coating, which immediately formed a layer on the surface of the OPC paste specimen (thermal stable up to 250°C [8]). This is clearly seen in Fig. 6, which presents paraffin and silicone specimens after the compressive strength test was performed.

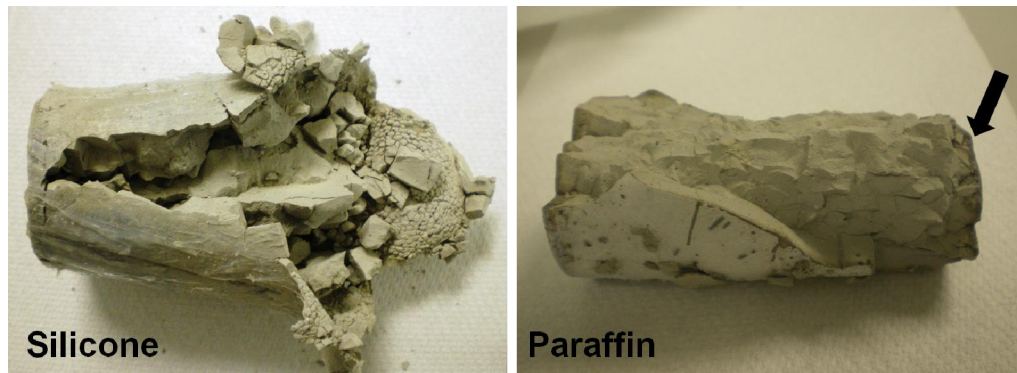


Fig. 6 OPC paste specimens coated with silicone or paraffin (after compressive strength tests)

It is possible to see that there is a difference in the type of fracture presented by the OPC paste specimens coated with silicone or paraffin. The specimen coated with silicone seems to have formed a thick flexible skin caused by the silicone coating, but a crumbled interior. For the specimen coated with paraffin this was not found, being in accordance with the higher residual strength for these specimens, 6 times greater than the specimens coated with silicone. Also in Fig. 6, a darker line of approximately 2 mm can be seen near the surface of the OPC paste coated with paraffin (black arrow, Fig. 6). This confirms that the melted paraffin penetrated into the paste, possibly creating a barrier for the air moisture ingress and therefore the rehydration of CaO.

3.3 Infrared spectroscopy

Infrared spectroscopy (IR) was conducted to determine whether CaO rehydration into CaOH_2 has taken place. The choice of this technique to determine the presence of CaOH_2 was first due to the efficiency of the method in determining CaOH_2 , as reported by previous studies [13-15]. Second, it was due to IR being capable of readily being utilised immediately after compressive strength tests were performed, therefore, assuring precision in determining CaOH_2 presence, considering its variation with time [3, 4].

In the IR spectrum, the peak at approximately 3644 cm^{-1} relates to CaOH_2 [13-16]. Fig. 7 shows the different spectra obtained for OPC pastes coated with silicone, paraffin and uncoated ('air moisture').

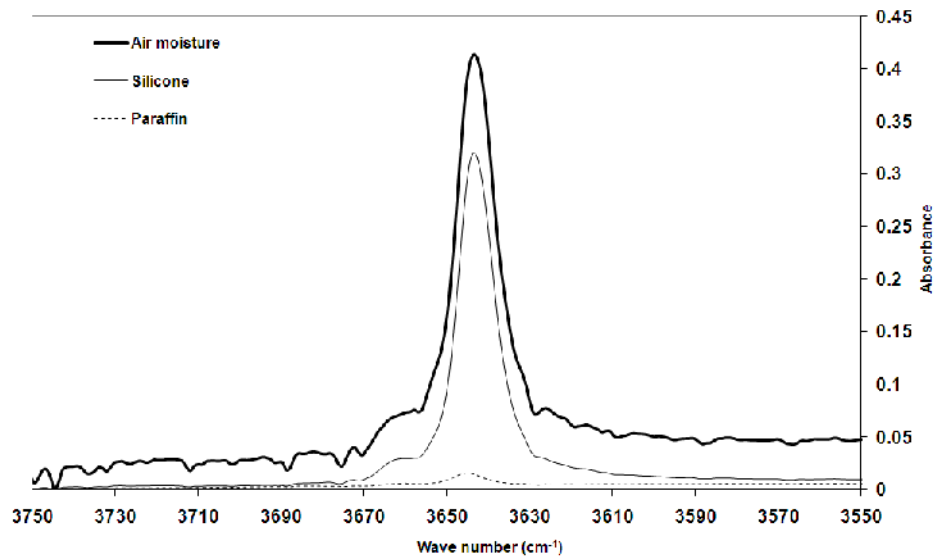


Fig. 7 IR spectra of the OPC pastes after exposure to 800°C , followed by air moisture exposure for 1 week

The uncoated OPC paste ('air moisture') has a CaOH_2 peak intensity almost 1.3 times greater than the OPC paste coated with silicone. In addition, a significant less intense peak is observed for the OPC paste coated with paraffin. Its peak is 16 times less intense than the OPC paste coated with silicone. Therefore, it can be concluded that the paraffin has acted as an effective barrier for moisture ingress, reducing the occurrence of the CaO rehydration.

Furthermore, Fig. 8 presents the IR wave number ranges related to paraffin (a) and silicone (b).

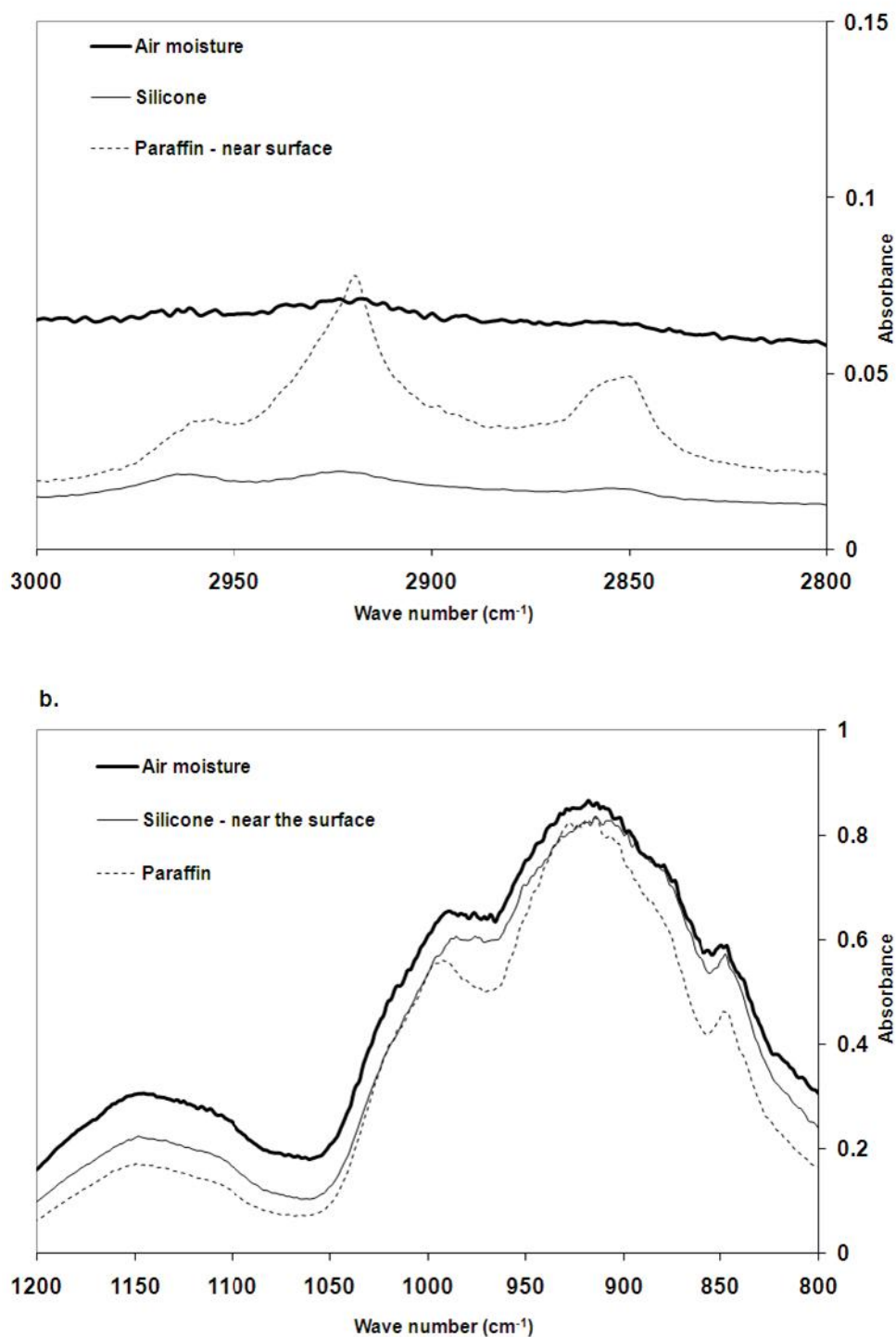


Fig. 8 IR spectra of the OPC pastes after exposure to 800°C, followed by air moisture exposure for 1 week (a. wave number range related to paraffin and b. wave number range related to silicone)

Fig. 8a presents the spectrum of samples obtained from the near surface of the specimen, showing that the paraffin has penetrated into the OPC specimen (as indicated in Fig. 6). In contrast, Fig. 8b shows the absence of the silicone peak for the silicone coated specimens (samples obtained from the near surface), confirming that the penetration of silicone into the OPC specimens did not occur.

4 Conclusions

The present work investigated the use of two sealants (silicone and paraffin) to reduce the negative effects of CaO rehydration on the mechanical properties of OPC pastes exposed to elevated temperatures.

It was found that 1 week after exposure to air moisture, the 800°C heat exposed OPC pastes coated with paraffin presented 15% of residual strength. On the other hand, the OPC pastes coated with silicone presented less than 2.5% of residual strength while the uncoated specimens presented total strength loss and complete disintegration. The total strength loss is a result of the dehydration of CaOH_2 during heating followed by the rehydration of CaO during cooling and exposure to air moisture.

Infrared spectroscopy revealed that uncoated OPC pastes presented the highest peak intensity for CaOH_2 , confirming the strength results trend. OPC pastes coated with silicone had a CaOH_2 peak 16 times more intense than the OPC pastes coated with paraffin. The OPC pastes coated with paraffin presented a very minor CaOH_2 peak intensity, showing the efficiency of this material in acting as a barrier to reduce the moisture ingress and therefore, CaO rehydration. This is in accordance with the compressive strength results obtained.

The finding from this study has practical relevance for repair of concrete structures with OPC as the binder following a fire event, since it has identified the progressive deterioration and impairment of compressive strength due to ingress of airborne water vapour. The concrete following a fire exposure may be immediately protected by a coating that will ensure that some residual strength is partially retained, avoiding complete deterioration that was shown to occur for uncoated specimens.

The authors recommend future research in different sealant materials in order to achieve an optimal system.

Acknowledgements

The authors gratefully acknowledge the Australian Research Council Discovery Grant No. DP0558463 for this research project.

5 References

1. Lea FC, Stradling RE (1922) The resistance to fire of concrete and reinforced concrete. *Engineering* 144: 341-344; 380-382
2. Dias WPS, Khoury GA, Sullivan PJE (1990) Mechanical Properties of Hardened Cement Paste Exposed to Temperatures up to 700°C (1292°F). *ACI Materials Journal* 87: 160-166
3. Mendes A, Sanjayan J, Collins F (2008) Phase transformations and mechanical strength of OPC/Slag pastes submitted to high temperatures. *Materials and Structures* 41: 345-350
4. Mendes A, Sanjayan J, Collins F (2009) Long-term progressive deterioration following fire exposure of OPC versus slag blended cement pastes. *Materials and Structures* 42: 95-101
5. Petzold A, Rohrs M (1970) *Concrete for high temperatures*. 2nd edition, Maclaren and Sons Ltd, London
6. Khoury GA (1992) Compressive strength of concrete at high temperatures: a reassessment. *Magazine of Concrete Research* 44: 291-309
7. Mehta PK, Monteiro PJM (2006) *Concrete microstructure, properties and materials*. McGraw-Hill, New York
8. Clarson SJ (2003) Silicones and Silicone-Modified Materials: A Concise Overview, in *ACS Symposium Series*. Washington, DC. American Chemical Society 838: 1-10

9. Colas A (2007) Silicones in Industrial Applications, in Inorganic Polymers, Jaeger R and Gleria M, Editors, Nova Science Publishers, pp. 61-161
10. Sharma A, Sharma SD, Buddhi D (2002) Accelerated thermal cycle test of acetamide, stearic acid and paraffin wax for solar thermal latent heat storage applications. *Energy Conversion and Management* 43: 1923-1930
11. Gontard N, Marchesseau S, Cuq JL, Guilbert S (1995) Water vapour permeability of edible bilayer films of wheat gluten and lipids. *International Journal of Food Science and Technology* 30: 49-56
12. Short NR, Purkiss JA, Guise SE (2001) Assessment of fire damaged concrete using colour image analysis. *Construction and Building Materials* 15: 9-15
13. Gao XF, Lo Y, Tam CM, Chung CY (1999) Analysis of the infrared spectrum and microstructure of hardened cement paste. *Cement and Concrete Research* 29: 805-812
14. Hanna RA, Barrie PJ, Cheeseman CR, Hills CD, Buchler PM, Perry R (1995) Solid state ^{29}Si and ^{27}Al NMR and FTIR study of cement pastes containing industrial wastes and organics. *Cement and Concrete Research* 25: 1435-1444
15. Mollah MYA, Yu W, Schennach R, Cocke DL (2000) A Fourier transform infrared spectroscopy investigation of the early hydration of Portland cement and the influence of sodium lignosulfonate. *Cement and Concrete Research* 30: 267-273
16. Mollah MYA, Kesmez M, Cocke DL (2004) An X-ray diffraction (XRD) and Fourier transform infrared spectroscopy (FT-IR) investigation of the long-term effect on the solidification/stabilization (S/S) of arsenic (V) in Portland cement type V. *Science of the Total Environment* 325: 255-262

Chapter 6

NMR, XRD, IR and Synchrotron NEXAFS

Spectroscopic Studies of OPC and OPC/Slag Cement Paste Hydrates

6.1 Overview

Chapters 2 to 5 discussed the negative effects of the calcium hydroxide (CaOH_2) dehydration and calcium oxide (CaO) rehydration on the mechanical properties of ordinary Portland cement (OPC) pastes exposed to elevated temperatures. The present Chapter 6 shows that most of the available literature on the effects of elevated temperatures on the cement paste has focused on the role of the paste hydrate CaOH_2 . On the other hand, very few studies have investigated the role of the other paste hydrates, such as calcium silicate hydrate (C-S-H), ettringite and monosulphate hydrate.

This chapter is based on the publication of the same name as the chapter title submitted to Materials and Structures Journal in January 2010. This paper investigates the fundamental similarities and/or differences between OPC and OPC/slag paste hydrates at room temperature, forming the basis to assist in the identification of changes in the paste hydrates after exposure to elevated temperatures. The following techniques are used in the present investigation: silicon and aluminium nuclear magnetic resonance (^{29}Si NMR and ^{27}Al NMR), X-ray diffraction (XRD), infrared (IR) and synchrotron Si K-edge near edge X-ray absorption fine structure (NEXAFS) spectroscopy.

6.2 Declaration for Thesis Chapter 6

Declaration by candidate

In the case of Chapter 6, the nature and extent of my contribution to the work was the following:

| Nature of contribution | Extent of contribution (%) |
|---|----------------------------|
| Developing outline of research objective and hypothesis Laboratory/experimental investigation and analysis of results Writing, reviewing and editing of paper | 85 |

The following co-authors contributed to the work. Co-authors who are students at Monash University must also indicate the extent of their contribution in percentage terms:

| Name | Nature of contribution | Extent of contribution (%) for student co-authors only |
|---------------|---|---|
| Jay Sanjayan | Developing outline of research objective and hypothesis Reviewing of paper | 2.5 |
| Frank Collins | Developing outline of research objective and hypothesis Reviewing of paper | 2.5 |
| Will P Gates | Developing outline of research objective and hypothesis Reviewing of paper | 10 |

Candidate's
Signature



30 September 2010

Declaration by co-authors

The undersigned hereby certify that:

- (1) the above declaration correctly reflects the nature and extent of the candidate's contribution to this work, and the nature of the contribution of each of the co-authors.
- (2) they meet the criteria for authorship in that they have participated in the conception, execution, or interpretation, of at least that part of the publication in their field of expertise;
- (3) they take public responsibility for their part of the publication, except for the responsible author who accepts overall responsibility for the publication;
- (4) there are no other authors of the publication according to these criteria;

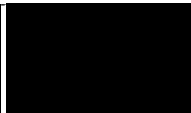
- (5) potential conflicts of interest have been disclosed to (a) granting bodies, (b) the editor or publisher of journals or other publications, and (c) the head of the responsible academic unit; and
- (6) the original data are stored at the following location(s) and will be held for at least five years from the date indicated below:

Location(s)


| |
|--|
| Department of Civil Engineering, Monash University |
|--|

[Please note that the location(s) must be institutional in nature, and should be indicated here as a department, centre or institute, with specific campus identification where relevant.]

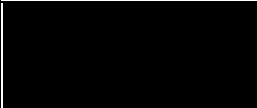
Signature 1

| | |
|---|--------------------------|
|  | 30 September 2010 |
|---|--------------------------|

Signature 2

| | |
|--|--------------------------|
|  | 30 September 2010 |
|--|--------------------------|

Signature 3

| | |
|---|--------------------------|
|  | 30 September 2010 |
|---|--------------------------|

6.3 Publication

NMR, XRD, IR and Synchrotron NEXAFS Spectroscopic Studies of OPC and OPC/slag cement paste hydrates

Alessandra Mendes, Will P Gates, Jay G Sanjayan, Frank Collins

Department of Civil Engineering, Monash University, Wellington Road, Clayton VIC
3800 Australia

Alessandra.mendes@monash.edu, ph. +61 3 9905 1849, fax +61 3 9905 4944

Abstract

This work aims to determine the fundamental similarities and/or differences between OPC and OPC/slag paste hydrates. OPC and 35% slag pastes are investigated using five techniques: ^{29}Si NMR, ^{27}Al NMR, X-ray diffraction (XRD), infrared (IR) and synchrotron near edge X-ray absorption fine structure (NEXAFS) spectroscopy. ^{29}Si NMR provides valuable information related to the formation of the C-S-H gel, the main hydrated phase of the cement paste. ^{27}Al NMR is a useful tool to characterize calcium aluminates and aluminate hydrates such as ettringite and monosulphate hydrate. XRD identifies polycrystalline phases of the hardened cement paste, including ettringite, monosulphate and CaOH_2 . Vibrational frequencies in IR assist in identifying the silicate, sulphate and carbonate phases of the cement paste. As far as we are aware, Si K-edge NEXAFS has never been applied in cement research and its advantages and disadvantages are discussed. Using these techniques, a comparison between OPC and 35% slag paste hydrates is made, shedding light on differences in the amount and form of hydrated phases present, especially the absence of ettringite in the 35% slag paste.

Keywords: cement, slag, paste hydrates, NMR, XRD, IR

1 Introduction

For decades ground granulated blast furnace slag ('ggbfs' or 'slag') has been widely used as a partial replacement for ordinary Portland cement (OPC) in concrete. The use of slag as a partial substitute for OPC in blended cements not only utilizes waste produced by the steel industry, but most importantly reduces the carbon dioxide emissions arising from cement making [1]. In addition, using slag as a partial substitute for OPC in concrete include an improvement in certain properties: e.g., lower heat of hydration, which decreases the cracking risk within large concrete pores; increased durability to sulphate attack; and better resistance to chloride diffusion which is known to pose a corrosion risk to reinforcement materials [2].

Those and other properties that lead to enhanced practical performance of cement/concrete are directly related to the presence and amount of paste hydrated within the paste. Chemical and physical properties are directly dependent on these cement paste hydrates.

The hydrated ordinary Portland cement paste is formed by many constituents. The calcium silicate hydrate (C-S-H) phase is the main product of Portland cement hydration. Portlandite, or calcium hydroxide CaOH_2 , is the second most abundant product in the hydrated Portland cement paste. It is present in the form of relatively large crystalline aggregates [3]. The AFt (ettringite) and AFm (monosulphate hydrate) phases are present in amounts that depend on the amount of tricalcium aluminate (C_3A) and ferrite phases in the original cement. Ettringite has needle-shaped prismatic crystal form and will eventually transform into monosulphate hydrate, having hexagonal-plate crystal form. The degree of AFt to AFm conversion differs in different cements [3]. Minor constituents of the hydrated Portland cement paste may include a poorly crystalline siliceous hydrogarnet which accommodates a significant fraction of the iron originally present in the ferrite phase [3]. The amount of 'bound' ('combined') water present in the hardened Portland cement paste depends on the phase composition of the original cement, on the degree of hydration and also on the way in which the term 'bound water' has been defined [3].

When ordinary Portland cement is partially replaced with slag the hydration products are expected to be similar to those formed in the OPC hydrated paste [4]. However, the quantities of $\text{Ca}(\text{OH})_2$ in OPC/slag blends are expected to be lower than the quantities found in OPC pastes [4].

As will be discussed in detail (Section 3), numerous studies have focused on cement paste hydrates, especially for OPC pastes. However, a greater number of those studies have focused on the C-S-H phase, probably due to its relationship with paste strength. Limited studies have focused on the possible roles the other paste hydrates, e.g., ettringite and monosulphate hydrate, may play on the chemical and physical properties of the cement paste. For OPC/slag blends those studies are even more limited.

Previous work by the authors [1, 5] identified the difference between CaOH_2 content in OPC and OPC/slag pastes at room temperature as the main cause for deterioration of OPC mechanical properties after exposure to elevated temperatures. When OPC is heated above 400°C , CaOH_2 dehydrates into CaO causing the OPC paste to contract, resulting in microcracks. After cooling and during exposure to air moisture, CaO rehydrates into CaOH_2 causing the OPC paste to expand and ultimately disintegrate. In comparison, for OPC/slag pastes, during hydration slag consumes most of the available CaOH_2 , consequently reducing or even eliminating the negative effects caused by CaOH_2 dehydration and CaO rehydration when cement paste is submitted to elevated temperatures.

However, it is important to identify the contributions, if any, of the other hydrates such as C-S-H, ettringite and monosulphate hydrate to the deterioration of the mechanical properties of OPC and OPC/slag pastes after exposure to elevated temperatures.

Therefore, the main aim of this study is to identify the fundamental similarities and/or differences between OPC and OPC/slag paste hydrates at room temperature using the following techniques: silicon and aluminium nuclear magnetic resonance (^{29}Si NMR and ^{27}Al NMR), X-ray diffraction (XRD), infrared (IR) and synchrotron Si K-edge near edge X-ray absorption fine structure (NEXAFS) spectroscopy. The present study will also attempt to correlate the data obtained from each of the above techniques. This ensures that the uncertainties and

limitations of each technique are minimized and a more comprehensive and accurate conclusion is drawn. This information forms the basis to assist in the identification of changes in the paste hydrates in OPC and OPC/slag blends after exposure to elevated temperatures. The contribution of the paste hydrates to the deterioration of the mechanical properties of the cement paste will be also addressed. This secondary aim is currently underway and will be reported in a later date.

As described previously, five different techniques will be used in the present investigation: ^{29}Si NMR, ^{27}Al NMR, XRD, IR and NEXAFS. As a bulk method, NMR probes the local environment surrounding particular nuclei, i.e., at the scale of nearest-neighbour (NN) and next-nearest-neighbour (NNN). An NMR signal is independent on sample crystallinity and largely dependent on the symmetry about the nuclei. Thus phases that may be undetected by XRD or IR can be observed using solid state silicon (^{29}Si) and aluminium (^{27}Al) NMR spectroscopy, which provides the opportunity to characterize the various phases present in cement pastes. For ^{27}Al NMR, the coordination environment about Al can be readily discerned, with chemical shifts occurring between (-10 and 15 ppm) for octahedral and (50 and 80 ppm) for tetrahedral coordination [6]. Shifts within these ranges are as much a function of bond length and bond valence as they are related to polymerisation. For ^{29}Si NMR, the chemical shift is strongly indicative of the degree of polymerization and hydration of the silicate phases, since silicon nearly ubiquitously has tetrahedral coordination. Paramagnetic nuclei (i.e., Fe, Mn) can result loss in ^{29}Si , and particularly ^{27}Al signal, if present in significant amounts, generally greater than ~ 3 wt% [6].

X-ray diffraction is a bulk technique, but specifically provides information only on the crystalline minerals present in cements, which are a complex mixture of highly crystalline, poorly crystalline and even amorphous phases. Generally, poorly crystalline mineral phases lack long-range order, and therefore high periodicity in interatomic distances in repeated structural units, and result in broadened diffraction bands of low intensity [7]. Highly crystalline mineral phases are generally observed as sharp and intense reflections, whereas amorphous (or X-ray transparent) materials will be only observed as an increased background underlying the reflections of the more crystalline phases.

Infrared is a bulk method that probes all anionic functional groups having vibrating dipole moments, making it useful as a tool for studying cements. The interaction of infrared radiation with material depends in part upon the short range distributions and symmetry of ligands, and also the bond-valence of the ligand dipole under study [8]. Particularly useful are the vibrational dipoles of hydroxyl (OH), bound or H-bonded water (HOH), carbonate (CO_3), sulphate (SO_4) and silicate (SiO_2) ligands.

Diffuse reflectance Fourier transform infrared (DRIFT IR) spectroscopy enhances the intensities of many mid IR bands associated with the O-H, C-O and S-O ligands, with respect to Si-O ligand [9]. DRIFT IR also requires minimal sample handling and spectral manipulation post collection.

Synchrotron based NEXAFS spectroscopy is another bulk method that, because of the ability to 'tune' the incident X-ray source to energies specific to an element of interest, can be used to study components containing individual elements. The processes responsible for NEXAFS spectra are related to the ejection of core electrons to unoccupied electronic states as well as into 'continuum states', the latter which involve single and multiple scattering events off the first few atomic shells surrounding the absorber [10]. Thus, NEXAFS spectroscopy contains information regarding the electronic configuration of the absorbing atom [11] which is related to the average local chemical and bonding environment (NN and NNN), but also beyond NNN due to multiple scattering processes in the continuum. For the 2p elements (e.g., Al and Si) the K-edge amplitude and position are dependent on site symmetry, bond angles, inter-atomic distances and NN/NNN identity [12].

2 Experimental procedure

2.1 Materials

Ordinary Portland cement (OPC) and ground granulated blast furnace slag (GGBFS or “slag”), conforming with the requirements of Australian Standard AS 3972 [13] were used as binder materials. The chemical composition and properties of the binders are presented in Table 1. The OPC used in this study has a low C_3A content of < 5%.

Table 1 Chemical composition and properties of the binders

| Constituent/property % | OPC | Slag |
|----------------------------------|-------|------|
| SiO ₂ | 19.90 | 32.5 |
| Al ₂ O ₃ | 4.70 | 13 |
| Fe ₂ O ₃ T | 3.38 | 0.22 |
| MgO | 1.30 | 5.47 |
| CaO | 63.93 | 42.1 |
| Na ₂ O | 0.17 | 0.21 |
| TiO ₂ | 0.245 | 1.08 |
| K ₂ O | 0.446 | 0.25 |
| MnO | 0.079 | 5.47 |
| P ₂ O ₅ | 0.063 | bd* |
| SO ₃ | 2.54 | 4.1 |
| LOI | 2.97 | 0.35 |
| Fineness, m ² /kg | 360 | 435 |
| Specific gravity | 3.15 | 2.92 |

*bd: below detection

In this investigation OPC was partially replaced with 35% by weight with slag. The term water/binder (w/b) ratio is used instead of the water/cement ratio to include both binder types mentioned above. The w/b ratio used was 0.5.

Cylinder specimens of diameter 50 mm and length 100 mm were investigated. The specimens consisted of pastes, thus overcoming uncertainties arising from paste-aggregate differential properties.

Two different mixtures (i.e., replacement 0 and 35% by weight with slag) were prepared. Water was first added, followed by the binders. The mixing was conducted in a mechanical mixer of 20 litres of capacity, 80 rpm, for five minutes each mixture. The specimens were cast using a vibration table for better

compaction. Specimens were sealed with a plastic sheet and demolded after 24 hours.

Demolding was followed by 28 days curing in lime-saturated water bath at 23°C. Following curing, the specimens were oven-dried for 2 days at 60°C and tested immediately after by using the different techniques described below.

2.2 Methods

Nuclear Magnetic Resonance (NMR)

Solid-state NMR analysis was performed using a Bruker AM300 instrument equipped with a Bruker 4 mm solid-state probe operating 59.6 MHz for ^{29}Si and 78.2 MHz for ^{27}Al . The chemical shifts were referenced to external samples of tetramethylsilane (TMS) for ^{29}Si and aqueous $\text{Al}(\text{OH})_3$ for ^{27}Al . The samples were analysed neat and all of the spectra were collected using a magic angle spinning (MAS) speed of 8 KHz. For the single ($\sim 90^\circ$ flip) pulse ^{27}Al NMR experiments a recycle delay of 2 seconds was used, with a 2.7 μsec pulse length and 200 Hz line broadening. For the single ($\sim 30^\circ$ flip) pulse ^{29}Si NMR experiments a pulse length of 3.5 μsec was used, with a delay time of 10 seconds and 100 Hz line broadening. The NMR data were processed by adopting a base line correction to flatten the background and normalising to the maximum signal intensity, to enable comparison across samples. The decompositions were accomplished by employing a Lorentzian profile for each component using the Equation 1 below. Components were initially placed using inflections and changes of slope in the spectrum as a guide to their possible presence and estimates of width (half width at half maximum), amplitude and centre were initially adjusted manually. All components were summed across the entire region of interest and the summed components (together forming the “fit spectrum”) were compared to the original spectrum using Least Square minimizations. The amplitude, height and width of each component were iteratively adjusted either independently (i.e., initially) or in combination (as the fit became “realistic”). Chi Square was calculated as an assessment of quality of fit. The integrated area of each component was calculated and if any component was less than 2-3% of the total signal, it was removed and the other components allowed to compensate. The ^{27}Al NMR data was processed as per above, except that an additional broad feature had to be added due to increased line broadening

of the octahedral Al signal. The generalised expression used for Lorentzian distribution is represented below by Equation 1.

$$y = \frac{A}{1 + \left(\frac{x - C}{B} \right)^2} \quad (1)$$

Where y is the resulting component magnitude at each x ; x is the position in ppm of the NMR signal; A , B and C are, respectively, the component amplitude, width and centre.

X-Ray Diffraction (XRD)

Powder X-ray traces were collected on a Phillips 1710 diffractometer modified with an electronic stepper motor using a Cu Ka radiation source within the range of 2 to 60°2 θ using step size of 0.02°2 θ and a scan rate of 1°2 θ per minute. Random powdered samples were back-pressed into aluminium sample supports onto frosted glass slide to minimise any preferred orientation effects. Mineral phases present in the traces were identified from auto-selected references in the international crystallographic diffraction database (ICDD) using the program XPLOT (CSIRO).

Infrared Spectroscopy (IR)

Diffuse reflectance IR spectroscopy was conducted using a FTS 3000 MX Excalibur Series Digilab fitted with a glow bar radiation source, a DTGS detector, dry CO₂-free air purge and an extended KBr beamsplitter. The sample space was continuously purged with dry nitrogen. As many as 512 acquisitions were co added at a resolution of 2 cm⁻¹ on powdered specimens mixed (~ 5%) with sodium chloride (ACS). Each spectrum was referenced to NaCl and converted to Kubelka-Munk absorbance units for comparison. Assignments of IR active bands present in the spectra were based on previously published works reported in Table 5.

Near Edge X-Ray Absorption Fine Structure (NEXAFS)

X-ray absorption spectroscopy was performed at the Australian Synchrotron as part of the commissioning of the “soft X-ray beamline” (14ID-01). Total electron yield (measured as drain current) Si K near edge X-ray absorption fine structure (NEXAFS) spectra, in the energy range of ~1840 to ~1890 eV, were collected on undiluted powdered samples pressed onto carbon tape. Steps of 0.1 eV and acquisition times 1 s were used. A minimum of 2 scans were co-added after

adjusting for instrumental energy drift and compared to reference minerals and from the survey work of Li et al. [14, 15]. Spectra were processed following typical procedures [10] by base-line correcting and intensity normalisation. Energies were adjusted to match the maximum intensity of the main peak of α -SiO₂, and intensities were normalised to a value of 1.0 at 1880 eV.

3 Results and discussion

3.1 Nuclear magnetic resonance (NMR)

²⁹Si NMR

Solid state ²⁹Si magic-angle spinning (MAS) NMR offers an efficient method to follow the hydration of C₃S in a qualitative and semi quantitative way because Si chemical shifts reflect the degree of condensation of SiO₂ tetrahedra [16]. This gives valuable information related to the formation of the calcium silicate hydrate (C-S-H) gel.

Interpretation of ²⁹Si NMR spectra provides the local silicate tetrahedral environment, designated as Qⁿ, where 'Q' represents the silicon tetrahedron bonded to four oxygen atoms and 'n' is the connectivity, i.e., the number of other 'Q' units attached to the SiO₄ tetrahedron under study. An increase in the number of SiO₄ units bonded to each Si centre produces an increase in the average electron density around the central Si atom, leading to a more negative chemical shift, relative to tetramethylsilane (TMS), for successively increasing 'n' values in Qⁿ [17]. Thus, Q⁰ denotes the monomeric orthosilicate anion SiO₄⁴⁻ (nesosilicate) typical of anhydrous silicate of cement (C₃S and C₂S), Q¹ represents an end group of a chain of C-S-H, Q² a middle group of C-S-H chain, and Q³ and Q⁴ are representative of points where branching in the silicate structure may occur [18]. Typical values are: Q⁰ = -70, Q¹ = -80 and Q² = -88 ppm [17].

Lippmaa et al. [19] pioneered successful application of ²⁹Si NMR in the study of C₃S hydration. Their work reported 6 peaks for pure C₃S identified as Q⁰ ranging from -69.2 to -73.8 ppm. In addition, after 130 days of hydration, hydrated C₃S presented 3 peaks: Q⁰, Q¹ and Q², respectively at -74, -79.1 and -85.4 ppm. They also noted that the signals of hydration products are broader than the signals of pure C₃S. This is due to a greater range in inter-atomic distances, and therefore a range in electron

density about the Si nucleus, of hydration products when compared to that of the starting material.

Hjorth et al. [16] studied the rate of disappearance and formation of the individual SiO_4 and condensed SiO_4 tetrahedra in C_3S by ^{29}Si NMR. They reported peaks for hydrated C_3S at: $Q^0 = -68$ to -76 ppm; $Q^1 = -76$ to -82 ppm; $Q^2 = -82$ to -88 ppm and $Q^4 = -110$ ppm, the latest being related to the addition of highly cross-linked amorphous silica to the system. They observed that hydration products of OPC cements had the same chemical shifts as those for the hydration products of synthetic crystalline C_3S . However, doped C_3S were found to present different ^{29}Si NMR spectra [20], giving broader signals with complex line shape than pure C_3S .

A correlation between the degree of C_3S hydration and compressive strength was performed using ^{29}Si NMR [21]. It was found that the silicon spectrum is essentially a function of the degree of polymerization of the constituent silicate groups. Therefore, measurements of the relative intensities of Q^0 to Q^4 can be used to monitor the progress of hydration/polymerization. For the OPC in study, the following peaks were found after hydration: $Q^0 = -71$ ppm (normalised); $Q^1 = -79$ ppm and $Q^2 = -84$ ppm. It was concluded that Si NMR provided excellent correlation between degree of hydration and compressive strength.

Johansson et al. [22] used ^{29}Si NMR to characterise OPC/silica fume blends. They reported the following Si NMR peaks: unhydrated Si sites = -69.2 , -71.4 , -72.0 , -73.5 ppm, Q^1 and $Q^2 = -78.9$, -81.5 , -84.4 , -91 ppm; $Q^4 = -111$ ppm for the silica fume. They used integrated peak intensity to estimate relative amounts of Q sites in solid silicates and to quantify the degree of polymerization and connectivities in the micronet of hydrated cements. C_3S was described as a fast reacting component in cement blends and C_2S as reacting slowly with water. Furthermore, their work reported that the Q^1/Q^2 ratio decreases with time while the high compressive strength of cement pastes can be correlated with a high value of Q^2/Q^1 ratio. Sun et al. [23] made similar observations when studying the hydration of pure C_3S . It was reported $Q^0 = -69$ and -73.2 ppm and a sharp peak at -71.2 ppm which they assigned to $\beta\text{-C}_2\text{S}$. They reported that presence of $\beta\text{-C}_2\text{S}$ resulted in persistence of the unhydrated Q^0 peak.

Schneider et al. [24] affirmed that the extent of incorporation of Al into the C-S-H can be obtained from the ^{29}Si NMR spectra. Their work found that Al substitutions in tetrahedral sites are detected only as $\text{Q}^2(1\text{Al})$ groupings. Silicon vacancies or Al substitutions can occur at special sites of the chain corresponding to tetrahedral not linked to calcium atoms, the so-called bridging tetrahedra. It was also reported that the Q^1 resonance corresponded to silicates forming dimmers or located at chain ends and $\text{Q}^2(1\text{Al})$ and Q^2 resonances should be associated to mid chain locations, respectively, with and without an Al substituted tetrahedron. Their work reported the following peaks for activated slags: $\text{Q}^1 = -78$ ppm; $\text{Q}^2(1\text{Al}) = -81$ ppm and $\text{Q}^2 = -84$ ppm.

Similar findings were also reported by Wang and Scrivener [25] while analysing activated slags. They stated that the ^{29}Si chemical shift is affected by the presence of Al in the first coordination shell and $\text{Q}^2(1\text{Al})$ is used to denote the Si underlined in Si-Si-Al-Si-Si groups. According to them, Al substitution for Si is confined to the bridging tetrahedron. They reported the following peaks for activated slags: $\text{Q}^0 = -74$ ppm for unhydrated slag; $\text{Q}^1 = -78.8$ ppm and $\text{Q}^2(1\text{Al}) = -81.5$ ppm.

Richardson and Groves [26] studied blends of white cement paste (WCP) and slag and reported that for a 1/1 slag/WPC blend, $\text{Q}^1 = -78.9$, $\text{Q}^2(1\text{Al}) = -81.5$ and $\text{Q}^2 = -84.5$ ppm. Similar values were also reported for a 9/1 slag/WPC blend: $\text{Q}^1 = -79.9$, $\text{Q}^2(1\text{Al}) = -81.1$ and $\text{Q}^2 = -84.5$ ppm. They concluded that Al substitutes for Si only occurred in the central tetrahedron of pentameric silicate chains. In addition, they concluded that similar structural models apply to C-S-H gel in a wide range of hardened cement pastes.

In a later study of WPC, Richardson [27] reported the following chemical shifts for a hydrated WPC: $\text{Q}^0 = -71.3$ (unreacted belite), $\text{Q}^1 = -79$ and $\text{Q}^2 = -85$ ppm. For a 50% WPC/50% slag blend it was reported: unreacted belite = -71.3 , unreacted slag = -73 ppm (broad peak). There appeared to be 3 hydrate peaks, however it was stated that more information was needed to deconvolute the spectrum. According to Richardson [15] such information can be obtained by activating the blends with 5M KOH solution. He reported the following chemical shifts for a 50% WPC/50% slag + 5M KOH: $\text{Q}^1 = -79$, $\text{Q}^2(1\text{Al}) = -82$ and $\text{Q}^2 = -85$ ppm and stated that for the activated blends the C-S-H is structurally better ordered, resulting in narrow NMR linewidths and so improved resolution.

For WPC with fly ash replacement, Richardson [28] again found Al incorporated in the C-S-H. It was reported the following peaks for the 70% WPC/30 % fly ash blend: $Q^1 = -79.1$, $Q^2(1Al) = -81.1$ and $Q^2 = -84.6$ ppm. For WPC with kaolinite, Skibsted and Hall [29] reported a chemical shift at $Q^3 = -91.5$ ppm, which was assigned to the kaolinite.

Sun et al. [30] described the C-S-H of slag and fly ash based cements as often high in Al. They affirmed that tobermorite and C-S-H peak at -81.5 ppm has been well assigned to Si on Q^2 sites with 1 tetrahedral Si NNN and 1 tetrahedral Al NNN ($Q^2(1Al)$). Its increase in intensity with increasing Al/(Si+Al) ratio and simultaneous loss of intensity for the Q^1 peak indicate that Al enters the tetrahedral chain sites and that the Al-Si chains become progressively more polymerized with increasing Al/(Si + Al). According to Sun et al. [18], structurally it is more likely that Al will enter the bridging tetrahedra, because Al[4]-O bonds are typically 0.1\AA longer than Si-O bonds, and the larger Al-O tetrahedra have more room to fit into the structure at the bridging sites.

^{29}Si NMR was also used in the study of anhydrous and hydrated phases in CEM V cement pastes [31]. A CEM V blended cement paste contains both pulverized fly ash and blast furnace slag. For this blend the following chemical shifts were found: $C_2S = -71.3$, $C_3S = -68.9$, -71.7 , -73.5 ppm, slag = -75.8 and PFA = -107 ppm = Q^4 . In addition, it was reported that generally, a broad resonance peak line is observed between -73 and 75 ppm depending on the type of slag.

An investigation of the intercalation potential of polyethylene glycol (PEG) with synthetic and pre-treated C-S-H was conducted using ^{29}Si NMR [32]. For a synthetic C-S-H the following chemical shifts were reported: $Q^1 = -79.3$ and $Q^2 = -85.2$ ppm.

More recently, Si NMR has been applied in the study of the chemical changes and phase analysis of OPC pastes carbonated at different CO_2 concentrations [33]. It was reported that carbonation induces both loss of Ca and polymerization of the C-S-H gel with the formation of Ca modified silica gel. The degree of polymerization increases with the CO_2 concentration. For example, OPC paste presented the following chemical shifts: $Q^0 = -74.6$ (C_2S), $Q^1 = -82.5$ and $Q^2 = -87.8$ ppm. Naturally carbonated pastes presented chemical shifts: $Q^0 = -74.4$, $Q^1 = -82.7$, $Q^2 = -88.3$, Q^3

= -98.3 and Q^4 = -112.1 ppm (close to silica gel) while for the 3% CO₂ samples a different scenario was found. The C-S-H gel (Q^1 and Q^2) is still present but intensity decreases in comparison with the reference sample, and the polymerization of the silicates is appreciably higher (Q^3 and Q^4). The 100% CO₂ sample show a complete decomposition of the C-S-H gel to a silica gel with no unhydrated phase [33].

For the present work, ²⁹Si NMR spectra for OPC and 35% slag paste samples are presented in Fig. 1. A summary of the chemical shifts observed and the related assignments are presented in Table 2.

Table 2 Results from decomposition of ²⁹Si NMR spectra of OPC and 35% slag pastes

| Sample | Centre ppm (relative to TMS) | FWHM* | Relative Area (%) | Assignment | Sums of square | Chi square |
|----------|---------------------------------|-------|----------------------|------------|----------------------|---------------|
| OPC | -70.0 | 4.97 | 11.59 | Q^0 | 0.0260 | 0.0938 |
| | -71.3 | 2.49 | 14.09 | Q^0 | | |
| | -73.8 | 4.98 | 10.89 | Q^0 | | |
| | -77.4 | 3.23 | 5.07 | Q^1 | | |
| | -79.0 | 4.12 | 20.72 | Q^1 | | |
| | -81.2 | 4.33 | 13.22 | $Q^2(1Al)$ | | |
| | -84.4 | 5.57 | 24.41 | Q^4 | | |
| 35% Slag | -68.8 | 7.15 | 10.85 | Q^0 | 0.0199 | 0.0815 |
| | -71.1 | 2.80 | 12.72 | Q^0 | | |
| | -73.9 | 4.35 | 6.53 | Q^0 | | |
| | -76.5 | 5.04 | 11.22 | Q^1 | | |
| | -79.1 | 4.69 | 24.87 | Q^1 | | |
| | -81.5 | 4.78 | 15.70 | $Q^2(1Al)$ | | |
| | -84.5 | 4.95 | 18.11 | Q^4 | | |

*Full width at half maximum

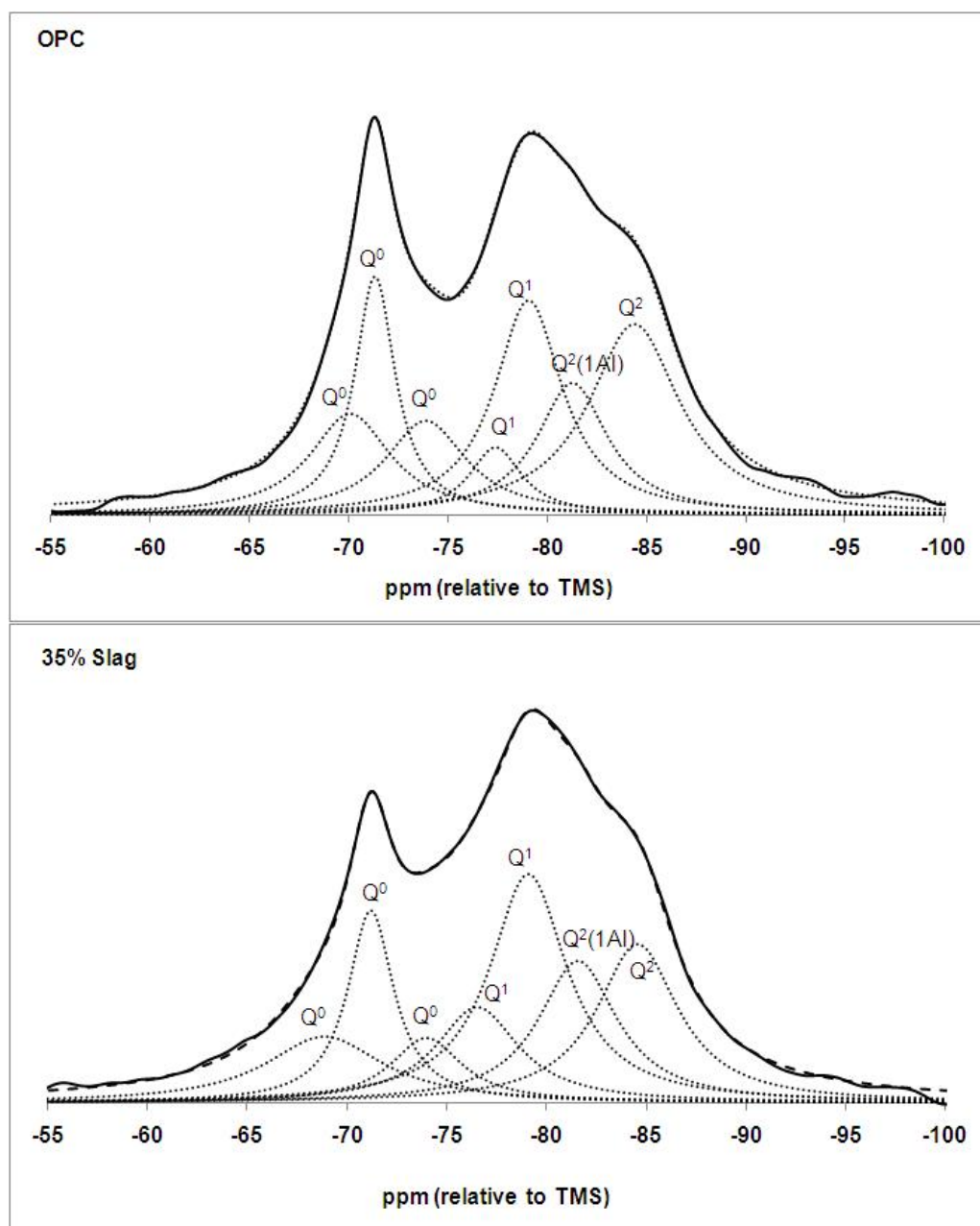


Fig. 1 Single pulse ^{29}Si NMR spectra of OPC and 35% slag pastes. Results of best least-squares fit decomposition are also displayed

For the OPC samples, 6 chemical shifts are observed and related assignments are presented in Table 2 and Fig. 1. Peaks related to Q^0 are observed at -70.0, -71.3, -73.8 ppm in accordance with previous works [16, 22, 31], with the sharp peak at -71.3 ppm relating to belite/larnite (C_2S) [18, 22, 27]. Peaks related to Q^1 are observed at -77.4 and -79.0 ppm [16, 24-28, 32] and those related to $Q^2(1Al)$ at -81.2 ppm and Q^2 at -84.4 ppm [16, 21, 22, 24, 26-28, 32]. As previously discussed in this section, the chemical shift $Q^2(1Al)$ at -81.2 ppm relates to the Al substitution for Si confined to the bridging tetrahedron [24-28].

Similarly, the 35% slag samples also presented 6 chemical shifts and related assignments are also presented in Table 2 and Fig. 1. The Q^0 chemical shifts at -68.8, -71.1, -73.9 ppm are in accordance with previous works [16, 22, 31] with the chemical shift at -73.9 ppm relating to unreacted slag [26, 27] and the sharp peak at -71.1 ppm relating to belite/larnite (C_2S) [18, 22, 27]. The peaks for Q^1 are located at -76.5 and -79.1 ppm [16, 24-28, 32] and for $Q^2(1Al)$ at -81.5 ppm and Q^2 at -84.5 ppm [16, 21, 22, 24, 26-28, 32]. As for the OPC paste, the chemical shift $Q^2(1Al)$ at -81.5 ppm relates to the Al substitution for Si confined to the bridging tetrahedron [24-28].

In summary, although minor differences are present as described above, no major differences are observed between the silicate phases of OPC and OPC partially replaced by slag (35%).

²⁷Al NMR

Solid state ²⁷Al magic-angle spinning (MAS) NMR has been useful in characterizing calcium aluminates and aluminate hydrates (ettringite and monosulphate hydrate), which are of importance in the chemistry of cements [34]. Generally, ²⁷Al MAS NMR has been concerned with the distinction between tetrahedrally (Al(4)) and octahedrally (Al(6)) coordinated aluminium, using the distinct chemical shift difference of about 60 ppm for these two coordination environments [34]. Al(4) is generally observed between 50 and 80 ppm, while Al(6) normally resonates between -20 and 20 ppm [35]. However, ²⁷Al MAS NMR spectroscopy has the disadvantage that spectra can be difficult to interpret, as ²⁷Al can be affected by quadrupolar interactions leading to a field-dependent shift in resonance position as well as an asymmetric broadening of the peaks [35].

Skibsted et al. [34] observed that hydration of C_3A calcium aluminate phases in OPC cements initially produces the sulphate containing phase ettringite, which slowly converts to the thermodynamically stable monosulphate. They reported the following chemical shifts for the spectrum of OPC hydrated for 1 day: narrow resonance at 13 ppm assigned as ettringite and weak shoulder at 5 ppm assigned to minor amounts of monosulphate hydrate and/or C_4AH_{13} . A broad centred resonance from 80 to 40 ppm was assigned as unhydrated material [34]. After 28 days of hydration the following chemical shifts were assigned as: 13 ppm = ettringite, 9 ppm = monosulphate and 7 ppm = C_4AH_{13} [34]. In the absence of the calcium sulphate in Portland cement, C_3A can react with $CaOH_2$ and water to form the hydrate C_4AH_{13} . This reaction may occur in Portland cements with a low SO_3/Al_2O_3 ratio, where the small amount of SO_3 is consumed during the initial formation of ettringite [34].

Hanna et al. [35] studied the hydration product of OPC in the presence of heavy metal containing stabilized waste. Their work reported one narrow chemical shift at 13.2 ppm and a broader signal at 8.5 ppm. Comparing those with the values obtained for pure aluminate hydrate (ettringite = -13.1 and monosulphate = -11.8 ppm) their work concluded that the peak at 13.2 ppm represented ettringite while the peak at 8.5 ppm related to the monosulphate hydrate [35].

Schneider et al. [24] used a cross-polarization (CP) technique in combination with magic-angle spinning (MAS) in the study of activated slags. Cross polarization is less efficient for Al(4) than Al(6) atoms, indicative of a low number of attached OH groups in Al(4). For pure slag a broad resonance peak centred at 64.1 ppm was reported, indicating Al was located only in tetrahedral sites. For hydrated pastes two chemical shifts were reported at 3.5 and 8.5 ppm, which they assigned as hydrated phases (hydrogarnet), possibly 2 different phases identified as C_3AH_6 and CAH_{10} using XRD [24]. It was also reported a chemical shift at 12 ppm assigned as ettringite. For the tetrahedral sites two peaks were observed: 66 and 72 ppm, with the 72 ppm being sharper and more resolved. For this reason the peak at 72 ppm was assigned to Al in the C-S-H chains [24].

Studying the incorporation of aluminium in the C-S-H of white Portland cements (WPC), Andersen et al. [36] observed 3 chemical shifts in the WPC ^{27}Al NMR spectrum: 13, 9.8 and 5 ppm. The first chemical shift was assigned to ettringite and

the peak at 9.8 ppm was assigned to monosulphate. The chemical shift at 5 ppm was denominated as a third aluminate phase which was not present in earlier studies of OPC [36]. In the tetrahedral region the Al substitution in the C-S-H reported at 69.5 ppm (14.09T) and 72.3 ppm (21.15T) [36].

Murgier et al. [37] studied slag activated with OPC and reported the following chemical shifts: 12 ppm (ettringite), 9 ppm (monosulphate), 3.5 ppm (non-assigned) and 71 ppm (Al substitution in C-S-H).

In 2006, Andersen et al. [38] characterized the third aluminate phase reported in 2003 [36]. The new aluminate phase reported for WPC is denoted as TAH. According to Andersen et al. [38] TAH has a chemical shift of 5 ppm. ^{27}Al NMR recorded at different magnetic fields have demonstrated that TAH is an amorphous or disordered species. It was also reported that the quantity of TAH increases with the hydration time and it is most likely formed at the expense of ettringite and Al^{3+} incorporated in alite and belite. TAH does not contain sulphate ions and an increase in sulphate content reduces TAH formation [38]. In addition, TAH has been detected in C-S-H phases when Ca/Si ratio is above 0.83. It was concluded that TAH is an amorphous aluminium hydroxide or a poorly disordered calcium aluminate hydrate [38].

Brunet et al. [31] concluded that the range for chemical shifts for tetrahedral aluminosilicates is generally around 70-85 ppm, which would according to them correspond to the structure of blast furnace slag (BFS).

For the present work, the ^{27}Al NMR spectra for OPC and 35% slag pastes are presented in Fig. 2. A summary of the chemical shifts observed and the related assignments are presented in Table 3. For the OPC paste two Al(4) and three Al(6) sites are observed. The Al(4) sites are located at 69.8 and 58.7 ppm. According to the previous works described above [24, 36, 37], the chemical shift at 69.8 ppm is attributed to Al substitution within a C-S-H phase, also observed in the ^{29}Si NMR results presented in the previous section. The Al(4) site located at 58.7 ppm is likely to refer to unhydrated material [24, 34]. The Al(6) sites in OPC have the following chemical shifts: 14.6, 9.6 and 5.0 ppm. The first two chemical shifts are in accordance with the resonance peaks reported in the literature for, respectively, ettringite and monosulphate hydrate [34-37]. The chemical shift reported at 5.0 ppm

can be possibly assigned to the previously reported chemical shifts for TAH (5 ppm) [36, 38] or C_4AH_{13} (7 ppm) [34]. However, the ^{27}Al NMR spectrum does not enable a definite assignment of this particular feature. XRD tests conducted in OPC pastes are discussed further in an attempt to determine which hydrate phase this peak may represent. Furthermore, the very broad fitted feature with a chemical shift at -7.9 ppm may be due to quadrupolar broadening of the Al(6) signal.

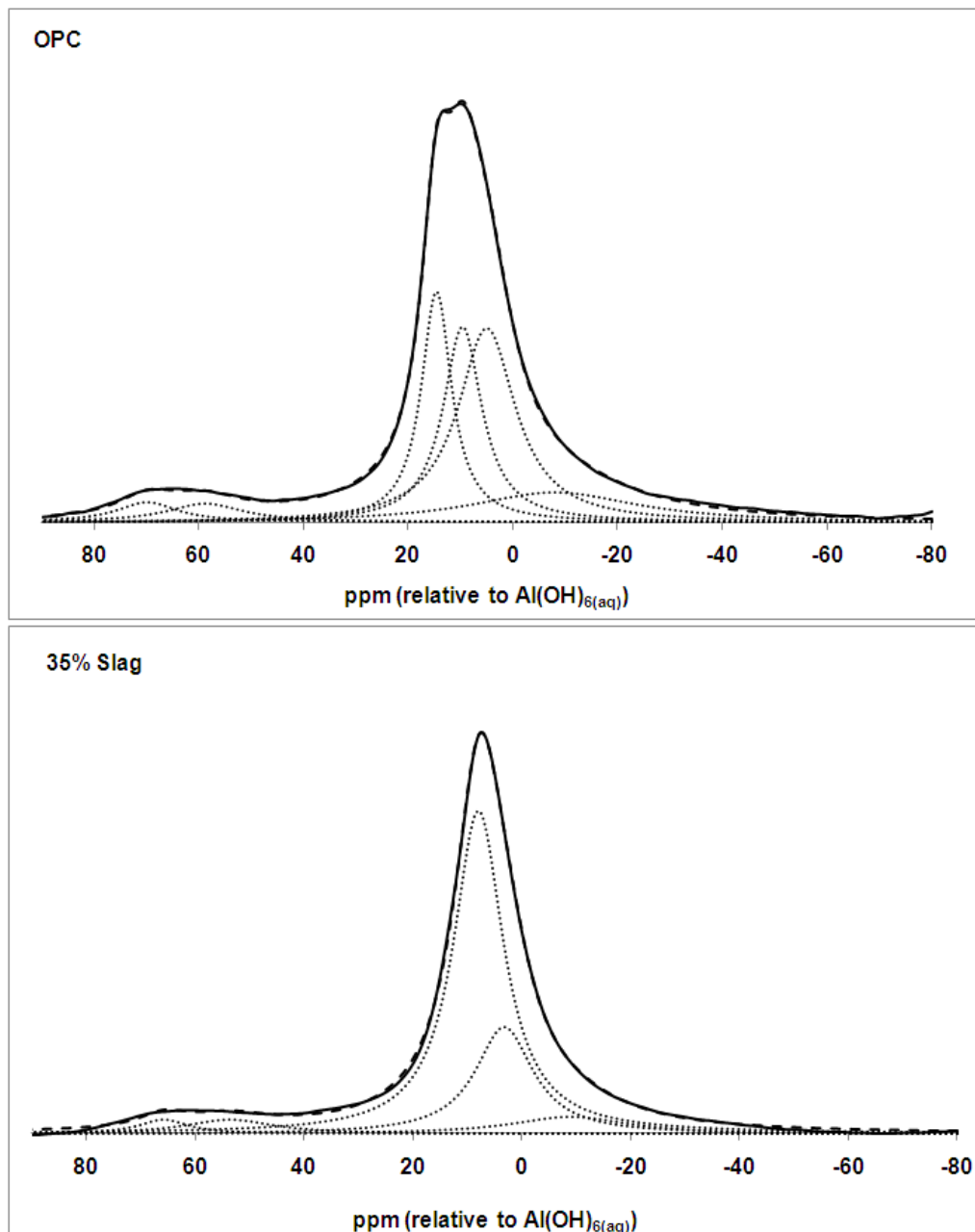


Fig. 2 Single pulse ^{27}Al NMR spectra of OPC and 35% slag pastes. Results of best least-squares fit decompositions are also displayed

Table 3 Results from decomposition of ^{27}Al NMR spectra of OPC and 35% slag pastes

| Sample | Centre ppm (relative to $\text{Al}(\text{OH})_6$ (aq)) | FWHM* | Relative Area (%) | Assignment | Sums of square | Chi square |
|----------|---|-------|----------------------|---------------|----------------------|---------------|
| OPC | 69.8 | 14.06 | 3.53 | Al^4 | 0.0446 | 0.686 |
| | 58.7 | 17.75 | 4.04 | Al^4 | | |
| | 14.6 | 7.00 | 21.62 | Al^6 | | |
| | 9.6 | 8.95 | 23.27 | Al^6 | | |
| | 5.0 | 13.35 | 33.88 | Al^6 | | |
| | -7.9 | 38.80 | 13.66 | Quadrupolar | | |
| 35% Slag | 66.1 | 11.03 | 3.20 | Al^4 | 0.0103 | 5.34 |
| | 53.9 | 19.75 | 5.42 | Al^4 | | |
| | 8.1 | 11.78 | 58.98 | Al^6 | | |
| | 3.4 | 12.90 | 24.82 | Al^6 | | |
| | -8.8 | 26.11 | 7.57 | Quadrupolar | | |

*Full width at half maximum

For the 35% slag paste, two $\text{Al}(4)$ sites and two $\text{Al}(6)$ sites are observed. The $\text{Al}(4)$ sites are located at 66.1 and 53.9 ppm. As per the OPC paste, the chemical shift at 66.1 ppm is attributed to Al substitution within a C-S-H phase [24, 36, 37]. This was also observed in the ^{29}Si NMR results presented in the previous section. The chemical shift at 53.9 ppm is possibly an unhydrated material [24, 34], due to slag addition to the system. The $\text{Al}(6)$ sites observed have chemical shifts at 8.1 and 3.4 ppm. The chemical shift at 8.1 ppm is in accordance with the resonance peak reported in the literature for monosulphate hydrate [34-37]. Murgier et al. [37] reported but was unable to assign a peak having a chemical shift at 3.5 ppm, whereas Schneider et al. [24] assigned a chemical shift at 3.5 ppm as a hydrogarnet CAH_{10} phase based on XRD results. XRD tests were performed in 35% slag pastes and are discussed further to confirm whether the 3.4 ppm chemical shift can be assigned to CAH_{10} . The broad fitted feature with a chemical shift at -8.8 ppm may be due to quadrupolar broadening, however this feature is less obvious than the one observed in the OPC pastes.

In summary, the major differences between the OPC and the 35% slag pastes were in the number and position of the $\text{Al}(6)$ sites. In the OPC paste, three $\text{Al}(6)$ environments were identified, positioned at 14.6 (ettringite), 9.6 (monosulphate) and 5.0 ppm (not yet assigned). The 5.0 ppm peak represented nearly 30% of the total signal. For the 35% slag paste, only two $\text{Al}(6)$ sites were observed, 8.1 ppm

(monosulphate hydrate) contributing to nearly 60% of the total signal and 3.4 ppm (not yet assigned). It is important to state that no ettringite was observed when OPC was partially replaced with slag, i.e., for 35% slag pastes.

X-ray diffraction (XRD)

X-ray diffraction (XRD) is used to identify the polycrystalline phases of cement and hardened cement paste through the recognition of the X-ray patterns for each of the crystalline phases [39]. Therefore, XRD is a useful tool to detect crystalline hydrates such as ettringite, monosulphate hydrate, portlandite (CaOH_2), calcium carbonate, and calcium silicate hydrate, as well as the various calcium silicate, calcium aluminate and aluminosilicate phases possibly present. In 1976, Breval [40] used X-ray studies to investigate C_3A hydration and identified the stable cubic C_3AH_6 as the main product.

XRD has also been utilized to complement other techniques. As described in the previous section, Schneider et al. [24] used XRD experiment to identify non-assigned peaks observed in ^{27}Al NMR spectra as CAH_{10} and C_3AH_6 .

The present work characterizes OPC and 35% slag pastes using XRD, aiming to identify the crystalline phases present in each of these pastes. In addition, an attempt is made to identify the unassigned hydrates detected by ^{27}Al NMR. The XRD spectra obtained for OPC and 35% slag pastes are presented in Fig. 3. The phases identified by XRD are summarized in Table 4. The related references to each phase are also presented in Table 4.

Both blends presented unhydrated starting materials as larnite, C_3A and also the hydrated phase C-S-H. The main phases observed for OPC paste (Table 4 and Fig. 3) are: CaOH_2 , calcite (CaCO_3) and ettringite. For 35% slag pastes similar phases were found, however CaOH_2 and calcite were present in less quantity and ettringite was not detected. The absence of ettringite in the 35% slag paste XRD spectrum is in accordance with the ^{27}Al NMR results. In contrast, 35% slag pastes presented monosulphate hydrate, which is absent in the OPC pastes XRD spectrum.

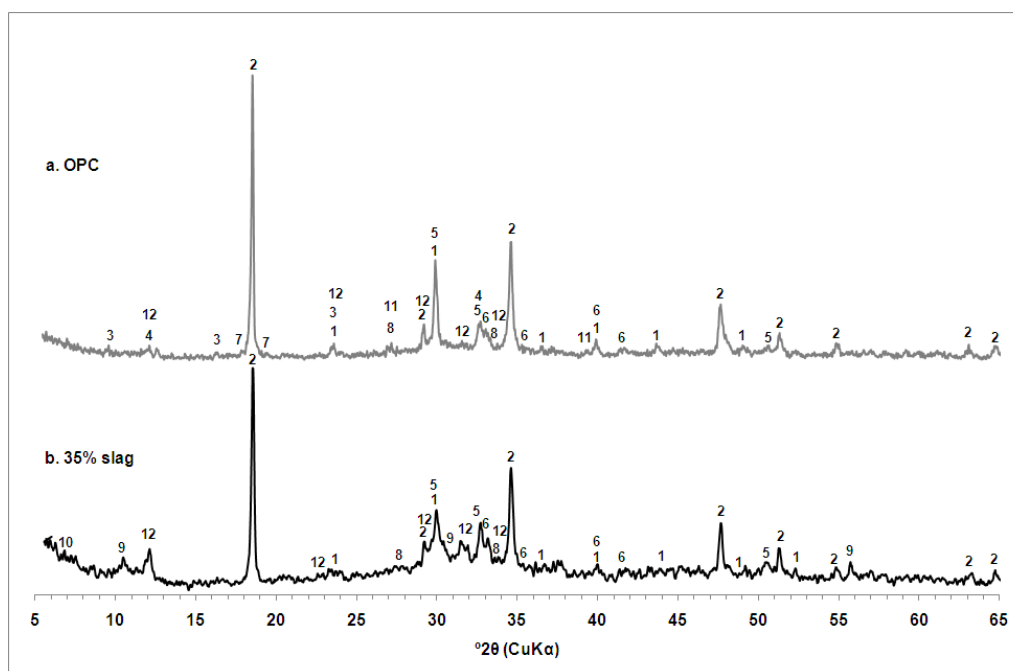


Fig. 3 X-ray traces of OPC (a) and 35% slag (b) pastes. 1. Calcite (CaCO_3); 2. Portlandite (CaOH_2); 3. Ettringite; 4. Brownmillerite; 5. C-S-H (calcium silicate hydrate); 6. Larnite (C_2S); 7. Hydrogarnet; 8. C_3A ; 9. Monosulphate hydrate; 10. CAH_{10} ; 11. C_3AH_6 ; 12. C_4AH_x

With regards to the CAH_{10} detected in the 35% slag samples, Schneider et al. [24] having observed this phase on their XRD spectra, have assigned this to the phase not identified by ^{27}Al NMR with chemical shift at 3.5 ppm. In the present study, a similar peak at 3.4 ppm was detected reported in the ^{27}Al NMR and has not yet been assigned. However, it is not believed that CAH_{10} is the phase fully responsible for the non-assigned chemical shift at 3.4 ppm (Fig. 2). The reason being that the chemical shift observed at 3.4 ppm (Fig. 2) corresponds to nearly 25% of the total signal in the ^{27}Al NMR, but only very weak signals are observed for CAH_{10} in the present XRD spectrum (Fig. 3). Due to the low presence of aluminate phases in the XRD spectrum it is believed that the phase in question cannot be attributed to a highly crystalline phase, but instead to a very disordered or amorphous constituent of the cement paste.

Table 4 Mineral phases present in OPC and 35% slag cement pastes. Only the most intense peaks are listed

| Mineral Phase | OPC | 35% Slag | $2\theta(\text{Cu K}\alpha)$ | Reference |
|----------------------------------|-------|----------|------------------------------|------------------|
| CaOH ₂ (Portlandite) | Major | Major | 18.1 | [18, 33, 41, 42] |
| | | | 29 | |
| | | | 34.1 | |
| | | | 47.2 | |
| | | | 51 | |
| CaCO ₃ (Calcite) | Major | Minor | 54.5 | [18, 33, 43] |
| | | | 23 | |
| | | | 29.3 | |
| | | | 39.4 | |
| | | | 43.2 | |
| Monosulphate hydrate | Nil | Minor | 48.6 | [41] |
| | | | 9.9 | |
| | | | 31.1 | |
| Brownmillerite | Minor | Nil | 55.1 | [18] |
| | | | 12.2 | |
| | | | 32.1 | |
| C-S-H (Calcium silicate hydrate) | Minor | Minor | 33.9 | [24] |
| | | | 29.6 | |
| | | | 32.2 | |
| AFt (Ettringite) | Minor | Nil | 50.1 | [18, 33, 41, 42] |
| | | | 9.1 | |
| | | | 15.8 | |
| | | | 23 | |
| Larnite (C ₂ S) | Trace | Trace | 32.4 | [18] |
| | | | 32.2 | |
| | | | 32.6 | |
| | | | 34.3 | |
| | | | 39.5 | |
| CAH ₁₀ | Nil | Trace | 41.2 | [24] |
| C ₃ AH ₆ | Trace | Nil | 7 | [24, 44] |
| | | | 11.6 | |
| | | | 23.6 | |
| Hydrogarnet | Trace | Nil | 39.3 | [41] |
| | | | 17.5 | |
| C ₃ A | Trace | Trace | 18.9 | [43] |
| | | | 33.0 | |
| C ₄ AH _x | Trace | Trace | 33.3 | [42] |
| | | | 11.5 | |
| | | | 22 | |
| | | | 23 | |
| | | | 29.3 | |
| | | | 31 | |
| | | | 36 | |

*Estimated composition. Major > 40%; Minor 5 - 40%; Trace < 5%; Nil not observed.

For the OPC paste, the non-assigned 5.0 ppm peak in the ^{27}Al NMR (Fig. 2) is also probably not related to a crystalline phase. For the same reason as explained above, the 5.0 ppm chemical shift is strong, corresponding to nearly 30% of the total signal. As for the 35% slag sample, no crystalline aluminate phase is observed with an intensity in the XRD spectrum suggestive of this phase. Therefore, the ^{27}Al chemical shift at 5.0 ppm probably represents a very poorly crystalline or even amorphous aluminate phase, and not the crystalline C_4AH_{13} reported previously for OPC [34]. It is more likely that the 5.0 ppm peak relates to the amorphous TAH reported in previous works [36, 38].

In addition to the differences in mineral phases discussed above, the trace for the 35% slag sample is noisier and also has an elevated background in the range 20-40 $^{\circ}2\theta$, indicative of a greater amount of amorphous, disordered materials.

Infrared Spectroscopy (IR)

Infrared spectroscopy (IR) is used in the areas of determination of molecular structure, identification of chemical species, quantitative/qualitative determination of chemical species [45]. Vibrational frequencies measured by IR can provide valuable information regarding the silicate, sulphate, and carbonate phases [35].

In 1968, Bensted and Prakash [46] studied calcium sulphate using IR. Their work reported SO_4 frequencies in the range of 1004 to 1120 cm^{-1} . In 1971, when studying ettringite and its derivatives, Bensted and Varma [47] determined three types of IR absorption bands in the region between 650 and 4000 cm^{-1} : stretching bands of sulphate, stretching and bending bands of water and/or hydroxyl and stretching bands of metal-hydroxyl pairs.

Bensted and Varma [48] also investigate the aluminate phase monosulphate hydrate using IR. Their work described the hydration reaction of the cement starting material C_3A . It was reported that gypsum tends to inhibit the formation of hexagonal plate calcium aluminate hydrates C_3AH_6 and C_4AH_{13} , resulting in ettringite as the primary hydration product [48]. Ettringite is a high sulphate form of calcium sulphotoaluminate and will remain in the C_3A paste until all the added gypsum has been consumed. Subsequent hydration of C_3A leads to the decomposition of the hexagonal prism phase of ettringite. A hexagonal plate of monosulphate, the low sulphate form of calcium sulphotoaluminate is then formed.

Although both monosulphate and ettringite contain sulphate, aluminate and water groups, there are major differences regarding the shapes and positions of their IR bands [48], thus IR is a useful tool to characterize those hydrates in the cement pastes.

For the present work, IR spectra of OPC and 35% slag are presented in Fig. 4. The assignments for the main bands as well as their references from previous published works are summarized in Table 5.

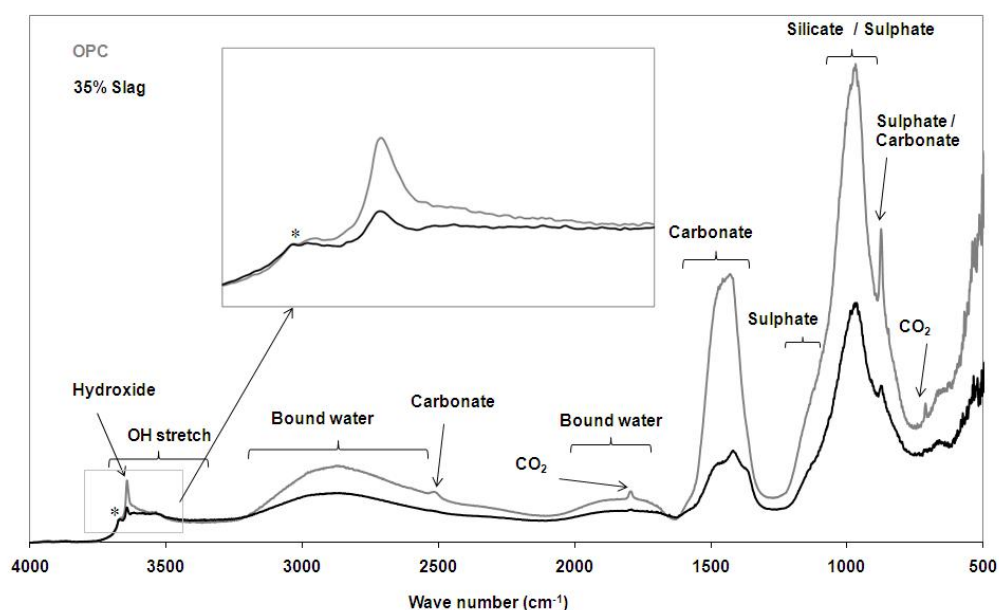


Fig. 4 FTIR spectra of OPC and 35% slag pastes. Spectra have been normalised to the OH bands near 3670 cm⁻¹ to better display differences

Table 5 Assignments of major bands observed in the FTIR spectra of OPC and 35% slag pastes

| Bands wave number (cm ⁻¹) | | Assignment | Reference |
|---------------------------------------|----------|---|---------------------------------|
| OPC | 35% Slag | | |
| 3672 | 3672 | M-OH stretch | [8, 47, 49-51] |
| 3666 | 3665 | M-OH stretch | [8, 47, 49-51] |
| 3654 | 3654 | M-OH stretch | [8, 47, 49-51] |
| 3644 | 3644 | CaOH ₂ OH stretch | [35, 52-54] |
| 3616 | 3616 | HOH stretch | [8, 47, 49-51] |
| 3580 | 3580 | OH stretch | [8, 47, 49-51] |
| 3535 | 3535 | OH stretch | [8, 47, 49-51] |
| 2970 | 2966 | Bound water HOH stretch | [8] |
| 2954 | 2952 | Bound water HOH stretch | [8] |
| 2508 | 2506 | Carbonate CO stretch | [55, 56] |
| 1880 | 1880 | Bound water HOH bend | [8] |
| 1792 | 1792 | CO ₂ CO stretch | [55, 56] |
| 1730 | 1730 | Bound water HOH bend | [8] |
| 1680 | 1660 | Bound water HOH bend | [8, 35, 47, 50, 51] |
| 1470 | 1472 | Carbonate CO stretch | [35, 55-57] |
| 1427 | 1415 | Carbonate CO stretch | [50-56] |
| 1367 | 1363 | Carbonate CO stretch | [55, 56] |
| 1130 | 1130 | Sulphate SO stretch | [47-49, 51, 58, 59] |
| 998 | 1002 | Silicate SiO stretch / Sulphate SO stretch | [8, 35, 46, 49, 50, 54, 59, 60] |
| 968 | 963 | Silicate SiO stretch | [8, 35, 49, 50, 54, 61] |
| 874 | 873 | Sulphate SO stretch / Carbonate CO bend | [35, 50, 51, 54, 55, 57, 59-61] |
| 710 | - | Carbonate CO bend | [54, 57] |

Five main bands have been identified for both the OPC and 35% slag spectra. In Fig. 4, starting from the left, the sharp peak at approximately 3644 cm⁻¹ relates to CaOH₂. This is in accordance with previous studies as referenced in Table 5. The lower intensity bands near 3670 and 3530 cm⁻¹ relate to M-O-H stretching of structural hydroxyl associated with other hydrous mineral phases. The broad peak centred near 2900 cm⁻¹ relates to the O-H stretch of strongly polarised H-bonded waters associated with cementitious minerals. The peaks near 1450 cm⁻¹ are due to C-O stretch of CaCO₃, and the peak near 977 cm⁻¹ is referent to the Si-O stretch mainly representing the C-S-H gel and other silicate phases (e.g. larnite) of the cement paste. A band for S-O stretch occurs near 1130 cm⁻¹ and is partially covered by the Si-O stretch. All related references are described in Table 5.

Large differences are observed in the IR spectra of the OPC and the 35% slag pastes (Fig. 4). In general, the O-H (CaOH_2), HOH, carbonate, silicate and possibly sulphate bands are all more intense in the OPC sample relative to the 35% slag sample. The OPC peaks for CaOH_2 and bound water are twice as intense than the peaks observed for 35% slag. This is in accordance with the present XRD findings and previous works by the authors [1, 5]. The carbonate and sulphate bands are nearly three times more intense in OPC pastes than in the 35% slag pastes. This is also in accordance with XRD results for calcite in OPC as a major phase. In addition, the OPC paste contained CO_2 , which was not observed in the 35% slag sample.

The sulphate SO stretch band at approximately 1130 cm^{-1} is of interest as it can provide information regarding the sulphoaluminate phase in both OPC and 35% slag samples. As discussed earlier, both ettringite (the high sulphate form of calcium sulphoaluminate) and monosulphate (the low sulphate form of calcium sulphoaluminate) contain sulphate, aluminate and water groups, however there are major differences regarding the shapes and positions of their IR wavebands [48].

Ettringite is reported to have a singlet centred at 1120 cm^{-1} while monosulphate is expected to have doublet centred on 1100 and 1170 cm^{-1} [47-49]. Corresponding to these differences, there are also differences in the bound water HOH bending bands at approximately 1650 cm^{-1} and also in the HOH stretching bands of water above 3000 cm^{-1} [49]. In the present work it is not possible to determine (Fig. 4) whether the S-O stretch band is a singlet (ettringite) or a doublet (monosulphate). Bensted and Varma [49] reported that after one day ettringite had already started converting to monosulphate while C-S-H was also been formed. In fact after seven days there was so much C-S-H present that the monosulphate bands in the region 1100 cm^{-1} were being encompassed by the C-S-H band centred on 970 cm^{-1} [49]. Likewise, in the spectra presented in Fig. 4 the silicate Si stretch at 968 and 963 cm^{-1} (for OPC and 35% slag, respectively) is encompassing the sulphate band, thus not enabling precise determination of the phase in question using this band.

However, as indicated by Bensted and Varma [49], the differences between ettringite and monosulphate bound water HOH bending bands at approximately 1650 cm^{-1} and OH stretching bands of water above 3000 cm^{-1} might provide useful information in the determination of ettringite and monosulphate phases. Their work

reported OH stretching bands at 3500, 3540, 3675 cm^{-1} for monosulphate. For ettringite, OH stretching bands at 3420 and 3635 cm^{-1} [49]. In Fig. 4 it is possible to observe a low-intensity OH stretching band centred at approximately 3666 cm^{-1} (expanded and represented by *) in the 35% slag spectrum (this occurs as a weak shoulder in the OPC spectrum). This possibly indicates the presence of monosulphate OH stretching water, suggesting that the encompassed sulphate band at 1130 cm^{-1} might be a monosulphate band. As discussed in the previous sections, monosulphate hydrate was present in both OPC and 35% slag pastes according to ^{27}Al NMR. In addition, XRD detected the presence of monosulphate hydrate in the 35% slag pastes while no ettringite was detected in these pastes by either ^{27}Al NMR or XRD.

Si NEXAFS

Few studies have been conducted on minerals using Si NEXAFS spectroscopy. Li et al. [15] reported the main Si NEXAFS peak positions with a limited number of corresponding ^{29}Si NMR chemical shifts for a variety of Q^n silicates. It is unlikely that the OPC or 35% slag pastes contain any of the silicates listed in their exact chemical makeup. However, in general, the main peak in the Si NEXAFS spectrum shifts to higher energy with increasing degree of polymerisation.

The Si K-edge NEXAFS spectra of OPC and 35% slag pastes are dominated by peaks at ~ 1847 eV, 1849 eV and 1863 eV (Fig. 5). The first two are single electron $1s \rightarrow \sigma^*_{\text{Si-O}}$ transitions of silicate [14, 15]. The latter band is due to a broad $\sigma^*_{\text{Si-O}}$ continuum resonance [14] and is probably made up of several overlapping σ^* (antibonding) orbitals due to differences in inter-atomic distances. The broad feature near 1855 eV is probably due to Si-O-O-Si multiple scattering (m.s.) [14].

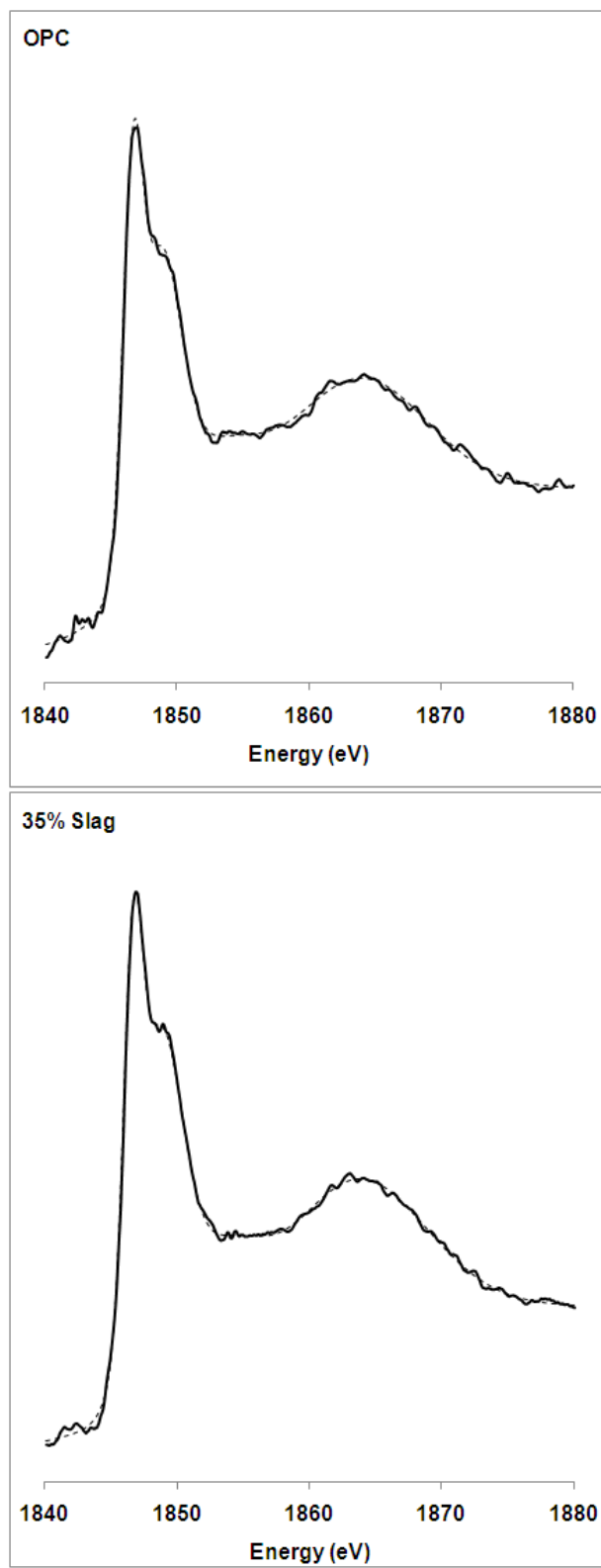


Fig. 5 Si NEXAFS spectra of OPC and 35% slag pastes

Table 6 Results of Si NEXAFS spectra of OPC and 35% slag pastes. Transitions assignments are also indicated

| Sample | Centre eV (relative to αSiO_2) | Assignment |
|------------------|---|--|
| OPC and 35% slag | 1847.0 | $\text{Q}^0 1s \rightarrow \sigma^*_{\text{Si-O}}$ |
| | 1849.0 | $\text{Q}^0 1s \rightarrow \sigma^*_{\text{Si-O}}$ |
| | 1855.0 | m.s.* |
| | 1863.0 | $\text{Q}^0 \sigma_{\text{Si-O}} \text{ res}$ |

*Multiple scattering

According to Li et al. [15] while the degree of silicate polymerisation in general corresponds to a shift to a higher energy, hydrated phases tend to have a relatively constant maximum energy, regardless of the degree of polymerisation. Table 6 shows that both OPC and 35% slag NEXAFS spectra present 3 major peaks, all related to Q^0 [15]. The spectra do not allow differentiation of any possible contribution of Q^1 and Q^2 units in the material.

As shown in Fig. 5, no significant differences are observed between OPC and 35% slag. Therefore, only minor differences between the Q^0 resonances of these pastes are likely to be present. This confirms the ^{29}Si NMR results reported in this study.

Further interpretation of the Si NEXAFS spectra at present is confounded by multiple factors affecting the X-ray absorption process. Without available reference spectra, Si NEXAFS technique is unlikely to provide more details on the similarities and/or differences between OPC and OPC/slag pastes.

4 Conclusions

The present work investigated the fundamental similarities and/or differences between OPC and OPC/slag paste hydrates. The use of the following techniques ^{29}Si NMR, ^{27}Al NMR, XRD, IR and NEXAFS enabled the following conclusions:

1. ^{29}Si NMR spectra showed that there are no major differences between the silicate phases of OPC pastes and 35% slag pastes. Both pastes presented 3 chemical shifts assigned as Q^0 , 2 chemical shifts assigned as Q^1 and 1 chemical shift assigned as Q^2 . In addition, both OPC and 35% slag pastes presented $Q^2(1\text{Al})$ chemical shifts related to the Al substitution for Si confined to the bridging tetrahedron.

2. ^{27}Al NMR spectra detected 3 octahedral and 2 tetrahedral sites for OPC. The following phases were assigned for the octahedral sites: ettringite, monosulphate hydrate and a non-assigned peak at 5.0 ppm (33% of the total signal). For the 35% slag paste, 2 octahedral and 2 tetrahedral sites were observed and the following assignments were made for the octahedral sites: monosulphate hydrate and a non-assigned peak at 3.4 ppm (25% of the signal). Thus, the main difference between OPC and 35% paste is the presence of ettringite in OPC pastes only. For the tetrahedral sites, Al substitutions in the C-S-H were detected for both OPC and 35% slag pastes confirming suitability of ^{27}Al NMR in detecting those substitutions.

3. XRD spectra showed 3 main phases for OPC: CaOH_2 , calcite and ettringite. For 35% slag no ettringite was detected confirming the ^{27}Al NMR results. The very low peak intensities for the aluminate phases in the XRD spectra indicate that the non-assigned chemical shifts observed in the ^{27}Al NMR are possibly not crystalline phases as CAH_{10} or C_4AH_{13} . It is more likely that the ^{27}Al NMR 5.0 and 3.4 ppm chemical shifts (found for OPC and 35% slag, respectively) relate to an amorphous, disordered phase. These phases are probably similar to the phase previously reported TAH [36, 38].

4. IR spectra confirmed previous reports [1, 5] that OPC presents more CaOH_2 than 35% slag pastes. It was also observed that OPC carbonate bands were three times more intense than the 35% slag bands. The knowledge of the sulphate SO stretch

and water bands for ettringite and monosulphate indicated that it is likely that these bands refer to monosulphate hydrate, especially for the 35% slag pastes. This in accordance with the ^{27}Al NMR and XRD results confirming that only monosulphate hydrate is present in 35% slag pastes.

5. Si NEXAFS results showed that there are no major differences between the Q^0 resonances of OPC and 35% slag pastes, confirming the ^{29}Si NMR results. Si NEXAFS technique was limited in providing detailed information on the similarities and/or differences between OPC and OPC/slag pastes due to the lack of available reference spectra. Therefore, future work is recommended in this area.

Acknowledgements

The authors gratefully acknowledge the Australian Research Council Discovery Grant No. DP0558463 for this research project. Part of this research was undertaken on beamline 14ID-01 at the Australian Synchrotron, Victoria Australia. The views expressed are those of the authors and not necessarily those of the owner or operator of the Australian Synchrotron. J Cashion, B Cowie and R Hocking all kindly provided assistance. Finally, the authors would like to gratefully acknowledge Dr Jenny Pringle from Monash School of Chemistry for assistance with all NMR experiments.

5 References

1. Mendes A, Sanjayan J, Collins F (2008) Phase transformations and mechanical strength of OPC/Slag pastes submitted to high temperatures. *Materials and Structures* 41: 345-350
2. A Guide to the Use of Slag in Roads (2002) - Australasian Slag Association Inc. 19-21
3. Odler I (1998) *Lea's Chemistry of Cement and Concrete* Fourth ed., Elsevier, Oxford, UK
4. Taylor HFW (1997) *Cement chemistry*. Redwood Books, Wiltshire
5. Mendes A, Sanjayan J, Collins F (2009) Long-term progressive deterioration following fire exposure of OPC versus slag blended cement pastes. *Materials and Structures* 42: 95-101
6. Kirkpatrick RJ (1988) MAS NMR Spectroscopy of Minerals and Glasses, in *Spectroscopy Methods in Mineralogy and Geology*, Ribbe PH, Editor. Mineralogical Society of America, Chelsea, Michigan, pp. 341-387
7. Moore DM, Reynolds RC (1987) *X-ray Diffraction and the Identification and Analysis of Clay Minerals*. Oxford University Press, New York
8. Farmer VC (1974) The layer silicates, in *The IR Spectra of Minerals*, Farmer VC, Editor. Mineralogical Society, London pp. 539
9. Griffiths PR, deHasseth JA (1986) *Fourier Transform Infrared Spectroscopy*. Wiley and Sons, New York
10. Gates WP (2006) X-ray Absorption Spectroscopy, in *Handbook of Clay Science*, Bergaya F, Theng BKG, and Lagaly G, Editors, Elsevier, Amsterdam pp. 789 - 864
11. Bianconi A (1988) XANES spectroscopy, in *X-ray absorption: Principals, Applications, Techniques of EXAFS, SEXAFS and XANES*, Prins DCKaR, Editor. John Wiley and Sons, New York, pp. 573-662

12. Wu Z, Marcelli A, Giulli G, Paris E, Seifert F (1996) Effects of higher coordination shells in garnets detected by X-ray absorption spectroscopy at the Al k-edge. *Physics Review B* 54: 2969-2979
13. AS 3972 - 1997: Portland and blended cements. Standards Australia.
14. Li D, Bancroft GM, Kasrai M, Fleet ME, Secco RA, Feng XH, Tan KH, Yang BX (1994) X-ray absorption spectroscopy of silicon dioxide (SiO₂) polymorphs: The structural characterisation of opal. *American Mineralogist* 79: 622-632
15. Li D, M G, Bancroft, Fleet ME, Feng XH (1995) Silicon K-edge XANES spectra of silicate minerals. *Physics and Chemistry of Minerals* 22: 115-122
16. Hjorth J, Skibsted J, Jakobsen HJ (1988) ²⁹Si MAS NMR studies of portland cement components and effects of microsilica on the hydration reaction. *Cement and Concrete Research* 18: 789-798
17. MacLaren DC, White MA (2003) Cement: Its Chemistry and Properties. *Journal of Chemical Education* 80: 623-635
18. Alonso C, Fernandez L (2004) Dehydration and rehydration processes of cement paste exposed to high temperature environments. *Journal of Materials Science* 39: 3015-3024
19. Lippmaa E, Mägi M, Tarmak M, Wieker W, Grimmer AR (1982) A high resolution ²⁹Si NMR study of the hydration of tricalciumsilicate. *Cement and Concrete Research* 12: 597-602
20. Stephan D, Dikoundou SN, Sieber GR (2008) Influenced of combined doping of tricalcium silicate with MgO, Al₂O₃ and FeO₃: synthesis, grindability, X-Ray diffraction and ²⁹Si NMR. *Materials and Structures* 41: 1729-1740
21. Parry-Jones G, Al-Tayyib AJ, Al-Dulaijan SU, Al-Mana AI (1989) ²⁹Si MAS-NMR hydration and compressive strength study in cement paste. *Cement and Concrete Research* 19: 228-234
22. Johansson K, Larsson C, Antzutkin ON, Forsling W, Kota HR, Ronin V (1999) Kinetics of the hydration reactions in the cement paste with

- mechanochemically modified cement ^{29}Si magic-angle-spinning NMR study. Cement and Concrete Research 29: 1575-1581
23. Sun G, Brough AR, Young JF (1999) ^{29}Si NMR study of the hydration of Ca_2SiO_5 and $\text{b-Ca}_2\text{SiO}_4$ in the presence of silica fume. J Am Cer Soc 82: 3225-3230
 24. Schneider J, Cincotto MA, Panepucci H (2001) ^{29}Si and ^{27}Al high-resolution NMR characterization of calcium silicate hydrate phases in activated blast-furnace slag pastes. Cement and Concrete Research 31: 993-1001
 25. Wang S-D, Scrivener KL (2003) ^{29}Si and ^{27}Al NMR study of alkali-activated slag. Cement and Concrete Research 33: 769-774
 26. Richardson IG, Groves GW (1997) The structure of the calcium silicate hydrate phases present in hardened pastes of white Portland cement/blast-furnace slag blends. Journal of Materials Science 32: 4793-4802
 27. Richardson IG (1999) The nature of C-S-H in hardened cements. Cement and Concrete Research 29: 1131-1147
 28. Richardson IG (2008) The calcium silicate hydrates. Cement and Concrete Research 38: 137-158
 29. Skibsted J, Hall C (2008) Characterization of cement minerals, cements and their reaction products at the atomic and nano scale. Cement and Concrete Research 38: 205-225
 30. Sun GK, Young JF, Kirkpatrick RJ (2006) The role of Al in C-S-H: NMR, XRD, and compositional results for precipitated samples. Cement and Concrete Research 36: 18-29
 31. Brunet F, Charpentier T, Chao CN, Peycelon H, Nonat A (2009) Characterization by solid-state NMR and selective dissolution techniques of anhydrous and hydrated CEM V cement pastes. Cement and Concrete Research 40: 208-219
 32. Beaudoin JJ, Drame H, Raki L, Alizadeh R (2009) Formation and properties of C-S-H-PEG nano structures. Materials and Structures 42: 1003-1014

33. Castellote M, Fernandez L, Andrade C, Alonso C (2009) Chemical changes and phase analysis of OPC pastes carbonated at different CO₂ concentrations. *Materials and Structures* 42: 515-525
34. Skibsted J, Henderson E, Jakobsen HJ (1993) Characterization of calcium aluminate phases in cements by ²⁷Al MAS NMR spectroscopy. *Inorganic Chemistry* 32: 1013-1027
35. Hanna RA, Barrie PJ, Cheeseman CR, Hills CD, Buchler PM, Perry R (1995) Solid state ²⁹Si and ²⁷Al NMR and FTIR study of cement pastes containing industrial wastes and organics. *Cement and Concrete Research* 25: 1435-1444
36. Andersen MD, Jakobsen HJ, Skibsted J (2003) Incorporation of Aluminium in the Calcium Silicate Hydrate (C-S-H) of Hydrated Portland Cements A High Filed ²⁷Al and ²⁹Si MAS NMR investigation. *Inorganic Chemistry* 42: 2280-2287
37. Murgier S, Zanni H, Gouvenot D (2004) Blast furnace slag cement: a ²⁹Si and ²⁷Al NMR study. *C. R. Chimie* 7: 389-394
38. Andersen MD, Jakobsen HJ, Skibsted J (2006) A new aluminium-hydrate species in hydrated Portland cements characterized by ²⁷Al and ²⁹Si MAS NMR spectroscopy. *Cement and Concrete Research* 36: 3-17
39. Roncero J, Valls S, Gettu R (2002) Study of the influence of superplasticizers on the hydration of cement paste using nuclear magnetic resonance and X-ray diffraction techniques. *Cement and Concrete Research* 32: 103-108
40. Breval E (1976) C₃A Hydration. *Cement and Concrete Research* 6: 129-138
41. Ramlochan T, Zacarias P, Thomas MDA, Hooton RD (2003) The effect of pozzolans and slag on the expansion of mortars cured at elevated temperature Part I: Expansive behaviour. *Cement and Concrete Research* 33: 807-814
42. Bertron A, Duchesne J, Escadeillas G (2007) Degradation of cement pastes by organic acids. *Materials and Structures* 40: 341-354

43. Kourounis S, Tsivilis S, Tsakiridis PE, Papadimitriou GD, Tsibouki Z (2007) Properties and hydration of blended cements with steelmaking slag. *Cement and Concrete Research* 37: 815-822
44. Christensen AN, Scarlett NVY, Madsen IC, Jensen TR, Hanson JC (2003) Real time study of cement and clinker phases hydration. *Dalton Trans.* 1529-1536
45. Ghosh SN (2002) Infrared Spectroscopy in Cement Chemistry, in *Advances in Cement Technology*, Ghosh SN, Editor. Tech Books International, New Delhi, pp. 709-734
46. Bensted J, Prakash S (1968) Investigation of the Calcium Sulphate-Water System by Infrared Spectroscopy. *Nature* 219: 60-61
47. Bensted J, Varma SP (1971) Studies of Ettringite and its derivatives. *Cement Technology* May/June: 73-77
48. Bensted J, Varma SP (1973) Studies of Ettringite and its derivatives, Part 4: The low-sulphate form of calcium sulfoaluminate (monosulphate). *Cement Technology* May/June: 112-115
49. Bensted J, Varma SP (1974) Some applications of infrared and Raman spectroscopy in cement chemistry Part 3 - Hydration of Portland cement and its constituents. *Cement Technology* September/October: 440-450
50. Barnett SJ, Macphee DE, Lachowski EE, Crammond NJ (2002) XRD, EDX and IR analysis of solid solutions between thaumasite and ettringite. *Cement and Concrete Research* 32: 719-730
51. Gastaldi D, Canonico F, Boccaleri E (2009) Ettringite and calcium sulfoaluminate cement: investigation of water content by near-infrared spectroscopy. *Journal of Materials Science* 44: 5788-5794
52. Gao XF, Lo Y, Tam CM, Chung CY (1999) Analysis of the infrared spectrum and microstructure of hardened cement paste. *Cement and Concrete Research* 29: 805-812
53. Mollah MYA, Yu W, Schennach R, Cocke DL (2000) A Fourier transform infrared spectroscopy investigation of the early hydration of Portland cement

and the influence of sodium lignosulfonate. *Cement and Concrete Research* 30: 267-273

54. Mollah MYA, Kesmez M, Cocke DL (2004) An X-ray diffraction (XRD) and Fourier transform infrared spectroscopy (FT-IR) investigation of the long-term effect on the solidification/stabilization (S/S) of arsenic (V) in Portland cement type V. *Science of the Total Environment* 325: 255-262
55. Adler HH, Kerr PF (1963) Infrared spectra, symmetry and structure relations of some carbonate minerals. *American Mineralogist* 48: 839-853
56. White WB (1971) Infrared characterisation of water and hydroxyl ion in the basic magnesium carbonate minerals. *American Mineralogist* 56: 43-56
57. Teleb SM, Nassr DE-S, Nour EM (2004) Synthesis and infrared spectra of alkaline earth metal carbonates by the reaction of metal salts with urea at high temperature. *Bulletin Material Science* 27: 483-485
58. Hall C, Barnes P, Billimore AD, Jupe AC, Turrillas X (1996) Thermal decomposition of ettringite $\text{Ca}_6[\text{Al}(\text{OH})_6]_2(\text{SO}_4)_3 \cdot 26\text{H}_2\text{O}$. *Journal of the Chemical Society, Faraday Transactions* 92: 2125-2129
59. Nosov VN, Frolova NG, Kamyshev VF (1976) IR Spectra of calcium sulphate semihydrate. *Zhurnal Prikladnoi Spektroskopii* 24: 713-715
Translated from Russian March 1976.
60. Adler HH, Kerr PF (1965) Variations in infrared spectra, molecular symmetry and site symmetry of sulphate minerals. *American Mineralogist* 50: 132-147
61. Piasta J, Sawicz Z, Rudzinski L (1984) Changes in the structure of hardened cement paste due to high temperature. *Materials and Structures* 17: 291-296

Chapter 7

NMR, XRD, IR and Synchrotron NEXAFS

Spectroscopic Studies of OPC and OPC/Slag Cement Paste Hydrates after Exposure to Elevated Temperatures

7.1 Overview

Chapter 6 investigated the fundamental similarities and/or differences between ordinary Portland cement (OPC) and OPC/slag paste hydrates at room temperature, forming the basis to assist in the identification of changes in the paste hydrates after exposure to elevated temperatures. The present Chapter 7 aims to identify these changes in OPC and OPC/slag paste hydrates.

This chapter is based on the publication of the same name as the chapter title submitted to Cement and Concrete Research Journal in July 2010. The effects of elevated temperatures on the silicate and aluminate phases of OPC and OPC/slag pastes are investigated by the following techniques: silicon and aluminium nuclear magnetic resonance (^{29}Si NMR and ^{27}Al NMR), X-ray diffraction (XRD), infrared (IR) and synchrotron Si K-edge near edge X-ray absorption fine structure (NEXAFS) spectroscopy.

7.2 Declaration for Thesis Chapter 7

Declaration by candidate

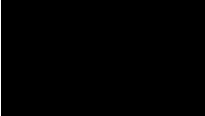
In the case of Chapter 7, the nature and extent of my contribution to the work was the following:

| Nature of contribution | Extent of contribution (%) |
|---|----------------------------|
| Developing outline of research objective and hypothesis Laboratory/experimental investigation and analysis of results Writing, reviewing and editing of paper | 85 |

The following co-authors contributed to the work. Co-authors who are students at Monash University must also indicate the extent of their contribution in percentage terms:

| Name | Nature of contribution | Extent of contribution (%) for student co-authors only |
|---------------|---|---|
| Jay Sanjayan | Developing outline of research objective and hypothesis Reviewing of paper | 2.5 |
| Frank Collins | Developing outline of research objective and hypothesis Reviewing of paper | 2.5 |
| Will P Gates | Developing outline of research objective and hypothesis Reviewing of paper | 10 |

Candidate's
Signature



30 September 2010

Declaration by co-authors

The undersigned hereby certify that:

- (1) the above declaration correctly reflects the nature and extent of the candidate's contribution to this work, and the nature of the contribution of each of the co-authors.
- (2) they meet the criteria for authorship in that they have participated in the conception, execution, or interpretation, of at least that part of the publication in their field of expertise;
- (3) they take public responsibility for their part of the publication, except for the responsible author who accepts overall responsibility for the publication;
- (4) there are no other authors of the publication according to these criteria;

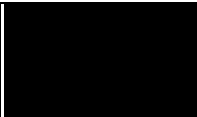
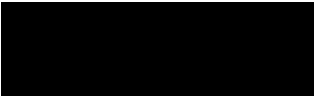
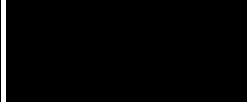
- (5) potential conflicts of interest have been disclosed to (a) granting bodies, (b) the editor or publisher of journals or other publications, and (c) the head of the responsible academic unit; and
- (6) the original data are stored at the following location(s) and will be held for at least five years from the date indicated below:

Location(s)

| |
|--|
| Department of Civil Engineering, Monash University |
|--|

[Please note that the location(s) must be institutional in nature, and should be indicated here as a department, centre or institute, with specific campus identification where relevant.]

Signature 1

| | |
|---|--------------------------|
|  | 30 September 2010 |
|  | 30 September 2010 |
|  | 30 September 2010 |

Signature 2

Signature 3

7.3 Publication

NMR, XRD, IR and Synchrotron NEXAFS Spectroscopic Studies of cement paste hydrates after exposure to elevated temperatures

Alessandra Mendes¹, Will P Gates¹, Jay G Sanjayan², Frank Collins¹

¹Civil Engineering Department, Monash University, Clayton VIC, Australia

²Faculty of Engineering and Industrial Sciences, Swinburne University of Technology, Hawthorn VIC, Australia

Phone: + 61 3 9905 5022, fax: + 61 3 9905 4944

Alessandra.mendes@monash.edu

Abstract

The present work investigates the contributions of paste hydrates such as C-S-H, ettringite and monosulphate, to the deterioration of the mechanical properties of OPC (ordinary Portland cement) and OPC/slag pastes after exposure to elevated temperatures. OPC/slag paste is compared because it does not deteriorate to the same extent as OPC paste. The study used five techniques, namely, ²⁹Si and ²⁷Al nuclear magnetic resonance (NMR), X-Ray Diffraction (XRD), Infrared Spectroscopy (IR) and Near Edge X-Ray Absorption Fine Structure (NEXAFS). The use of five different techniques was intended to minimise the uncertainties and limitations of any one technique. The tests results revealed that, after 800°C, OPC paste presented total loss of the C-S-H gel while the OPC/slag paste still presented some polymerized material. In addition, after 800°C, the aluminate phase of OPC experienced rehydration while this was not observed for the OPC/slag paste.

Keywords: B. Hydration products; D. Cement paste; A. Elevated temperatures; C. Mechanical properties; B. Spectroscopy

1 Introduction

The fire resistance of concrete has been the focus of researchers since 1922 [1]. When concrete is exposed to elevated temperatures, as in a fire event, physical and chemical transformations take place resulting in deterioration of its mechanical properties.

Above 400°C, one of the main hydrates of the OPC cement paste, calcium hydroxide (CaOH_2) dehydrates into calcium oxide (CaO) causing the OPC paste to shrink and crack [1-3]. After cooling and in the presence of air moisture, CaO rehydrates into CaOH_2 causing expansion, total strength loss and complete disintegration of the OPC paste [3-5].

Previous studies reported that the dehydration of CaOH_2 and rehydration of CaO caused no significant deterioration in pastes where OPC was partially replaced with slag [3, 4, 6]. Ground granulated blast furnace slag (GGBFS or 'slag') is a by-product of the iron and steel industries. Following grinding and blending with OPC the granulated, ground slag is cementitious. During hydration slag consumes most of the available CaOH_2 [7], consequently reducing or even eliminating the negative effects caused by the CaOH_2 dehydration and CaO rehydration when the cement paste is submitted to elevated temperatures.

On the other hand, very little research has been conducted in order to determine the contribution, if any, of the other cement paste hydrates to the deterioration of mechanical properties after exposure to elevated temperatures. Once the OPC paste hydration is complete, four main hydrates are formed: calcium silicate hydrate (C-S-H gel), CaOH_2 , ettringite and monosulphate hydrate. Partial replacement of OPC with slag leads to similar paste hydrates [8, 9], although as described above, the CaOH_2 amount is expected to be lower [7, 9].

Furthermore, deeper understanding of the performance of cement based materials requires knowledge at the microstructural level [10]. Therefore, it is of importance to identify the contributions, if any, of the other paste hydrates to the deterioration of the mechanical properties after exposure to elevated temperatures.

Some studies have attempted to characterize OPC hydrates after exposure to elevated temperatures and will be discussed here. In contrast, there is no such data for pastes where OPC has been partially replaced with slag. Thus, the present work investigates OPC and OPC/slag paste hydrates after exposure to elevated temperatures. In this investigation the following techniques are used: 1. Silicon nuclear magnetic resonance (^{29}Si NMR); 2. Aluminium nuclear magnetic resonance (^{27}Al NMR); 3. X-ray diffraction (XRD); 4. Infrared spectroscopy (IR) and 5. Synchrotron Si K-edge near edge X-ray absorption fine structure (NEXAFS) spectroscopy. The use of five different techniques was intended to minimise the uncertainties and limitations of any one technique, and to allow more comprehensive and accurate conclusions to be drawn.

2 Materials and Methods

2.1 Materials

Ordinary Portland cement (OPC) and ground granulated blast furnace slag (GGBFS or “slag”), conforming with the requirements of Australian Standard AS 3972 [11] were used as binder materials. The chemical composition and properties of the binders are presented in Table 1. The OPC used in this study has a low C_3A content of < 5%.

Table 1 Chemical composition and properties of the binders

| Constituent/property % | OPC | Slag |
|----------------------------------|-------|------|
| SiO_2 | 19.90 | 32.5 |
| Al_2O_3 | 4.70 | 13 |
| $\text{Fe}_2\text{O}_3\text{T}$ | 3.38 | 0.22 |
| MgO | 1.30 | 5.47 |
| CaO | 63.93 | 42.1 |
| Na_2O | 0.17 | 0.21 |
| TiO_2 | 0.245 | 1.08 |
| K_2O | 0.446 | 0.25 |
| MnO | 0.079 | 5.47 |
| P_2O_5 | 0.063 | bd* |
| SO_3 | 2.54 | 4.1 |
| LOI | 2.97 | 0.35 |
| Fineness, m^2/kg | 360 | 435 |
| Specific gravity | 3.15 | 2.92 |

*bd: below detection

In this investigation OPC was partially replaced with 35% by weight with slag. The term water/binder (w/b) ratio is used instead of the water/cement ratio to include both binder types mentioned above. The w/b ratio used was 0.5.

Cylinder specimens of diameter 50 mm and length 100 mm were investigated. The specimens consisted of pastes.

The two different mixtures (i.e., replacement 0 and 35% by weight with slag) were prepared by adding water followed by the binders. Each mixture was prepared in a mechanical mixer of 20 litres of capacity, 80 rpm, for five minutes. The specimens were cast using a vibration table for better compaction. Specimens were sealed with a plastic sheet and demolded after 24 hours. Demolding was followed by 28 days curing in lime-saturated water bath at 23°C.

2.2 Methods

Heat treatment

Before exposure to high temperatures, the specimens were oven-dried for 2 days at 60°C. Following drying, heat treatment was conducted in a Tetlow furnace. The heat treatment was as follows: constant heating rate of 6.25°C/min until 50°C below the desired temperature, then 1 hour until the desired temperature was reached, followed by 1 hour at the desired temperature. For example, at 800°C heat treatment, constant heating rate of 6.25°C/min until 750°C, then 1 hour between 750-800°C, and finally 1 hour in 800°C.

Three different temperatures were applied: 400, 500 or 800°C. Following heating the specimens were allowed to cool down inside the furnace until room temperature was reached. After cooling, the heat treated OPC and 35% slag pastes were investigated using solid-state NMR analysis, X-ray diffraction, Infrared and Si NEXAFS spectroscopy. The reference specimens (not heat treated) were tested immediately after drying to avoid further hydration. The heat treated specimens were investigated immediately after cooling to avoid rehydration.

Nuclear Magnetic Resonance (NMR)

Solid-state NMR analysis was performed using a Bruker AM300 instrument equipped with a Bruker 4 mm solid-state probe operating 59.6 MHz for ^{29}Si and 78.2 MHz for ^{27}Al . The chemical shifts were referenced to external samples of tetramethylsilane (TMS) for ^{29}Si and aqueous $\text{Al}(\text{OH})_3$ for ^{27}Al . The samples were analysed neat and all of the spectra were collected using a magic angle spinning (MAS) speed of 8 KHz. For the single ($\sim 90^\circ$ flip) pulse ^{27}Al NMR experiments a recycle delay of 2 seconds was used, with a 2.7 μsec pulse length and 200 Hz line broadening. For the single ($\sim 30^\circ$ flip) pulse ^{29}Si NMR experiments a pulse length of 3.5 μsec was used, with a delay time of 10 seconds and 100 Hz line broadening. The NMR data were processed by adopting a base line correction to flatten the background and normalising to the maximum signal intensity, to enable comparison across samples. The decompositions were accomplished by employing a Lorentzian profile for each component using the Equation 1 below. Components were initially placed using inflections and changes of slope in the spectrum as a guide to their possible presence and estimates of width (half width at half maximum), amplitude and centre were initially adjusted manually. All components were summed across the entire region of interest and the summed components (together forming the “fit spectrum”) were compared to the original spectrum using Least Square minimizations. The amplitude, height and width of each component were iteratively adjusted either independently (i.e., initially) or in combination (as the fit became “realistic”). Chi Square was calculated as an assessment of quality of fit. The integrated area of each component was calculated and if any component was less than 2-3% of the total signal, it was removed and the other components allowed to compensate. The ^{27}Al NMR data was processed as per above, except that an additional broad feature had to be added due to increased line broadening of the octahedral Al signal. The generalised expression used for Lorentzian distribution is represented below by Equation 1.

$$y = \frac{A}{1 + \left(x - \frac{C}{B}\right)^2} \quad (1)$$

Where y is the resulting component magnitude at each x ; x is the position in ppm of the NMR signal; A , B and C are, respectively, the component amplitude, width and centre.

X-Ray Diffraction (XRD)

Powder X-ray traces were collected on a Phillips 1710 diffractometer modified with an electronic stepper motor using a Cu K α radiation source within the range of 2 to 60°2 θ using step size of 0.02°2 θ and a scan rate of 1°2 θ per minute. Random powdered samples were back-pressed into aluminium sample supports onto frosted glass slide to minimise any preferred orientation effects. Mineral phases present in the traces were identified from auto-selected references in the international crystallographic diffraction database (ICDD) using the program XPLOT (CSIRO).

Infrared Spectroscopy (IR)

Diffuse reflectance IR spectroscopy was conducted using a FTS 3000 MX Excalibur Series Digilab fitted with a glow bar radiation source, a DTGS detector, dry CO₂-free air purge and an extended KBr beamsplitter. The sample space was continuously purged with dry nitrogen. As many as 512 acquisitions were co added at a resolution of 2 cm⁻¹ on powdered specimens mixed (~ 5%) with sodium chloride (ACS). Each spectrum was referenced to NaCl and converted to Kubelka-Munk absorbance units for comparison.

Near Edge X-Ray Absorption Fine Structure (NEXAFS)

X-ray absorption spectroscopy was performed at the Australian Synchrotron as part of the commissioning of the “soft X-ray beamline” (14ID-01). Total electron yield (measured as drain current) Si K near edge X-ray absorption fine structure (NEXAFS) spectra, in the energy range of ~1840 to ~1890 eV, were collected on undiluted powdered samples pressed onto carbon tape. Steps of 0.1 eV and acquisition times of 1 second were used. A minimum of 2 scans were co-added after adjusting for instrumental energy drift and compared to reference minerals and from the survey work of Li et al. [12, 13]. Spectra were processed following typical procedures [14] by base-line correcting and intensity normalisation. Energies were adjusted to match the maximum intensity of the main peak of α -SiO₂, and intensities were normalised to a value of 1.0 at 1880 eV.

3 Results and discussion

3.1 ^{29}Si NMR

Solid state ^{29}Si magic-angle spinning (MAS) NMR offers an efficient method to follow the hydration of C_3S in a qualitative and semi quantitative way because Si chemical shifts reflect the degree of condensation of SiO_2 tetrahedra [15]. This gives valuable information related to the formation of the calcium silicate hydrate (C-S-H) gel.

Interpretation of ^{29}Si NMR spectra requires knowledge of the local silicate tetrahedral environment, which can be designated as Q^n , where 'Q' represents the silicon tetrahedron bonded to four oxygen atoms and 'n' is the connectivity, i.e., the number of other 'Q' units attached to the SiO_4 tetrahedron under study. An increase in the number of SiO_4 units bonded to each Si centre produces an increase in the average electron density around the central Si atom, leading to a more negative chemical shift, relative to tetramethylsilane (TMS), for successively increasing n values in Q^n [16].

Thus, Q^0 denotes the monomeric orthosilicate anion SiO_4^{4-} (nesosilicate) typical of anhydrous silicate of cement (C_3S and C_2S), Q^1 represents an end group of a chain of C-S-H, Q^2 a middle group of C-S-H chain, and Q^3 and Q^4 are representative of points where branching in the silicate structure may occur [17]. Typical values for cement ^{29}Si NMR are: $\text{Q}^0 = -70$, $\text{Q}^1 = -80$ and $\text{Q}^2 = -88$ ppm [16].

In the present work, ^{29}Si NMR was conducted on OPC and 35% slag pastes exposed to 400, 500 and 800°C. The results are compared to the reference specimens named 'RT' (room temperature).

Fig. 1 presents the spectra for OPC and 35% slag specimens. A summary of the chemical shifts observed and the related assignments is presented in Table 2.

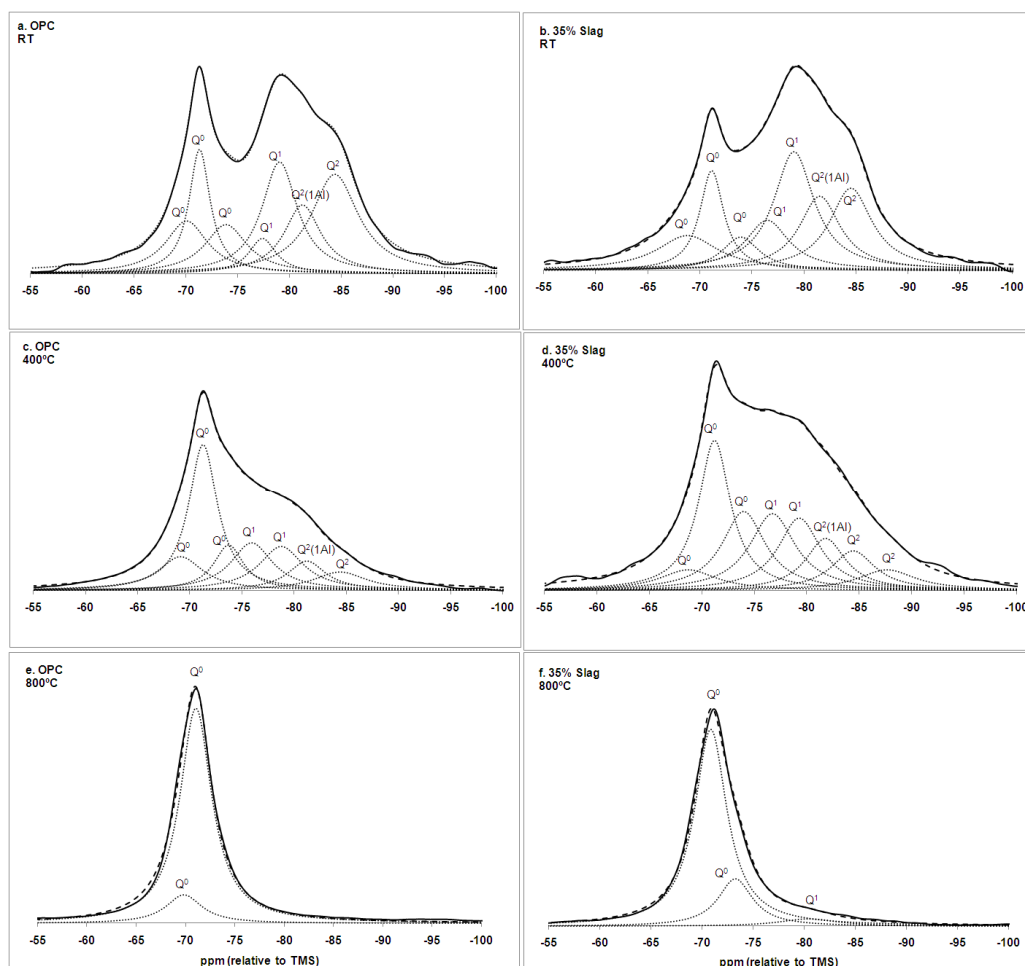


Fig. 1 Single pulse ^{29}Si NMR spectra of OPC and 35% slag pastes. Results of best least-squares fit decompositions are also displayed

Table 2 Results from decomposition of ^{29}Si NMR spectra of OPC and 35% slag pastes

| Sample | Q ⁰ | | | Q ⁰ | | | Q ⁰ | | |
|----------------|----------------|-------------|-------------------|----------------|------------|-------------------|----------------------|------------|-------------------|
| | Centre (ppm) | FWHM* (ppm) | Relative area (%) | Centre (ppm) | FWHM (ppm) | Relative area (%) | Centre (ppm) | FWHM (ppm) | Relative area (%) |
| OPC RT | -70.0 | 4.97 | 11.59 | -71.3 | 2.49 | 14.08 | -73.8 | 4.98 | 10.89 |
| OPC 400°C | -69.1 | 5.17 | 11.44 | -71.2 | 3.35 | 32.65 | -73.7 | 3.48 | 10.41 |
| OPC 500°C | -69.0 | 6.77 | 14.85 | -71.1 | 3.30 | 30.73 | -73.6 | 3.79 | 9.14 |
| OPC 800°C | -69.8 | 4.44 | 12.92 | -71.0 | 3.93 | 87.08 | - | - | - |
| 35% slag RT | -68.8 | 7.15 | 10.85 | -71.1 | 2.80 | 12.72 | -73.9 | 4.35 | 6.53 |
| 35% slag 400°C | -68.7 | 6.63 | 5.55 | -71.2 | 3.67 | 23.11 | -74.0 | 5.01 | 16.33 |
| 35% slag 500°C | -68.3 | 7.04 | 9.33 | -71.2 | 3.68 | 24.05 | -74.0 | 5.21 | 19.35 |
| 35% slag 800°C | - | - | - | -70.8 | 3.85 | 76.00 | -73.3 | 4.09 | 19.28 |
| Sample | Q ¹ | | | Q ¹ | | | Q ² (1Al) | | |
| | Centre (ppm) | FWHM (ppm) | Relative area (%) | Centre (ppm) | FWHM (ppm) | Relative area (%) | Centre (ppm) | FWHM (ppm) | Relative area (%) |
| OPC RT | -77.4 | 3.22 | 5.07 | -79.0 | 4.16 | 20.72 | -81.2 | 4.33 | 13.22 |
| OPC 400°C | -75.9 | 4.85 | 15.20 | -78.4 | 5.13 | 14.79 | -81.2 | 4.37 | 8.36 |
| OPC 500°C | -75.5 | 5.18 | 15.63 | -78.6 | 5.43 | 14.91 | -81.3 | 4.78 | 8.01 |
| OPC 800°C | - | - | - | - | - | - | - | - | - |
| 35% slag RT | -76.5 | 5.04 | 11.22 | -79.1 | 4.69 | 24.87 | -81.5 | 4.77 | 15.70 |
| 35% slag 400°C | -76.7 | 5.28 | 16.66 | -79.3 | 4.92 | 14.64 | -81.8 | 4.64 | 9.99 |
| 35% slag 500°C | -76.8 | 5.35 | 16.73 | 79.3 | 4.93 | 13.36 | -81.6 | 4.49 | 8.75 |
| 35% slag 800°C | - | - | - | -80.4 | 7.03 | 4.72 | - | - | - |
| Sample | Q ² | | | Q ² | | | Sum of squares | Chi square | |
| | Centre (ppm) | FWHM (ppm) | Relative area (%) | Centre (ppm) | FWHM (ppm) | Relative area (%) | | | |
| OPC RT | -84.4 | 5.57 | 24.41 | - | - | - | 0.0260 | 0.0938 | |
| OPC 400°C | -84.4 | 6.14 | 7.15 | - | - | - | 0.0068 | 0.0422 | |
| OPC 500°C | -84.8 | 9.11 | 6.72 | - | - | - | 0.1847 | 0.1091 | |
| OPC 800°C | - | - | - | - | - | - | 0.0473 | 0.4795 | |
| 35% slag RT | -84.5 | 4.95 | 18.11 | - | - | - | 0.0199 | 0.0815 | |
| 35% slag 400°C | -84.4 | 5.05 | 8.14 | -87.6 | 6.64 | 5.58 | 0.0221 | 0.3130 | |
| 35% slag 500°C | -84.3 | 4.18 | 4.26 | -87.3 | 7.08 | 4.17 | 0.0079 | 0.0395 | |
| 35% slag 800°C | - | - | - | - | - | - | 0.1285 | 0.5072 | |

*Full width at half maximum

For the OPC reference samples, 6 chemical shifts are observed (Table 2 and Fig. 1a). Three Q^0 resonances are detected at -70.0, -71.3, -73.8 ppm. This is in accordance with previous works [15, 18, 19]. The sharp peak at -71.3 ppm relates to belite/larnite (C_2S) [17, 19, 20].

Two Q^1 chemical shifts are detected at -77.4 and -79.0 ppm [15, 20-25] while $Q^2(1Al)$ is observed at -81.2 ppm and Q^2 at -84.4 ppm [15, 19-24, 26]. The chemical shift $Q^2(1Al)$ at -81.2 ppm relates to the Al substitution for Si confined to the bridging tetrahedron [20, 22-25].

Similarly, 6 chemical shifts are observed for the 35% slag reference samples (35% slag RT), Table 2 and Fig. 1b. For Q^0 the following chemical shifts are detected at -68.8, -71.1, -73.9 ppm. This is in accordance with previous works [15, 18, 19], in which the chemical shift at -73.9 ppm relates to unreacted slag [20, 23] and the sharp peak at -71.3 ppm relates to belite/larnite (C_2S) [17, 19, 20].

For the Q^1 resonance two chemical shifts are observed at -76.5 and -79.1 ppm [15, 20-25]. Furthermore, the resonance $Q^2(1Al)$ is observed at -81.5 ppm while Q^2 is detected at -84.5 ppm [15, 19-24, 26]. As for the OPC paste, the chemical shift $Q^2(1Al)$ at -81.5 ppm relates to the Al substitution for Si confined to the bridging tetrahedron [20, 22-25].

When heated to 400°C, differences are found between OPC and 35% slag pastes (Fig. 1c and d, respectively). For the OPC pastes, in general, there was an increase in the relative area (%) of Q^0 resonances, while a decrease in the relative area (%) of Q^1 , $Q^2(1Al)$ and Q^2 resonances was observed. It is also noted that the FWHM (full width at half maximum) for the Q^1 and Q^2 chemical shifts increased with heating. According to Alonso and Fernandez [17] this is due to a more disordered structure of the amorphous C-S-H with heating. Alonso and Fernandez [17] investigated the effects of elevated temperatures on the microstructure of OPC pastes. Above 450°C, their OPC paste no longer presented the chemical shift related to Q^2 while a new Q^0 and Q^1 peaks were observed above this temperature.

For the 35% slag specimens (Fig. 1d), there was also an increase in the relative area (%) of the Q^0 resonances, in particular for the chemical shifts at -71.2 ppm (referent to C_2S) and -74 ppm (referent to the unreacted slag). A decrease in the

relative area (%) of Q^1 , $Q^2(1Al)$ and Q^2 resonances was observed while a new resonance at -87.6 ppm was detected, having a small relative area of ~ 5.5%. This new resonance is assigned as Q^2 and was possibly being encompassed by the other resonances at room temperature (RT). It is important to note that with the increase of temperature to 400°C, the 35% slag pastes remained more polymerized than OPC pastes. This indicates that the OPC C-S-H gel has been more affected by temperature than the 35% slag C-S-H. From 400 to 500°C, while some changes in the FWHM and relative areas of the components occurred, the chemical shifts remained essentially unchanged for both OPC and 35% slag (Table 2).

After exposure to 800°C, the OPC paste shows a total transformation of the initial C-S-H gel structure (Q^1 and Q^2) (Fig. 1e), in accordance with the observations of Alonso and Fernandez [17]. The OPC paste has no detectable Q^1 or Q^2 . Two Q^0 resonances are now observed instead of the 3 observed at room temperature (RT). The resonance at -69.8 ppm remained almost unchanged with the increase in temperature while the resonance at -71.0 ppm (related to C_2S) significantly increased in relative area (from ~ 14% at room temperature to 87%).

The 35% slag paste shows a very different behaviour after exposure to 800°C (Fig. 1f). The Q^2 and $Q^2(1Al)$ resonances detected in samples heated to as high as 500°C are no longer detected above 800°C. However, in contrast to OPC, a small resonance Q^1 at -80.4 ppm (~5% relative area) is still observed, indicating that the 35% slag remained slightly more polymerized than OPC after exposure to 800°C. Differences were also observed for the resonances related to Q^0 . While the Q^0 resonance at -68.8 ppm (room temperature) was not detected, the Q^0 resonance at -70.8 ppm (referent to C_2S) increased in relative area (~13% at room temperature to 75%). In addition, the Q^0 resonance at -73.3 ppm (related to the unreacted slag) was also detected with its relative area having increased from ~ 6.5% at room temperature to 20%.

In summary, there are no major differences in the C-S-H gel composition of OPC and 35% slag pastes at room temperature. However, a different scenario is observed with the increase in temperature. Above 400°C, the 35% slag pastes remained more polymerized than the OPC pastes. After exposure to 800°C, the OPC paste completely lost its hydrated materials and presented only the Q^0 resonances at -69.8 and -71.0 ppm (12.92% and 87.08% of relative area,

respectively). On the other hand, the 35% slag paste presented Q^0 resonances at -70.8 and -73.3 ppm (76.0% and 19.28% of relative area, respectively) and a small Q^1 resonance at -80.4 ppm. This indicates that the 35% slag pastes remained slightly more polymerized than the OPC pastes after exposure to 800°C. As discussed previously, after exposure to 800°C, OPC paste completely disintegrates and crumbles. In contrast, 35% slag paste has a residual compressive strength of more than 30% [3]. This difference in deterioration of mechanical properties was attributed to differences in the $CaOH_2$ hydrate content between OPC and 35% slag paste. However, the present ^{29}Si NMR shows that OPC and 35% slag C-S-H gels differ with the increase in temperature. The C-S-H gel has been described by Mehta and Monteiro [27] as the most important phase determining the properties of the paste. As described above, beyond 400°C, the 35% slag paste retained more polymerized material than the OPC paste. Therefore, it is likely that the further deterioration on the mechanical properties observed for the OPC paste in comparison to 35% slag paste can also be attributed to the differences in the silicate phases between these pastes after exposure to temperatures above 400°C.

3.2 ^{27}Al NMR

Solid state ^{27}Al magic-angle spinning (MAS) NMR has been useful in characterizing calcium aluminates and aluminate hydrates (ettringite and monosulphate hydrate), which are of importance in the chemistry of cements [28]. Generally, ^{27}Al MAS NMR has been concerned with the distinction between tetrahedrally ($Al(4)$) and octahedrally ($Al(6)$) coordinated aluminium, using the distinct chemical shift difference of about 60 ppm for these two coordination environments [28]. $Al(4)$ is generally observed between 50 and 80 ppm, while $Al(6)$ normally resonates between -20 and 20 ppm [29]. However, ^{27}Al MAS NMR spectroscopy has the disadvantage that spectra can be difficult to interpret, as ^{27}Al can be affected by quadrupolar interactions. This leads to a field-dependent shift in resonance position as well as an asymmetric broadening of the peaks [29].

Fig. 2 presents the spectra for OPC and 35% slag specimens. A summary of the chemical shifts observed and the related assignments is presented in Table 3.

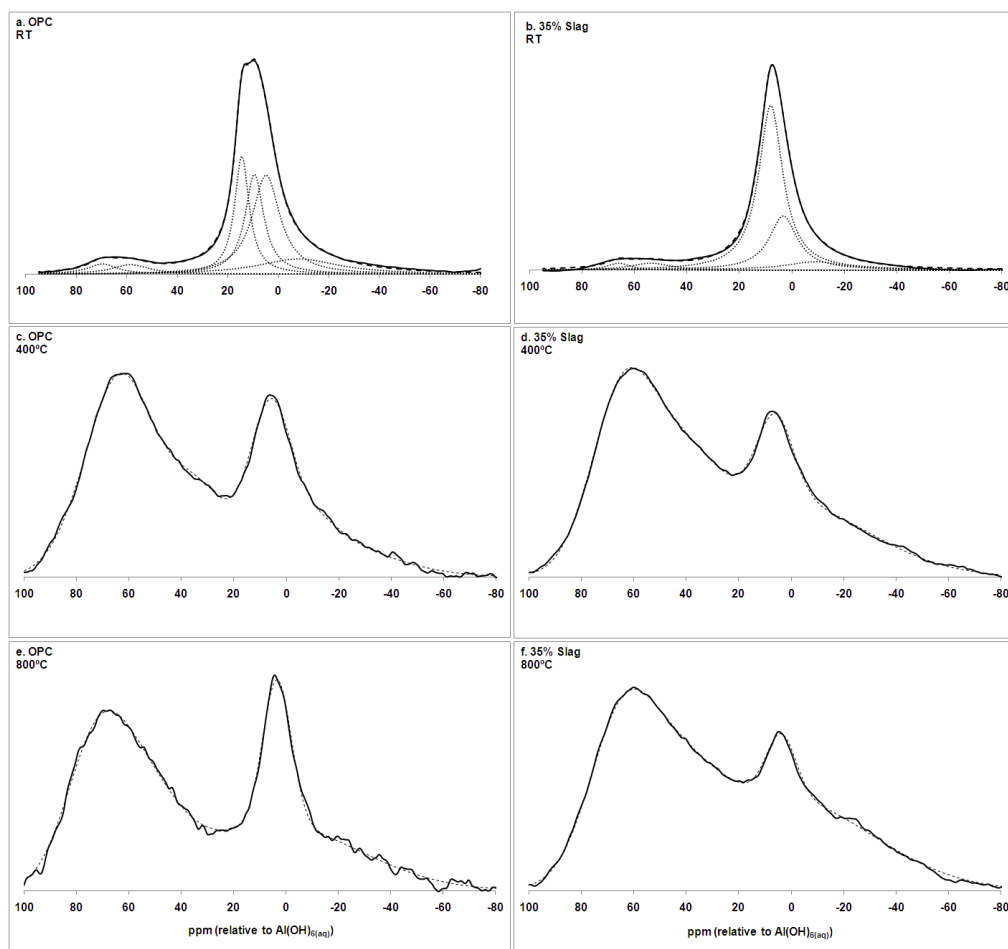


Fig. 2 Single pulse ^{27}Al NMR spectra of OPC and 35% slag pastes. Results of best least-squares fit decompositions are also displayed for the room temperature samples

Table 3 Results from decomposition of ^{27}Al NMR spectra of OPC and 35% slag pastes RT

| Sample | Centre ppm (relative to $\text{Al}(\text{OH})_3(\text{aq})$) | FWHM* (ppm) | Relative Area (%) | Assignment | Sums of square | Chi square |
|-------------|--|----------------|----------------------|---------------|----------------------|---------------|
| OPC RT | 69.8 | 14.06 | 3.53 | Al^4 | 0.0446 | 0.686 |
| | 58.7 | 17.75 | 4.04 | Al^4 | | |
| | 14.6 | 7.00 | 21.62 | Al^6 | | |
| | 9.6 | 8.95 | 23.27 | Al^6 | | |
| | 5.0 | 13.35 | 33.88 | Al^6 | | |
| | -7.9 | 38.80 | 13.66 | Quadrupolar | | |
| 35% Slag RT | 66.1 | 11.03 | 3.20 | Al^4 | 0.0103 | 5.34 |
| | 53.9 | 19.75 | 5.42 | Al^4 | | |
| | 8.1 | 11.78 | 58.98 | Al^6 | | |
| | 3.4 | 12.90 | 24.82 | Al^6 | | |
| | -8.8 | 26.11 | 7.57 | Quadrupolar | | |

*Full width at half maximum

The major differences in the ^{27}Al NMR spectra between OPC and the 35% slag RT pastes are in the number and position of the Al(6) sites. In the OPC RT, two Al(4) and three Al(6) sites are observed. The Al(4) sites are located at 69.8 and 58.7 ppm. According to previous works [24, 30, 31] the chemical shift at 69.8 ppm is attributed to Al substitution within a C-S-H phase, also observed in the ^{29}Si NMR results presented in the previous section. The Al(4) site located at 58.7 ppm is likely to refer to unhydrated material [24, 28]. The Al(6) sites in OPC have the following chemical shifts: 14.6, 9.6 and 5.0 ppm. The first two chemical shifts are in accordance with the resonance peaks reported in the literature for, respectively, ettringite and monosulphate hydrate [28-31]. The chemical shift reported at 5.0 ppm can be possibly assigned to the previously reported chemical shifts for TAH (5 ppm) [30, 32] or C_4AH_{13} (7 ppm) [28]. However, the ^{27}Al NMR spectrum does not enable a definite assignment of this particular feature. XRD tests conducted in OPC pastes are discussed further in an attempt to determine which hydrate phase this peak may represent. Furthermore, the very broad fitted feature with a chemical shift at -7.9 ppm is may be due to quadrupolar broadening of the Al(6) signal.

For the 35% slag RT, two Al(4) sites and only two Al(6) sites are observed. The Al(4) sites are located at 66.1 and 53.9 ppm. As per the OPC paste, the peak fitted with a chemical shift at 66.1 ppm is attributed to Al substitution within a C-S-H phase [24, 30, 31]. Such phase was also observed by ^{29}Si NMR. The peak fitted with a chemical shift at 53.9 ppm is likely to refer to unhydrated material [24, 28] possibly slag. The Al(6) sites observed have chemical shifts at 8.1 and 3.4 ppm. The chemical shift at 8.1 ppm is in accordance with the resonance peak reported in the literature for monosulphate hydrate [28-31]. Murgier et al. [31] reported but was unable to assign a peak having a chemical shift at 3.5 ppm, whereas Schneider et al. [24] assigned a chemical shift at 3.5 ppm as a hydrogarnet CAH_{10} phase based on XRD results. XRD tests were performed in 35% slag pastes and are discussed further to confirm whether the 3.4 ppm chemical shift can be assigned to CAH_{10} . Furthermore, as for the OPC, the chemical shift at -8.8 ppm is likely to be due to quadrupolar broadening of the Al(6) signal.

Due to excessive line broadening and poor signal to noise, the Al NMR spectra at elevated temperature (above 400°C) could not be satisfactorily fit, therefore only the spectra are presented. Fig. 2c and d (OPC and 35% slag, respectively) shows that with the increase of temperature to 400°C there is a significant conversion of octahedral sites Al(6) to tetrahedral sites Al(4). This conversion is very similar for both the OPC and 35% slag paste showing that with an increase in temperature the hydrated Al(6) dehydrates into Al(4) unhydrated materials. Furthermore, following exposure to 800°C, the conversion is sustained and both Al(6) and Al(4) are present in the OPC and 35% slag pastes (Fig. 2e and f, respectively). However, Fig. 2e shows that the octahedral Al(6) component of the OPC paste increased from 400°C to 800°C. This indicates that rehydration occurred in the OPC paste, either during cooling or transition from furnace to the NMR experiment, showing that OPC pastes are more prone to rehydration than the 35% slag pastes.

Although ^{27}Al NMR has been limited in characterizing the aluminate phases after exposure to elevated temperatures, Fig. 2 shows that the aluminate phases of OPC and 35% pastes differ significantly after exposure to elevated temperatures, especially in relation to octahedral Al(6) sites, possibly due to the rehydration of OPC pastes. Therefore, it is likely that the aluminate phases play a role in the differences found in the deterioration of mechanical properties between OPC and 35% slag pastes after exposure to 800°C.

3.3 X-ray diffraction (XRD)

X-ray diffraction (XRD) is used to identify the polycrystalline phases of cement and hardened cement paste through the recognition of the X-ray patterns for each of the crystalline phases [33]. Therefore, XRD is a useful tool to detect crystalline hydrates such as ettringite, monosulphate hydrate, portlandite (CaOH_2), calcium carbonate, and calcium silicate hydrate, as well as the various calcium silicates, calcium aluminate and aluminosilicate phases possibly present.

The XRD spectra (Fig. 3) shows that at room temperature, both blends presented unhydrated starting materials such as larnite (C_2S), C_3A and also the hydrated phase C-S-H. The main phases observed for OPC paste RT are: calcium hydroxide or portlandite (CaOH_2), calcite (CaCO_3) and ettringite (Fig. 3). For 35% slag pastes similar phases were found, however CaOH_2 and calcite were present in less

quantity and ettringite was not detected. The absence of ettringite in the 35% slag paste XRD spectrum is in accordance with the ^{27}Al NMR results. In contrast, 35% slag pastes presented monosulphate hydrate, which is absent in OPC pastes XRD spectrum.

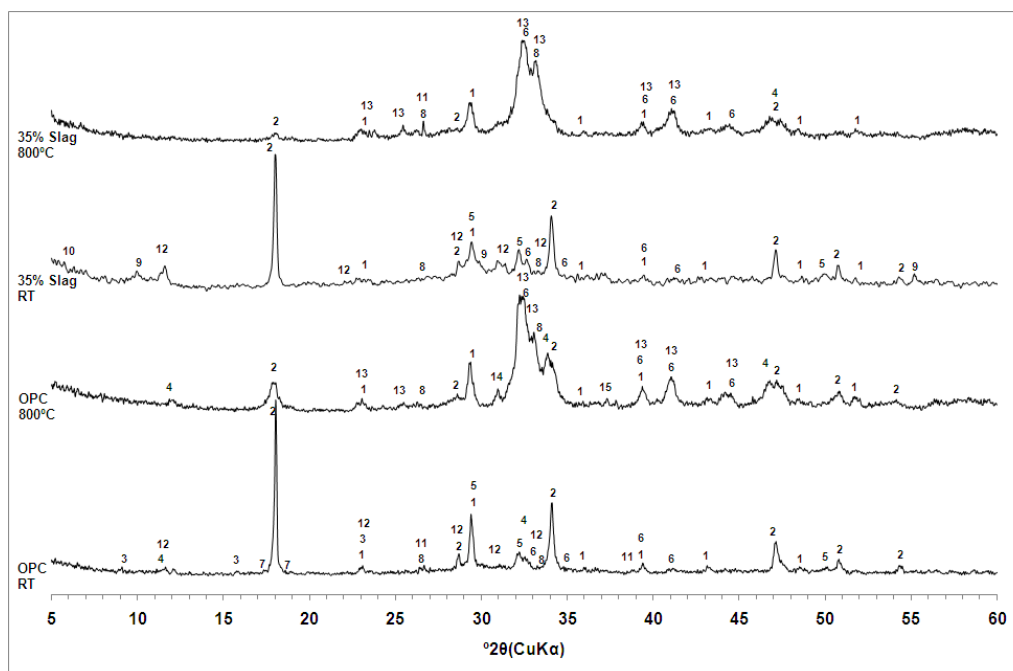


Fig. 3 X-ray spectra of OPC and 35% slag pastes RT and 800°C. 1. Calcite (CaCO_3); 2. Portlandite (CaOH_2); 3. Ettringite; 4. Brownmillerite; 5. C-S-H (calcium silicate hydrate); 6. Larnite (C_2S); 7. Hydrogarnet; 8. C_3A ; 9. Monosulphate hydrate; 10. CAH_{10} ; 11. C_3AH_6 ; 12. C_4AH_x ; 13. Calcium silicate; 14. Al_2O_3 and 15. Lime (CaO)

As described by Alonso and Fernandez [17], after OPC paste exposure to 800°C (Fig. 3), brownmillerite remains present while the CaOH_2 peak significantly decreases [17, 34]. According to Alonso and Fernandez [17] a well identified peak for lime CaO was also present but this is not observed in the present work. This is possibly due to poor crystallinity of the present CaO .

For the 35% slag specimens, exposure to 800°C also significantly reduced the CaOH_2 peak, almost completely (Fig. 3). No CaO peak is present, also possibly due to its poor crystallinity as well as to the significantly lower amounts of CaO present in 35% slag pastes when compared to OPC pastes.

In summary, exposure to 800°C dehydrates both OPC and 35% slag crystalline phases in a similar way. Both OPC and 35% slag presented starting materials as larnite, calcium silicate, C₃A as major phases after 800°C. The key difference between OPC and 35% slag pastes after 800°C being related to the intensity in the CaOH₂ peak. This is in accordance with previous works by the authors [3, 4], in which the higher content of CaOH₂ in OPC pastes, was found to be the cause to the greater deterioration of mechanical properties of these pastes after exposure to 800°C. This deterioration was significantly lower for pastes where OPC has been partially replaced with slag [3, 4].

The very low peak intensities for the aluminate phases in the 800°C XRD spectra confirms that the unassigned chemical shifts observed in the ²⁷Al NMR are possibly related to an amorphous, disordered aluminate phase.

3.4 Infrared Spectroscopy (IR)

Infrared spectroscopy (IR) is useful for determination of molecular structure, identification of chemical species, quantitative/qualitative determination of chemical species [35]. Vibrational frequencies measured by IR can provide valuable information regarding the silicate, sulphate, and carbonate phases [29].

At room temperature, five main bands have been identified for both the OPC and 35% slag spectra. In Fig. 4 starting from the left, the sharp peak at approximately 3644 cm⁻¹ relates to CaOH₂. This is in accordance with previous studies [29, 36-38]. The lower intensity bands near 3670 and 3530 cm⁻¹ relate to M-O-H stretching of structural hydroxyl associated with other hydrous mineral phases [39-43]. The broad peak centred near 2900 cm⁻¹ relates to the O-H stretch of strongly polarised H-bonded waters associated with cementitious minerals [42]. The peaks near 1450 cm⁻¹ are due to C-O stretch of CaCO₃ [44]. The peak near 977 cm⁻¹ is referent to the Si-O stretch mainly representing the C-S-H gel and other silicate phases (e.g. larnite) of the cement paste [45]. A band for S-O stretch occurs near 1130 cm⁻¹ and is partially covered by the Si-O stretch [40, 41, 43, 46-48].

Furthermore, large differences are observed in the spectra of the OPC and the 35% slag pastes RT (Fig. 4). In general, the O-H (CaOH₂), HOH, carbonate, silicate and possibly sulphate bands are all more intense in the OPC specimens relative to the

35% slag. The OPC peaks for CaOH_2 and bound water are twice as intense as the peaks observed for 35% slag. This is in accordance with the present XRD findings and previous works by the authors [3, 4]. For the carbonate and sulphate bands, these are nearly three times more intense in OPC than in the 35% slag pastes. This is also in accordance with XRD results for calcite in OPC as a major phase. In addition, the OPC specimens also contained CO_2 , which was not observed for the 35% slag.

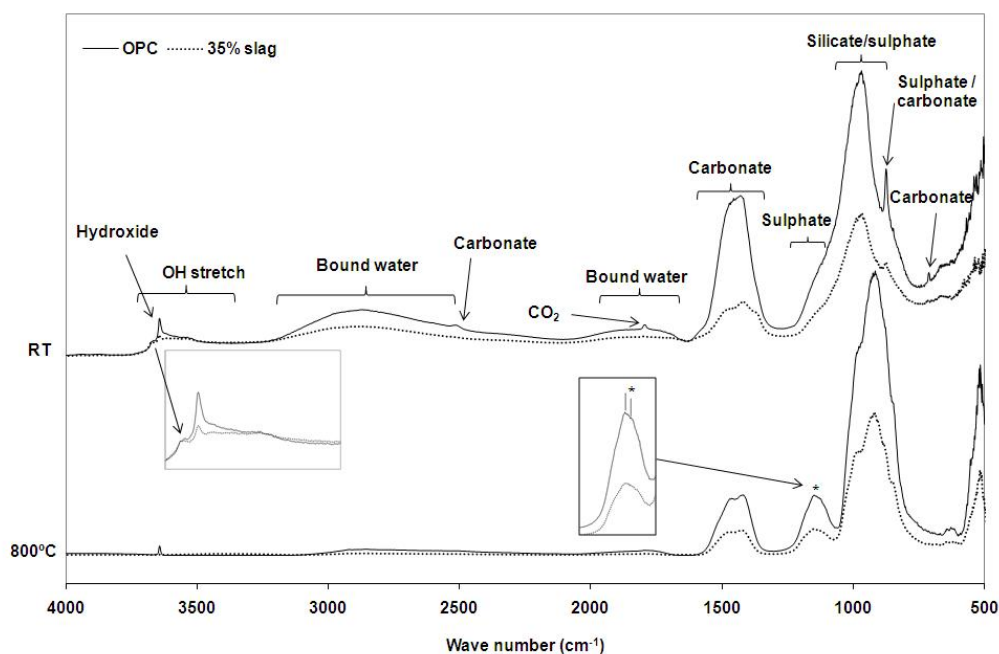


Fig. 4 FTIR spectra of OPC and 35% slag pastes RT and 800°C. Spectra have been normalised to the OH bands near 3670 cm^{-1} to better display differences

After exposure to 800°C, the main changes observed for OPC and 35% slag pastes are (Fig. 4, from left to right): decreased CaOH_2 peak intensity (35% slag is almost absent); significant decrease in the bound water stretch at $\sim 2900 \text{ cm}^{-1}$; disappearance of CO_2 peak present in OPC paste RT; significant decrease in the carbonate peak (as also observed in XRD studies by Alonso and Fernandez [17]); shift of the silicate/sulphate peak stretch to lower wave bands as a result of depolymerization [49].

The sulphate SO stretch band at approximately 1130 cm^{-1} is of interest as it can provide information regarding the sulphoaluminate phase in both OPC and 35% slag specimens. At room temperature, the silicate Si stretch at 968 and 963 cm^{-1}

(for OPC and 35% slag, respectively) is encompassing the sulphate band, thus not enabling precise determination of the phase in question. However, as indicated by Bensted and Varma [41], the differences between ettringite and monosulphate bound water HOH bending bands at approximately 1650 cm^{-1} and OH stretching bands of water above 3000 cm^{-1} might provide useful information in the determination of ettringite and monosulphate phases. Their work reported OH stretching bands at 3500 , 3540 , 3675 cm^{-1} for monosulphate. For ettringite, OH stretching bands at 3420 and 3635 cm^{-1} [41]. In Fig. 4 (enlargement on the left), for the RT spectra, it is possible to observe a low-intensity OH stretching band centred at approximately 3666 cm^{-1} in the 35% slag RT spectrum (this occurs as a weak shoulder in the OPC spectrum). This possibly indicates the presence of monosulphate OH stretching water, suggesting that the encompassed sulphate band at 1130 cm^{-1} might be a monosulphate band. As discussed in the previous sections, monosulphate was present in both OPC and 35% slag samples according to ^{27}Al NMR. In addition, XRD detected the presence of monosulphate in the 35% slag pastes while no ettringite was detected for 35% slag pastes in either ^{27}Al NMR or XRD.

After exposure to 800°C , the sulphate SO stretch band is no longer encompassed by the SiO stretch and it can be observed at $\sim 1130\text{ cm}^{-1}$ (Fig. 5). The enlargement insert shows a doublet present at 1120 and 1145 cm^{-1} . According to Bensted and Varma [41], during hydration, gypsum converts into ettringite followed by monosulfate formation. Their work reported that gypsum presents a doublet peak centred at 1120 and 1145 cm^{-1} [41]. Therefore, it can be concluded that exposure to 800°C possibly converts ettringite and/or monosulfate into the starting material gypsum. Fig. 4 shows this is more pronounced for OPC pastes, with the gypsum IR peak being three times more intense for OPC relative to 35% slag. The conversion from aluminate hydrate phases into products similar to the starting materials is in accordance with ^{27}Al NMR findings (increase in the tetrahedral Al(4) sites with heating). Furthermore, the increase in the OPC octahedral Al(6) observed by the ^{27}Al NMR and related to rehydration after 800°C is in accordance with the IR spectra regions between $3000\text{--}2500\text{ cm}^{-1}$ and $2000\text{--}1500\text{ cm}^{-1}$. This regions show a slope relating to bound water for the OPC pastes after exposure to 800°C . This is not observed for the 35% slag pastes after exposure to 800°C .

3.5 NEXAFS

The Si NEXAFS spectra of OPC and 35% slag pastes before and after exposure to 800°C is presented in Fig. 5. The present analysis is based on the work conducted by Li et al. [13]. Their work lists the main Si K-edge NEXAFS peak positions with a limited number of corresponding ^{29}Si NMR chemical shifts for a variety of Q^n silicates. In general, the main peak in the Si NEXAFS spectrum shifts to higher energy with increasing degree of polymerisation [13].

The Si K-edge NEXAFS spectra of OPC and 35% slag pastes are dominated by peaks at ~ 1847 eV, 1849 eV and 1863 eV (Fig. 5). The first two are single electron $1s \rightarrow \sigma^*_{\text{Si-O}}$ transitions of silicate [12, 13]. The latter band is due to a broad $\sigma^*_{\text{Si-O}}$ continuum resonance [12] and is probably made up of several overlapping σ^* (antibonding) orbitals due to differences in inter-atomic distances. The broad feature near 1855 eV is probably due to Si-O-O-Si multiple scattering [12].

Fig. 5 shows that both OPC and 35% slag spectra present 3 major peaks related to Q^0 [13]. The spectra do not allow differentiation of any possible contribution of Q^1 and Q^2 units in the material. For the RT pastes, OPC and 35% slag spectra are very similar and there are no significant differences between the Q^0 resonances of these pastes. This confirms the ^{29}Si NMR results reported in this study.

However, with heating to 800°C, the peak at 1847 eV shifts to a lower energy, indicating loss of polymerization [13]. This is observed for both OPC and 35% slag pastes. In addition, for both pastes, the peak at 1849 eV increases significantly after exposure to 800°C. According to Li et al. [13], this peak relates to Q^0 and its increase is possibly a result of depolymerization due to rise in temperature. After 800°C, the peaks at 1847 and 1849 eV are higher in intensity for OPC pastes relative to 35% slag pastes. This suggests that after exposure to 800°C, the OPC paste is less polymerized than the 35% slag paste. This was observed in the ^{29}Si NMR results reported in this study.

It is important to note that while the spectra presented are limited in scope, Si K-edge NEXAFS ability to characterize Q^0 might indicate suitability of this technique to study the hydration of the cement paste.

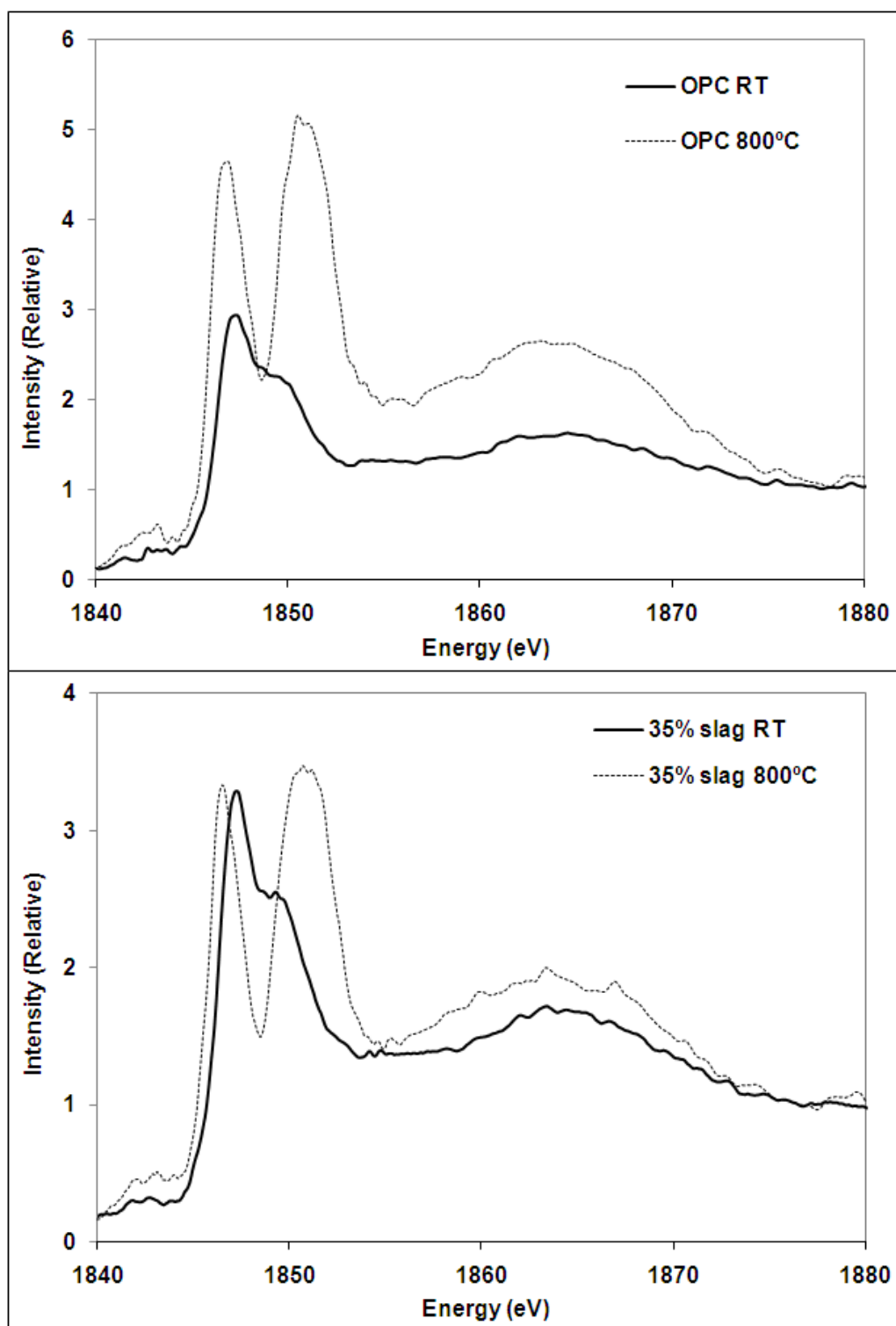


Fig. 5 Si NEXAFS spectra of OPC and 35% slag pastes RT and 800°C

4 Conclusions

The present work investigated the contributions of paste hydrates to the deterioration of the mechanical properties after exposure to elevated temperatures.

^{29}Si NMR spectra showed that at room temperature there are no major differences between the silicate phases of OPC and 35% slag pastes. Both pastes presented 3 Q^0 resonances, 2 Q^1 resonances and 1 Q^2 resonance. In addition, both OPC and 35% slag pastes presented $\text{Q}^2(1\text{Al})$ chemical shifts related to the Al substitution for Si confined to the bridging tetrahedron. However, with the temperature increase, ^{29}Si NMR spectra showed differences in the C-S-H gel of OPC and 35% slag pastes. Above 400°C, the 35% slag paste remained slightly more polymerized than the OPC paste. After exposure to 800°C, the OPC paste completely lost its hydrated materials and presented only Q^0 resonances while the 35% slag pastes presented Q^0 resonances and a small Q^1 resonance. This indicates that the 35% slag pastes remained slightly more polymerized than the OPC paste. This is an important finding as it is likely that the further deterioration of mechanical properties observed for the OPC paste in comparison to 35% slag paste can also be attributed to the differences in the silicate phases between these pastes after exposure to temperatures above 400°C.

^{27}Al NMR was limited in characterizing the aluminate phases after exposure to elevated temperatures. However, above 400°C, a conversion of octahedral Al(6) sites to tetrahedral Al(4) sites was observed for both OPC and 35% spectra. This shows that with an increase in temperature, the hydrated Al(6) dehydrates into Al(4) unhydrated materials. After exposure to 800°C, the conversion was sustained for both pastes however, the octahedral Al(6) component of the OPC paste increased from 400°C to 800°C. This indicates that rehydration occurred in the OPC pastes. Therefore, it is likely that the aluminate phases also play a role in the further deterioration of mechanical properties experienced by OPC pastes when compared to 35% slag pastes.

XRD showed that after exposure to 800°C, the very low peak intensities for the aluminate phases suggest that the unassigned chemical shifts observed in the ^{27}Al

NMR spectra are possibly related to an amorphous, disordered phase. These phases are probably dehydrated forms of the previously reported TAH phase.

IR showed that after exposure to 800°C, ettringite and/or monosulfate are possibly converted into the starting material gypsum. The gypsum IR peak was three times more intense for OPC relative to 35% slag.

The Si NEXAFS spectra of OPC and 35% slag pastes at room temperature show no significant differences between the Q^0 resonances of these pastes. This confirms the ^{29}Si NMR results reported in this study. However, after exposure to 800°C, the OPC paste was found to be less polymerized than the 35% slag paste, also in agreement with the ^{29}Si NMR results.

Acknowledgements

The authors gratefully acknowledge the Australian Research Council Discovery Grant No. DP0558463 for this research project. Part of this research was undertaken on beamline 14ID-01 at the Australian Synchrotron, Victoria Australia. The views expressed are those of the authors and not necessarily those of the owner or operator of the Australian Synchrotron. J Cashion, B Cowie and R Hocking all kindly provided assistance. Finally, the authors would like to gratefully acknowledge Dr Jenny Pringle from Monash School of Chemistry for assistance with all NMR experiments.

5 References

1. Lea FC, Stradling RE (1922) The resistance to fire of concrete and reinforced concrete. *Engineering* 144: 341-344
2. Dias WPS, Khoury GA, Sullivan PJE (1990) Mechanical Properties of Hardened Cement Paste Exposed to Temperatures up to 700°C (1292°F). *ACI Mater J* 87: 160-166
3. Mendes A, Sanjayan J, Collins F (2008) Phase transformations and mechanical strength of OPC/Slag pastes submitted to high temperatures. *Mater Struct* 41: 345-350
4. Mendes A, Sanjayan J, Collins F (2009) Long-term progressive deterioration following fire exposure of OPC versus slag blended cement pastes. *Mater Struct* 42: 95-101
5. Petzold A, Rohrs M (1970) Concrete for high temperatures. second ed., Maclaren and Sons Ltd, London
6. Khoury GA (1992) Compressive strength of concrete at high temperatures: a reassessment. *Mag Conc Res* 44: 291-309
7. Taylor HFW (1997) Cement chemistry. Redwood Books, Wiltshire
8. Regourd M, Thomassin JH, Baillif P, Touray JC (1983) Blast-furnace slag hydration. Surface analysis. *Cem Concr Res* 13: 549-556
9. Richardson IG, Groves GW (1992) Microstructure and microanalysis of hardened cement pastes involving ground granulates blast-furnace slag. *J Mater Sci* 27: 6204-6212
10. Richardson IG (2000) The nature of the hydration products in hardened cement pastes. *Cem Concr Compos* 22: 97-113
11. AS 3972-1997: Portland and blended cements. Standards Australia.
12. Li D, Bancroft GM, Kasrai M, Fleet ME, Secco RA, Feng XH, Tan KH, Yang BX (1994) X-ray absorption spectroscopy of silicon dioxide (SiO₂) polymorphs: The structural characterisation of opal. *Am Mineral* 79: 622-632

13. Li D, M G, Bancroft, Fleet ME, Feng XH (1995) Silicon K-edge XANES spectra of silicate minerals. *Phys Chem Miner* 22: 115-122
14. Gates WP (2006) X-ray Absorption Spectroscopy, in *Handbook of Clay Science*, Bergaya F, Theng BKG, and Lagaly G, Editors, Elsevier, Amsterdam, pp. 789 - 864
15. Hjorth J, Skibsted J, Jakobsen HJ (1988) ^{29}Si MAS NMR studies of portland cement components and effects of microsilica on the hydration reaction. *Cem Concr Res* 18: 789-798
16. MacLaren DC, White MA (2003) Cement: Its Chemistry and Properties. *J Chem Ed* 80: 623-635
17. Alonso C, Fernandez L (2004) Dehydration and rehydration processes of cement paste exposed to high temperature environments. *J Mater Sci* 39: 3015-3024
18. Brunet F, Charpentier T, Chao CN, Peycelon H, Nonat A (2009) Characterization by solid-state NMR and selective dissolution techniques of anhydrous and hydrated CEM V cement pastes. *Cement and Concrete Research* 40: 208-219
19. Johansson K, Larsson C, Antzutkin ON, Forsling W, Kota HR, Ronin V (1999) Kinetics of the hydration reactions in the cement paste with mechanochemically modified cement ^{29}Si magic-angle-spinning NMR study. *Cement and Concrete Research* 29: 1575-1581
20. Richardson IG (1999) The nature of C-S-H in hardened cements. *Cement and Concrete Research* 29: 1131-1147
21. Beaudoin JJ, Drame H, Raki L, Alizadeh R (2009) Formation and properties of C-S-H-PEG nano structures. *Materials and Structures* 42: 1003-1014
22. Richardson IG (2008) The calcium silicate hydrates. *Cement and Concrete Research* 38: 137-158
23. Richardson IG, Groves GW (1997) The structure of the calcium silicate hydrate phases present in hardened pastes of white Portland cement/blast-furnace slag blends. *Journal of Materials Science* 32: 4793-4802

24. Schneider J, Cincotto MA, Panepucci H (2001) ^{29}Si and ^{27}Al high-resolution NMR characterization of calcium silicate hydrate phases in activated blast-furnace slag pastes. *Cem Concr Res* 31: 993-1001
25. Wang S-D, Scrivener KL (2003) ^{29}Si and ^{27}Al NMR study of alkali-activated slag. *Cement and Concrete Research* 33: 769-774
26. Parry-Jones G, Al-Tayyib AJ, Al-Dulaijan SU, Al-Mana AI (1989) ^{29}Si MAS-NMR hydration and compressive strength study in cement paste. *Cement and Concrete Research* 19: 228-234
27. Mehta PK, Monteiro PJM (2006) *Concrete microstructure, properties and materials*. McGraw-Hill, New York
28. Skibsted J, Henderson E, Jakobsen HJ (1993) Characterization of calcium aluminate phases in cements by ^{27}Al MAS NMR spectroscopy. *Inorg Chem* 32: 1013-1027
29. Hanna RA, Barrie PJ, Cheeseman CR, Hills CD, Buchler PM, Perry R (1995) Solid state ^{29}Si and ^{27}Al NMR and FTIR study of cement pastes containing industrial wastes and organics. *Cem Concr Res* 25: 1435-1444
30. Andersen MD, Jakobsen HJ, Skibsted J (2003) Incorporation of Aluminium in the Calcium Silicate Hydrate (C-S-H) of Hydrated Portland Cements A High Field ^{27}Al and ^{29}Si MAS NMR investigation. *Inorg Chem* 42: 2280-2287
31. Murgier S, Zanni H, Gouvenot D (2004) Blast furnace slag cement: a ^{29}Si and ^{27}Al NMR study. *C. R. Chimie* 7: 389-394
32. Andersen MD, Jakobsen HJ, Skibsted J (2006) A new aluminium-hydrate species in hydrated Portland cements characterized by ^{27}Al and ^{29}Si MAS NMR spectroscopy. *Cem Concr Res* 36: 3-17
33. Roncero J, Valls S, Gettu R (2002) Study of the influence of superplasticizers on the hydration of cement paste using nuclear magnetic resonance and X-ray diffraction techniques. *Cem Concr Res* 32: 103-108
34. Handoo SK, Agarwal S, Agarwal SK (2002) Physicochemical, mineralogical, and morphological characteristics of concrete exposed to elevated temperatures. *Cem Concr Res* 32: 1009-1018

35. Ghosh SN (2002) Infrared Spectroscopy in Cement Chemistry, in *Advances in Cement Technology*, Ghosh SN, Editor. Tech Books International, New Delhi, pp. 709-734
36. Gao XF, Lo Y, Tam CM, Chung CY (1999) Analysis of the infrared spectrum and microstructure of hardened cement paste. *Cem Concr Res* 29: 805-812
37. Mollah MYA, Kesmez M, Cocke DL (2004) An X-ray diffraction (XRD) and Fourier transform infrared spectroscopy (FT-IR) investigation of the long-term effect on the solidification/stabilization (S/S) of arsenic (V) in Portland cement type V. *Sci Total Environ* 325: 255-262
38. Mollah MYA, Yu W, Schennach R, Cocke DL (2000) A Fourier transform infrared spectroscopy investigation of the early hydration of Portland cement and the influence of sodium lignosulfonate. *Cem Concr Res* 30: 267-273
39. Barnett SJ, Macphee DE, Lachowski EE, Crammond NJ (2002) XRD, EDX and IR analysis of solid solutions between thaumasite and ettringite. *Cem Concr Res* 32: 719-730
40. Bensted J, Varma SP (1971) Studies of Ettringite and its derivatives. *Cem Technol* May/June: 73-77
41. Bensted J, Varma SP (1974) Some applications of infrared and Raman spectroscopy in cement chemistry Part 3 - Hydration of Portland cement and its constituents. *Cem Technol* September/October: 440-450
42. Farmer VC (1974) The layer silicates, in *The IR Spectra of Minerals*, Farmer VC, Editor. Mineralogical Society, London, pp. 539
43. Gastaldi D, Canonico F, Boccaleri E (2009) Ettringite and calcium sulfoaluminate cement: investigation of water content by near-infrared spectroscopy. *J Mater Sci* 1-7
44. Stevulova N, Balintova M, Briancin J, Szeghyova Z (2007) Mechanochemical Synthesis of Belite Cements from Coal Fly Ash/Portlandite Mixture. *Chem Sust Environ* 15: 225-229

45. Hidalgo A, Domingo C, Garcia C, Petit S, Andrade C, Alonso C (2008) Microstructural changes induced in Portland cement-based materials due to natural and supercritical carbonation. *J Mater Sci* 43: 3101-3111
46. Bensted J, Varma SP (1973) Studies of Ettringite and its derivatives, Part 4: The low-sulphate form of calcium sulphoaluminate (monosulphate). *Cem Technol* May/June: 112-115
47. Hall C, Barnes P, Billimore AD, Jupe AC, Turrillas X (1996) Thermal decomposition of ettringite $\text{Ca}_6[\text{Al}(\text{OH})_6]_2(\text{SO}_4)_3 \cdot 26\text{H}_2\text{O}$. *J Chem Soc, Faraday Transactions* 92: 2125-2129
48. Nosov VN, Frolova NG, Kamyshev VF (1976) IR Spectra of calcium sulphate semihydrate. *Zhurnal Prikladnoi Spektroskopii* 24: 713-715
Translated from Russian March 1976.
49. Piasta J, Sawicz Z, Rudzinski L (1984) Changes in the structure of hardened cement paste due to high temperature. *Mater Struct* 17: 291-296

Chapter 8

Effects of Slag and Cooling Method on the Progressive Deterioration of Concrete after Exposure to Elevated Temperatures as in a Fire Event

8.1 Overview

Chapters 3 to 7 reported the effects of elevated temperatures on the microstructure and mechanical properties of ordinary Portland cement (OPC) and OPC/slag pastes. The present Chapter 8 investigates the effects of elevated temperatures on the mechanical properties of OPC and OPC/slag concretes.

This chapter is based on the publication of the same name as the chapter title in Materials and Structures Journal, DOI 10.1617/s11527-010-9660-2, published online on the 31st of August 2010. The paper investigates the effects of slag replacement and different cooling methods on concrete exposed to elevated temperatures. In this study, OPC and OPC slag concretes were heat exposed to 400°C and 800°C. Following heating, specimens were cooled by either furnace or water cooling. Infrared spectroscopy (IR) was used to analyse the phase transformations that resulted from slag replacement, exposure to elevated temperatures and different cooling methods.

8.2 Declaration for Thesis Chapter 8

Declaration by candidate

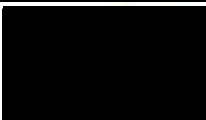
In the case of Chapter 8, the nature and extent of my contribution to the work was the following:

| Nature of contribution | Extent of contribution (%) |
|---|----------------------------|
| Developing outline of research objective and hypothesis Laboratory/experimental investigation and analysis of results Writing, reviewing and editing of paper | 90 |

The following co-authors contributed to the work. Co-authors who are students at Monash University must also indicate the extent of their contribution in percentage terms:

| Name | Nature of contribution | Extent of contribution (%) for student co-authors only |
|---------------|---|---|
| Jay Sanjayan | Developing outline of research objective and hypothesis Reviewing of paper | 5 |
| Frank Collins | Developing outline of research objective and hypothesis Reviewing of paper | 5 |

Candidate's
Signature

| | |
|---|-------------------|
|  | 30 September 2010 |
|---|-------------------|

Declaration by co-authors

The undersigned hereby certify that:

- (1) the above declaration correctly reflects the nature and extent of the candidate's contribution to this work, and the nature of the contribution of each of the co-authors.
- (2) they meet the criteria for authorship in that they have participated in the conception, execution, or interpretation, of at least that part of the publication in their field of expertise;
- (3) they take public responsibility for their part of the publication, except for the responsible author who accepts overall responsibility for the publication;
- (4) there are no other authors of the publication according to these criteria;
- (5) potential conflicts of interest have been disclosed to (a) granting bodies, (b) the editor or publisher of journals or other publications, and (c) the head of the responsible academic unit; and

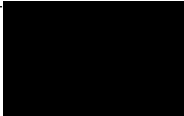
(6) the original data are stored at the following location(s) and will be held for at least five years from the date indicated below:

Location(s)


| |
|--|
| Department of Civil Engineering, Monash University |
|--|

[Please note that the location(s) must be institutional in nature, and should be indicated here as a department, centre or institute, with specific campus identification where relevant.]

Signature 1

| | |
|---|--------------------------|
|  | 30 September 2010 |
|---|--------------------------|

Signature 2

| | |
|---|--------------------------|
|  | 30 September 2010 |
|---|--------------------------|

8.3 Publication

Effects of slag and cooling method on the progressive deterioration of concrete after exposure to elevated temperatures as in a fire event

Alessandra Mendes · Jay G. Sanjayan ·
Frank Collins

Received: 17 February 2010 / Accepted: 16 August 2010
© RILEM 2010

Abstract In the present work OPC and OPC/slag concretes were exposed to elevated temperatures, 400 and 800°C. The critical temperature of 400°C has been reported for OPC paste. Above 400°C, the paste hydrate $\text{Ca}(\text{OH})_2$ dehydrates into CaO causing the OPC paste to shrink and crack. After cooling and in the presence of air moisture, CaO rehydrates into $\text{Ca}(\text{OH})_2$, resulting in disintegration due to re-expansion of OPC paste. Therefore, the present work assessed whether this also applies to OPC concretes. Two cooling methods were used: furnace and water cooling. Following the heat treatment/cooling method, compressive tests and Infrared (IR) spectroscopic studies were conducted. Results showed that after 400°C, water cooling caused all concrete, regardless of the type of blended cement binder, a further 20% loss in the residual strength. After 800°C, water cooling caused OPC concrete a further 14% loss while slag blends presented around 5% loss. IR indicated that the further loss observed in the OPC concrete is due to the accelerated CaO rehydration into $\text{Ca}(\text{OH})_2$. Afterward, the non-wetted furnace

cooled specimens were exposed to air moisture for one week, resulting in further strength loss of 13%. IR results suggested that slow rehydration of CaO occur with exposure to air moisture. In conclusion, water cooling caused more damage in OPC concrete, while the concrete that has not been wetted undergoes progressive deterioration. This indicates a need to monitor the non-wetted concrete after a fire event has occurred for potential further deterioration.

Keywords OPC · Slag · Concrete · Elevated temperatures · Cooling methods · Progressive deterioration

1 Introduction

The structural safety of concrete structures exposed to fire is a major design consideration [1], therefore leading to extensive research and consequently, published data in the behaviour of concrete made with ordinary Portland cement (OPC).

When concrete is submitted to high temperatures as in a fire, physical and chemical transformations take place resulting in deterioration of its mechanical properties [2]. A common way of investigating those physical and chemical transformations is dividing the investigation in two steps: (i) the cement paste and (ii) the concrete as a whole, i.e., paste, aggregates and the interface between paste and aggregate.

A. Mendes (✉) · F. Collins
Civil Engineering Department, Monash University,
Clayton, VIC, Australia
e-mail: Alessandra.mendes@monash.edu

J. G. Sanjayan
Faculty of Engineering and Industrial Sciences,
Swinburne University of Technology, Hawthorn,
VIC, Australia

Published online: 31 August 2010



In previous studies the authors investigated (i), the cement paste [3, 4]. The critical temperature of 400°C for OPC paste was confirmed. This is in accordance with previous studies [5, 6]. Above 400°C, one of the main hydrates of the OPC paste, calcium hydroxide Ca(OH)_2 , dehydrates into CaO [7], causing the OPC paste to shrink and crack. After cooling and in the presence of air moisture, CaO rehydrates into Ca(OH)_2 , resulting in disintegration due to re-expansion of OPC paste [3, 4, 6, 8].

Previous studies [3, 4, 9] also reported that dehydration of Ca(OH)_2 and rehydration of CaO had no significant deterioration in pastes where OPC was partially replaced with ground granulated blast furnace slag (slag), a by-product of the iron blast furnace industry. Following grinding and blending with OPC the granulated, ground slag is cementitious. During hydration slag consumes most of the available Ca(OH)_2 , consequently reducing or even eliminating the negative effects caused by the Ca(OH)_2 dehydration and CaO rehydration when cement paste is submitted to elevated temperatures.

The present work investigates (ii), the concrete as whole. It focuses on the deterioration of its mechanical properties after exposure to elevated temperatures. Two temperatures will be investigated, 400°C (below Ca(OH)_2 dehydration) and 800°C. Two types of cooling method are used namely, furnace cooling and water cooling. Furnace cooling is the most reported cooling method for concrete exposed to elevated temperatures. It consists of turning the furnace off and letting the specimens cool down until room temperature is eventually reached. However, furnace cooling does not represent a real life fire extinguishing method, due to the slow rate of cooling, whereas water extinguishing is used in cases of a fire event. Furnace cooling would represent, in a fire event, the concrete that has not been wetted during the fire extinguishment.

Previous studies have investigated the effects of different cooling methods on the residual mechanical properties of concrete exposed to elevated temperatures [10–15]. However, they only investigated the effects of the cooling methods on the properties of OPC concrete, not OPC/slag concrete. Further, the previous studies did not include the long term deterioration of concrete after fire exposure, and the effect of cooling method on the type of deterioration.

Sharshar [15] reported that OPC concrete made with Lytag aggregate exposed to 520°C and quenched

with water presented a slight decrease in relative strength when compared with specimens submitted to furnace cooling. He attributed this slight decrease to thermal stresses caused by the thermal shock when concrete is exposed to water.

Sakr and Hakim [14] studied the effects of different cooling methods on heavy weight concrete. It was found that air cooled concrete had 22.1 MPa after exposure to 500°C, while water cooling resulted in a strength of 13.25 MPa. After 750°C, furnace cooling resulted in a maximum compressive strength of 13.1 and water cooling 5.40 MPa.

Luo et al. [12] investigated the effect of cooling in concrete made with OPC, fly ash and granite aggregate. Their work reported that the residual compressive strength of the concrete exposed to furnace cooling was 45% while specimens exposed to water cooling presented a residual strength of 32% after heat treatment of 800°C, a difference of 13%. For the specimens exposed to 1000°C the residual compressive strength was 8.3% for the furnace cooling and 7.4% for the water cooling. It was concluded that the thermal gradient induced by the cooling methods was not the key cause of sample damage, whereas the residual pore volume and pore size distribution following cooling had a more significant effect on residual strength.

Abramowicz and Kowalski [10] investigated concrete made with siliceous aggregate heated to temperatures of 270, 370 and 500°C. Cooling by 10 s immersion in water was found not to produce any significant decrease of concrete strength; most likely due to insufficient thermal gradient arising within the short (10 s) immersion duration.

Kowalski [11] analysed the effects of cooling on the properties of concrete made with fly ash and siliceous aggregate. His work found that rapid cooling of the heated concrete had the highest influence on the strength loss when the maximum temperature was 330°C. Specimens cooled in laboratory air lost about 10% of their strength, while specimens cooled rapidly in water lost about 35% (5 min in water) and 55% (20 min in water). Kowalski [11] attributed the reason for strength loss to microcracks that formed as a result of stresses induced by a temperature gradient. In the case of maximum temperature of 550°C, he suggested that the strength loss depended much less on the cooling process because, if the concrete has already been damaged during heating to 550°C its internal stiffness



would have been reduced and hence the induced stresses and resultant microcracking during cooling would be lower.

Similar observations were made by Nassif et al. [13]. Their work investigated the impact of water cooling on limestone concrete using a stiffness damage test. They stated that sudden cooling would unbalance internal equilibrium resulting in significant internal stresses and loss of stiffness.

In the present work, the following procedures were conducted to investigate the effects of the cooling methods on the mechanical properties of OPC and OPC/slag concretes:

- (1) Heat treatments (400 and 800°C) followed by either furnace or water cooling;
- (2) Compressive strength tests; and
- (3) Infrared (IR) spectroscopic studies.

The temperature of 400°C was chosen for a comparison with 800°C. This enables determination whether rehydration of CaO has a negative effect in OPC concrete as it has in OPC pastes [3–6]. The compressive strength tests assist in the determination of any effects of the cooling methods on the mechanical properties of OPC and OPC/slag concretes. In addition, whether the different cooling methods affect the OPC and the OPC/slag concretes differently. Furthermore, IR spectroscopy was conducted to complement the results providing information on whether CaO rehydration into Ca(OH)_2 has occurred and whether that has any relationship with the cooling methods. IR is used in the areas of determination of molecular structure, identification of chemical species and quantitative/qualitative determination of chemical species [16]. Ca(OH)_2 has been successfully identified in cement paste using IR by previous studies [17–19].

2 Experimental procedure

Ordinary Portland cement and ground granulated blast furnace slag (slag), conforming with the requirements of Australian Standard AS 3972 [20] were used as binder materials. Pakenham Blue Metal (Old Basalt) crushed type was used as coarse aggregate with the following properties: Maximum size = 14 mm; specific gravity = 2.95; and absorption = 1.2%. Lyndhurst washed fine sand was used as the fine aggregate with the

following properties: specific gravity = 2.65; absorption = 0.5%. All concrete mixtures contained water reducer WRDA GWA Grace Construction products 4.03 ml/kg of total cementitious materials; Total cementitious content = 300 kg/m³; and Coarse aggregate = 1100 kg/m³.

Measurements of the moisture contents of the aggregates were taken the day before and on the day of the concrete mixing. The aggregate weights were adjusted to saturated and surface dry condition.

In this investigation OPC was partially replaced (i.e., 35, 50% by weight of binder) with slag. The term water/binder (w/b) ratio is used instead of the water/cement ratio (w/c) to include both binder types mentioned above. The w/b ratio used was 0.63.

Cylinder specimens, with diameter 100 mm and length 200 mm were investigated.

Mixing was conducted and specimens were cast using a vibration table for better compaction. Specimens were sealed with a plastic sheet and demoulded after 24 h, followed by 28 days curing in lime-saturated water bath at 23°C. Specimens were then placed in a controlled temperature room for drying, at 23°C and 50% of relative humidity. The length of drying was of approximately 60 days.

Following drying, heat treatment was conducted in a Tetlow furnace. The heat treatment was as follows: constant heating rate of 6.25°C/min until 50°C below the desired temperature, then 1 h until the desired temperature was reached, followed by 1 h at the desired temperature. For example, at 800°C heat treatment, constant heating rate of 6.25°C/min until 750°C, then 1 h between 750 and 800°C, and finally 1 h in 800°C.

Two different peak temperatures were applied within the furnace, namely 400 and 800°C, as well as two types of cooling methods, furnace and water cooling.

Thermocouples were placed in the centre and surface of the specimens in order to monitor the differential gradient between those (Fig. 1).

Furnace cooling consisted of turning the furnace off and letting the specimens cool down until room temperature is reached. Water cooling consisted of removing the specimens out of the furnace once heat treatment was finished, i.e., at either 400 or 800°C, and placing the specimens in a container with 75 l of capacity, filled up with 30 l of water at temperature $20 \pm 2^\circ\text{C}$ for 10 min.

Specimens were tested for compressive strength in a Baldwin—Universal Testing Machine (120 WHVL—



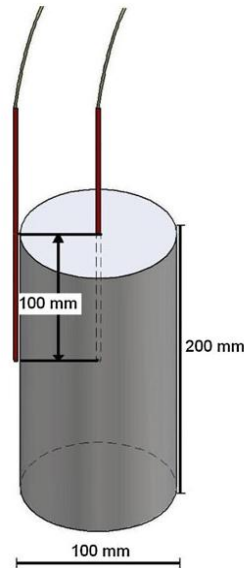


Fig. 1 Thermocouples distribution, inside (*centre*) and on the surface of the specimen

120000 LB. CAP.), using loading rate of 20 MPa/min. The results reported are an average of 2 specimens of each mixture for each temperature. Compressive strength tests were conducted 1 day and 1 week after the heat treatment and cooling have taken place.

Diffuse reflectance IR spectroscopy was conducted using a FTS 3000 MX Excalibur Series Digilab fitted with a glow bar radiation source, a DTGS detector, dry air purge and an extended KBr beamsplitter for the near IR (NIR) and the mid IR (MIR). The sample space was continuously purged with dry nitrogen. As many as 512 acquisitions were co added at a resolution of 2 cm^{-1} on powdered specimens mixed ($\sim 5\%$) with sodium chloride (ACS). Each spectrum was referenced to NaCl and converted to Kubelka–Munk absorbance units for comparison.

3 Results and discussion

Figure 2 presents the curves for the 400 and 800°C heat treatments applied to the OPC and OPC/slag concretes. In both heat treatments, the temperature of

OPC and 35% slag concrete surface and the furnace environment were the same throughout the heat treatment and therefore are represented by only one (1) curve namely 'surface'. In addition, the curve for the 50% slag followed the same trend as 35% slag, and for better visualization of the curves is not presented in Fig. 2.

The temperature in the centre of the specimens did not follow the same trend, showing that the heat transfer between the surface and centre of the specimen of OPC and 35% slag are different.

For the 400°C heat treatment, Fig. 2 shows that 35% slag concrete specimens conducted the heat faster than OPC concrete specimens. However, the temperature difference between the centre of the OPC and the 35% slag specimens did not exceed 28.8°C.

It is important to note that for the 400°C heat treatment the maximum temperature reached in the centre of 35% slag specimen was 350.1 and 321.3°C for the OPC concrete specimen. The maximum surface/furnace environment temperature reached was 379.2°C. Therefore, it is unlikely that dehydration of Ca(OH)_2 occurred on either of those specimens since the critical temperature of 400°C was not attained.

For the 800°C heat treatment, a similar behavior to the 400°C was found (Fig. 2). The 35% slag concrete also conducted the heat faster than the OPC concrete. Temperature differential between the centre of the OPC concrete specimen and the 35% slag specimen reached 47.3°C. As both surface and centre of the specimen have reached temperatures above 400°C, dehydration of the Ca(OH)_2 is likely to have occurred on those specimens.

The compressive strength tests were carried out 1 day and 1 week after the heating and cooling treatments have taken place.

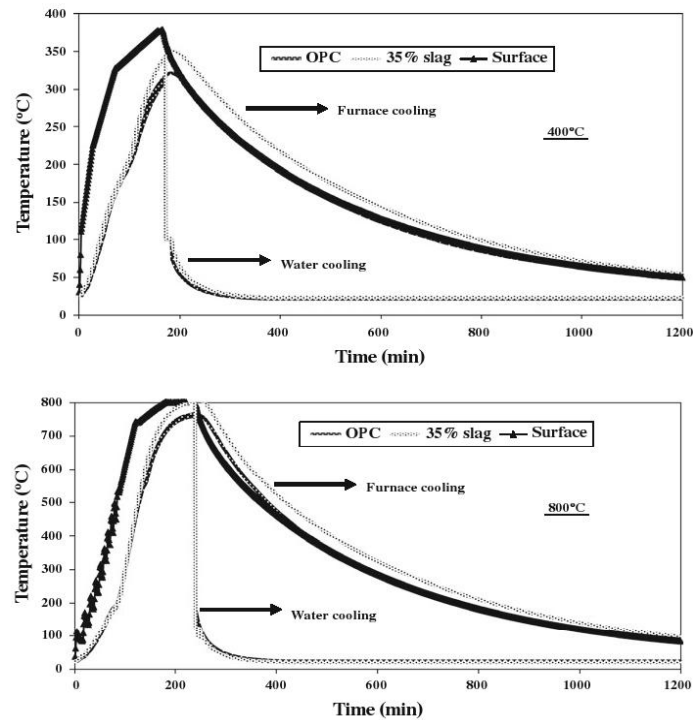
3.1 One day after the heat treatment/cooling

A comparison of the residual strength of the different concrete blends 1 day after exposure to either 400 or 800°C and followed by either furnace or water cooling is presented in Fig. 3.

After the 400°C heat treatment, water cooling causes a further 20% loss in the residual compressive strength when compared with furnace cooling, for all specimens, i.e., OPC, 35 and 50% slag concrete specimens. Considering that 400°C was not reached inside or on the surface of the specimens, Ca(OH)_2



Fig. 2 OPC and 35% slag heat curves for the 400 and 800°C heat treatments



dehydration of the cement paste cannot be the cause of this further loss of compressive strength once specimens were cooled with water. In addition, the loss in residual strength was similar in all specimens, and the heat transfer from the surface to the centre of the specimens does not seem to vary considerably with the type of binder (OPC or OPC/slag). This suggests that the strength loss is a consequence of thermal stresses caused by thermal shock of the concrete specimen when in contact with water at $20 \pm 2^\circ\text{C}$.

For the 800°C heat treatment a different scenario was found. Fig. 3 shows that after 800°C, the difference between the residual strength after furnace and water cooling was not the same among the concrete blends. The variation on the residual strength of OPC concrete, when comparing furnace with water cooling, was in the range of 14%. For the slag blends, i.e., for the 35 and 50% slag concrete

specimens this difference was significantly smaller, 4 and 5%, respectively.

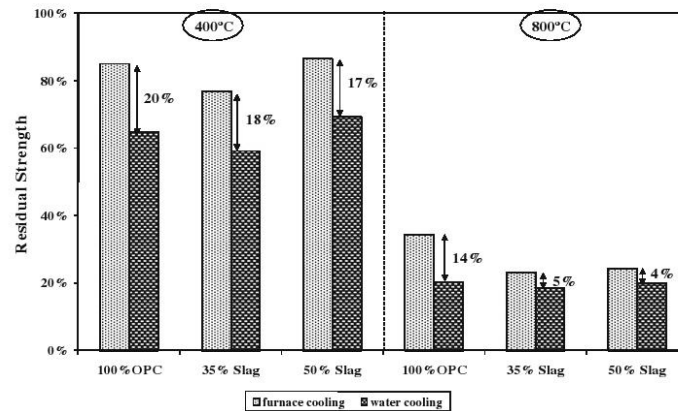
As seen for the 400°C heat treatment, thermal shock seems to be the cause for the loss of strength of all blends. However, thermal shock cannot be solely accounted for the greater loss of compressive strength of OPC concrete specimens exposed to 800°C and water cooling.

Ca(OH)_2 is expected to have dehydrated after 800°C, this is above the critical temperature of 400°C for OPC pastes [3, 4, 6]. This suggests that the more severe deterioration of OPC concrete when cooled with water might be due to the rehydration of CaO into Ca(OH)_2 .

Based on that, IR was conducted to determine whether the CaO rehydration into Ca(OH)_2 was the cause of the more severe deterioration found for OPC concrete submitted to 800°C and water cooling.



Fig. 3 Comparison of the residual strength of the different concrete specimens 1 day after exposure to 400 and 800°C and followed by either furnace or water cooling



The choice of this technique to determine the amount of Ca(OH)_2 in the different specimens was first due to the efficiency of the method in determining Ca(OH)_2 as reported by previous studies [17–19], but also due to the availability of the equipment immediately after the cooling had occurred, therefore assuring precision in determining Ca(OH)_2 presence in the different samples, considering its variation with time [3, 4].

Figure 4 shows the different spectra obtained when comparing the different blends with the different cooling methods, after exposure to 800°C heat treatment, therefore above the temperature of 400°C necessary for the dehydration of Ca(OH)_2 .

The peak reference to the wave number around 3640 cm^{-1} corresponds to the Ca(OH)_2 content in the cement paste [17–19]. Figure 4a shows that immediately after the furnace cooling, the peak intensity (absorbance) slightly differs for OPC and 35% slag specimens. The peak intensity is higher for OPC, while is close to zero for the 35% slag specimen. Slag blends at room temperature have less Ca(OH)_2 than OPC, and therefore less CaO available to rehydrate into Ca(OH)_2 , resulting in less intensity.

However, for the water cooling (Fig. 4b) both peaks increase, especially for OPC specimens. Ca(OH)_2 was found in previous studies for slag blends, however, in lower quantities and with the Ca(OH)_2 dehydration and CaO rehydration not having severe effects on those blends [3, 4].

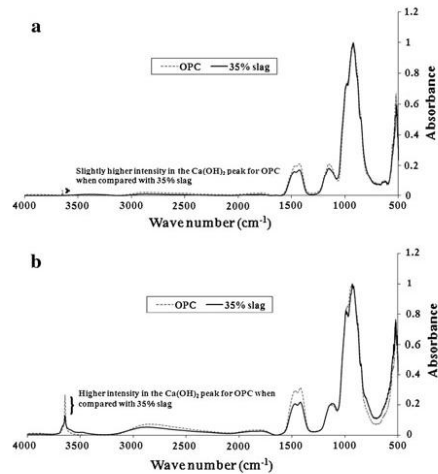


Fig. 4 IR spectra of OPC and 35% slag samples 1 day after the 800°C heat treatment and cooling (a) furnace cooling and b) water cooling)

Due to the difference between residual strength of OPC specimens when exposed to 800°C and cooled with furnace or water, a comparison between furnace and water cooling OPC IR spectra is made and presented in Fig. 5.

When analysing Fig. 5, it is possible to see that for OPC specimens, the intensity of the Ca(OH)_2



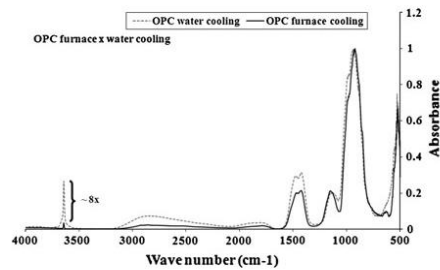


Fig. 5 OPC IR spectra comparison between furnace and water cooling

increases significantly after the water cooling. The peak in water cooling is approximately eight times more intense than furnace cooling specimens. This suggests that the water cooling provides a plentiful supply of water that results in an acceleration of the CaO rehydration into Ca(OH)_2 , resulting in more damage for the OPC specimens when compared with specimens submitted to furnace cooling.

However, it is of interest how a slow rehydration of CaO would affect the concrete, as in a furnace cooled sample exposed to air moisture. This would represent the concrete that in a fire event that has not been wetted during fire extinguishment, following exposure to elevated temperatures.

In an attempt to reproduce the effects of a slower rehydration of CaO, the OPC and OPC/slag specimens submitted to 800°C followed by furnace cooling were stored in a controlled room exposed to 23°C and 50% of relative humidity for one (1) week.

3.2 One week after the heat treatment/cooling

To determine the impact of air moisture on the rehydration of CaO and possible deterioration of concrete mechanical properties, OPC and OPC/slag specimens submitted to 800°C followed by furnace cooling were exposed to air moisture for 1 week. The specimens were then tested for compressive strength. The results are presented in Fig. 6 and a comparison with the results obtained 1 day after the heat treatment/cooling is made.

In Fig. 6 it is possible to see that the difference initially found between furnace and water cooling has been reduced after the furnace cooled specimens have been exposed to air moisture. Especially for

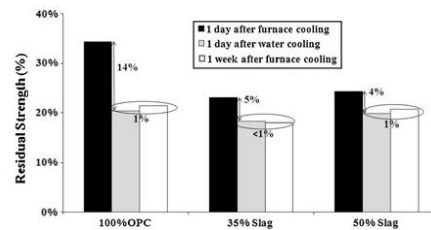


Fig. 6 Residual strength of the different blends 1 day after furnace and water cooling and 1 week after furnace cooling

OPC, the difference found between water and furnace cooling specimens after 1 day was of 14%. The difference after 1 week exposure to air moisture is now 1%. This indicates progressive deterioration of furnace cooled OPC concrete after exposure to air moisture. To a lesser extent, for the slag specimens, the initial difference of 4–5% has now been reduced to $\sim 1\%$.

It is very likely that the cause of this progressive deterioration, especially for OPC, is due to the slower but continuous rehydration of CaO, as a result of exposure to air moisture.

In order to confirm that rehydration of CaO took place, IR tests were conducted on the specimens after 1 week exposure to air moisture. The results are presented in Fig. 7.

Figure 7a compares 800°C heat treated OPC specimens submitted to furnace cooling. The specimens were tested 1 day and 1 week after the heat treatment/cooling. It can be concluded that there is an increase in the Ca(OH)_2 peak intensity after 1 week exposure to air moisture. The absorbance intensity is almost 12.5 times higher than for the furnace cooled specimens tested 1 day after the cooling took place. This suggests that the progressive deterioration on the mechanical properties of furnace cooled specimens after 1 week exposure to air moisture (especially for OPC) is due to the slow rehydration of CaO into Ca(OH)_2 .

In addition, to confirm that the water cooling method provides a plentiful supply of water that results in an acceleration of the CaO rehydration into Ca(OH)_2 , OPC specimens submitted to water cooling and tested 1 day after cooling, were compared with OPC water cooled specimens submitted to air moisture exposure for 1 week. The results are presented in

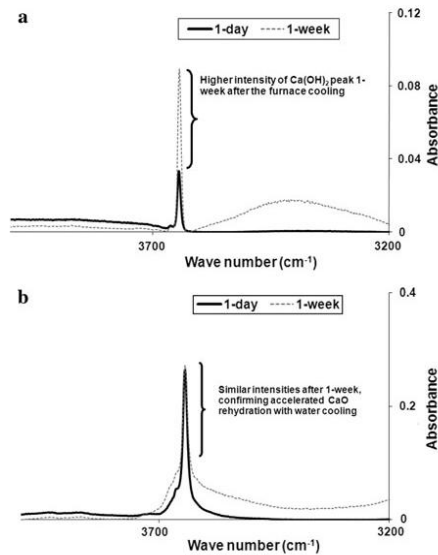


Fig. 7 Enlargements of the Ca(OH)_2 intensity peaks in **a** OPC submitted to furnace cooling (1 day and 1 week after the cooling) and **b** OPC submitted to water cooling (1 day and 1 week after cooling)

Fig. 7b. The intensities of the Ca(OH)_2 peaks are the same for both samples (tested 1 day and 1 week after the heat treatment/cooling and exposure to air moisture). This indicates that water cooling method leads to an accelerated rehydration of CaO resulting in no further rehydration of CaO, thus no further deterioration of the concrete that has been wetted during cooling. It is important to note that no further mechanical deterioration was observed for water cooled specimens exposed to air moisture for 1 week.

As discussed previously, similar mechanical deterioration was found for water cooled specimens 1 day after heating/cooling and furnace cooled specimens 1 week after exposure to air moisture. For the water cooled specimens, deterioration was caused by accelerated CaO rehydration. For the furnace cooled specimens, the deterioration was due to the slow CaO rehydration after exposure to air moisture for 1 week. However, the amount of Ca(OH)_2 formed and detected by IR was not similar.

OPC furnace cooled specimens exposed to air moisture for 1 week presented Ca(OH)_2 peak

absorbance intensity of 0.09. OPC water cooled specimens tested 1 day after the heating/cooling presented Ca(OH)_2 absorbance intensity of 0.26. Therefore, even though the slower CaO rehydration caused the furnace cooled specimens the same deterioration as the accelerated CaO rehydration (water cooled), the amounts of Ca(OH)_2 formed differed. The amount of Ca(OH)_2 necessary to cause the same very deterioration on the furnace cooled specimens after 1 week of air moisture exposure is at least three times less than the amount necessary for the water cooled specimens.

The authors believe that the explanation for this phenomenon is related to the nature of the crystal growth. Different crystals growth would lead to different deterioration. Water cooling and air moisture exposure provide different environments for the growth of the Ca(OH)_2 crystal, resulting in different final crystals. Chatterji [21] investigated the crystal growth during hydration of CaO. He stated that hydration of CaO may cause volume expansion and damage in hardened cement paste and concrete. Ramachandran et al. [22, 23] analysed the hydration of CaO pressed compacts exposed to either a limited quantity of liquid water or to water vapour. The compacts are reported to have a void content of 46% by volume and a CaO content of 54%. For the liquid water the compact remained strong and undamaged. In contrast, for the compact exposed to water vapour, volume increase was observed resulting in disintegration. According to Ramachandran et al. [22, 23], liquid water hydration would result in a through-solution growth mechanism while vapour hydration would result in a solid-state-hydration [22, 23].

Chatterji [21] concluded that not every crystal growth lead to disintegration of the constraining body. Therefore, although water is a source for CaO rehydration in concrete exposed to elevated temperatures, the extent of the damage will depend on the form of water provided (liquid, vapour). In the case of the OPC in study, the water cooling 1 day after the heat treatment resulted in deterioration of the mechanical properties. Less CaO rehydration was necessary after 1 week of air moisture exposure to lead to the same deterioration as the one caused by water cooling.

Finally, 50% slag specimens, although not tested by IR spectroscopy, are unlikely to show significant differences to 35% slag, with Ca(OH)_2 peak intensities expected to be slightly lower.



4 Conclusions

The present work investigated the effects of different cooling methods (furnace and water cooling) on the mechanical properties of OPC and OPC slag concretes exposed to 400 and 800°C. The key findings were:

- (1) One day after the 400°C heat treatment, all concrete blends (OPC and OPC/slag) presented strength loss of approximately 20% when comparing furnace cooled with water cooled specimens. The further loss of strength found for the water cooling is likely to be due to thermal stresses caused by the thermal shock experienced by the concrete specimens once in contact with water;
- (2) One day after the 800°C heat treatment, strength loss was in the range of 14% for OPC concrete and 4–5% for the slag blends when comparing furnace with water cooled specimens;
- (3) Considering the similar strength losses at 400°C for all the blends once cooled with water, the higher strength loss for OPC concrete exposed to 800°C and water cooling cannot be attributed solely to stresses due to thermal shock;
- (4) IR spectroscopy demonstrated an increase in the intensity of the Ca(OH)_2 peak of water cooled specimens when compared to furnace cooled specimens (after 800°C). This was significantly more pronounced for OPC specimens. The higher intensity of the Ca(OH)_2 peak for OPC specimens suggests that water cooling provides a plentiful supply of water that results in an acceleration of the CaO rehydration into Ca(OH)_2 , resulting in more damage for the OPC concrete specimens;
- (5) One week after the 800°C/furnace cooling took place, further deterioration of the mechanical properties was found for all specimens, especially for OPC specimens. The same deterioration caused by water cooling (1 day) was found for furnace cooled specimens after 1 week exposure to air moisture. This is of importance when assessing fire damaged structures;
- (6) IR showed that air moisture also caused rehydration of CaO into Ca(OH)_2 in the concrete that has not been wetted. This rehydration was slower (1 week) when compared to the accelerated rehydration caused by the water cooling;
- (7) IR also indicated that although the deterioration caused by 1 week exposure to air moisture was similar to the one caused by water cooling, the amount of CaO rehydration necessary to cause the same deterioration differed. The 1 week exposure to air moisture presented 3 times less Ca(OH)_2 formed than the amount found for the water cooled specimens;
- (8) The source of water (liquid, vapour) impacts on the Ca(OH)_2 crystal growth. This is likely to be the determining factor on how the rehydration of CaO will impact on the concrete exposed to elevated temperatures, especially for OPC specimens.

Acknowledgment The authors gratefully acknowledge the Australian Research Council Discovery Grant No. DP0558463 for this research project.

References

1. Crozier DA, Sanjayan JG (1999) Chemical and physical degradation of concrete at elevated temperatures. *Concrete in Australia*, March–May, pp 18–20
2. Khoury GA (2000) Effect of fire on concrete and concrete structures. *Prog Struct Eng Mater* 2:429–447
3. Mendes A, Sanjayan J, Collins F (2008) Phase transformations and mechanical strength of OPC/Slag pastes submitted to high temperatures. *Mater Struct* 41:345–350
4. Mendes A, Sanjayan J, Collins F (2009) Long-term progressive deterioration following fire exposure of OPC versus slag blended cement pastes. *Mater Struct* 42:95–101
5. Lea FC, Stradling RE (1922) The resistance to fire of concrete and reinforced concrete. *Engineering* 144: 341–344
6. Dias WPS, Khoury GA, Sullivan PJE (1990) Mechanical properties of hardened cement paste exposed to temperatures up to 700°C (1292 F). *ACI Mater J* 87:160–166
7. Noumowe A (2005) Mechanical properties and microstructure of high strength concrete containing polypropylene fibres exposed to temperatures up to 200°C. *Cem Concr Res* 35:2192–2198
8. Petzold A, Rohrs M (1970) *Concrete for high temperatures*, 2nd edn. Maclaren and Sons Ltd, London
9. Khoury GA (1992) Compressive strength of concrete at high temperatures: a reassessment. *Mag Concr Res* 44:291–309
10. Abramowicz M, Kowalski R (2005) The influence of short time water cooling on the mechanical properties of concrete heated up to high temperature. *J Civil Eng Manag* XI:85–90
11. Kowalski R (2007) The effects of the cooling rate on the residual properties of heated-up concrete. *Struc Concr* 8:11–15
12. Luo X, Sun W, Chan S (2000) Effect of heating and cooling regimes on residual strength and microstructure of normal strength and high performance concrete. *Cem Concr Res* 30:379–383



13. Nassif AY, Rigden S, Burley E (1999) The effects of rapid cooling by water quenching on the stiffness properties of fire-damaged concrete. *Mag Concr Res* 51:255–261
14. Sakr K, El-Hakim E (2005) Effect of high temperature or fire on heavy weight concrete properties. *Cem Concr Res* 35:590–596
15. Sarshar R (1989) Effect of elevated temperatures on the strength of different cement pastes and concretes. Department of Civil Engineering, University of London, London
16. Gosh SN (2002) Advances in cement technology—infrared spectroscopy in cement chemistry. Teck Books International, New Delhi
17. Gao XF, Lo Y, Tam CM, Chung CY (1999) Analysis of the infrared spectrum and microstructure of hardened cement paste. *Cem Concr Res* 29:805–812
18. Hanna RA, Barrie PJ, Cheeseman CR, Hills CD, Buchler PM, Perry R (1995) Solid state ^{29}Si and ^{27}Al NMR and FTIR study of cement pastes containing industrial wastes and organics. *Cem Concr Res* 25:1435–1444
19. Mollah MYA, Yu W, Schennach R, Cocke DL (2000) A Fourier transform infrared spectroscopy investigation of the early hydration of Portland cement and the influence of sodium lignosulfonate. *Cem Concr Res* 30:267–273
20. Australia Standard AS 3972-1997 Portland and blended cements
21. Chatterji S (2005) Aspects of generation of destructive crystal growth pressure. *J Cryst Growth* 277:566–577
22. Ramachandran VS, Sereda PJ, Feldman RF (1964) Mechanism of hydration of calcium oxide. *Nature* 201:288
23. Ramachandran VS, Sereda PJ, Feldman RF (1967) Discussion on 'The volume expansion of hardened cement paste due to the presence of 'dead burnt' CaO ' by S Chatterji and J W Jeffrey. *Mag Concr Res* 19:49–50



Chapter 9

Differences in the Behaviour of Cement Paste and Concrete after Exposure to Elevated Temperatures, as in a Fire Event

9.1 Overview

Chapter 8 revealed that ordinary Portland cement (OPC) concrete does not disintegrate or present total strength loss after exposure to elevated temperatures as OPC paste. Therefore, Chapter 9 investigates the differences in the behaviour of OPC paste and concrete after exposure to elevated temperatures.

This chapter is based on the publication of the same name as the chapter title submitted to Cement and Concrete Composites Journal in June 2010. This paper investigates why calcium oxide (CaO) rehydration causes total strength loss of OPC paste but only 65% strength loss of OPC concrete after exposure to 800°C. As the rehydration of CaO is a result of water absorption by the specimen after heating, techniques such as water sorptivity, solvent sorptivity, solvent exchange method (porosity) and nitrogen adsorption were used to assess the differences between paste and concrete.

9.2 Declaration for Thesis Chapter 9

Declaration by candidate

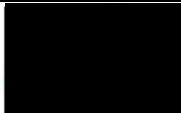
In the case of Chapter 9, the nature and extent of my contribution to the work was the following:

| Nature of contribution | Extent of contribution (%) |
|---|----------------------------|
| Developing outline of research objective and hypothesis Laboratory/experimental investigation and analysis of results Writing, reviewing and editing of paper | 85 |

The following co-authors contributed to the work. Co-authors who are students at Monash University must also indicate the extent of their contribution in percentage terms:

| Name | Nature of contribution | Extent of contribution (%) for student co-authors only |
|---------------|---|---|
| Jay Sanjayan | Developing outline of research objective and hypothesis Reviewing of paper | 5 |
| Frank Collins | Developing outline of research objective and hypothesis Reviewing of paper | 5 |
| Will P Gates | Developing outline of research objective and hypothesis Reviewing of paper | 5 |

**Candidate's
Signature**

| | |
|---|--------------------------|
|  | 30 September 2010 |
|---|--------------------------|

Declaration by co-authors

The undersigned hereby certify that:

- (1) the above declaration correctly reflects the nature and extent of the candidate's contribution to this work, and the nature of the contribution of each of the co-authors.
- (2) they meet the criteria for authorship in that they have participated in the conception, execution, or interpretation, of at least that part of the publication in their field of expertise;
- (3) they take public responsibility for their part of the publication, except for the responsible author who accepts overall responsibility for the publication;
- (4) there are no other authors of the publication according to these criteria;

- (5) potential conflicts of interest have been disclosed to (a) granting bodies, (b) the editor or publisher of journals or other publications, and (c) the head of the responsible academic unit; and
- (6) the original data are stored at the following location(s) and will be held for at least five years from the date indicated below:

Location(s)

| |
|--|
| Department of Civil Engineering, Monash University |
|--|

[Please note that the location(s) must be institutional in nature, and should be indicated here as a department, centre or institute, with specific campus identification where relevant.]

Signature 1



30 September 2010

Signature 2



30 September 2010

Signature 3



30 September 2010

9.3 Publication

Differences in the behaviour of cement paste and concrete after exposure to elevated temperatures, as in a fire event

Alessandra Mendes¹, Jay G Sanjayan², Will P Gates¹, Frank Collins¹

¹*Civil Engineering Department, Monash University, Wellington Rd, 3800 Clayton VIC, Australia*

²*Faculty of Engineering and Industrial Sciences, Swinburne University of Technology, Hawthorn VIC, Australia*

Phone: + 61 3 9905 5022, fax: + 61 3 9905 4944

Alessandra.mendes@eng.monash.edu.au

Abstract

This study investigates why CaO rehydration causes total strength loss of OPC paste compared to only 65% loss of OPC concrete after 800°C exposure. Subsequent water sorptivity tests revealed paste reacted instantaneously with water, completely disintegrating within minutes. This was attributed to an accelerated rehydration of CaO into Ca(OH)₂. This was not observed in concrete. Sorptivity tests using acetone eliminated the disintegration due to CaO reaction with water. Porosity tests indicated a higher porosity and coarser capillary pore size distribution (PSD) in paste over paste in concrete. This has an influence on the rate of water absorption. The rate of water absorption determines the growth rate of Ca(OH)₂ crystals and ultimately the type of Ca(OH)₂ crystals formed. Different crystals cause different levels of deterioration, not always leading to the total disintegration. Therefore, the rate of water absorption is the determining factor controlling the extent of deterioration caused by CaO rehydration.

Keywords: cement paste; concrete; elevated temperatures; strength loss; water absorption

1 Introduction

The behaviour of cement paste and concrete after exposure to elevated temperatures, as in a fire event, has been of interest to many researchers for decades. One of the first studies was conducted by Lea in 1920 [1].

When concrete is subjected to high temperatures, physical and chemical transformations take place resulting in deterioration of its mechanical properties [2].

A common way of investigating those physical and chemical transformations is by dividing the investigation into two steps: (i) the cement paste and (ii) the concrete as a whole, i.e., paste, aggregates and the interface between paste and aggregate. Investigating (i), the cement paste, Lea and Stradling [3] reported that one product of hydration of ordinary Portland cement (OPC) paste is calcium hydroxide (CaOH_2). This compound decomposes at about 400°C into calcium oxide (CaO) and water. In addition, they proposed that the high loss of water that occurs between 300 and 500°C is due to the breaking up of the CaOH_2 .

Dias et al. [4] reported that although no initial signs of distress were visible on OPC pastes heated to 400°C or above and cooled to room temperature, all specimens exhibited severe cracking to the point of disintegration after a few days. According to Petzold and Rohrs [5], the reason for this cracking is the expansive and hence disruptive rehydration (due to reaction with airborne water vapour) of previously dissociated CaOH_2 which is accompanied by a 44% volume increase.

Studies by the authors revealed similar findings [6, 7]. The critical temperature of 400°C for OPC pastes was confirmed. Above this temperature, OPC pastes presented total strength loss due to dehydration of CaOH_2 and rehydration of CaO . However, dehydration of CaOH_2 and rehydration of CaO had no impact in pastes where OPC was partially replaced with ground granulated blast furnace slag (slag), a by-product of the iron blast furnace industry. This is illustrated in Fig. 1. During hydration slag consumes most of the available CaOH_2 , consequently reducing or even eliminating the negative effects caused by the CaOH_2 dehydration and CaO rehydration when cement paste is submitted to elevated temperatures. The

compressive strength of OPC and 50% slag pastes after exposure to temperatures up to 800°C is presented in Fig. 2.

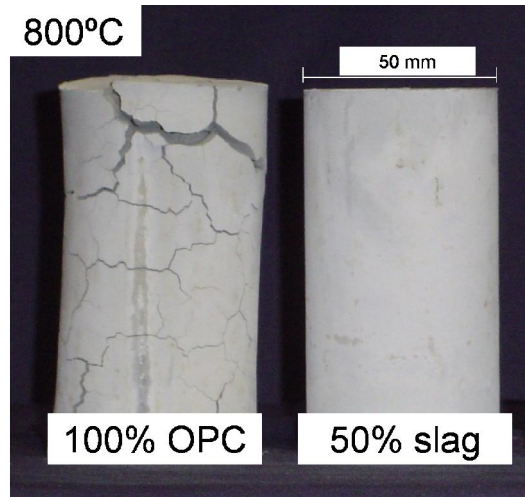


Fig. 1 OPC and 50% slag pastes after exposure to 800°C.

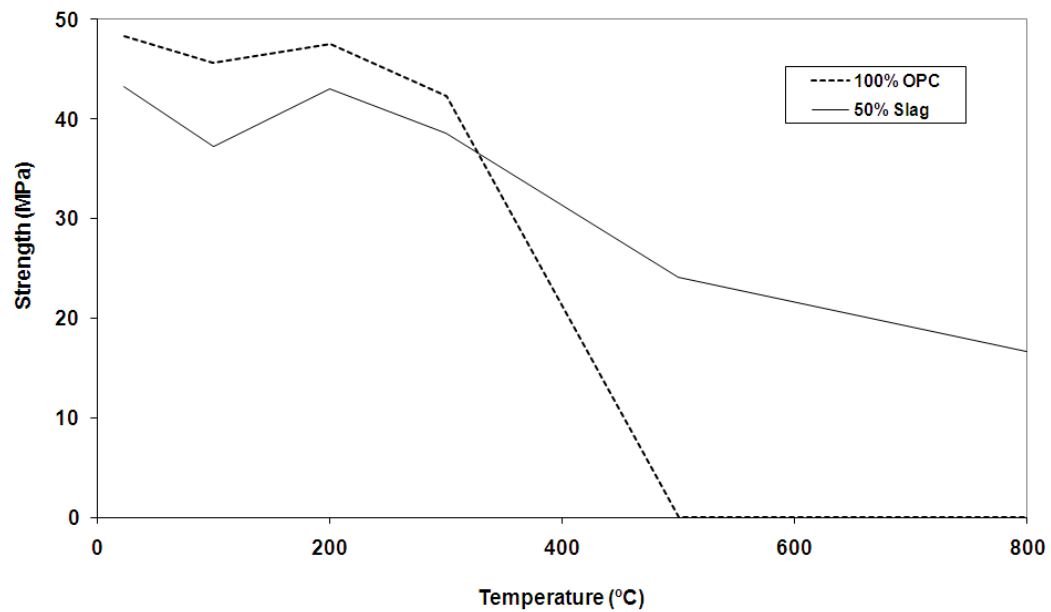


Fig. 2 Compressive strength of OPC and 50% slag pastes at different temperatures.

Following the investigation of the cement paste, Lea and Stradling [8] assessed the effects of elevated temperatures on (ii), the concrete as a whole. Their work stated that specimens of OPC concrete made with Rowley Rag aggregate (volcanic dolerite stone) exposed to 700°C crumbled to pieces six days after the heat treatment.

Khoury [9] stated that, following Lea and Stradling, it was recognized that the CaOH_2 problem could be the Achilles' heel of concrete in high temperature applications.

Moreover, other researchers reported strength loss of OPC concrete when submitted to temperatures as high as 1200°C, but no significant disintegration or crumbling were found [10-13]. In addition, Khoury [9] affirmed that there was scope for improvement within the temperature range of 300-600°C. In 2000, Khoury [2] suggested that the deterioration of the mechanical properties of concrete can be reduced by judicious design of concrete mix, with the choice of aggregate possibly the most important factor. Flint or Thames gravel is said to break up at relatively low temperatures ($< 350^\circ\text{C}$), while granite is expected to exhibit thermal stability up to 600°C. Basalt aggregate was reported not to undergo phase changes at temperatures up to 800°C [2, 14].

The authors have also performed tests on concrete [15]. The concrete specimens were made with the same OPC cement and slag blends as the one used for the paste in which OPC pastes disintegrated [15]. The coarse aggregate used was basalt, as described above as having high thermal stability. Fig. 3 presents the residual compressive strength for the OPC and 50% slag concretes after exposure to 800°C followed by either furnace or water cooling. It was found that even though dehydration of CaOH_2 and rehydration of CaO were determined to have occurred by infrared spectroscopy (IR), the OPC concrete did not disintegrate or crumble even months after the heat treatment.

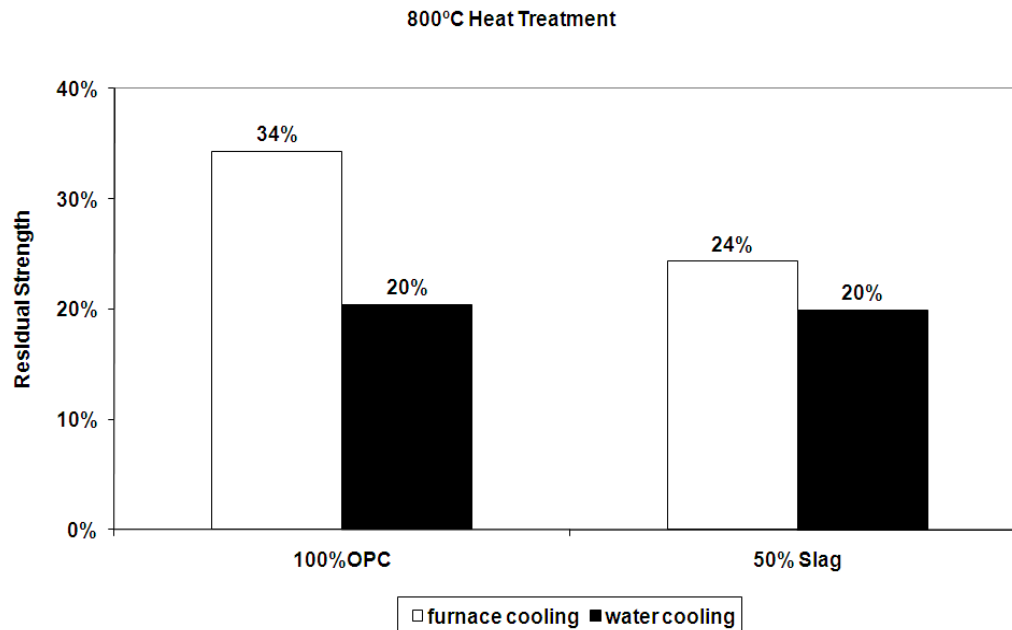


Fig. 3 Residual strength of OPC and OPC/slag concretes after exposure to 800°C.

The authors have also reported the long-term effects of the CaO rehydration on OPC pastes [7]. It was reported that one year after the 800°C heat exposure, the OPC paste has been reduced to a powder. This was confirmed to be due to continuous rehydration of CaO via airborne water vapour throughout the year.

Based on that, it is expected that the OPC cement paste in the concrete would disintegrate, even if over longer time periods, independently of the thermal stability of the aggregate. However, it is clear from the discussion above that after exposure to elevated temperatures, the OPC paste test results does not represent the same deterioration behaviour of the OPC paste present in concrete.

Therefore, the present work aims to identify why the dehydration of CaOH_2 and rehydration of CaO is not detrimental for the OPC paste in concrete as it is for an OPC paste specimen (Fig. 1). Thus, the present work investigates differences in the dehydration/rehydration process of cement paste and concrete. Based on that, it focuses on distinguishing how the water is absorbed by the cement paste and concrete subsequent to heating. Firstly, water sorptivity tests were conducted. Secondly, sorptivity tests using a solvent instead of water were performed without damage to the specimens caused by reaction of water & CaO. Thirdly, an attempt to determine the porosity of the pastes and concretes using a solvent was made.

Afterward, nitrogen adsorption was performed to provide information regarding the pore size distribution of the specimens. Discussion of each technique is presented in the relevant sections.

2 Materials and methods

Paste

Ordinary Portland cement (OPC) and ground granulated blast furnace slag (GGBFS or “slag”) conforming to the requirements of Australian Standard AS 3972 were used as binder materials. The chemical composition and properties of the binders are presented in Table 1. The OPC used in this study has a low C_3A content of < 5%. In this investigation OPC was partially replaced (i.e., 50% by weight) with slag. The term water/binder (w/b) ratio is used instead of the water/cement ratio to include both binder types mentioned above. The (w/b) ratio used was 0.5.

Table 1 Chemical composition and properties of the binders.

| Constituent/property % | OPC | Slag |
|----------------------------------|-------|------|
| SiO ₂ | 19.90 | 32.5 |
| Al ₂ O ₃ | 4.70 | 13 |
| Fe ₂ O ₃ T | 3.38 | 0.22 |
| MgO | 1.30 | 5.47 |
| CaO | 63.93 | 42.1 |
| Na ₂ O | 0.17 | 0.21 |
| TiO ₂ | 0.245 | 1.08 |
| K ₂ O | 0.446 | 0.25 |
| MnO | 0.079 | 5.47 |
| P ₂ O ₅ | 0.063 | bd* |
| SO ₃ | 2.54 | 4.1 |
| LOI | 2.97 | 0.35 |
| Fineness, m ² /kg | 360 | 435 |
| Specific gravity | 3.15 | 2.92 |

*below detection

Concrete

Identical binders to the paste specimens were used. Pakenham Blue Metal (Old Basalt) crushed type was used as coarse aggregate with the following properties: Maximum size = 14 mm; specific gravity = 2.95; and absorption = 1.2%. Lyndhurst washed fine sand was used as the fine aggregate with the following properties: specific gravity = 2.65; absorption = 0.5%. The w/b ratio used was 0.63. All concrete mixtures contained water reducer WRDA GWA Grace Construction

products 4.03 ml/kg of total cementitious materials; Total cementitious content = 300 kg/m³; and Coarse aggregate = 1100 kg/m³.

Measurements of the moisture contents of the aggregates were taken the day before and on the day of the concrete mixing. The aggregate weights were adjusted to saturated and surface dry condition.

Mixing and Heat Treatment

For the paste, water was first added, followed by the binders. The mixing was conducted in a mechanical mixer of 20 litres of capacity, 80 rpm, for five minutes each mixture. For the concrete, the first step was the mixing of aggregates with a third of the water for 30 seconds. The second step was the addition of the binders and remaining water, followed by two minutes of mixing. The mixture was set to rest for an extra two minutes. The final step consisted of adding the water reducer during the last two minutes of mixing. For both paste and concrete, the specimens were compacted using a vibration table for better compaction. Specimens were sealed with a plastic sheet and demolded after 24 hours and cured for 28 days in lime-saturated water at 23°C. Specimens were then placed in a controlled temperature room for drying during 30 days, at 23°C and 50% of relative humidity.

Following drying, the heat exposure was conducted in a muffle furnace. The heat exposure was as follows: constant heating rate of 6.25°C/min until 750°C, than 1 hour between 750-800°C, and finally 1 hour in 800°C.

Paste and concrete specimens were assigned as 'RT' for room temperature and '800°C' for the 800°C heat exposed specimens.

Water and Solvent Sorptivity

Two specimens of each mix (for both paste and concrete) were tested. Sorptivity tests were conducted in accordance with ASTM C 1585 – 04 Standard Test Method for Measurement of Rate of Absorption of Water by Hydraulic Cement Concretes. The test specimen's size for pastes and concrete specimens was 100 mm x 50 mm. The specimens were oven dried for 3 days at 50°C followed by 15 days sealed storage. The 800°C heat treated specimens were tested immediately after the heat treatment took place. The solvent sorptivity test was performed as per water

sorptivity. Acetone ACS reagent grade $\geq 99.5\%$ was used. The test was conducted inside desiccators in order to avoid acetone evaporation.

Porosity – Solvent Exchange Method

Three specimens of each mix were tested. For the concrete specimens, only the mortar part of the specimen was tested (no coarse aggregate). No pre-drying was performed except for the specimens that were exposed to heat tests. The specimens were saturated with acetone in a sealed container until constant mass. The pycnometer test was based in the ASTM D854-05 Standard Test Methods for Specific Gravity of Soil Solids by Water Pycnometer. Acetone density was determined by the pycnometer test.

Nitrogen Adsorption

Nitrogen adsorption and desorption tests were conducted using a Coulter "Omnisorp 360CX" gas sorption analyzer. Outgas was at 3.5×10^{-5} torrs, 40°C for approximately 30 hours. Specific surface areas were calculated by the Brunauer, Emmet and Teller (BET) method over a relative pressure range of 0.05-0.25 on the adsorption/desorption isotherm. Total cumulative pore volume available to nitrogen (1-40 nm pore radius range) and pore size distribution were calculated by the Barrett, Joyner, Hallenda (BJH) method [16] using data from the desorption isotherm.

3 Results and discussions

3.1 Water sorptivity

Sorptivity tests were conducted to determine any difference in the water absorption process of paste and concrete. A difference in water absorption leads to differences in the CaO rehydration process. Sorption is a term used for water ingress into pores under unsaturated conditions due to capillary suction [17]. Sorptivity testing has been previously used as a measure of the ability of concrete to absorb water [17, 18]. The specimens in comparison consisted of room temperature 'RT' (not exposed to heat) and '800°C' heat exposed (followed by cooling to room temperature) paste and concrete specimens. For comparison, specimens with partial replacement of OPC with slag (50% by weight) were also tested.

During sorptivity testing, the OPC paste 800°C immediately upon contact with water released significant heat and cracked. The heat was so intense that the sealing plastic was partially melted. Within a few minutes, the specimen had disintegrated completely (Fig. 4). Similar disintegration is seen when the OPC paste 800°C is exposed to air moisture for a few days [6], however the excessive heat is not apparent. Therefore, the authors believe that this abrupt disintegration of OPC paste 800°C in water was due to an accelerated rehydration of CaO. Therefore, the same heat exposure as described in Section 2 was performed in a CaO sample. It was observed that immediately after cooling, and in the presence of water, the CaO reacted instantly, with the temperature reaching ~ 80°C within 30 seconds. Thus, confirming that immersing OPC paste 800°C in water provided an accelerated exothermic rehydration of CaO.



Fig. 4 OPC paste 800°C. Left, after 800°C heat treatment. Middle, immediately after water immersion. Right, few minutes after water immersion.

None of the remaining specimens (OPC concrete and 50% slag paste and concrete) presented the significant deterioration found for the OPC paste 800°C and therefore, in those specimens, sorptivity tests were possible. The slag specimens (both concrete and paste) presented slightly higher sorptivity values when compared to OPC, this is in accordance with previous work [19]. However, the differences between OPC and 50% slag pastes and concretes were not significant. Therefore, for better visualization Fig. 5 presents only 50% slag specimens. In Fig. 5, the test time has been truncated to show sorption differences at earlier times.

The specimens are represented by 'paste and concrete' and 'RT' (not exposed to heat) and '800°C'. When comparing the paste with the concrete it should be taken into account that the concrete specimens consist of approximately 20% paste.

Therefore, to enable accurate comparison, the differential mass ($\Delta\text{Mass} \%$) of each specimen was calculated [20] and is plotted against the time ($\text{s}^{1/2}$) in Fig. 5.

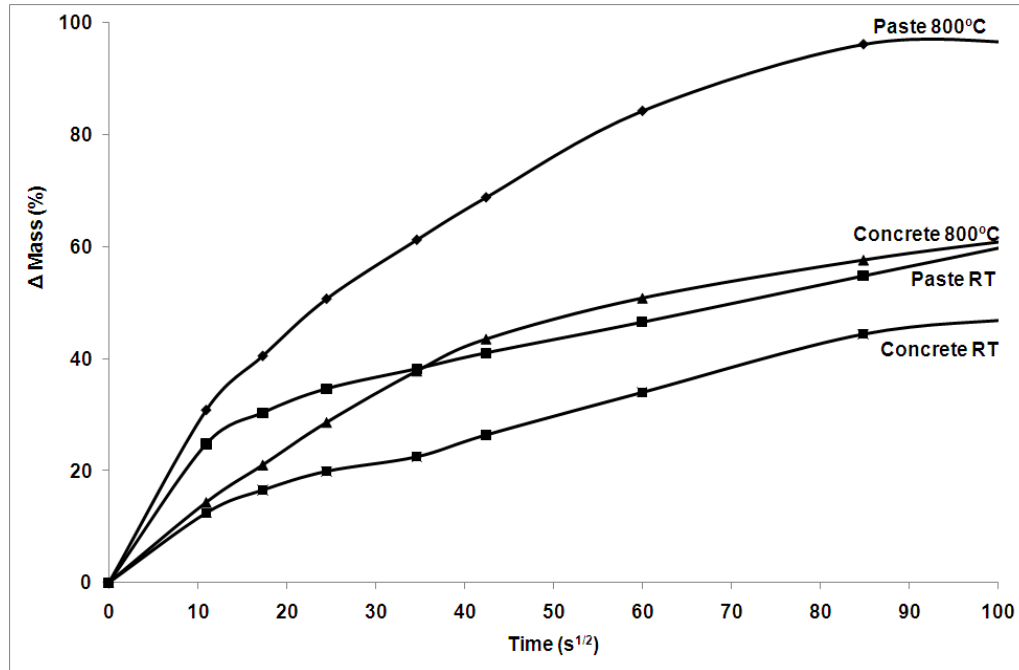


Fig. 5 Water sorptivity test results for the different specimens (50% slag blend).

It is clear from Fig. 5 that paste 800°C absorbs water at a significantly faster rate than concrete 800°C, paste RT and concrete RT. Therefore, this results in more available water for the rehydration of CaO in a shorter period of time. Fig. 5 shows that after 100 $\text{s}^{1/2}$ (~ 3 hours) of exposure to water, the paste 800°C absorbed ~ 97% of the total amount of water absorbed, while the concrete 800°C absorbed ~ 60%. When comparing the pastes RT and 800°C, it is possible to see that the heat exposure caused the water absorption to increase from 47 to 85% in 60 $\text{s}^{1/2}$ (1 hour). On the other hand, for the concrete, the increase from RT to 800°C after 1 hour exposure to water was 17%, showing that the effects of the heat treatment on the absorption of concrete were not as severe as for the paste.

3.2 Solvent Sorptivity

In the water sorptivity test, the OPC paste 800°C crumbled and completely disintegrated during the first few minutes of the test, inhibiting completion of the test, and consequently, determination of its capacity to absorb water. As explained above, the instantaneous disintegration is a result of the accelerated rehydration of CaO caused by the reaction of the dehydrated OPC paste with water. Hence, the need to find a way of determining the absorption of this paste is necessary.

Two issues were of concern when performing the water sorptivity test: the pre-treatment required (drying) and rehydration of CaO leading to damage in the presence of water.

Regarding the pre-treatment required, the fine pore structure of concrete is very sensitive to drying procedures, which might result in microstructural damage [21]. Previous works have used temperatures as high as 105°C as a pre-treatment prior to porosity test techniques such as sorptivity, MIP or vacuum saturation [22-29]. It is generally considered that, at 105°C, only free water (evaporable water) is removed from the pore spaces of most materials [23]. However, it has been reported that ettringite crystallinity is readily destroyed, with loss of water, by heating in air ~ 100 – 105°C [30]. In addition, drying may result in structural and physical collapse of other hydrates as monosulfate hydrate (AFm) and C-S-H [30]. The temperature at which the decomposition of C-S-H initiates is not well established but C-S-H is partially dehydrated at 105°C [23]. Furthermore, it has been reported that even drying temperatures as low as 50°C may not be appropriate for all concretes [17]. This is because the concretes with low water/cement ratio dry at a much slower rate than those with high water/cement ratio [21]. In addition, drying can introduce microcracks that influence the measured sorptivity.

The other concern relates to the rehydration of CaO in the presence of water. Especially for the 800°C specimens, on exposure to water, the dried material may also rehydrate [31, 32], affecting the accuracy of the sorptivity test measurement.

An alternative to the use of the water as the wetting medium in the sorptivity test is the use of a solvent. The solvent acetone was chosen for the present work because: (i) water is miscible in it, thus it will remove strongly bound pore water; (ii)

it has a lower dielectric than water, thus it will be less likely to hydrogen-bond strongly to surfaces; and (iii) it has a lower capacity of formation of covalent bonding to oxides such as CaO, thus will be less likely to significantly react with the highly reactive components in heated cements than water. Acetone has been successfully used to remove free water from cement paste and concrete, i.e., as a drying method prior to mercury intrusion porosimetry (MIP) [33, 34]. Therefore, while acetone will remove the capillary water from both the cement paste and concrete, it will penetrate essentially the same pore space as water via capillary attraction, enabling the determination of each specimen's sorption. However, the viscosity and density of acetone and water differ enough to possibly affect some of the results.

Further, the effects of acetone in the microstructure of the cement paste have been the focus of previous works. The main concern being that acetone would impact on an accurate quantitative determination of the CaOH_2 content of the hardened cement paste [33]. It is suggested that the length of CaOH_2 crystals increased when immersed in acetone [35]. This finding is not expected to significantly impact on the current experiment, especially for the 800°C specimens, as those have experienced complete CaOH_2 dehydration. In addition, Taylor and Turner [36] reported that in the presence of acetone, C_3S paste quickly turned yellow, the colour deepening after a few days to a reddish yellow. This was not observed in the present experiment and may be an artefact of their experiment. Furthermore, acetone quenching was reported to have preserved the pores better than other drying techniques (freeze drying, oven drying, and vacuum drying) [23, 33, 37, 38].

Thus, the sorptivity test was repeated using acetone. Fig. 6 presents the acetone sorptivity results for all OPC specimens, as completion of OPC paste 800°C sorptivity test was now possible without the reaction of CaO with water that lead to completely disintegration. The 50% slag specimens presented similar acetone sorptivity results as OPC, and for better visualization, only OPC specimens are presented in Fig. 6. It is possible to see that concrete RT (room temperature) absorbs acetone slowly, approximately 9% in $60 \text{ s}^{1/2}$ (first hour). In a faster rate than concrete RT, paste RT absorbed ~ 29% in the same period of $60 \text{ s}^{1/2}$. Interestingly, a slower rate of acetone sorption was observed for the paste and concrete RT in comparison to the rate of water sorption as seen in Fig. 5. This may be a result of the acetone reaction with CaOH_2 as described by others [33, 35]. In addition, the

slower rate may be also a result of the lower surface tension of acetone compared to water; the very small pores present in concrete RT (see BET section) may be less accessible to acetone than water.

For the concrete 800°C, a different scenario was found. While the acetone absorption of this specimen was quite fast, 82% in 60 s^{1/2} (first hour - Fig. 6), the water absorption was much slower 32% in the same period (Fig. 5). This suggests that although the OPC concrete 800°C capacity to absorb a liquid is significant, when the liquid is water this absorption is quite slow. The slower rate is also related to the greater viscosity and density of water compared to acetone.

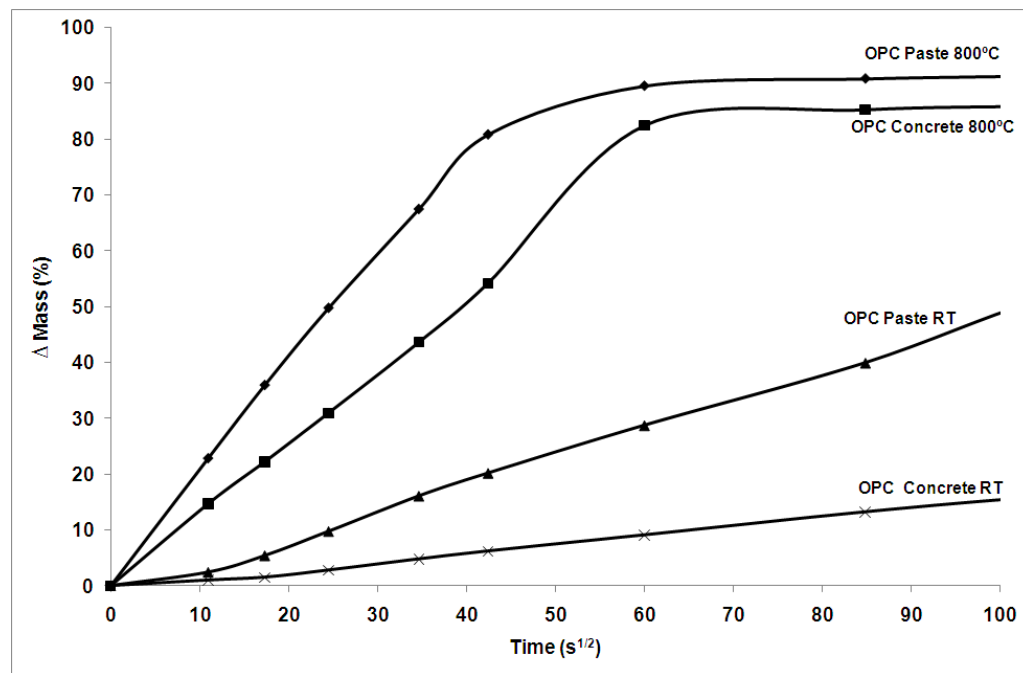


Fig. 6 Acetone sorptivity test results for the different OPC specimens.

The OPC paste 800°C absorbed ~ 89% of the total amount of acetone absorbed in 60 s^{1/2} (first hour). This shows the higher capacity of this specimen to absorb a liquid when compared to the remaining specimens.

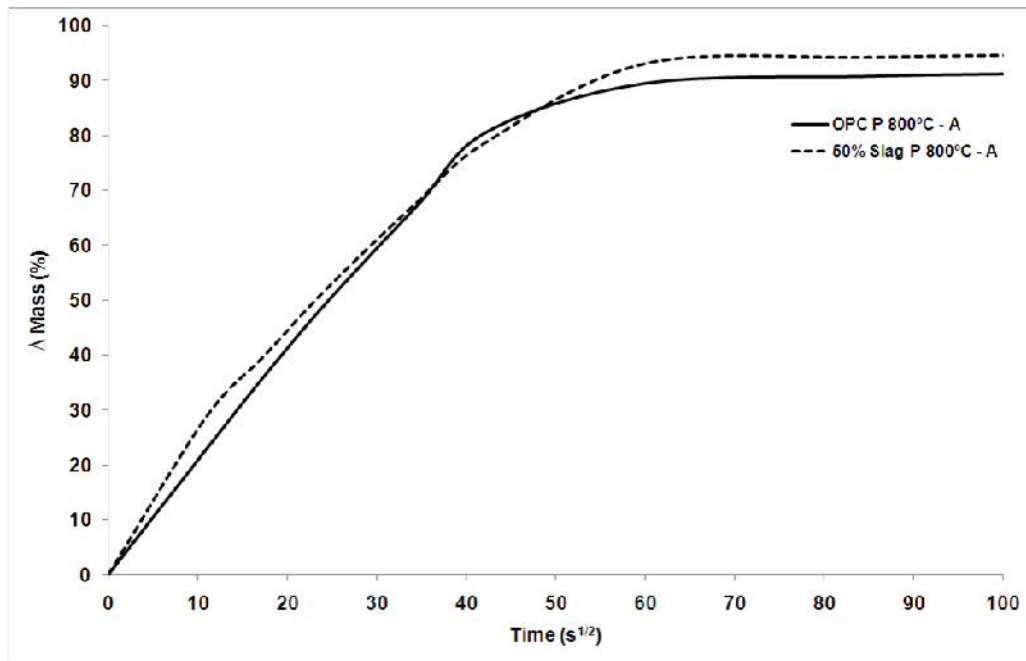


Fig. 7 Comparison between OPC and 50% slag pastes 800°C (acetone sorption).

Fig. 7 presents the acetone absorption for the OPC and 50% slag paste 800°C. It can be seen that OPC and 50% slag pastes 800°C presented similar acetone absorption. Therefore, the 50% slag water absorption results would provide an indication of the OPC paste 800°C rate of water absorption (Fig. 8 – dashed line). For the 50% slag paste 800°C, water and acetone were absorbed in a very similar way, approximately 85% of water and 93% of acetone absorption in 60 s^{1/2} (first hour). Based on this, as the OPC paste 800°C acetone absorption is in the range of 92% in the same period of 60 s^{1/2}, very similar to the 93% found for the slag specimen, the water absorption would be expected to be similar. Considering the 50% slag paste 800°C rate of water absorption of 84% in the first hour, it is reasonable to expect that the OPC paste 800°C rate would be of similar value for the same period. This is represented in Fig. 8 (dashed line) and is expected to be the minimum amount absorbed during the first 100 s^{1/2} (~ 3 hours). In addition, as described in the previous section, OPC paste 800°C disintegrated minutes after being in the presence of water. The reason for this fast disintegration was attributed to the rehydration of CaO. Therefore, indicating that in the OPC paste 800°C this reaction is almost instantaneous.

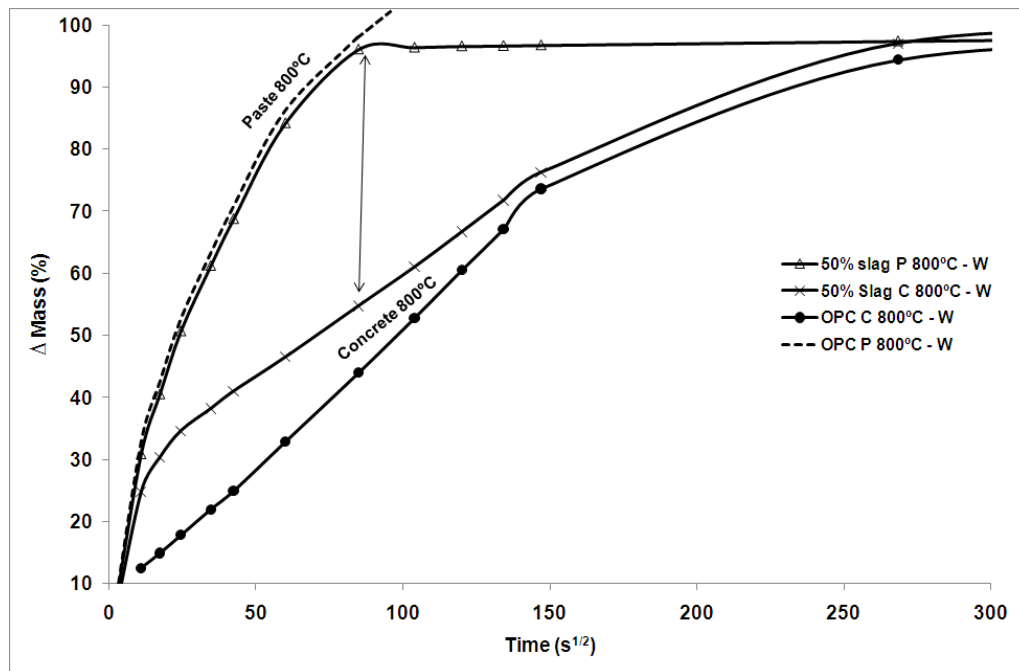


Fig. 8 Water absorption of OPC and 50% slag blends 800°C. Dashed line indicates expected absorption for the OPC paste 800°C.

This is an important finding as shows that the OPC paste 800°C rate of water absorption (expected to be ~ 85% in 1 hour and > 90% after 3 hours) occurs in a much faster way compared to OPC concrete 800°C (approximately 32% in 1 hour and 53% after 3 hours). This is represented in Fig. 8 by the arrow, with the top indicating paste 800°C and the bottom, concrete 800°C.

Differences in rate of water absorption lead to differences in growth rates of CaOH_2 . Fast growth of crystals favours crystal growth at selected faces of the crystal, the crystals are acicular [39]. A slow growth yields equant crystals [39]. Faster water absorption leads to faster CaO rehydration, and consequently faster growth of CaOH_2 . Acicular and fast crystal growth are more conducive of causing damage to a porous matrix than slow and equant crystal growth [39]. Equant growth may not cause any damage [39]. Ramachandran et al. [40, 41] analysed the hydration of CaO pressed compacts exposed to either a limited quantity of liquid water or to water vapour. The compacts are reported to have a void content of 46% by volume and a CaO content of 54%. For the liquid water the compact remained strong and undamaged. In contrast, for the compact exposed to water vapour, a volume

increase was observed resulting in disintegration. Chatterji [39] concluded that not all crystal growth leads to disintegration of the constraining body.

Thus, the differences in the rate of water absorption observed for the OPC paste and concrete 800°C lead to differences in the growth rate of CaOH_2 crystals during rehydration of CaO . The different CaOH_2 crystals formed will lead to different deteriorations. This explain why OPC paste disintegrates after exposure to 800°C followed by air moisture and/or water (CaO rehydration), and why, on the other hand, the OPC concrete does not disintegrate, even though CaO rehydration has been confirmed to take place.

In conclusion, the dehydration of CaOH_2 and rehydration of CaO might cause damage to OPC paste and concrete after exposure to temperatures above 400°C followed by exposure to air moisture. However, the extent of the deterioration is not only related to the rehydration occurrence, but most importantly it is related to the rate of how the rehydration occurs, i.e., the rate of water absorption.

3.3 Porosity – Solvent Exchange Method

The fast rate of acetone absorption of both paste and concrete 800°C, in which reaction is expected to be minimal, indicates differences in the porosity of those specimens when compared to the RT specimens. As reported previously [24, 42], the porosity of concrete allows movement and retention of water and other substances.

An accurate measurement of porosity and pore size distribution of hardened cement paste is extremely difficult to obtain [37, 43]. While determining porosity, there are evidences that the fragile microstructure of the cement matrix can be damaged by two causes: by the drying procedure itself and/or, by the measurement technique employed for the pore structure determination [37, 38, 44].

Based on that, the present work used the solvent exchange method to minimize the effects of both pre drying and the technique itself. No drying is required using the solvent exchange method. Parrot [45] used methanol as a drying treatment prior to nitrogen adsorption and concluded that the pore structure had not been excessively disturbed and that subsequent desorption and adsorption of methanol rather than

nitrogen might be used to study pore structure. In 1984, Parrot [46] concluded that solvent exchange can provide a simple physical measure of diffusion in cementitious pastes, that can reflect the effects of pore structure alterations arising from previous drying. Robler and Odler [34] used an acetone-ether extraction to determine the porosity of the cement paste. Having free water removed by acetone-ether and bound water by loss of ignition, it was concluded that an accurate measurement of porosity was obtained [34]. Day and Marsh [43] concluded the alcohol exchange process, followed by removal of the alcohol may be a preferred drying method if accurate pore size distributions are to be obtained.

The acetone used in the present work, as described in the previous section, is expected to have a low detrimental impact on the microstructure of the specimen.

Saturating the specimen with acetone enabled estimation of porosity. It is assumed that total penetration of the acetone into the pores occurred. The total mass of acetone absorbed by each specimen was recorded. As the acetone's density at the test temperature is known, the volume of acetone in the specimen can then be determined. In a similar way, the volume of the specimen can be determined by the known mass and bulk density. The porosity is then determined by the equation 1 below:

$$P (\%) = V_a/V_s \quad (1)$$

Where, $P (\%)$ refers to the porosity of the specimen in percentage, V_a the volume of acetone inside the specimen and V_s the volume of the specimen. For comparison, a pycnometer of known volume was weighed, filled with a known mass of finely ground specimen and acetone until saturation, followed by weighing. With the mass and density of acetone and total volume known, the volume of the sample and its particle density can be calculated. Finally, with the known bulk density (ρ_{bulk}) and particle density ($\rho_{particle}$) the porosity $P (\%)$ can be determined by the equation 2 below:

$$P (\%) = \rho_{bulk}/\rho_{particle} \quad (2)$$

Both the solvent exchange method and the pycnometer method provided very similar results and those are presented in Fig. 9. For the concrete specimens the porosity results are related to the paste in concrete only, not considering aggregates and ITZ porosities. For the room temperature specimens, as expected, paste is more porous compared to the paste in concrete [26]. In addition, partial replacement of OPC with slag tends to slightly increase the porosity of concrete RT and 800°C and paste RT. This is in accordance with previous work [33]. For the paste 800°C, a different scenario was found, with the OPC paste presenting higher porosity than 50% slag paste, possibly due to the higher deterioration occurred due to the CaOH_2 dehydration. The higher porosity of OPC paste 800°C is in accordance with same trend found for the compressive strength, in which higher porosity lead to a higher deterioration of mechanical properties. This is in accordance with previous works [11, 22, 34].

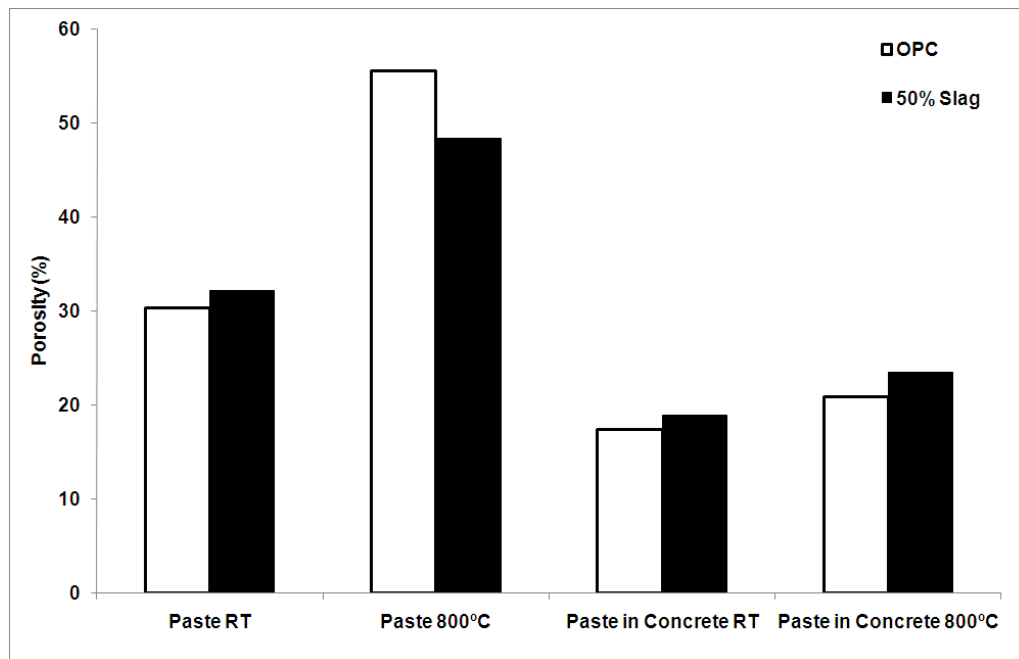


Fig. 9 Porosities determined by the solvent exchange method using acetone, for both OPC and 50% slag specimens.

3.4 Nitrogen adsorption

As described by Day and Marsh [43], when only one porosity measurement technique is used during an examination, interpretation of results is restricted because the method is based on a number of underlying assumptions. As an example, differences in viscosity, density and surface tension for acetone and water

mean that slightly different pores will be accessed by these two solvents. While the authors believe the differences will have minimal effect on the bulk results, it is useful to have another means to prove the specimen pore space. Therefore, nitrogen adsorption technique was performed to complement the porosity characterisation obtained by the acetone exchange methods described in the previous section. It must be noted that nitrogen absorption/desorption isotherms only prove a specific range of pore sizes, thus is also limited in its ability as a stand-alone technique in characterising the porosity of paste and concrete.

Adsorption measurements using various adsorbates (N_2 , H_2O , Kr, etc.) generate values of specific surface areas and cumulative pore volumes [31]. The cement paste has by volume a relatively large porosity, which can be defined in terms of void volume, capillary pores and gel pores. The voids are formed on mixing when air is entrapped into the mixture and the resulting voids can vary in size from approximately 1 to 500 μm . Capillary pores have an average radius greater than 50 \AA and are originally water filled. When interconnected these pores dominate water transport [47]. Gel pores have a radius less than 50 \AA [47]. The water present in gel pore is more strongly bound water and can be removed only by drying [31] or by solvent exchange.

In the case of heat exposed specimens, structural changes which may result from dehydration processes are predominantly effectual in a pore radius range below 40 \AA [48]. The occurrence of structural changes in this range might be investigated by N_2 adsorption [48].

Fig. 10 presents the adsorption isotherms for OPC paste and concrete, RT and 800°C. In general, the results are in accordance with the porosity results presented in Fig. 9. OPC paste RT has a N_2 adsorption volume of $\sim 52 \text{ cm}^3/\text{g}$ while paste in concrete RT has an adsorption volume of $\sim 20 \text{ cm}^3/\text{g}$. A higher adsorption is found for the OPC paste 800°C at the same p/p_0 compared to the paste RT. The OPC paste 800°C has an adsorption volume of $\sim 70 \text{ cm}^3/\text{g}$ while OPC paste in concrete 800°C has $\sim 26 \text{ cm}^3/\text{g}$. This supports the findings described in the previous section, as the OPC paste 800°C presented higher total adsorption, and therefore greater porosity, when compared to the OPC paste in concrete 800°C.

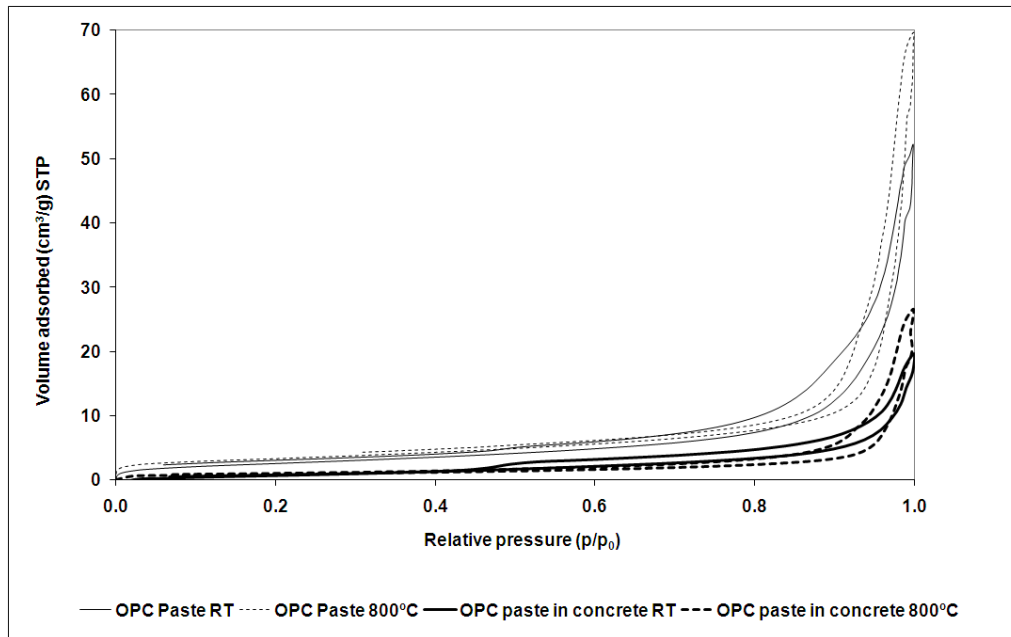


Fig. 10 Nitrogen adsorption isotherms for OPC paste and concrete, RT and 800°C.

Fig. 11A and B present the BJH desorption cumulative pore size distribution for the different OPC specimens. In Fig. 11A, a comparison between paste RT and 800°C is made in order to determine the effects of the heat exposure on the pore size distribution of the cement paste. For both RT and 800°C the peaks near 5 nm relates to the gel pores [47] which are of a size that is not conducive to unsaturated flow by capillary attraction. As discussed above, the water present in the gel pores is more strongly bound water and can be removed only by drying [31]. After exposure to 800°C, it can be seen that the gel pores have drastically decreased. This is evidenced by the increase in capillary pores and microcracks, which when interconnected dominate the water transport [47]. Thus, this change in pore size, and change in the volume of pores of different sizes (i.e. gel and capillary), facilitates the absorption of water in the system.

In Fig. 11B, OPC paste 800°C is compared to paste in concrete 800°C so that the differences between the pore size distributions of those specimens can be determined. Regarding the gel pores, the heat treatment seems to result in similar loss of gel pores volume, as a result of the dehydration due to the loss of bound water. However, regarding the capillary pores, the OPC paste 800°C presents a greater volume of the coarser pore size distribution. As discussed above, the capillary pores dominate the water transport, therefore leading to greater absorption

of water by the paste 800°C when compared to the paste in concrete 800°C. This is in accordance with the sorptivity tests discussed in the previous sections, confirming that OPC paste 800°C absorbs water at a faster rate when compared to OPC paste in concrete 800°C. This results in different CaO rehydration process between those specimens.

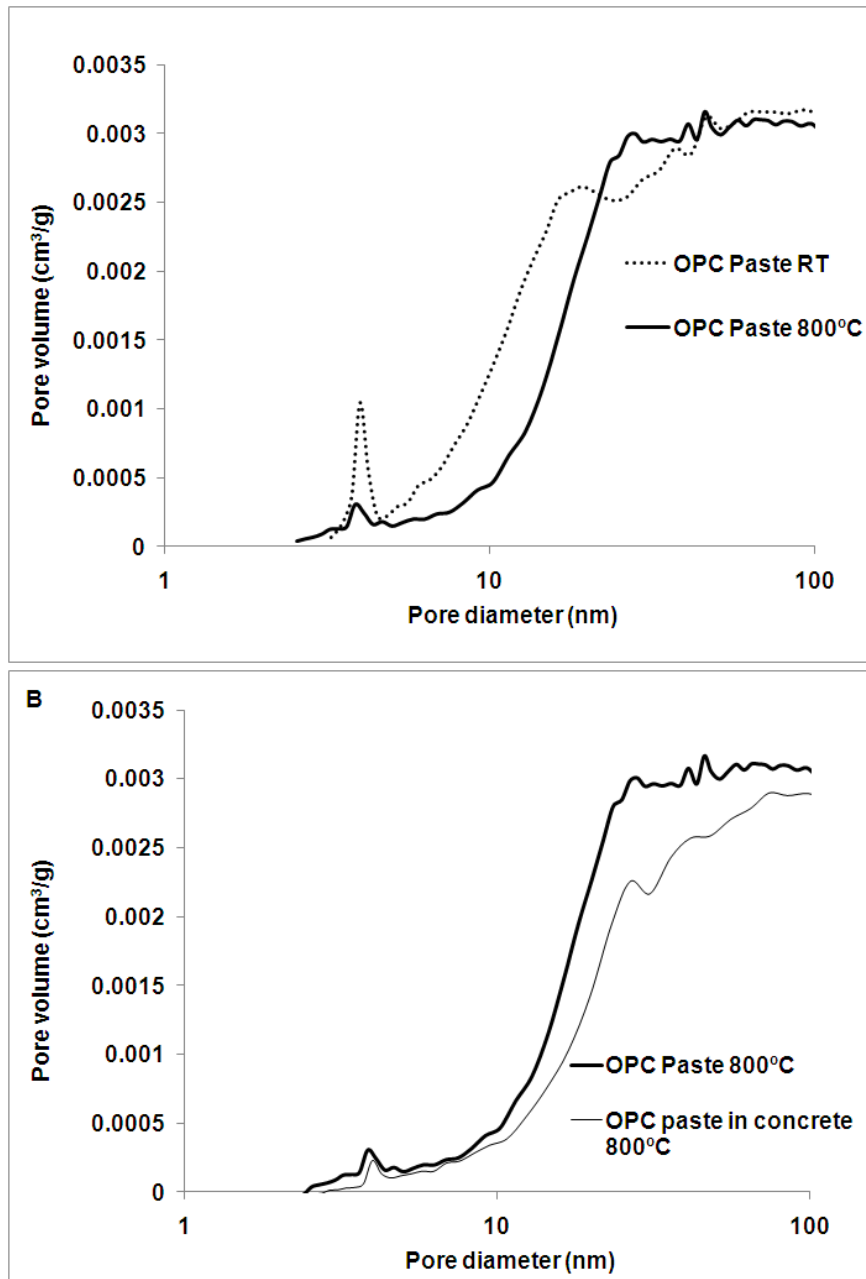


Fig. 11 BJH desorption pore size distributions. 'A' OPC paste RT and 800°C. 'B' OPC paste and paste in concrete 800°C.

4 Conclusions

The present work investigated why, after exposure to 800°C, rehydration of CaO causes total strength loss in OPC paste, leading to complete disintegration of the paste yet only 65% strength loss in OPC concrete.

Water sorptivity tests have shown that OPC paste 800°C specimens reacted instantaneously with water, releasing heat and disintegrating, inhibiting test completion. This was found to be due to an accelerated rehydration of CaO in the presence of water; an expansive, exothermic and instantaneous reaction.

Acetone sorptivity tests provided an indication of the OPC paste 800°C rate of water absorption. Based on that, it was concluded that OPC paste 800°C absorbed water faster than OPC concrete.

The rate of water absorption determines the growth rate of CaOH_2 crystals and ultimately the type of CaOH_2 crystals formed. Therefore, the faster rate of water absorption observed for OPC paste 800°C compared to OPC concrete 800°C, led to different CaOH_2 crystal formation in each specimen. Different crystals cause different levels of deterioration, not always leading to the total disintegration of the constraining body.

This explain why OPC paste disintegrates after exposure to 800°C followed by air moisture and/or water (CaO rehydration), and why, on the other hand, the OPC concrete 800°C does not disintegrate, even though CaO rehydration has been confirmed to have taken place.

Therefore, the extent of the deterioration is not only related to the CaO rehydration occurrence, but most importantly it is related to the rate at which rehydration occurs, i.e., the rate of water absorption. The rate of water absorption is the determining factor controlling the extent of deterioration caused by CaO rehydration.

The solvent exchange method using acetone provided a good indication of the porosity of the specimens. In addition, it eliminated the negative effects of the pre-

drying required by other porosity testing techniques such as mercury intrusion porosimetry (MIP). The porosity was significantly higher for the paste 800°C compared to the paste in concrete 800°C.

Nitrogen adsorption tests confirmed the porosities results obtained with acetone exchange method. A greater volume of the coarser pore size distribution, capillary pores (radius greater than 50 Å), known for dominating the water transport, was found in the OPC paste 800°C in comparison to the paste in concrete 800°C. This supports the finding that paste 800°C absorbs water faster than the paste in concrete 800°C.

Acknowledgments

The authors gratefully acknowledge the Australian Research Council Discovery Grant No. DP0558463 for this research project.

5 References

1. Lea FC (1920) The effect of temperature on some of the properties of materials. Engineering
2. Khoury GA (2000) Effect of fire on concrete and concrete structures. Progress in Structural Engineering and Materials 2: 429-447
3. Lea FC, Stradling RE (1922) The resistance to fire of concrete and reinforced concrete. Engineering 144: 341-344
4. Dias WPS, Khoury GA, Sullivan PJE (1990) Mechanical Properties of Hardened Cement Paste Exposed to Temperatures up to 700°C (1292F). ACI Materials Journal 87: 160-166
5. Petzold A, Rohrs M (1970) Concrete for high temperatures. 2nd edition ed., Maclaren and Sons Ltd, London
6. Mendes A, Sanjayan J, Collins F (2008) Phase transformations and mechanical strength of OPC/Slag pastes submitted to high temperatures. Materials and Structures 41: 345-350

7. Mendes A, Sanjayan J, Collins F (2009) Long-term progressive deterioration following fire exposure of OPC versus slag blended cement pastes. *Materials and Structures* 42: 95-101
8. Lea FC, Stradling RE (1922) The resistance to fire of concrete and reinforced concrete. *Engineering* 144: 380-382
9. Khoury GA (1992) Compressive strength of concrete at high temperatures: a reassessment. *Magazine of Concrete Research* 44: 291-309
10. Arioiz O (2007) Effects of elevated temperature on properties of concrete. *Fire Safety Journal* 42: 516-522
11. Chan SYN, Peng GF, Chan JKW (1996) Comparison between high strength concrete and normal strength concrete subjected to high temperature. *Materials and Structures* 29: 616-619
12. Chen B, Li C, Chen L (2009) Experimental study of mechanical properties of normal-strength concrete exposed to high temperatures at an early age. *Fire Safety Journal* 44: 997-1002
13. Handoo SK, Agarwal S, Agarwal SK (2002) Physicochemical, mineralogical, and morphological characteristics of concrete exposed to elevated temperatures. *Cement and Concrete Research* 32: 1009-1018
14. Khoury GA, Grainger BN, Sullivan PJE (1985) Transient thermal strain of concrete: literature review, conditions within the specimen and behaviour of individual constituents. *Magazine of Concrete Research* 37: 131-144
15. Mendes A, Sanjayan JG, Collins F (2010) Effects of slag and cooling method on the progressive deterioration of concrete after exposure to elevated temperatures as in a fire event. *Materials and Structures* DOI 10.1617/s11527-010-9660-2: Published online 31 August 2010
16. Gregg SJ, Sing KSW (1967) Adsorption, surface area and porosity. Academic Press, London
17. Nokken MR, Hooton RD (2002) Dependence of Rate of Absorption on Degree of Saturation of Concrete. *Journal of Cement, Concrete and Aggregates (CCA)* 24: 20-24

18. Lockington D, Parlange JY, Dux P (1999) Sorptivity and the estimation of water penetration into unsaturated concrete. *Materials and Structures* 32: 342-347
19. Ho DWS, Hinczak I, Conroy JJ, Lewis RK. Influence of Slag Cement on the Water Sorptivity of Concrete. in *Proceedings Second International Conference*. 1986. Madrid, Spain: ACI SP 91 1463-1473
20. Baroghel-Bouny V (2007) Water vapour sorption experiments on hardened cementitious materials: Part I: Essential tool for analysis of hygral behaviour and its relation to pore structure. *Cement and Concrete Research* 37: 414-437
21. Safiuddin M, Hearn N (2005) Comparison of ASTM saturation techniques for measuring the permeable porosity of concrete. *Cement and Concrete Research* 35: 1008-1013
22. Chan YN, Luo X, Sun W (2000) Compressive strength and pore structure of high-performance concrete after exposure to high temperature up to 800°C. *Cement and Concrete Research* 30: 247-251
23. Gallé C (2001) Effect of drying on cement-based materials pore structure as identified by mercury intrusion porosimetry: A comparative study between oven, vacuum, and freeze-drying. *Cement and Concrete Research* 31: 1467-1477
24. Gonen T, Yazicioglu S (2007) The influence of compaction pores on sorptivity and carbonation of concrete. *Construction and Building Materials* 21: 1040-1045
25. Gopalan MK (1996) Sorptivity of Fly Ash Concretes. *Cement and Concrete Research* 26: 1189-1197
26. Kayali OA (1987) Porosity of concrete in relation to the nature of the paste-aggregate interface. *Materials and Structures* 20: 19-26
27. Li YX, Chen YM, Wei JX, He XY, Zhang HT (2006) A study on the relationship between porosity of cement paste with mineral additives and compressive strength of mortar based on this paste. *Cement and Concrete Research* 36: 1740-1743

28. Okpala DC (1989) Pore structure of hardened cement paste and mortar. *The International Journal of Cement Composites and Lightweight Concrete* 11: 245-254
29. Wilson MA, Carter MA, Hoff WD (1999) British Standard and RILEM water absorption tests: A critical evaluation. *Materials and Structures* 32: 571-578
30. Zhang L, Glasser FP (2000) Critical examination of drying damage to cement pastes. *Advances in Cement Research* 12: 79-88
31. Korpa A, Trettin R (2006) The influence of different drying methods on cement paste microstructures as reflected by gas adsorption: Comparison between freeze-drying (F-drying), D-drying, P-drying and oven-drying methods. *Cement and Concrete Research* 36: 634-649
32. Ramachandran VS, Feldman RF, Beaudoin JJ (1981) *Concrete science: treatise on current research* Heyden, London
33. Collier NC, Sharp JH, Milestone NB, Hill J, Godfrey IH (2008) The influence of water removal techniques on the composition and microstructure of hardened cement pastes. *Cement and Concrete Research* 38: 737-744
34. Robler M, Odler I (1985) Investigations on the relationship between porosity, structure and strength of hydrated portland cement pastes. *Cement and Concrete Research* 15: 320-330
35. Beaudoin JJ, Gu P, Marchand J, Tamtsia B, Myers RE, Liu Z (1998) Solvent replacement studies of hydrated portland cement systems: the role of calcium hydroxide. *Advn Cem Bas Mat* 8: 56-65
36. Taylor HFW, Turner AB (1987) Reactions of tricalcium silicate paste with organic liquids. *Cement and Concrete Research* 17: 613-623
37. Feldman RF, Beaudoin JJ (1991) Pretreatment of hardened hydrated cement pastes for mercury intrusion measurements. *Cement and Concrete Research* 21: 297-308
38. Konecny L, Naqvi SJ (1993) The effect of different drying techniques on the pore size distribution of blended cement mortars. *Cement and Concrete Research* 23: 1223-1228

39. Chatterji S (2005) Aspects of generation of destructive crystal growth pressure. *Journal of Crystal Growth* 277: 566-577
40. Ramachandran VS, Sereda PJ, Feldman RF (1964) Mechanism of Hydration of Calcium Oxide. *Nature* 201: 288
41. Ramachandran VS, Sereda PJ, Feldman RF (1967) Discussion on 'The volume expansion of hardened cement paste due to the presence of 'dead burnt' CaO by S Chatterji and J W Jeffrey. *Magazine of Concrete Research* 19: 49-50
42. Steffens A, Dinkler D, Ahrens H (2002) Modeling carbonation for corrosion risk prediction of concrete structures. *Cement and Concrete Research* 32: 935-941
43. Day RL, Marsh BK (1988) Measurement of Porosity in Blended Cement Pastes. *Cement and Concrete Research* 18: 63-73
44. Feldman RF (1984) Pore Structure Damage in Blended Cements Caused by Mercury Porosimetry Intrusion. *Journal of American Society* 67: 30
45. Parrott LJ (1981) Effect of drying history upon the exchange of pore water with methanol and upon subsequent methanol sorption behaviour in hydrated alite paste. *Cement and Concrete Research* 11: 651-658
46. Parrott LJ (1984) An examination of two methods for studying diffusion kinetics in hydrated cements. *Materials and Structures* 17: 131-137
47. Bordallo HN, Aldridge LP (2010) Concrete and Cement Paste Studied by Quasi-Elastic Neutron Scattering. *Z. Phys. Chem.* 224: 183-200
48. Rostásy FS, Wei R, Wiedemann G (1980) Changes of pore structure of cement mortars due to temperature. *Cement and Concrete Research* 10: 157-164

Chapter 10

Conclusions & Future Work

10.1 Summary and conclusions

Most of the current literature describing the effects of elevated temperatures on OPC concrete is contradictory, as outlined in Chapter 2 of this thesis. Above 400°C, one of the main hydrates of the cement paste, calcium hydroxide (CaOH_2) dehydrates into calcium oxide (CaO) causing the OPC paste to shrink and crack.

During cooling and following exposure to air moisture, CaO rehydrates into CaOH_2 causing expansion, disintegration and total strength loss of the OPC paste. Through this study, although the critical temperature of 400°C has been confirmed for OPC paste, this was not valid for OPC concrete. This highlights that the behaviour of paste and concrete, following exposure to elevated temperatures, can differ. The rate of water absorption, which enables the CaO rehydration, was found to be the key factor controlling the extent of deterioration of the mechanical properties of paste and concrete. This is further summarized, along with other key conclusions, in this chapter.

1. The dehydration of CaOH_2 and rehydration of CaO leads to total strength loss and complete disintegration of OPC pastes. As indicated by thermogravimetric analysis (TGA) and compressive strength tests, partial replacement of OPC with slag resulted in a significant and beneficial reduction of the amount of CaOH_2 . An increase in the proportion of slag in the cement paste led to an improvement in the mechanical properties following exposure to temperatures beyond 400°C. OPC/slag pastes presented compressive strength in the range of 15 MPa after exposure to 800°C, while OPC pastes presented total strength loss.
2. The CaO rehydration progresses with time resulting in severe deterioration of the OPC paste structure. After one year of exposure to air moisture, the CaO rehydration led the hardened OPC paste to completely disintegrate to powder. On the other hand, OPC/slag pastes were not affected by the progressive CaO

rehydration, presenting no visual or residual strength changes after one year of exposure to air moisture.

3. The use of sealants has proven to be a promising option to minimize the negative impact of CaO rehydration on OPC pastes exposed to elevated temperatures. After exposure to 800°C, the application of paraffin as a sealant resulted in OPC pastes retaining 15% of residual strength even after one week of exposure to air moisture. On the other hand, OPC pastes coated with silicone presented residual strength lower than 2.5%, indicating that silicone was not as successful as paraffin. Infrared spectroscopy (IR) tests revealed that OPC pastes coated with paraffin presented a very minor CaOH_2 peak intensity. This shows the efficiency of this sealant in acting as a barrier to reduce moisture ingress and therefore, minimize the CaO rehydration. In contrast, OPC pastes coated with silicone presented a CaOH_2 peak 16 times more intense than the OPC pastes coated with paraffin.
4. The role of other paste hydrates, rather than CaOH_2 , in the deterioration of the mechanical properties of OPC and OPC/slag pastes was determined using the following techniques: nuclear magnetic resonance (NMR), X-ray diffraction (XRD), infrared spectroscopy (IR) and Synchrotron NEXAFS. The behaviour of the calcium silicate hydrate (C-S-H gel) of OPC and OPC/slag pastes after exposure to elevated temperatures was found to differ. After exposure to 800°C, the C-S-H gel of OPC/slag pastes remained more polymerized than the C-S-H gel of OPC pastes. This is of importance as it indicates that the total loss of C-S-H gel for OPC pastes has also contributed to the greater deterioration of mechanical properties of these pastes when compared to OPC/slag pastes.
5. Furthermore, NMR, XRD and IR tests revealed that the aluminate phases of OPC and OPC/slag pastes differ after exposure to temperatures up to 800°C. The OPC pastes presented rehydration of the aluminate phases, while this was not observed for OPC/slag pastes. Therefore, it is likely that the aluminate phases also play a role in the greater deterioration of mechanical properties experienced by OPC pastes when compared to 35% slag pastes.

6. The temperature of 400°C is below the critical temperature necessary for CaOH_2 dehydration. OPC concrete heated to 400°C followed by exposure to air moisture presented strength loss of approximately 20%. When water cooling followed the exposure to 400°C, a further 20% strength loss was observed for the OPC concrete. OPC/slag concrete presented similar strength losses to OPC concrete. The further strength losses due to water cooling are a result of thermal stresses caused by the thermal shock experienced by concrete when in contact with water.
7. The temperature of 800°C is above the critical temperature necessary for CaOH_2 dehydration. OPC concrete heated to 800°C followed by exposure to air moisture presented strength loss of 65% while OPC pastes presented total strength loss and complete disintegration. Therefore, the dehydration of CaOH_2 and rehydration of CaO is significantly less detrimental for OPC concrete than it is for OPC paste.
8. OPC concrete heated to 800°C followed by water cooling presented a further strength loss of 14%. For OPC/slag concrete the further strength loss due to water cooling was approximately 5%, therefore, significantly less than the strength loss observed for OPC concrete. Infrared tests revealed that the greater strength loss observed for OPC concrete was a result of the accelerated rehydration of CaO caused by the water cooling method.
9. Exposure to 800°C followed by air moisture caused further deterioration in OPC and OPC/slag concretes. After one week exposure to air moisture OPC and OPC/slag concrete presented the same strength loss caused by water cooling, i.e., 14% and 5% respectively. IR tests showed that this further deterioration was caused by the slower rehydration of CaO as a result of exposure to air moisture. However, even though the different sources of water (air moisture and water cooling) caused similar deterioration, the amount of CaOH_2 formed by each source differed.
10. OPC pastes exposed to 800°C followed by cooling to room temperature were later investigated by water sorptivity tests. During testing, the OPC paste reacted instantaneously with water, releasing heat and disintegrating, inhibiting test completion. This was found to be due to an accelerated rehydration of

CaO in the presence of water; an expansive, exothermic and instantaneous reaction. Acetone sorptivity tests provided an indication of the rate of water absorption of OPC pastes previously exposed to 800°C. When compared to water sorptivity results for the OPC concrete (previously exposed to 800°C followed by cooling to room temperature), it was concluded that after exposure to elevated temperatures, OPC paste absorbs water at a faster rate than the OPC paste in concrete.

11. The rate of water absorption determines the growth rate of CaOH_2 crystals and ultimately the type of CaOH_2 crystals formed. Therefore, the faster rate of water absorption observed for OPC paste compared to the OPC paste in concrete, led to different CaOH_2 crystal formation in each specimen (previously exposed to 800°C followed by exposure to moisture). Different crystals cause different levels of deterioration, not always leading to the total disintegration of the constraining body. This explains why OPC paste disintegrates after exposure to 800°C followed by air moisture and/or water (CaO rehydration). And this also explains why, on the other hand, the OPC paste in concrete exposed to 800°C followed by air moisture and/or water does not disintegrate, even though CaO rehydration has been confirmed to have taken place.
12. The extent of the deterioration is therefore, not only related to the CaO rehydration occurrence, but most importantly it is related to the rate at which rehydration occurs, i.e., the rate of water absorption. The rate of water absorption is the determining factor controlling the extent of deterioration caused by CaO rehydration.
13. Nitrogen adsorption tests were conducted in OPC paste and concrete previously exposed to 800°C. Test results showed that a greater volume of the coarser pore size distribution (capillary pores with radius greater than 50 Å), known for dominating the water transport, was found in the OPC paste in comparison to the OPC paste in concrete. This supports the finding that OPC paste absorbs water at a faster rate than the OPC paste in concrete.

10.2 Suggestions for future work

This thesis investigated the effects of elevated temperatures on the mechanical properties of OPC and OPC/slag paste and concrete. The following suggestions are proposed to better supplement the findings of this thesis.

1. Study of different binders

The investigation of the effects of binders such as fly ash and silica fume on the microstructure and mechanical properties of OPC paste and concrete exposed to elevated temperatures is of interest as it would provide further information on how elevated temperatures impact on the OPC binder. In addition, different binders might result in better mechanical properties after exposure to elevated temperatures.

2. Thermal resistance under loading

The assessment of the impact of loading/unloading during exposure to elevated temperatures would provide additional information regarding the behaviour of concrete during a fire event.